UNIVERSITY OF ICELAND

Ph.D. Thesis

in Geology

Glacial geomorphology and dynamics of palaeo-ice streams in northeast Iceland

Nína Aradóttir

April 2024

FACULTY OF EARTH SCIENCES

Glacial geomorphology and dynamics of palaeo-ice streams in northeast Iceland

Nína Aradóttir

Dissertation submitted in partial fulfillment of a
Philosophiae Doctor degree in Geology

PhD Committee
Ívar Örn Benediktsson, supervisor
Institute of Earth Sciences, University of Iceland
Ólafur Ingólfsson, supervisor
Faculty of Earth Sciences, University of Iceland
Anders Schomacker
Department of Geosciences, UiT The Arctic University of Norway
Skafti Brynjólfsson
Icelandic Institute of Natural History

Opponents
Anna Hughes
Physical Geography and Quaternary Science, University of Manchester
Eiliv Larsen
Geological Survey of Norway

Faculty of Earth Sciences
School of Engineering and Natural Sciences
University of Iceland
Reykjavík, April 2024

Glacial geomorphology and dynamics of palaeo-ice streams in northeast Iceland
Dissertation submitted in partial fulfillment of a *Ph.D.* degree in Geology

Copyright © 2024 Nína Aradóttir
All rights reserved

Faculty of Earth Sciences
School of Engineering and Natural Sciences
University of Iceland
Askja, Sturlugata 7
IS-102, Reykjavik
Iceland

Telephone: 525 4000

Bibliographic information:
Nína Aradóttir, 2024, *Glacial geomorphology and dynamics of palaeo-ice streams in northeast Iceland*, PhD dissertation, Faculty of Earth Sciences, University of Iceland, 160 pp.

Author ORCID: 0000-0002-6584-8964
ISBN: 978-9935-9772-0-5

Abstract

This thesis describes the evidence of palaeo-ice streams in northeast Iceland. Ice streams within the Iceland Ice Sheet (IIS) had been previously proposed, but limited studies existed on their geomorphology. The aim of this study was to advance the understanding of the geomorphological imprint, configuration, and dynamics of palaeo-ice streams and their development during and following the Last Glacial Maximum by mapping glacial landforms and analyze their internal architecture.

The research focuses on streamlined subglacial bedforms (SSBs; drumlins and mega-scale glacial lineations), crevasse-squeeze ridges (CSRs), and ribbed moraines; however, glaciofluvial and ice-marginal landforms, as well as hummocky terrain were also mapped. The distribution and orientation of SSBs reveal four flow-sets of cross-cutting palaeo-ice streams that shifted in time and space, along with ice divides. During the maximum glaciation, ice flow was towards the north, unconstrained by the topography, but became confined to the fjords and valleys as the ice sheet thinned. The CSRs and ribbed moraines indicate ice-stream shutdown following glacier readvances during the Late Glacial. The variance in landform morphology and distribution is used to reconstruct the configuration and dynamics of the ice streams.

The results provide new insight into the dynamics of the IIS and palaeo-ice streams within it and are essential for constraining numerical modelling experiments of the ice sheet's evolution. This research has implications for our understanding of modern and palaeo-ice sheet behaviour during deglaciation and under warming climate, and paves the way for further studies and reconstructions of palaeo-ice streams in Iceland.

Útdráttur

Þessi ritgerð fjallar um ummerki og hegðun fornra ísstrauma á Norðausturlandi. Tilgátur hafa áður verið settar fram um ísstrauma í hinum íslenska meginjökli á síðasta jökulskeiði en takmarkaðar rannsóknir hafa verið gerðar á landmótun þeirra. Markmið verkefnisins var því að auka skilning á landmótun, útbreiðslu og virkni fornra ísstrauma og þróun þeirra á síðasta jökulskeiði með því að kortleggja og rannsaka jökulræn landform. Rannsóknir á innri byggingu landforma munu auka skilning okkar á tilurð og myndun þeirra ásamt hegðun ísstraumanna.

Í rannsókninni er lögð áhersla á straumlínulaga landform (jökulöldur og risakembur), sprungufyllingar og rifjagarða, en malarásar, leysingafarvegir, jökulgarðar og haugaruðningar eru einnig kortlagðir. Útbreiðsla og stefna straumlínulaga landforma benda til nokkurra ísstrauma sem hafa verið virkir á mismunandi tíma og færst til, ásamt ísaskilum. Á hámarki síðasta jökulskeiðs var ísflæði á rannsóknarsvæðinu til norðurs, án tilheyrandi áhrifa af undirliggjandi landslagi, en samhliða þynningu jökulþekjunnar varð ísflæðinu stjórnað æ meir af landslaginu. Sprungufyllingarnar og rifjagarðarnir eru til marks um stöðnun ísstrauma sem voru virkir á síðjökultíma. Breytileika í lögun og dreifingu landformanna er hægt að nýta til að skilja legu og virkni ísstraumanna.

Niðurstöðurnar veita nýja innsýn í útbreiðslu og virkni fornra ísstrauma á Íslandi og gagnast til að skorða líkanareikninga af íslenska meginjöklinum. Rannsóknin leggur grunn að áframhaldandi kortlagningu á fornum ísstraumum á Íslandi og eykur skilning á hegðun nútíma og fornra meginjökla og viðbrögðum óstöðugra ísstrauma við hlýnandi loftlagi.

Table of Contents

Útdráttur ..... **v**
List of Figures ..... **viii**
List of Tables ..... **ix**
List of Publications ..... **x**
Abbreviations ..... **xii**
Acknowledgements ..... **xiii**
1 Introduction **1**
1.1 Motivation 1
1.2 Objectives 2
1.3 Ice streams and geomorphology 3
1.4 The Iceland Ice Sheet 4
2 Study area **7**
2.1 Glacial history 7
3 Methods **11**
3.1 Geomorphological mapping 11
3.2 Morphological and spatial analysis 14
3.3 Sedimentology 16
3.4 Ground penetrating radar 17
4 Results: Summary of papers **19**
4.1 Paper I 20
4.2 Paper II 22
4.3 Paper III 24
4.4 Paper IV 27
5 Discussion **29**
5.1 Reconstruction of palaeo-ice streams 29
5.2 Implications for ice dynamics 31
5.3 Glacial history 33
6 Conclusion **37**
7 Future perspectives **39**
References **41**
Paper I **49**
Paper II **69**
Paper III **129**
Paper IV **131**

List of Figures

Figure 1.1 Overview of the geomorphological imprint of the IIS.. 2

Figure 2.1 Overview map of the study area in northeast Iceland with the elevation distribution. 9

Figure 3.1 Examples of the different data used to map the landforms from the Bustarfell drumlin field within the Jökuldalsheiði-Vopnafjörður flow-set.. 12

Figure 3.2 Field images. 13

Figure 3.3 Size-frequency distribution of the morphometrics of the SSBs, CSRs, ribbed moraines, and transverse ridges presented with boxplots.. 16

Figure 4.1 Composite map of glacial landforms in northeastern Iceland that are investigated in this thesis. 19

Figure 4.2 Hypothetical flow-sets of cross-cutting palaeo-ice streams in northeast Iceland from Paper I. 21

Figure 4.3 A conceptual model of the formation of the investigated drumlins from Paper II. 23

Figure 4.4 Conceptual landsystem model illustrating landforms associated with ice-stream shutdown in terrestrial environment based on observations from Bakkaflói and Þistilfjörður, northeast Iceland in Paper III. 25

Figure 4.5 Time slices highlighting the glacial history and possible ice-stream configuration and dynamics in Bakkaflói and Þistilfjörður during the A) YD and B) PB readvances. 26

Figure 4.6 Conceptual landsystem model illustrating ribbed moraines formed within the Vopnafjörður-Jökuldalsheiði flow-set from Paper IV.. 28

Figure 5.1 A) *Conceptual landsystem model of terrestrial palaeo-ice streams based on observations from the Vopnafjörður-Jökuldalsheiði, Bakkaheiði, Bakkaflói and Þistilfjörður flow-sets in northeast Iceland..* 30

Figure 5.2 Schematic diagram of the relative timing of the landforms comprising the palaeo-ice stream landsystem in northeast Iceland. 31

Figure 5.3 *A-D show the hypothesized configuration of palaeo-ice streams within the IIS at several stages during the last glaciation without absolute age constraints..* 35

List of Tables

Table 3.1 Landforms that have been mapped within the thesis and description of how they are identified. Also listed are their dimensions, location, number of mapped landforms, and the paper(s) in which they are discussed. 15

List of Publications

This thesis is based on five years of research carried out at the Institute of Earth Sciences, University of Iceland, including four field seasons. The PhD project was funded for three years by the University of Iceland Doctoral Research Fund and one year by The Icelandic Centre for Research (RANNÍS). Additional funding for the last year and the field work was by the Doctoral Teaching Assistant Grant, the Energy Research Fund of Landsvirkjun, the Icelandic Road and Coastal Administration Research Fund, and the Aðalsteinn Kristjánsson Memorial Fund. The outcome is presented in four manuscripts listed below as Appendices I-IV. Papers I-III are published, and paper IV is in preperation.

I. Benediktsson, Í.Ö., **Aradóttir, N.,** Ingólfsson., Ö., Brynjólfsson, S. 2022. *Cross-cutting palaeo-ice streams reveal shifting Icelandic Ice Sheet dynamics***.** Geomorphology, 396, 108009. https://doi.org/10.1016/j.geomorph.2021.108009

II. **Aradóttir, N.,** Benediktsson, Í.Ö., Ingólfsson, Ó., Sturkell, E., Brynjólfsson, S., Farnsworth, W.R., Phillips, E. 2023. *Drumlin formation within the Bustarfell drumlin field, northeast Iceland: integrating sedimentological and GPR data*. Journal of Quaternary Science, 38 (3), 386-402. https://doi.org/10.1002/jqs.3481

III. **Aradóttir, N.,** Benediktsson, Í.Ö., Ingólfsson, Ó., Brynjólfsson, S., Farnsworth, W.R., Benjamínsdóttir, M.M., Ríkharðsdóttir, L.B. 2023. *Ice-stream shutdown during deglaciation: Evidence from crevasse-squeeze ridges of the Iceland Ice Sheet*. Earth Surface Processes and Landforms, 48 (12), 2412-2430. https://doi.org/10.1002/esp.5636

IV. **Aradóttir, N.,** Benediktsson, Í.Ö., Helgadóttir, E.G., Ingólfsson, Ó., Brynjólfsson, S., Farnsworth, W.R. *Ribbed moraines formed during deglaciation of the Iceland Ice Sheet: Implications for ice-stream dynamics*. Submitted to Boreas special issue.

Contribution from the author.

Paper I: Fieldwork, aerial photograph and DEM analyses, geomorphological mapping, data interpretation, preparation of text and figures together with Ívar Örn Benediktsson.

Paper II: Fieldwork planning, fieldwork, aerial photograph and DEM analyses, geomorphological mapping, sedimentological analysis, ground penetrating radar, data interpretation, preparation of text and figures.

Paper III: Fieldwork planning. fieldwork, aerial photograph and DEM analyses, geomorphological mapping, sedimentological analysis, data interpretation, preparation of text and figures.

Paper IV: Fieldwork planning/leading, fieldwork, aerial photograph and DEM analyses, geomorphological mapping, data interpretation, preparation of text and figures.

Additionally, contributions were made to the following articles during the PhD period that are not included in the thesis:

Aradóttir, N., Ingólfsson, Ó., Noormets, R., Benediktsson, Í.Ö., Ben-Yehoshua, D., Håkansson, L., Schomacker, A. 2019. Glacial geomorphology of Trygghamna, western Svalbard - integrating terrestrial and submarine archives for a better understanding of past glacial dynamics. Geomorphology, 344, 75-89. https://doi.org/10.1016/j.geomorph.2019.07.007

Ben-Yehoshua, D., **Aradóttir, N.,** Ingólfsson, Ó., Benediktsson, Í.Ö., Farnsworth, W.R. 2023. Formation of crevasse-squeeze ridges at Trygghamna, Svalbard. Earth Surfaces, Processes and Landforms, 48 (12), 2334-2348. https://doi.org/10.1002/esp.5631

Principato, S., Mastro, H., Benediktsson, Í.Ö., **Aradóttir, N**. 2023. Morphometric analysis of ice scour lakes in Iceland: a proxy for ice sheet dynamics. Earth Surface Processes and Landforms, available online. https://doi.org/10.1002/esp.5693

Abbreviations

BP – Before present

C_{40} – Clast shape index

CSR – Crevasse-squeeze ridge

DEM – Digital elevation model

GIS – Greenland Ice Sheet

GPR – Ground penetrating radar

ER - Elongation ratio

IIS – Iceland Ice Sheet

ka – thousand years

LGM – Last Glacial Maximum

LIA – Little Ice Age

MSGL – Mega-scale glacial lineation

NLSI – National Land Survey of Iceland

PB – Preboreal

RA – Roundness index for angular clasts

SSB – Streamlined subglacial bedform

YD – Younger Dryas

WAIS – West Antarctic Ice Sheet

Acknowledgements

This PhD dissertation would never have been accomplished without the support of numerous people. First, my two supervisors, Ívar Örn Benediktsson and Ólafur Ingólfsson, I am very grateful to have gotten the chance to participate in this project and for all the excellent guidance they have given me. Óli is especially thanked for all the fascinating stories from Svalbard in his lectures during my undergraduate studies, which was the reason that I applied for exchange studies at The University Centre in Svalbard. During my stay there, my interest in glacial geology grew and there was no turning back. I did my BSc thesis with Óli and then moved back to Svalbard for my master's studies in glacial geology. Óli has therefore been a great influence in my studies. I thank Ívar for his endless support, encouragement, and patience throughout the project. Ívar's door has always been open, whatever the subject was. It has been a great pleasure to work with Ívar and Óli, both as supervisors and as friends.

I am grateful for the financial support the project received. It was funded by the University of Iceland Doctoral Research Fund, the Icelandic Centre for Research (RANNÍS), the Doctoral Teaching Assistant Grant, the Energy Research Fund of Landsvirkjun, the Icelandic Road and Coastal Administration Research Fund, and the Aðalsteinn Kristjánsson Memorial Fund.

The other members of my PhD committee, Anders Schomacker and Skafti Brynjólfsson, are thanked for participating in the field work, guidance, and reviewing the thesis right before Christmas. Skafti is also thanked for valuable comments when reading over the manuscripts and discussion on mapping, which will hopefully continue. I am grateful to Wesley Farnsworth for all the constructive feedback, motivation, and coffee during the whole process. It has been greatly appreciated and helpful. Erik Sturkell is thanked for lending us his GPR and for being patient while I tried to understand geophysics and ran into some problems in the field.

Many thanks to the master students that I collaborated with during the project, Erla Guðný Helgadóttir, Sigurrós Arnardóttir, Margrét Mjöll Benjamínsdóttir, Lena Björg Ríkarðsdóttir, and Eiður Daði Bjarkason. Not to mention other people who have joined the field work, Hreggviður Norðdahl, Eshter Ruth Guðmundsdóttir, Karl Stefánsson, Teitur Hinrichsen, and Emrys Phillips. This project could not have been completed without your contribution. Special thanks to Hreggi and Esther for their friendship throughout the years. The last field season with Erla Guðný and her field dog Buski was especially memorable for various reasons. The farmers and landowners in the study area are also greatly acknowledged for their assistance and for allowing us to dig through landforms on their land.

Everyone else I got to know during my time in Askja; Sif, Greta, Kate, Noemi, Eemu, Erna, Daniel, Sigga, Rebekka, Ásta, Rosie, Gro, Tingting, Ahmed, Araksan, Will, Jóhanna Kristín, Céline, Elisa, Anna Jóna, those I got to know through JÖRFÍ – and many more – thanks for all the enjoyable moments together. I am also grateful to my friends from my undergraduate studies, Margrét, Vigdís, Snjólaug, and Inga, for being there from the start.

Thanks to my ranger friends, Ágústa, Linda, Helga Hvanndal, Guðbjörg, Habba, Benni, and Álfur, that have helped me think about something else than the PhD. Your friendship means the world to me. The Svalbard reunion with Lis and Christine in

Akureyri last summer led to our meetings during the last phase of the PhD was exactly the motivation that I needed in the end – thanks for being there with me through it. Also, thanks to everyone who looked after Dreki and Gríma during my field work and travels.

Lastly, I want to thank my parents and siblings for their endless support throughout the whole process and for always showing interest in the project. All the travels in Iceland together with them, promoted me to respect nature, which is a big part of my life today. My mom and my sister Helga, I cannot express my gratitude enough for all the encouragement, love, and advice you have given me. I love you all!

1 Introduction

1.1 Motivation

Glaciers shape the landscape as they expand and retreat, leaving behind distinct fingerprints that become exposed after their demise. The landforms and sediments formed by the glaciers are used to reconstruct fluctuations and dynamics of former ice masses as well as processes occurring at the ice-bed interface or the ice margin. Therefore, glacial geomorphology is an essential tool for understanding the complex behavior of glaciers and their relationship to changes in climate (Benn and Evans, 2010). The information acquired from studying contemporary glacial environments can serve as analogs when investigating palaeo-ice sheets and -ice streams (Evans and Rea, 1999; Stokes, 2018).

The Icelandic landscape outside the active volcanic zone and in the surroundings of modern glaciers has been significantly modified by glacial processes. The glacial geomorphology and the sedimentary record in front of modern glaciers in Iceland are well-studied compared to the older glacial landscapes outside the Neoglacial or Little Ice Age (LIA) moraines (Benediktsson et al., 2024a). Data on the Pleistocene glacial landscapes are fragmentary and require additional information for a comprehensive understanding of the configuration and dynamics of the Iceland Ice Sheet (IIS) during the Late Weichselian (Fig. 1.1; Benediktsson et al., 2022a, b). Compared to other ice sheets in the northern hemisphere, our knowledge of the IIS during the Last Glacial Maximum (LGM) and the subsequent deglaciation is limited. Numerous studies exist on the configuration and behaviour of palaeo-ice streams within other Pleistocene ice sheets (e.g. Stokes and Clark, 2001; Kjær et al., 2003; Greenwood and Clark, 2009; Margold et al., 2015), but comparable studies from Iceland have been largely lacking.

Palaeo-ice streams within the IIS have been proposed with onshore and offshore geomorphological mapping of streamlined subglacial bedforms (SSBs; drumlins and mega-scale glacial lineations), glacial striae and large-scale topography (Fig. 1.1; Norðdahl, 1991; Norðdahl and Pétursson, 2005; Spagnolo and Clark, 2009; Clark and Spagnolo, 2016; Principato et al., 2016; Norðdahl et al., 2019; Arnardóttir, 2022), further supported with numerical modelling (Bourgeois et al., 2000; Hubbard et al., 2006; Patton et al., 2017). Despite these efforts, the configuration and cross-cutting relationships of palaeo-ice streams in Iceland are still poorly understood. Furthermore, no studies exist on the sedimentary record of glacial bedforms associated with palaeo-ice streams within the IIS. More geomorphological, sedimentological, and chronological data are necessary for future efforts to reconstruct the configuration and dynamics of the IIS and its palaeo-ice streams during the LGM and subsequent deglaciation.

The suggested rates of retreat during the collapse of the IIS in the Bølling interstadial are comparable to contemporary rates of mass loss of the Greenland Ice Sheet (GIS) (Ingólfsson and Norðdahl, 2001; Norðdahl and Ingólfsson, 2015; Patton et al., 2017). The development of the IIS during the deglaciation can therefore serve as a useful analog to the rapid retreat of ice sheets with similar characteristics in geothermally active areas, such as the Siple Coast in Antarctica, and northeast Greenland, due to the ongoing climate and sea level change (Hugonnet et al., 2021).

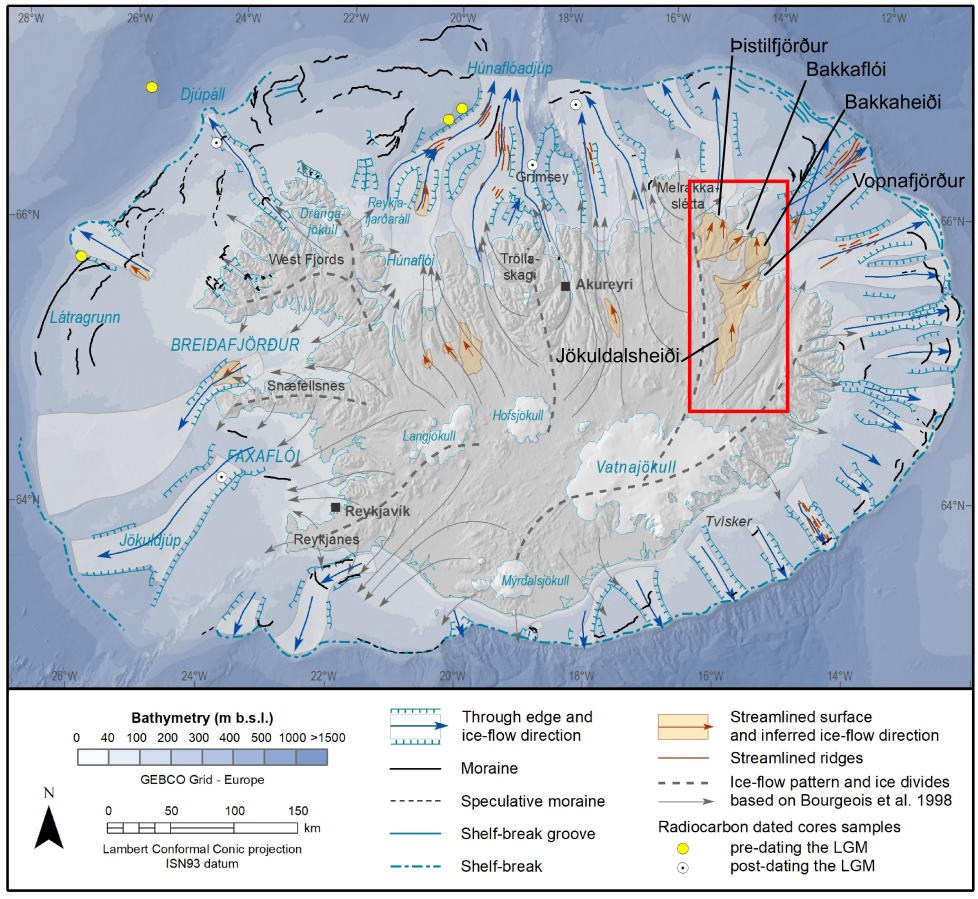

Figure 1.1 Overview of the geomorphological imprint of the IIS. The study area in northeast Iceland is located within the red box and the investigated fjord-valley systems are marked. The configuration of the terrestrial flow-sets in northwest and north Iceland is based on the mapping of SSBs (Principato et al., 2016; Arnardóttir, 2022) and on the results from Paper I within the study area. The offshore data is based on Spagnolo and Clark (2009), Clark and Spagnolo (2016), and Patton et al. (2017). Modified from Benediktsson et al. (2022b).

1.2 Objectives

The overall aim of this thesis is to identify and reconstruct the configuration and dynamics of palaeo-ice streams within the IIS in northeast Iceland. This is achieved by mapping and investigating glacial landforms and sedimentary records in the Þistilfjörður, Bakkaflói, Bakkaheiði, Vopnafjörður and Jökuldalsheiði areas (Fig. 1.1). Additionally, the internal architecture of key bedforms is analyzed. The findings advance our understanding of the configuration, geomorphological imprint, and deglaciation history of palaeo-ice streams in northeast Iceland and provide valuable insights into the basal processes, landform genesis, and ice-stream dynamics.

The main research questions of this thesis were:

- What was the configuration and relative timing of palaeo-ice streams in northeast Iceland during the Late Weichselian?
- Which glacial landforms characterize the palaeo-ice stream beds?
- What characterizes the morphology and internal architecture of the glacial bedforms and what does this imply about their formation as well as the behavior of palaeo-ice streams?
- What do glacial landsystems in northeast Iceland reveal about the dynamics of palaeo-ice streams and the development of the IIS in this region?
- How do the mapped flow-sets and landforms correlate with the known glacial history in northeast Iceland?

1.3 Ice streams and geomorphology

Ice streams are corridors of fast-flowing ice, bounded by slower-moving ice (Paterson, 1994). Their behaviour and location have a substantial effect on the stability and mass balance of ice sheets through the release of ice and sediments (Bennett, 2003). Most data on ice streams are on the mass balance and configuration (Stokes, 2018), and less is known about the basal environment as direct observation of the glacier bed remains difficult and is limited to boreholes and seismic investigations (Kamb, 2001; Bennett, 2003; Smith et al., 2021). Although there are still unanswered questions regarding the mechanism associated with their fast and variable flow, ice streaming is largely governed by processes at the ice-bed interface, where weak deformable till layer(s) and/or basal sliding facilitate increased flow rates (Kamb, 2001; Bennett, 2003; Alley et al., 2004; Stokes et al., 2007). Other potential forcings and factors must also be accounted for such as subglacial topography and bedrock composition (Winsborrow et al., 2010; Stokes et al., 2016), the size of the drainage basin (Ó Cofaigh et al., 2008), and atmospheric and oceanic changes (Joughin et al., 2012; Carr et al., 2013).

All contemporary ice streams are marine-terminating and exist within the Antarctic and Greenland ice sheets (Bennett, 2003). Their sensitivity to sea level and climate change is currently of great concern but the effect that these changes have on the behaviour and mechanisms of fast ice flow is, however, still not fully understood (e.g. Bennett, 2003; Alley et al., 2005; Joughin et al., 2014). Palaeo-ice streams are considered to have been present in former ice sheets, both terrestrial and marine-terminating (Stokes and Clark, 1999, 2001). To reconstruct palaeo-ice streams, geomorphological criteria is presented in a landsystem template by Stokes and Clark (1999), consisting of highly streamlined terrain, abrupt lateral margins, heterogeneous onset zones, and major sedimentary depocenters. The criteria have been used to infer where and when ice streams operated and to reconstruct former ice sheets (e.g. Evans et al., 2008; Ó Cofaigh and Stokes, 2008; Hughes et al., 2010; Livingstone et al., 2012; Eyles et al., 2018).

Elongated drumlins and mega-scale glacial lineations (MSGLs) are among the main indicators of fast ice flow (Briner, 2007; King et al., 2009; Stokes et al., 2013a). They are elongated in the direction of ice flow and are end members of a size and shape continuum (Ely et al., 2016; Sookhan et al., 2022) with the MSGLs being more elongated (Clark, 1993). The wide range of morphological characteristics and composition of drumlins (e.g. Menzies, 1979; Stokes et al., 2011; Maclachlan and Eyles, 2013) have led to several

hypotheses of their formation including; deformation of till around more competent cores (Smalley and Unwin, 1968; Boulton, 1987; Hart, 1997), catastrophic meltwater floods (Shaw, 2002), and instabilities at a flat-bed causing a rise in the till surface (Hindmarsh, 1998; Fowler, 2000; Stokes et al., 2013b; Fowler and Chapwanya, 2014). Hart (1997) classified drumlins into three types and suggested that they can be formed by either erosion, deposition, deformation, or a combination of all, although others have explained their formation to be solely erosional (Eyles et al., 2016). The recent investigation of a modern drumlin field in Iceland suggests that lower effective stresses occur over drumlins than between them, resulting in erosion on the drumlin sides and head and deposition of till on their top and lee slope (Benediktsson et al., 2016; McCracken et al., 2016; Iverson et al., 2017). The genesis of MSGLs has also been debated (e.g. Ó Cofaigh et al. 2013; Stokes et al., 2013a), although much fewer studies have focused on their internal architecture. However, one of the key aspects of their formation is their association with fast-flowing ice (Clark, 1993; King et al., 2009; Spagnolo et al., 2014).

Ribbed moraines and crevasse-squeeze ridges (CSRs) are not as widespread on palaeo-ice stream beds as drumlins and MSGLs but have been related to ice streaming and/or surging lobes. Ribbed moraines are clusters of subglacial ridges, formed transverse or oblique to ice flow (Hättestrand and Kleman, 1999; Dunlop and Clark, 2006) and can occur on a continuum with drumlins and MSGLs, where the transition from ribbed moraines to streamlined bedforms is related to increasing ice flow rates (Barchyn et al., 2016). They often occur in the core areas of former ice sheets related to ice-stream onset zones (De Angelis and Kleman, 2008) but the ridges can also be formed within the main trunk of the ice streams or in marginal settings (Vérité et al., 2021). Ribbed moraines are occasionally superimposed on SSBs and have been linked to ice-stream shutdowns (Stokes et al., 2006, 2008). CSRs are reticular ridges, orientated oblique or transverse to former ice flow formed by subglacial sediments squeezed into basal crevasses. They are well-known from modern surge-type glaciers (Sharp, 1985; Evans and Rea, 1999, 2003), but are also described in palaeo-settings where they have been connected to ice-stream or surging lobe shutdown (e.g. Evans et al., 2016; Kurjanski et al., 2019).

The geomorphology of ice stream beds is critical for understanding the behaviour of ice streams as the formation of bedforms can be linked to the mechanism of ice streaming (Stokes and Clark, 1999, 2001; Livingstone et al., 2012; Stokes, 2018). Furthermore, data (i.e. chronological and morphological) from palaeo-ice streams beds are essential for the modelling of past ice sheets and ice streams, which can further contribute to improved understanding of the linkage between ice stream development and climate change (Stokes and Clark, 2011; Patton et al., 2017).

1.4 The Iceland Ice Sheet

Iceland is located in the North Atlantic Ocean (63-67 °N and 13-24 °W), close to the boundary between warm currents from the south and cold polar currents from the north, making Icelandic glaciers highly sensitive to changes in climate and oceanic circulations (Eiríksson et al., 2000; Geirsdóttir, 2011; Benediktsson et al., 2022a). Icelandic landscape, both terrestrial and on the surrounding shelf, is therefore shaped by multiple glaciations during the Pleistocene. Most of the record from the LGM (c. 24.2-18.6 cal. ka BP) is offshore as terrestrial glacial landforms and sediments from the Late Weichselian are rare due to overprinting, volcanism, and erosional processes. The glacial imprints outside the modern glaciers are mainly from the following deglaciation (Benediktsson et al., 2022b). Therefore, the data set is limited, especially with sparse data from the eastern and northern

parts of Iceland, which prevents precise spatial and temporal reconstruction of the IIS and ice streams within it (Fig. 1.1).

The IIS is estimated to have been over 300.000 km^2 in size during the LGM, it probably extended to the shelf break and was largely grounded below sea level (Norðdahl and Pétursson, 2005; Hubbard et al., 2006; Norðdahl et al., 2008; Patton et al., 2017). The configuration and dynamics of the IIS have been reconstructed using numerical modelling together with empirical data (Fig. 1.1; Bourgeois et al., 2000; Norðdahl and Pétursson, 2005; Hubbard et al., 2006; Patton et al., 2017), such as bathymetrical- and geophysical data and sediment cores from the offshore record (e.g. Syvitski et al., 1999; Andrews et al., 2000; Eiríksson et al., 2000; Andrews and Helgadóttir, 2003; Spagnolo and Clark, 2009). Reconstructions of the ice sheet development during the deglaciation are supported by the extent of glacial till and geomorphological evidence, such as glacial striations, in the onshore record together with raised shorelines (e.g. Norðdahl, 1991; Norðdahl and Pétursson, 2005; Norðdahl et al., 2008). The deglaciation of the IIS is considered to have started around 18.6 cal. ka BP and a collapse of the ice sheet occurred between 15.3 and 14.6 cal. ka BP, which is thought to have been triggered by rapid global eustatic sea-level rise, causing extreme calving and retreat of the grounding line (Ingólfsson and Norðdahl, 2001; Norðdahl and Ingólfsson, 2015; Andrés et al., 2019; Benediktsson et al., 2023a). The ice margin retreated further inland during the Bølling-Allerød interstadial (Benediktsson et al., 2023b). Although the extent of the ice sheet is poorly constrained during that stage, it is based on numerical modelling (Patton et al., 2017), mapping of glacial landforms (i.e. raised shorelines and meltwater features) (Ingólfsson and Norðdahl, 2001; Norðdahl and Ingólfsson, 2015), and volcanic formations (Liccardi et al., 2007). Subsequently, two readvances occurred during the Late Glacial and the Early Holocene, associated with the Younger Dryas (YD; c. 12.9-11.7 cal. ka BP) and Early Preboreal (PB; c. 11.3-10.4 cal. ka BP) periods, respectively. The IIS is considered to have been mostly deglaciated at 8.7 cal. ka BP (e.g. Norðdahl and Pétursson, 2005; Norðdahl et al., 2008; Geirsdóttir et al., 2009; Larsen et al., 2012; Benediktsson et al. 2024a).

Modelling suggests that the IIS was up to 1500-2000 m thick with an elongated E-W orientated ice divide above the center of Iceland and radial ice discharge during the LGM (Norðdahl, 1991; Patton et al., 2017). Ice streams are thought to have regulated the IIS by discharging ice and sediment from the ice sheet interior towards the shelf edge. The location of ice streams within the IIS has been projected based on large-scale topography, streamlined subglacial bedforms, and glacial striae (Fig. 1.1; Bourgeois et al., 2000; Stokes and Clark, 2001; Norðdahl and Pétursson, 2005; Hubbard et al., 2006; Spagnolo and Clark, 2009; Clark and Spagnolo, 2016; Patton et al., 2017). Norðdahl (1991) depicted major ice streams in the main fjords of central north Iceland whereas Bourgeois et al. (2000) reconstructed flow patterns across the entire Iceland with topographic ice streams located in all major fjords, and ice divides over mountainous regions in between these fjords. Spagnolo and Clark (2009) concluded that major troughs and streamlined ridges on the Iceland shelf were imprints of palaeo-ice streams, and Clark and Spagnolo (2016) identified cross-cutting troughs indicative of multiple phases of shelf glaciation (Fig. 1.1). Principato et al. (2016) mapped and quantified the properties of SSBs in northwest Iceland, improving the understanding of the dynamics and extent of palaeo-ice streams in this region. Their study is the only one where the geomorphology of palaeo-ice streams in Iceland has been investigated in detail, besides master theses on the glacial geomorphology of the central north Iceland shelf (Höfer, 2019; OConnell, 2020), streamlined subglacial bedforms in Bárðardalur in north Iceland (McKenzie et al., 2017; Arnardóttir, 2022), and transverse ridges in northeast Iceland (Helgadóttir, 2020; Benjamínsdóttir, 2021).

2 Study area

The study area covers the northeastern part of Iceland and is focused on the three, major fjord-valley systems that dominate the coastal areas and extends back to associated uplands and plateaus towards the south or south-west. The area is divided into four separated subareas based on the mapping; (1) Þistilfjörður, a broad valley (~18-33 km) with low-lying plateaus; (2) Bakkaflói to the south-east, with subdued valleys and low-lying plateaus; (3) the Bakkaheiði plateau – a peninsula separating Bakkaflói and Vopnafjörður; (4) Vopnafjörður-Jökuldalsheiði, which is characterized by three narrow valleys (~1-6 km) reaching into the extensive highland plateau, Jökuldalsheiði (Figs 1.1 & 2.1). These fjord-valley systems are the result of repeated glaciations since the onset of the Quaternary (Benediktsson et al., 2022a). The bedrock in this region consists primarily of Miocene and Pliocene (>3.3-0.8 million years old) plateau basalts with intercalated sediment horizons. It mainly becomes progressively younger towards the west. In general, the basalts have a northward strike and are heavily intersected by N-S trending dykes, especially in the Bakkaheiði area (Sæmundsson, 1977; Jóhannesson and Sæmundsson, 2009). The study area is delineated to the west by an arcuate chain of Middle Pliocene (0.12-0.8 million years old) hyaloclastite ridges, Þríhyrnings- and Dimmifjallgarður, that stretch from the Vatnajökull ice cap in the south towards the northern coast and separate the area from the currently active northern volcanic rift zone (Hjartardóttir et al., 2010; Hjartarson and Sæmundsson, 2014). Hence, basal ice flow within the study area was not directly affected by volcanic activity and glacial landforms are not obscured by post-glacial lavas. To the south and southeast, the study area is delimited by the deep channel of the Jökulsá á Brú glacial river and the Smjörfjöll-Hellisheiði massif (Fig. 2.1).

2.1 Glacial history

Fast-flowing ice has been suggested in northeast Iceland with ice flow through the fjord-valley systems, Þistilfjörður, Bakkaflói, and Vopnafjörður, during the LGM (Bourgeois et al., 2000; Patton et al., 2017). The model by Patton et al. (2017) additionally suggests the flow-set draining from Jökuldalsheiði in the highlands through Vopnafjörður and onto the shelf, with support from mapping of bathymetric data in the offshore record (Spagnolo and Clark, 2009) (Fig. 1.1). Glacial landforms indicating former ice flow, such as glacial striations, are shown on geological and geomorphological maps (Sæmundsson, 1977; Norðdahl and Hjort, 1993; Sæmundsson, 1995). The striation pattern indicates an easterly flow from the highlands above Þistilfjörður towards a more northeasterly flow in the highlands above Vopnafjörður. The flow is generally towards the northeast in the coastal areas, parallel to the valleys. In Þistilfjörður and on the Bakkaheiði plateau the flow appears more towards the north (Fig. 1.1). Two sets of glacial striations were observed in several places, with the older ones orientated to the north and younger ones to the northeast. Main-ice divides during the Late Glacial were proposed on Þríhyrnings- and Dimmifjallgarður, Smjörfjöll-Hellisheiði massif and over Mt. Syðri- and Ytri-Hágöngur towards the center of Bakkaheiði. Earlier investigations within the study area have mainly focused on the deglaciation history of the IIS and shoreline displacement after the YD period, providing important constraints on the deglaciation in the area (Norðdahl and Hjort,

1993; Sæmundsson, 1995). Several ice-marginal positions were also inferred by Norðdahl and Hjort (1993) in Þistilfjörður and Bakkaflói and by Sæmundsson (1995) in the Vopnafjörður area. Although age constraints for these landforms are sparse, the ice-marginal positions are associated with glacier readvances during the YD or PB periods. Aðalsteinsson (1985, 1987) mapped a few moraines on Jökuldalsheiði that have been considered to be from the Early Holocene.

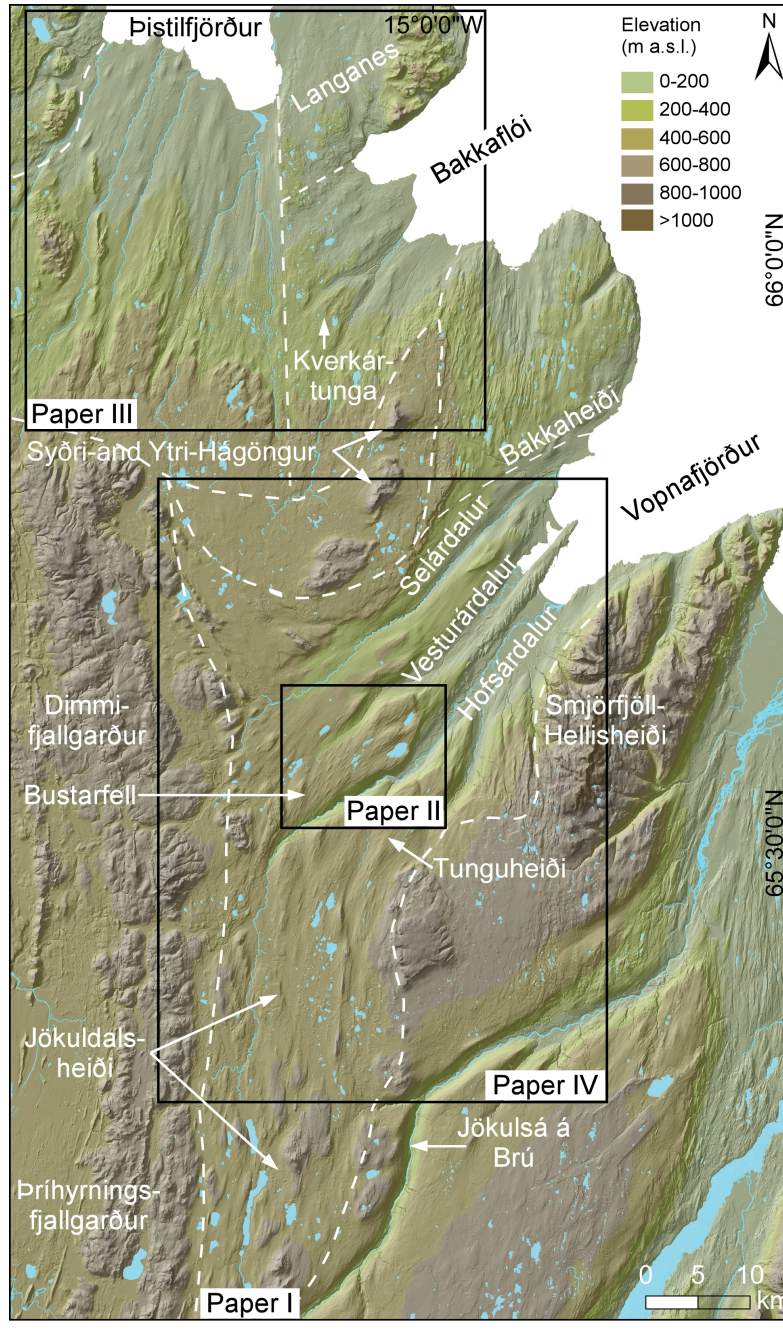

Figure 2.1 Overview map of the study area in northeast Iceland with the elevation distribution. The place names referred to in the thesis are marked together with outlines of the areas that are investigated in the papers. Paper I focuses on the whole study area within the white dashed lines, that furthermore mark the ice-stream flow-sets. Lakes and rivers are marked blue.

3 Methods

3.1 Geomorphological mapping

The resolution of digital elevation models (DEMs) and aerial images has improved greatly over the past decades and access to open data sets has increased (Chandler et al., 2018), allowing for more detailed mapping and analysis of glacial landforms. The principal data source used for mapping and analyzing the landforms for this thesis was the ArcticDEM with a 2 m vertical and <1 m horizontal resolution (Porter et al., 2018). The data has been corrected and mosaicked by the National Land Survey of Iceland (NLSI), the Icelandic Met Office, and the Polar Geospatial Center (Porter et al., 2018). Additionally, infrared Spot satellite images with 2.5 m resolution from NLSI and aerial images from Loftmyndir ehf., were used to facilitate the mapping (Fig. 3.1A-D). The mapping was verified by field checking selected areas within the study area (Fig. 3.2A, B). Geomorphological mapping of the landforms was undertaken following the guidelines of Chandler et al. (2018), by combining the interpretation of remotely sensed data and field data. Analysis of the data and mapping was conducted in ESRI ArcGIS 10.4-8 and finalized in Canvas X. The identification and mapping of the landforms were carried out at a scale of 1:1500-3000 based on the dimensions of the landforms and the scale of the map. All data were handled in the Lambert Conformal Conic reference system, and elevations are in meters above sea level.

Hillshaded relief models of the ArcticDEM were produced and used as a basis for the mapping. To avoid azimuth bias (Smith and Clark, 2005; Smith and Wise, 2007), the hillshades were illuminated from four different azimuths, 0°, 45°, 90°, and 315°, selected according to the orientation of the landforms, and one with the solar angle at 90° (i.e. overhead). The hillshades were vertically exaggerated by three to five with a solar angle of 25° to enhance subtle features (Fig. 3.1C, D, F). A slope map and contour lines (minimum of 2 m resolution) were generated from the ArcticDEM to help delineate the landforms (Fig. 3.1E, F). To minimize the influence of user bias, strict criteria were followed during the mapping (Smith and Clark, 2005; Hillier et al., 2015). For SSBs to be mapped, they had to show a clear orientation of elongation, be upstanding from the landscape in both axes and have a clear break of slope. Mapping was therefore carried out using a combination of the hillshades with different azimuths, infrared satellite and aerial images, slope maps, and contour lines. A polygon was drawn at the break of slope of each bedform (Fig. 3.1A-F). Although automated mapping techniques are increasingly being applied in glacial geomorphology, especially in areas with large numbers of similar features (>1000 to >10,000; Yu et al., 2015; Sookhan et al., 2016; Chandler et al., 2018), the landforms here were manually digitized due to the geospatial resolution and the relatively small number (<800).

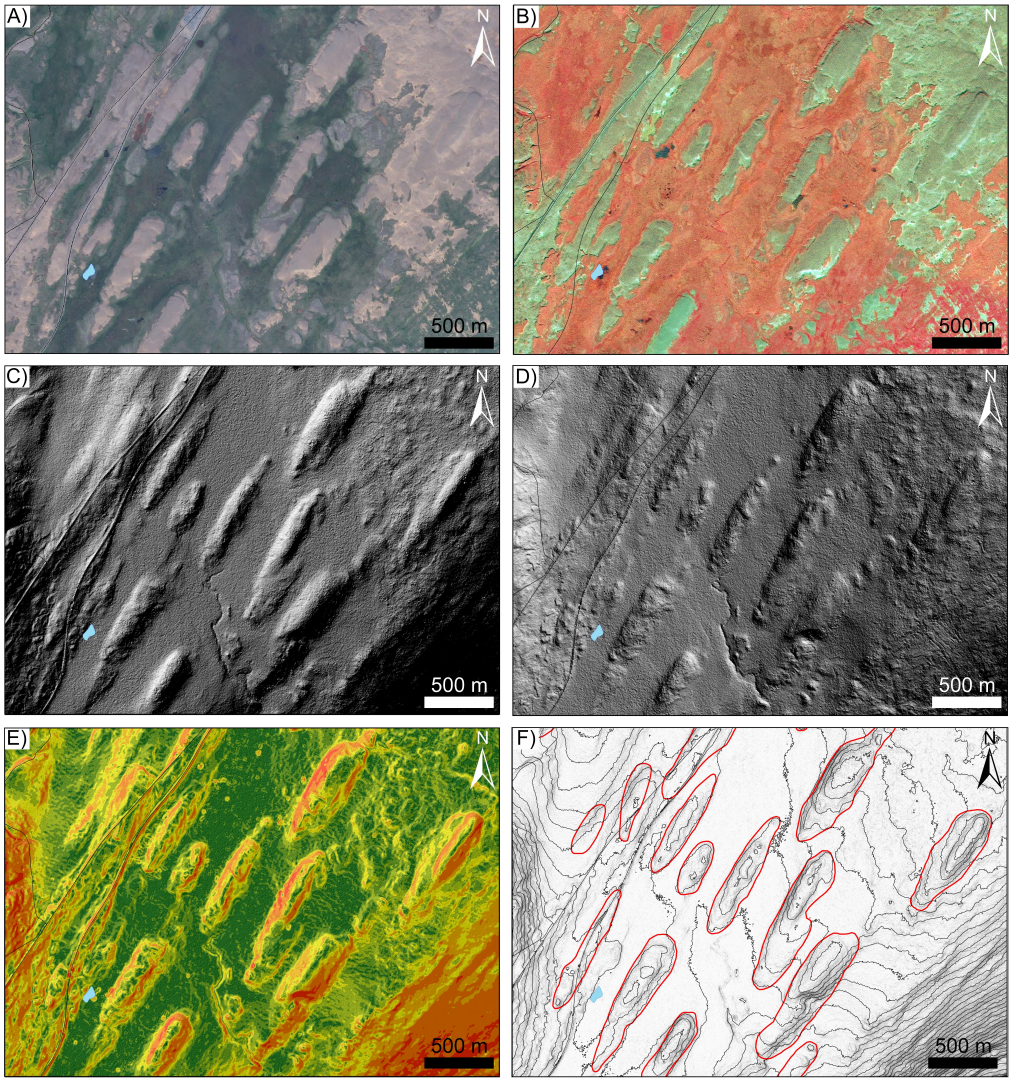

Figure 3.1 Examples of the different data used to map the landforms from the Bustarfell drumlin field within the Jökuldalsheiði-Vopnafjörður flow-set. A) Aerial image from Loftmyndir ehf. B) Infrared satellite image from the National Land Survey of Iceland. C) Hillshade generated from the 2 m ArcticDEM, illuminated from 315° with solar angle of 25° and vertical exaggeration by five. D) Hillshade generated from the 2 m ArcticDEM, illuminated from 45° with solar angle of 25° and vertical exaggeration by five. Figures C and D clearly demonstrate the importance of using different azimuths. E) Slope map generated from the ArcticDEM. The break of slope is often easier to distinguish using the slope map than the hillshades. F) Hillshade generated from the 2 m ArcticDEM, illuminated from 315° with solar angle of 90° (or directly above) and vertical exaggeration by five with 5-m contour lines generated from the ArcticDEM. The drumlins are mapped with a red polygon.



Figure 3.2 A) Field checking the ribbed moraines on Hauksstaðaheiði. B) Field checking segmented MSGL in eastern Þistilfjörður. C) Collection of a transverse GPR profile with a 100 MHz antenna on a drumlin in Bakkaflói. D) Preparing a section, dug with an excavator, in a drumlin on Bustarfell before analyzing it. E) A section dug with an excavator through a CSR in Þistilfjörður. F) Measuring clast fabric and collecting samples for grain-size analysis and clast morphology from the other section through a CSR in Þistilfjörður. Photos A, C, and D by Ívar Örn Benediktsson and E by Skafti Brynjólfsson.

Main emphasis was on mapping and investigating SSBs, ribbed moraines, and CSRs although glaciofluvial landforms, hummocky terrain, and ice-marginal landforms (i.e. moraines and channels) were included when applicable. Glacial landforms previously mapped in the area that were relevant to the study were digitized (Norðdahl and Hjort, 1993; Sæmundsson, 1995). The SSBs are classified into drumlins and MSGLs, with the latter having elongation ratios of >10:1 (Stokes and Clark, 1999). It is acknowledged that drumlins and MSGLs are part of a morphological continuum and that this strict boundary is arbitrary and up for debate (Spagnolo et al., 2014; Ely et al., 2016). Therefore, drumlins with elongation ratios <5:1 and 5-10:1 are separated for better visualization of the elongation ratio spectrum. If SSBs could not be delineated due to undiscernible break of slope but streamlining of the landscape was nonetheless clear, polylines were used to indicate the streamlining and mapped as glacial lineations. Despite the possibility that the streamlining of bedrock with negligible till cover may be the cumulative result of several ice sheet cycles (Hughes et al., 2010), we include streamlined bedrock in our mapping because of the difficulty in distinguishing separate glacial cycles in such areas. Further descriptions and classifications of the mapped landforms are listed in Table 1.

3.2 Morphological and spatial analysis

Morphological and spatial analysis of glacial landforms is essential for their interpretation as they are classified based on their size and shape and their distribution delimits past glacier flow. To investigate the morphology of the SSBs, CSRs, ribbed moraines, and transverse ridges, the length of the long axis, the width orthogonal to the long axis, and the orientation of the long axis were measured using the minimum bounding geometry tool in ArcGIS, as described by Napieralski and Nalepa (2010). The elongation ratio (ER) is found by dividing the length with the width. The data is illustrated with boxplots in Figure 3.3 and with histograms in the papers. The orientation of the landforms was compiled in rose diagrams. The prominence and symmetry of randomly chosen landforms were examined with the 3D profile tool in ArcGIS. Additionally, the spacing between the CSRs was measured using the average nearest neighbor tool in ArcToolbox (Paper III). To calculate the density of the landforms a point was created in the center of each bedform and the number of landforms within each 1 or 4 km^2 grid cell was calculated. The packing of the SSBs, i.e. the surface area of landforms per 4 km^2, was calculated with the Point Density tool in ArcToolbox with landform area as the population field (Paper II). The cell size was chosen considering both the dimensions of landforms and the map scale. In addition, qualitative descriptions of the mapped landforms are presented.

Table 3.1 Landforms that have been mapped within the thesis and description of how they are identified. Also listed are their dimensions, location, number of mapped landforms, and the paper(s) in which they are discussed.

Landform and papers	Characteristics	Dimensions and no. mapped	Location
Streamlined subglacial bedforms (SSBs) Paper I, II	Elongated hills, parallel to former ice flow. Asymmetric long profile. Often eroded by postglacial fluvial erosion. Define the four cross-cutting flow-sets.	Length: 101 – 3841 m Width: 36 – 942 m ER (:1): 1.9 – 16.8 797	All areas.
Glacial lineations Paper I	Streamlined terrain, parallel to former ice flow. The break of slope is not clear enough to be mapped as SSBs.	na 417	All areas.
Ribbed moraines Paper IV	Broad arcuate to rectangular ridges, transverse or oblique to former ice flow. Asymmetrical and symmetrical cross profile. Often eroded by postglacial fluvial erosion. Examples of them superimposed on SSBs.	Length: 28 – 539 m Width: 17 – 282 m ER (:1): 1.0 – 6.0 1190	Shallow basins on Hauksstaða-and Jökuldalsheiði and in eastern Þistilfjörður.
Crevasse-squeeze ridges (CSRs) Paper III	Reticular, interconnected ridges, transverse or oblique to former ice flow. Symmetrical cross profile. Examples superimposed on SSBs and are above the highest shoreline.	Length: 34 – 343 m Width: 19 – 52 m ER (:1): 1.2 – 2.8 403	Spatially restricted in Þistilfjörður and Bakkaflói.
Transverse ridges (Possibly CSRs) Paper IV	Interconnected ridges, generally transverse to former ice flow and with symmetrical cross profile.	Length: 20 – 78 m Width: 14 – 34 m ER (:1): 1.0 – 5.6 348	Selárdalur and surroundings.
Eskers Paper IV	Sinous to straight ridges composed of sorted sediments. Generally parallel to former ice low. Superimposed on ribbed moraines.	na	Jökuldalsheiði and few in Vopnafjörður, Bakkaflói and Þistilfjörður.
Moraines Paper IV	Ridges transverse to former ice flow. Asymmetric cross profile with a steeper proximal side. Often associated with ice-marginal channels and termination of eskers.	na	Jökuldalsheiði.
Ice-marginal channels Papers II, IV	Transverse channels. Often incised into SSBs and are interconnected. Can be associated with moraines.	na	All areas. Mainly on Bustarfell and Jökuldalsheiði.
Hummocky terrain Paper IV	Hummocky topography with unsorted to sorted sediments.	na	Selárdalur.
Raised shorelines Paper III	Terraces that are parallel to the modern coastline with washed surface.	na	Bakkaflói og Þistilfjörður.

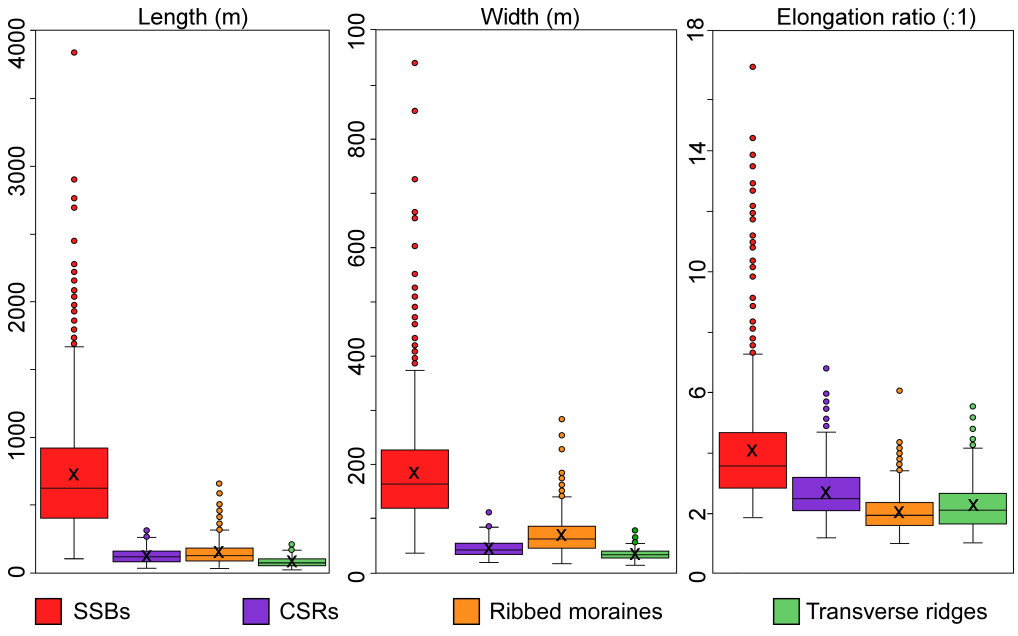

Figure 3.3 Size-frequency distribution of the morphometrics of the SSBs, CSRs, ribbed moraines, and transverse ridges presented with boxplots. The median and average of the datasets are denoted by the horizontal line and the 'x', respectively. Half (50%) of the values occur within the boxplots and the other half outside. The dots are outliers.

3.3 Sedimentology

The sedimentology and stratigraphy of the bedforms (SSBs, CSRs, and ribbed moraines) were investigated in five natural sections that were extended and cleaned by hand and six sections in pits that were dug with an excavator (Papers II-IV; Fig. 3.2D, F). Sediments exposed in the sections were documented at a scale of 1:20, using the data chart by Krüger and Kjær (1999) for glacial sediments, and the strike and dip of beds/structures were measured. The size of particles in sediment deposits contains information about the source of the material and the process of transportation, erosion, and deposition that have produced the material (Evans and Benn, 2004). Grain-size analyses of diamict units in the drumlin on Bustarfell and the CSRs in Bakkaflói and Þistilfjörður (Papers II and III) were carried out using standard sieving methods, starting by washing out materials finer than 0.063 mm (fines; clay and silt), followed by dry sieving to separate sand and gravel fractions. The sections and additional data were illustrated in Canvas X.

Clast fabric analysis is considered to reflect the behavior of the ice and is a quantitative tool to determine former ice flow directions and the depositional history of subglacial tills (Kjær and Krüger, 1998; Carr and Rose, 2003). Clast fabric measurements were collected from a 25x25 cm surface (if feasible), where the dip and dip direction were measured for at least 25 elongated clasts (a:b ratio >1.5:1) with an a-axis ranging in length from 0.6 to 6 cm (Kjær and Krüger, 1998). The measurements were then plotted and analyzed in the software Stereonet and the eigenvectors (V_1) and eigenvalues (S_1 and S_3) calculated. If the eigenvalue of the principal eigenvector was higher than 0.54, the clasts

were considered to show preferred orientation (Lawson, 1979). All compass measurements were corrected for the regional negative declination of 10° (in 2020).

Clast morphology is used to infer the process of transport and deposition and the amount of reworking (Lukas et al., 2013). To examine the clast morphology, fifty clasts, with an a-axis between 1.5 and 10 cm, were collected from 25x25 cm surfaces. The a (long)-, b (intermediate)- and c (short)-axes were measured and plotted in a ternary diagram (Evans and Benn, 2004). In addition, the roundness and texture of the clasts were estimated (Powers, 1953; Evans and Benn, 2004). The clast shape is presented as the C_{40} index (percentage of clasts with c:a axis ratio ≤0.4) and the clast roundness as the RA index (percentage of angular and very angular clasts) (Benn and Ballantyne, 1993). In addition, it was noted if the clasts contained striations, and were faceted or bullet-shaped (Evans and Benn, 2004).

3.4 Ground penetrating radar

Ground penetrating radar (GPR) can be a useful tool to examine the internal architecture of glacial landforms and to estimate the sediment thickness, especially where exposures are absent or few (Hubbard and Glasser, 2005). GPR profiles were acquired with a Malå Ramac/GPR CUII using both 50 and 100 MHz antennas, and antenna separation of 4 and 0.6 m, respectively. Surveys were made with a step size ranging from 0.02 to 0.5 m. Over fifty profiles on drumlins, ribbed moraines, and CSRs were acquired, transverse, longitudinal, and diagonal, across the targets (Fig. 3.2C). However, GPR was only presented in Paper II from the drumlins on Bustarfell. This is because the disturbances in the acquired data from the CSRs and ribbed moraines made the interpretations challenging. Thus, the data were not considered to significantly add to the overall interpretation of the internal architecture of the bedforms. Part of the profiles were collected along the sections to facilitate correlation between the GPR profiles and the sections. Data were processed with ReflexW 8.0 Sandmeier software, a GPR and seismic processing software, and topographic data from the ArcticDEM were used to rectify the profile elevation. The processing steps were done in this order (when deemed beneficial): *dewowing, move start time, energy decay, background removal, and elevation correction*. A velocity of 0.084 m/ns was used for depth conversion of the recorded two-way travel time based on common mid-point (CMP) measurements on a drumlin in Bakkaflói. This value is similar to other glacial sediments in Iceland (e.g. Kjær et al., 2004; Woodard et al., 2020) and to the tabulated range of 0.06-0.1 m/ns for saturated and damp sand (Jol and Bristow, 2003).

4 Results: Summary of papers

Here, the four papers (I-IV) are summarized while the full versions are presented in Appendices I-IV. Based on the mapping from all the papers a composite map of glacial landforms in northeastern Iceland is presented in this thesis (Fig. 4.1).

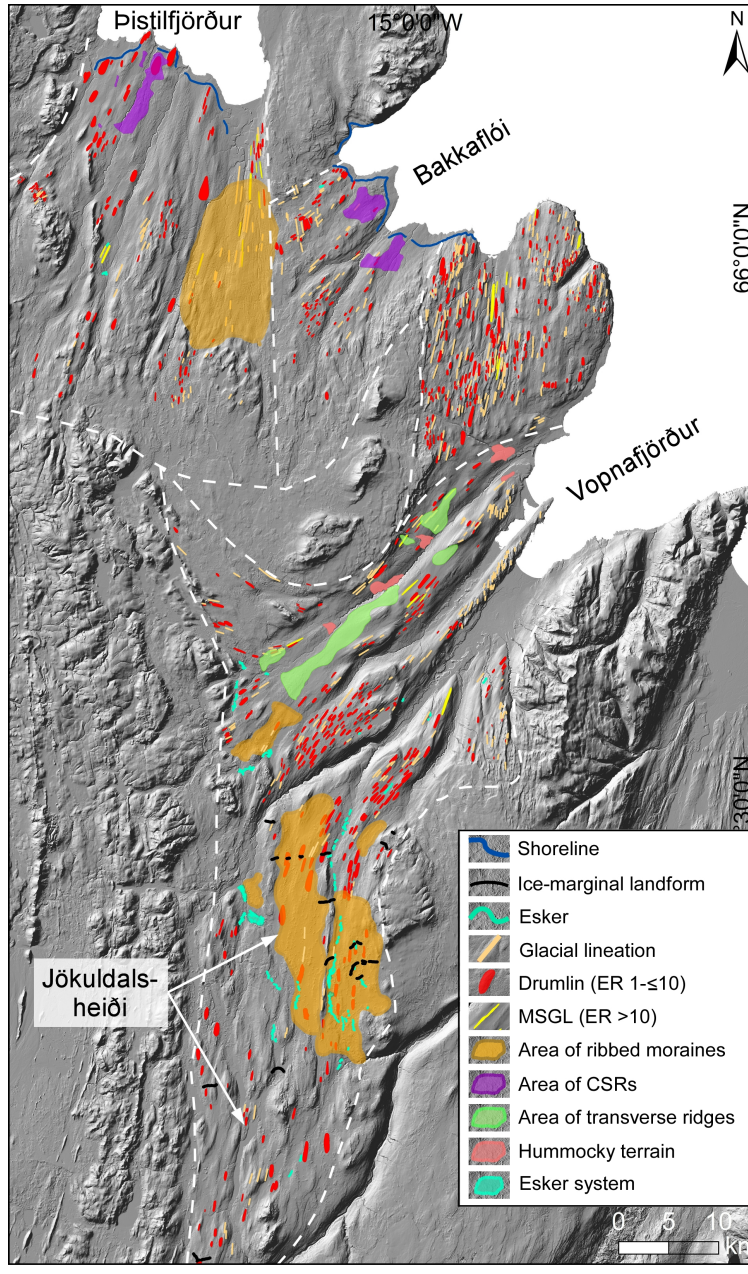

Figure 4.1 Composite map of glacial landforms in northeastern Iceland that are investigated in this thesis. Most of the landforms are based on mapping for Papers I-IV. The mapping of the shorelines in Þistilfjörður and Bakkaflói is based on Norðdahl and Hjort (1993). The outermost hummocky terrain in Vopnafjörður is based on Sæmundsson (1995). The two innermost ice-marginal landforms are from Aðalsteinsson (1985, 1987). MSGL = mega-scale glacial lineation, CSRs = crevasse-squeeze ridges. Not all ice-marginal channels are included on the map due to their resolution.

4.1 Paper I

Benediktsson, Í.Ö., Aradóttir, N., Ingólfsson., Ó., Brynjólfsson, S. 2022. *Cross-cutting palaeo-ice streams in NE-Iceland reveal shifting Icelandic Ice Sheet dynamics*. Geomorphology, 396, 108009. https://doi.org/10.1016/j.geomorph.2021.108009

- Mapping of SSBs (drumlins and MSGLs) reveals four flow-sets of palaeo-ice streams in northeast Iceland.
- Cross-cutting of the flow-sets reflects shifts in ice sheet dynamics and migration of ice divides.
- Ice streaming during maximum glaciation was towards the north from an E-W ice divide.
- During deglaciation the ice streams became topographically constrained from N-S and E-W ice divides.

In the first paper of this thesis, palaeo-ice streams in northeast Iceland are reconstructed by detailed mapping of SSBs and glacial lineations. The morphometrics, distribution, and orientation of the bedforms reveal flow-sets of four cross-cutting palaeo-ice streams together with migration of ice divides. The flow-sets are termed after their location; Þistilfjörður, Bakkaflói, Bakkaheiði, and Vopnafjörður-Jökuldalsheiði (Fig. 4.1). In total, ~800 SSBs and ~400 glacial lineations were mapped. Only 4% of the SSBs have an elongation ratio >10:1 and are classified as MSGLs. The morphometry of the SSBs is quite variable, which probably indicates diverse internal structure and maturity, as well as subglacial and glaciological processes responsible for their formation. The highest density and packing of the SSBs on the Bakkaheiði plateau, in the center of Vopnafjörður and the eastern margin of Þistilfjörður, might suggest the axial zones of the ice streams. This corresponds to the areas of SSBs with the highest elongation ratio. The SSBs are more common on the highland plateaus than in the valleys and mostly occur at altitudes between 250 and 650 m a.s.l. This is likely the result of non-erosive ice at higher elevations, near ice divides, and enhanced post-glacial erosion at lower elevations due to marine and fluvial processes.

North-trending SSBs on Jökuldalsheiði and Bakkaheiði plateaus and in Þistilfjörður suggest that during maximum glaciation and ice-sheet thickness, ice flow within the study area was largely unaffected by underlying topography allowing ice to flow northwards across valleys and fjords. This ice flow direction correlates with the orientation of previously identified troughs on the northeastern shelf. The pattern of ice flow suggests that an E-W orientated ice divide was located to the south of the study area, as has been previously proposed by modelling. During deglaciation and ice sheet thinning, a N-S orientated ice divide developed to the west of the study area. Palaeo-ice streams became confined to valleys and fjords resulting in younger flow-sets crosscutting the older ones (Fig. 4.2). The most visible evidence for this cross-cutting relationship can be seen at the

boundary between the Þistilfjörður and Bakkaflói flow-sets where younger SSBs overlay older bedforms as well as where the younger Vopnafjörður-Jökuldalsheiði flow-set cross-cuts the older Bakkaheiði flow-set close to the coast. The absolute ages of these flow-sets are uncertain, but the simplest interpretation is that the older ones pertain to the LGM and the younger sets relate to the following deglaciation. We also acknowledge that the variable dimensions of the SSBs might represent different generations of palaeo-ice streaming, while the well-developed drumlins fields are likely formed during the deglaciation.

The results of this study demonstrate the importance of glacial geomorphological mapping for the reconstruction of palaeo-ice streams and ice divides. Ultimately, finds improve our understanding of the evolution and shifts in ice dynamics of the IIS. Future efforts should strive to better constrain the chronology of the ice-stream retreat as well as to couple with an ice sheet model.

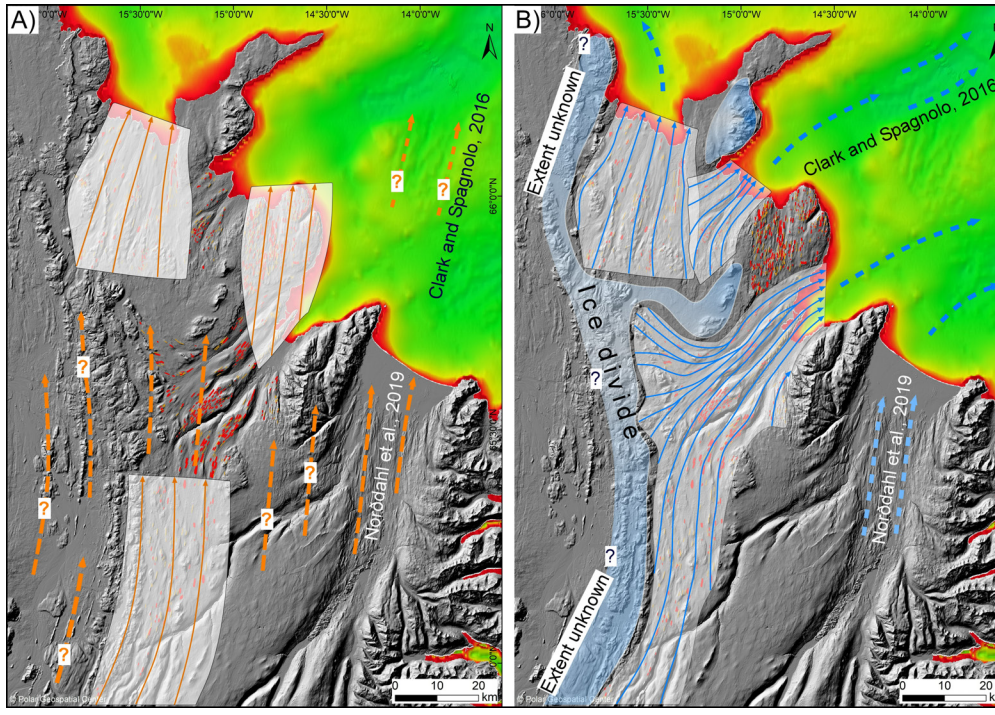

Figure 4.2 Hypothetical flow-sets of cross-cutting palaeo-ice streams in northeast Iceland. A) Northward trending flow-sets during a maximum phase of glaciation when ice flow was independent of the underlying topography. An E-W orientated ice divide was located above the present Vatnajökull ice cap (south of this map, see Fig. 1.1). B) Flow-sets related to deglaciation when the ice streams were topographically controlled. A N-S ice divide developed over the mountain range to the west of the study area and between Þistilfjörður and Vopnafjörður. Converging palaeo-ice stream flow characterized the areas of Jökuldalsheiði-Vopnafjörður, Bakkaflói, and Þistilfjörður. Ice flow during both phases corresponds to troughs on the shelf (indicated by dashed, orange, and blue arrows; described by Spagnolo and Clark, 2009). Note the cross-cutting of the older north-northeast trending trough (on A) by the younger northeast trending trough, as identified by Clark and Spagnolo (2016). Modified from Paper I.

4.2 Paper II

Aradóttir, N., Benediktsson, Í.Ö., Ingólfsson, Ó., Sturkell, E., Brynjólfsson, S., Farnsworth, W.R., Phillips, E. 2023. *Drumlin formation within the Bustarfell drumlin field, northeast Iceland: integrating sedimentological and GPR data*. Journal of Quaternary Science, 38 (3), 386-402. https://doi.org/10.1002/jqs.3481

- The unimodal shape and morphometry of the drumlins on Bustarfell suggest a similar formation process.
- The drumlins likely developed from erosional and depositional processes in addition to subglacial deformation, based on GPR and sedimentological data.
- Pre-existing glacial fluvial sediments form the core of the drumlins, which developed during readvance associated with the YD period.

The aim of this paper is to investigate the internal architecture of two drumlins in the Bustarfell drumlin field within the Vopnafjörður-Jökuldalsheiði flow-set to illuminate subglacial processes that contributed to drumlin formation. This was achieved by integrating sedimentological analysis and GPR (50 and 100 MHz). The investigated drumlin Thury is composed of two units of subglacial traction till, with interbedded glaciofluvial sediments. The volume of glaciofluvial sediments is greater at the stoss side than the lee side, suggesting a core of glaciofluvial outwash. The upper till and the glaciofluvial sediments are deformed. There is no evidence of a bedrock core in the investigated drumlins and the bedrock was estimated at ~10-12 m depth based on the GPR data. The core of glaciofluvial sediments suggests that the drumlin formed around well-drained patches (sticky spots) in the glacial bed that hindered local ice flow through increased basal drag and encouraged till deposition. Furthermore, GPR data from the drumlins indicate a combination of erosional and depositional processes. The unimodal shape, high spatial density, and similar morphometry of the drumlins within the Bustarfell drumlin field suggest a similar formation process.

Based on the correlation of the drumlin formation with the glacial history in northeast Iceland, the northward fabric in the lower till suggests that it was deposited during the maximum glaciation when ice flow was towards the north. As the ice margin retreated over the Bustarfell plateau during the Bølling-Allerød interstadial, glaciofluvial sediments were deposited in a proglacial setting. Small ice-marginal fans are considered to have formed from minor meltwater outlets on the Bustarfell plateau while the main volume of meltwater flowed down into the valleys on either side. The drumlins likely formed around these fans during a subsequent readvance associated with the YD period. During the Early Holocene deglaciation, the drumlins were exposed and transverse ice-marginal channels incised through the drumlin surface during a stepwise retreat of a passive terminus (Fig. 4.3). The GPR data show that the inter-drumlin areas are composed of up to ~8 m thick post-glacial sediments, reducing the apparent drumlin relief.

The sedimentological and GPR data are complimentary, although the deformation and lack of trace layers made the interpretation of the GPR profiles challenging. Integrating GPR data with sedimentological data in glacial environments in Iceland can be useful to investigate the internal architecture of glacial landforms and learn about processes operating at the beds of advancing glaciers and ice sheets.

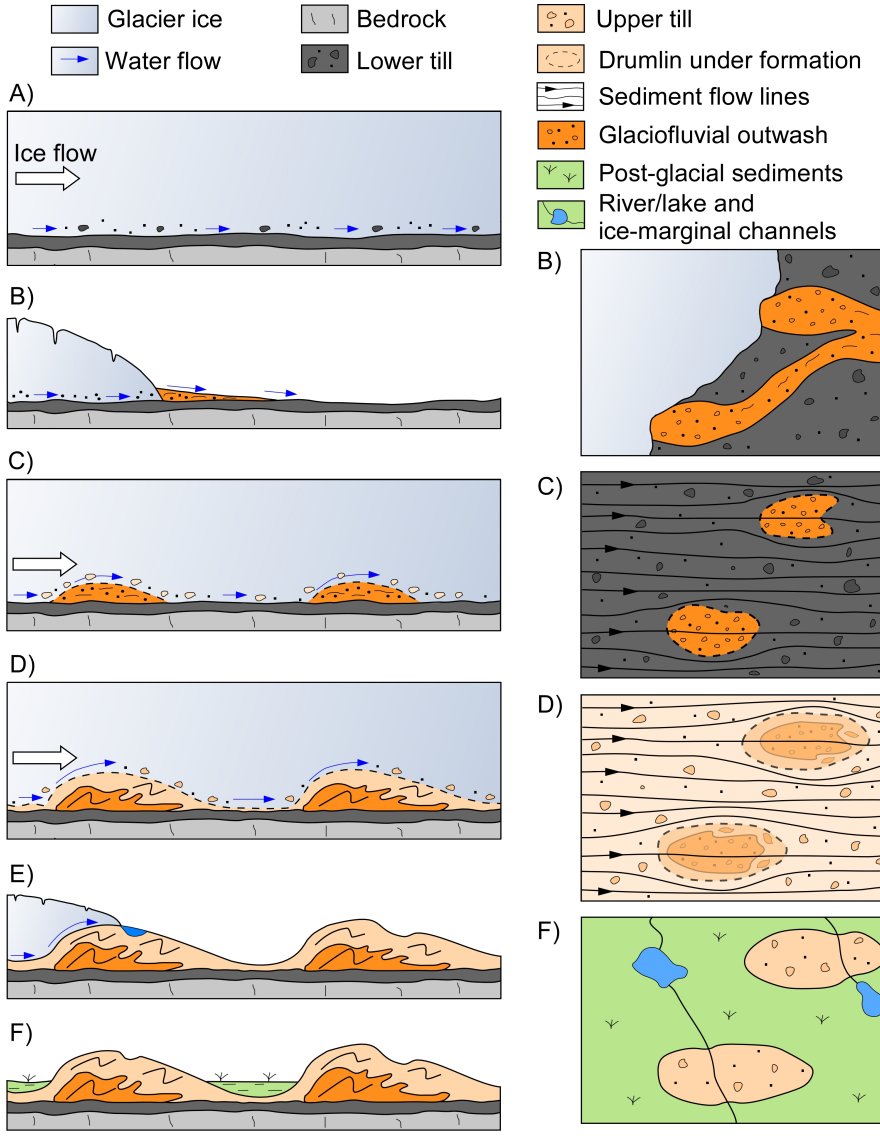

Figure 4.3 A conceptual model of the formation of the investigated drumlins from Paper II. A) Maximum glaciation. Deposition of subglacial traction till. B) Deglaciation. Ice-marginal outwash fans are deposited. C) Glacier readvance. The glaciofluvial material acts as sticky spots and initiates the drumlin formation. D) Drumlin formation. Deformation of the glaciofluvial core and draping of subglacial traction around it, followed by drumlinisation of the landscape. E) Deglaciation. The ice retreat is stepwise and ice-marginal channels are formed. F) Post-glacial sediments are deposited in the inter-drumlin areas. The scale is non-proportional. Modified from Paper II.

4.3 Paper III

Aradóttir, N., Benediktsson, Í.Ö., Ingólfsson, Ó., Brynjólfsson, S., Farnsworth, W.R., Benjamínsdóttir, M.M., Ríkharðsdóttir, L.B. 2023. *Ice-stream shutdown during deglaciation: Evidence from crevasse-squeeze ridges of the Iceland Ice Sheet*. Earth Surface Processes and Landforms, 48 (12), 2412-2430. https://doi.org/10.1002/esp.5636

- CSRs are described outside modern glaciers for the first time in Iceland, within the Bakkaflói and Þistilfjörður flow-sets.
- The landsystem in Bakkaflói and Þistilfjörður represents once active ice streams as well as ice-stream shutdown, summarized in a conceptual landsystem model.
- Reticular CSRs are formed near the marginal zone under various stress directions while linear CSRs are formed further upstream where longitudinal stress dominates.

The aim of this paper is to increase contemporary understanding of the dynamics of the IIS during deglaciation in northeast Iceland by investigating geometrical ridges (linear and reticular) within the Bakkaflói and Þistilfjörður flow-sets. The ridges were mapped in detail highlighting their cross-cutting relationship to other landforms in the area. The morphological data was combined with sedimentological analyses from the ridges. The ridges are interpreted as CSRs, based on their interconnected network, primary orientation transverse and/or oblique to former ice flow, and internal composition of homogenous subglacial till. CSRs are common in front of modern Icelandic glaciers but have not previously been described from the palaeo-record. In addition to the CSRs, the landsystem consists of SSBs, ice-marginal landforms, raised shorelines, and relict meltwater channels (Fig. 4.4). In both areas, the CSRs are superimposed on the SSBs, indicating that they post-date the SSBs and signify the waning stage of ice streaming. The overall landform assemblage in Bakkaflói and Þistilfjörður is interpreted to represent once active ice streams within the IIS during the LGM and the following ice-stream shutdown, during deglaciation.

Despite minimal chronological constraints in the area, we surmise that the CSRs were formed during the later stage of ice streaming at the end of the YD. It is unlikely that the CSRs would remain preserved if they formed earlier given the suggested YD age of the ice-marginal features by the present coast. The ice-marginal landforms just up-ice from the CSR areas are suggested to have formed during a PB readvance. While this advance may have overridden other CSRs further up-ice, it did not affect the CSR networks investigated in this study (Fig. 4.5). The preservation of the CSRs suggests downwasting following the readvance. The morphological difference of the CSRs between the flow-sets may relate to different kinematic settings within the ice streams; the linear CSRs in Bakkaflói formed further upstream where extensional forces parallel to ice flow were dominant, whereas the reticular CSRs in Þistilfjörður are more indicative of transverse and longitudinal forces near the terminal zone. The ice margin in Bakkaflói might therefore have extended further out into the marine environment at the time of formation of the linear CSRs (Fig. 4.5). High-resolution bathymetric data from the adjoining shelf, as well as an enhanced geochronological constraint in the area, are however necessary for further reconstructing past ice-sheet behaviour and ice-stream dynamics in the area. The paper provides palaeo-analogs to modern ice streams and surging lobe shutdown. Furthermore, findings enhance the knowledge of both modern and palaeo-ice sheet behavior during deglaciation under climate warming.

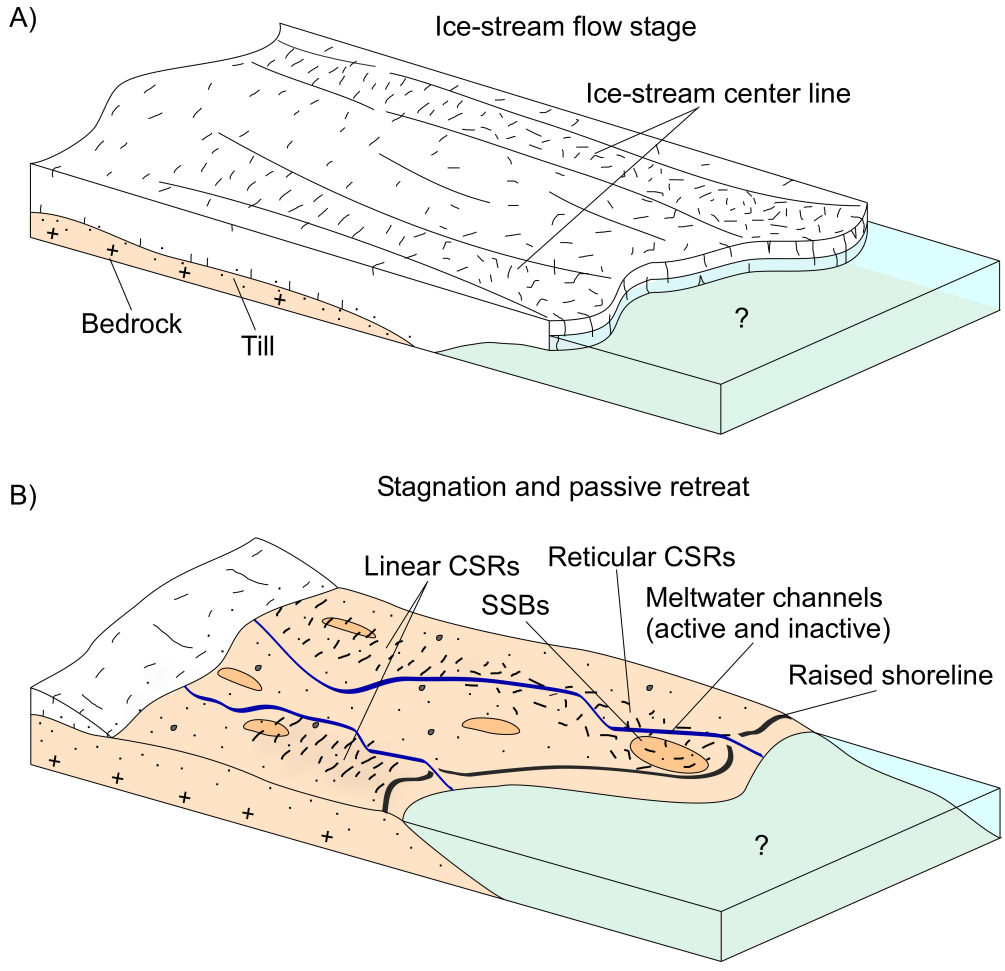

Figure 4.4 Conceptual landsystem model illustrating landforms associated with ice-stream shutdown in terrestrial environment based on observations from Bakkaflói and Þistilfjörður, northeast Iceland in Paper III. A) Flow stage of a terrestrial ice stream that extends into the marine environment. Corridors of relatively faster flow within the ice stream generate mainly transverse crevasses in the trunk flow zone due to dominating longitudinal tensile stresses while a combination of longitudinal and lateral stresses near the calving marginal zone generate crevasses with variable orientations. B) The ice-stream shutdown is followed by downwasting and passive retreat, allowing the preservation of CSRs in the terrestrial environment. Their distribution and orientation in the post-glacial landscape reflect the glacial stress regimes around the time of ice-stream shutdown. The question marks indicate that the landsystem in the marine environment is unknown as bathymetric data is lacking. Modified from Paper III.

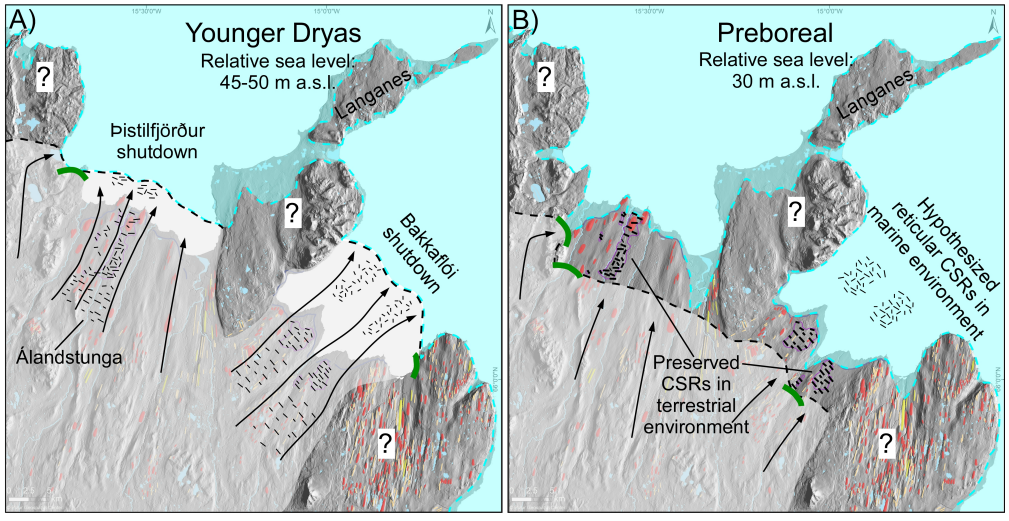

Figure 4.5 Time slices highlighting the glacial history and possible ice-stream configuration and dynamics in Bakkaflói and Þistilfjörður during the A) YD and B) PB readvances. The ice-marginal positions from Norðdahl and Hjort (1993) are marked with green and dashed line drawn between them to indicate the possible extent of the ice-margin. As Paper III only focuses on the glacial reconstruction within the study area, the areas outside are marked with question marks to indicate unknown ice extent. Modified from Paper III.

4.4 Paper IV

Aradóttir, N., Benediktsson, Í.Ö., Helgadóttir, E.G., Ingólfsson, Ó., Brynjólfsson, S., Farnsworth, W.R. *Ribbed moraines formed during deglaciation of the Iceland Ice Sheet: Implications for ice-stream dynamics*. Submitted to Boreas special issue.

- Ribbed moraines are described within Vopnafjörður-Jökuldalsheiði flow-set and for the first time in Iceland.
- The ribbed moraines are considered to form at the shear margin of a decaying ice stream resulting from velocity differences within it.
- A conceptual landsystem model highlights the spatial distribution of the landforms related to the dynamics of the ice stream during the deglaciation.

Paper IV describes ribbed moraines for the first time in Iceland and focuses on the deglaciation dynamics in the northeastern sector of the IIS. The ribbed moraines occur in shallow basins on the Hauksstaðaheiði and Jökuldalsheiði highland plateaus within the Vopnafjörður-Jökuldalsheiði flow-set. Additionally, other transverse ridges in Selárdalur and glaciofluvial deposits and ice-marginal landforms are mapped. Morphological data is combined with sedimentological analyses of the ribbed moraines to increase our understanding of their formation and implications for the dynamics of the IIS during deglaciation. The ribbed moraines generally have a broad arcuate or rectangular shape but examples of anastomosing and hummocky ridges also occur. Cross profiles are both symmetrical and asymmetrical and long-axis orientation is usually transverse or oblique to the former ice-flow. The ribbed moraines are composed of pre-existing material, a base of stratified glaciofluvial sediments draped with subglacial till. Both sedimentological units dip outward from the ridge crest and exhibit deformation/thrust structures. We interpret these characteristics as the result of compressional flow during ridge formation. In contrast, the ridges in Selárdalur are more linear, exhibiting similarity to CSRs. However, further studies are required to determine their origin. On Jökuldalsheiði, prominent transverse ridges, sometimes found in connection with inactive channels and eskers, are interpreted as ice-marginal moraines.

The formation of ribbed moraines is still debated and they have both been associated with the onsets and shutdown of ice-streaming. As the ribbed moraines in northeast Iceland superimpose SSBs and do not show any sign of being overridden, they probably signify the waning stage of ice streaming. Ribbed moraines are often considered to form at the transition zone between fast and slow ice flow. Our results agree and we suggest that the ridges formed under the lateral shear margin of an ice stream based on their distribution and often oblique orientation in relation to SSBs. Correlating the formation of the ribbed moraines with the known glacial history in this region we suppose that the ridges formed during ice-stream shutdown following the YD readvance. Eskers superimposed on ribbed moraines indicate channelized water drainage during the deglaciation and location within meltwater corridor. The eskers frequently terminate at ice-marginal positions on Jökuldalsheiði, implying stillstands or small readvances during the deglaciation. A conceptual landsystem model is presented based on the results that highlight the spatial distribution of the landforms related to the dynamics of the ice stream during the deglaciation (Fig. 4.6). This study has implications for the deglaciation behavior of ice streaming in the northeastern part of the IIS and sheds light on the role of ribbed moraines within the ice sheet for future work in Iceland.

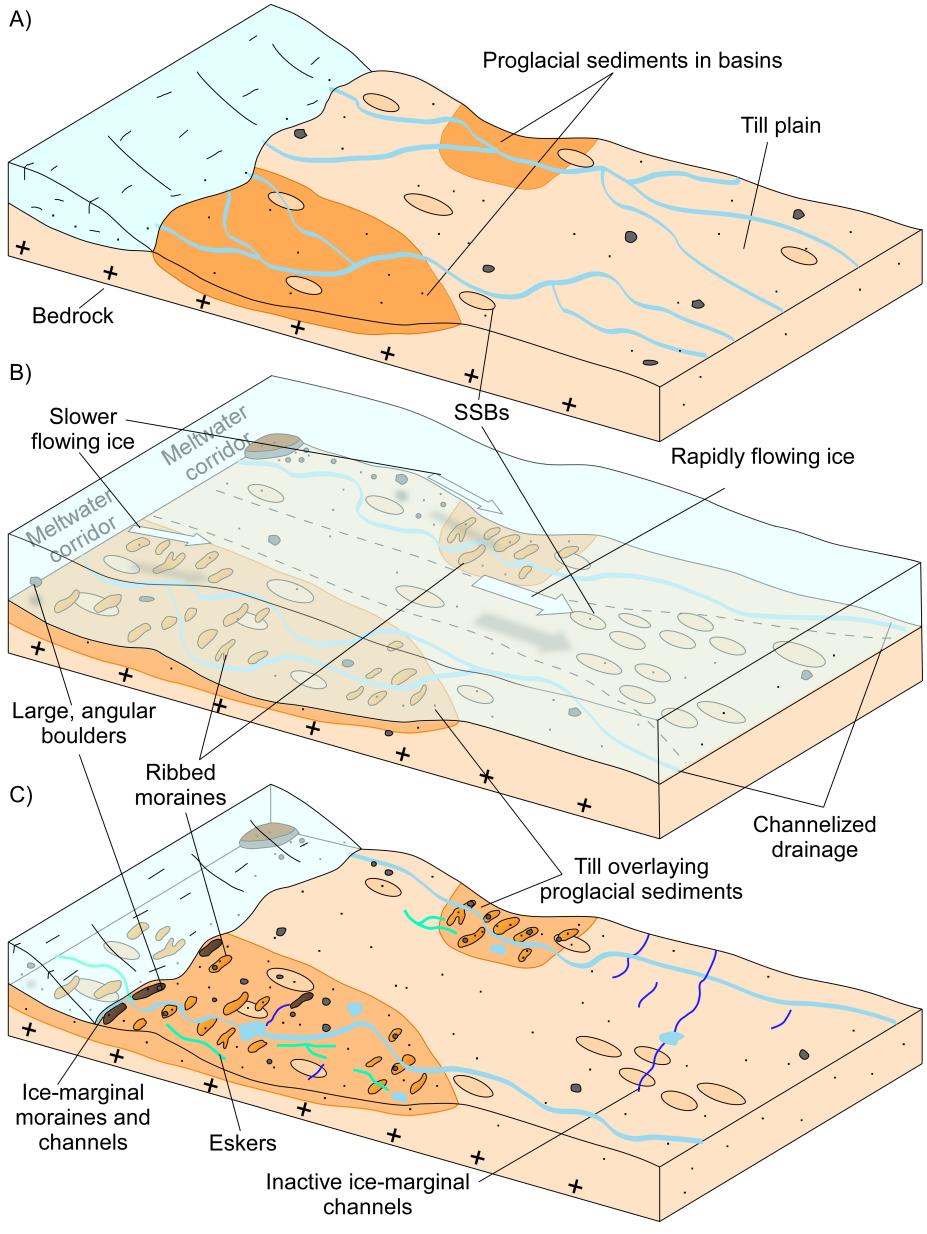

Figure 4.6 Conceptual landsystem model illustrating ribbed moraines formed within the Vopnafjörður-Jökuldalsheiði flow-set from Paper IV. A) Deglaciation. SSBs that formed during the last ice advance are exposed and glaciofluvial sediment is deposited, especially in basins. B) Ice stagnation following glacier readvance. Formation of SSBs continued within the ice-stream trunk during the readvance. Ribbed moraines are formed at the lateral shear margin of the ice stream due to changes in basal processes from the velocity difference within the ice. Eskers indicate that the drainage changes from distributed to channelized during deglaciation. Large and angular boulders are transported englacially from local bedrock outcrops. C) Deglaciation. Ice-marginal landforms indicate a stepwise retreat.

5 Discussion

5.1 Reconstruction of palaeo-ice streams

The glacial landsystem in northeast Iceland consists of SSBs, CSRs, ribbed moraines, eskers, hummocky terrain, ice-marginal landforms (moraines and channels), and postglacial raised marine shorelines. The configuration of cross-cutting flow-sets of palaeo-ice streams is reconstructed based on detailed mapping of the landforms, especially the SSBs (Fig. 4.1 & 4.2). A conceptual model is presented of the terrestrial assemblages of landforms that are characteristic of the palaeo-ice stream beds. The landforms in the model reflect variable periods of ice streaming from maximum glaciation to deglaciation when the palaeo-ice streams became constrained by the topography during ice sheet thinning and retreat. The final ice streaming terminated with a shutdown followed by downwasting, punctuated by short lived readvances or stillstands in some areas (Fig. 5.1A). A conceptual stratigraphical log is presented with the landsystem model to highlight the field observations of the internal architecture of the SSBs, CSRs, and ribbed moraines as well as the morphology. Two subglacial till units are observed in the SSBs, CSRs, and ribbed moraines, that are interbedded with deformed glaciofluvial sediments in the SSBs and ribbed moraines. The lower till is homogenous, and the measured clast fabric is towards the north. The upper till is more varied, generally showing signs of deformation and measured clast fabrics towards the northeast. Bedrock was observed at the base in some of the sections in the SSBs and ribbed moraines (Fig. 5.1B). In general, the sediment cover outside the landforms is thin with frequent outcrops of glacially sculptured bedrock. The relative timeline for the formation of the landforms is illustrated on Figure 5.2 and summarizes the conditions under which they are formed.

The reconstruction of palaeo-ice streams in this thesis correlates well with the offshore record, with troughs incised in a north-northeast and northeast direction, appearing as an extension of the onshore valleys. The troughs extend to the shelf edge and the streamlined sea floor outside Bakkaflói and Vopnafjörður coincides with the orientation of the troughs (Spagnolo and Clark, 2009; Clark and Spagnolo, 2016; Patton et al., 2017). Overlapping troughs at different depths, a shallower north-northeast trending one cross-cut by a deeper trough orientated towards the northeast, was observed by Clark and Spagnolo (2016). This cross-cutting was interpreted to represent different ice-flow directions (Figs 1.1 & 4.2) and is supported by the onshore evidence presented in Paper I proposing different palaeo-ice stream flow directions and migration of ice divides. During maximum glaciation, ice flow is suggested towards the north with negligible influence by the underlying topography. Upon ice thinning during deglaciation, ice-stream flow directions became progressively more controlled by the underlying topography (Figs 4.2 & 5.2). Modelling experiments suggested areas with faster-flowing ice extending out onto the shelf during the LGM and the subsequent deglaciation, especially in the Vopnafjörður area. However, the models do not assume northward flow during the maximum glaciation, such as ice-streaming over the Bakkaheiði plateau, as the northward trending SSBs do suggest (Bourgeois et al., 2000; Hubbard et al., 2006; Patton et al., 2017). This highlights the importance of geomorphological data for better constraining the modelling of palaeo-ice streams in Iceland and the dynamics of the IIS.

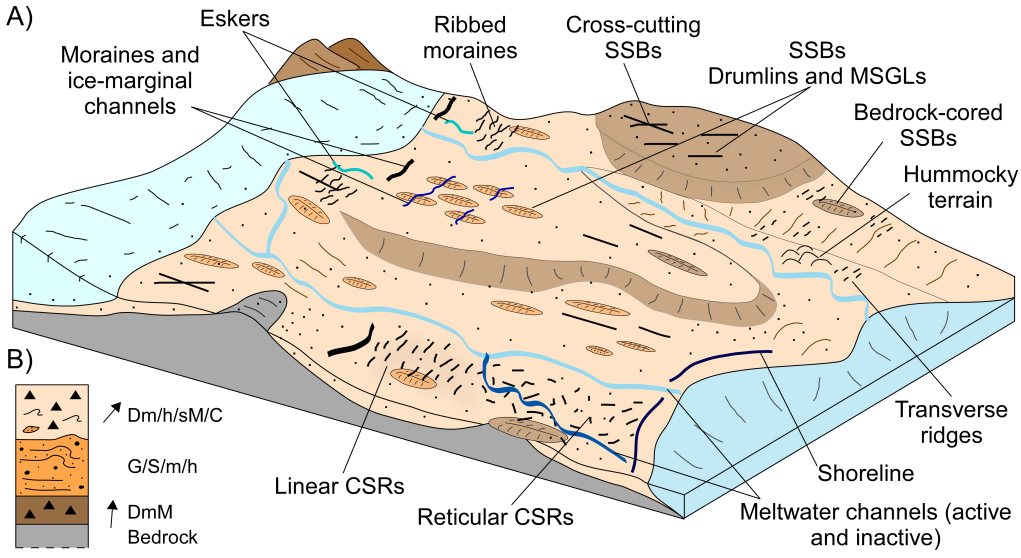

Figure 5.1 A) *Conceptual landsystem model of terrestrial palaeo-ice streams based on observations from the Vopnafjörður-Jökuldalsheiði, Bakkaheiði, Bakkaflói and Þistilfjörður flow-sets in northeast Iceland. The SSBs form during active ice streaming and their cross-cutting and distribution indicates that the ice flow became constrained by the topography during ice sheet thinning. Their variable size and shape represent different maturity and ice flow duration. During ice-stream shutdown, ribbed moraines form under the lateral shear margins of the ice streams and CSRs near the ice margin. Their preservation indicates downwasting but moraines and ice-marginal channels suggest that the retreat was punctuated by short lived readvances or stillstands. Eskers superimposing SSBs and ribbed moraines indicate that the drainage was channelized during the final deglaciation. B) Conceptual composite log of the stratigraphy in northeast Iceland based on the sedimentological work from SSBs, CSRs, and ribbed moraines, combined with the morphological observations. The arrows represent the general clast fabric orientation and the lithofacies code the general sediments facies (D=diamict, m=massive, h=heterogenous, s=stratified, M=medium-grained, C=coarse-grained, G=gravel, S=sand, m=massive, h=horizontal).*

Our results align with modelled ice divides and their migration, i.e. an E-W orientated central ice divide over the present Vatnajökull during maximum glaciation with northward flowing ice streams (Bourgeois et al., 2000; Patton et al., 2017). During deglaciation and ice sheet thinning, a N-S orientated ice divide formed over the Þríhyrningsfjallgarður-Dimmifjallgarður mountain range, and the ice streams became more topographically constrained. Previous reconstructions have suggested an ice divide in the area during the LGM (Bourgeois et al., 2000) or the following deglaciation (Norðdahl and Hjort, 1993). Local ice divides would also have formed over the Smjörfjöll-Hellisheiði massif and then progressively in elevated terrain between the different flow-sets, such as between Þistilfjörður and Bakkaflói as well as Þistilfjörður and Vopnafjörður, as the ice sheet continued to thin (Fig. 4.2). The proposed ice divides imply that the onset zone of the ice streaming during maximum glaciation may have originated near the present Vatnajökull ice cap but they might have shifted during the deglaciation as ice divides

migrated. No evidence of the ice stream onset zones was observed but they are rarely preserved because of reshaping during the continued glaciation and the following deglaciation (De Angelis and Kleman, 2008).

In the onshore record, previous studies of the geomorphology of palaeo-ice streams have focused on SSBs and streamlined terrain (Principato et al., 2016; Norðdahl et al., 2019; Arnardóttir, 2022). The ribbed moraines in northeast Iceland are the first to be described in Iceland and although CSRs have previously been described in front of modern surge-type glaciers (e.g. Ingólfsson et al., 2016 and references therein), this is the first description of them in the Icelandic palaeo-record. The resolution of aerial images and DEMs has improved significantly over the past years making it possible to identify landforms that might have been overlooked in previous studies, especially with the release of the ArcticDEM. The reconstruction from this study and the conceptual landsystem model of palaeo-ice streams in northeast Iceland provide an analogue for other palaeo-ice streams within the IIS.

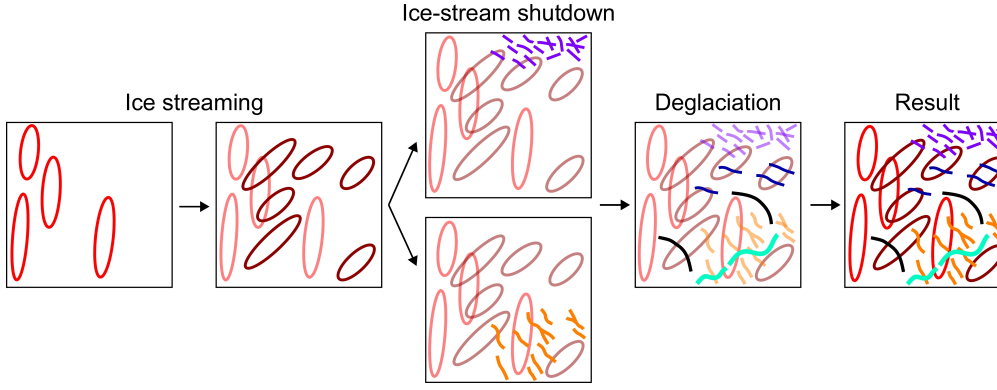

Figure 5.2 Schematic diagram of the relative timing of the landforms comprising the palaeo-ice stream landsystem in northeast Iceland. SSBs are formed during active ice streaming, younger (dark red) cross-cut the older (red). CSRs (purple) and ribbed moraines (orange) are superimposed on the SSBs and indicate ice-stream shutdown. During the deglaciation, eskers (turquoise) are formed time transgressively and ice-marginal channels (dark blue) and moraines (black) indicate stepwise retreat.

5.2 Implications for ice dynamics

Findings from this project add to the limited studies of the geomorphological record of palaeo-ice streams in Iceland. The results enhance our understanding and strengthen our reconstruction of the dynamics of the IIS. Comparison between the mapped landforms and the reconstruction of the palaeo-ice streams in this thesis with previous studies is restricted because of significant difference in resolution. The average elongation ratio of the SSBs in northeast Iceland is 4.0:1 and only 4% of the SSBs were classified as MSGLs. However, SSBs adjacent to the mapped MSGLs often have a rather high elongation ratio (>5:1). The average is lower than the SSBs analyzed in the Bárðardalur valley in northern Iceland by Arnardóttir (2022) (average elongation ratio = 8.9:1 and 30% = MSGLs) and in northwestern Iceland by Principato et al. (2016), (average elongation ratio = 6.4:1 and 14% = MSGLs). Smaller SSBs with lower elongation ratios might, however, be unidentified in northwestern Iceland due to lower resolution of remote sensing data than used in this

thesis. This difference may suggest that the ice streams in northwest and north Iceland experienced faster flow or persisted for a longer time (Stokes et al., 2013a; Ely et al., 2016; Sookhan et al., 2021, 2022). This is supported by deeper and wider troughs identified in the offshore record in northern Iceland (Spagnolo and Clark, 2009; Clark and Spagnolo, 2016; Höfer, 2019) and by modelling experiments proposing larger ice streams in the north and northwest Iceland (Bourgeois et al., 2000; Hubbard et al., 2006; Patton et al., 2017). The results from Principato et al. (2016) also suggest that the three flow-sets of palaeo-ice streams in northwest Iceland merged on the shelf to feed a larger ice stream, while the offshore record from northeast Iceland implies that they drained through separate troughs (Clark and Spagnolo, 2016). As detailed mapping of the northeast Iceland shelf has not been conducted, a meaningful comparison between these records is limited. Other factors affecting the elongation ratio of the SSBs should also be considered, such as the variation in the substratum (i.e. lithology, sedimentology, and topography) at a local scale (e.g. Greenwood and Clark, 2009; Sookhan et al., 2021). However, ice velocity and glaciological processes are generally considered to be the main controls on the morphology of subglacial bedforms (Ely et al., 2016). The variations in geothermal heat flux also need to be accounted for when comparing the behaviour of ice streams in different areas as enhanced heat flow, concurrent with the volcanically active zone, influences ice streaming (Bourgeois et al., 1998, 2000). This could explain the apparent high ice velocities in the Bárðardalur ice stream, which is located on the flank of the northern volcanic zone.

The areas with the highest density and packing of the SSBs roughly coincide with the areas with the highest elongation ratio, suggesting the axial zones of ice streaming. These areas are usually in the center of the valley-fjord systems (Principato et al., 2016), except in Þistilfjörður where it is located at the eastern margin of the valley. Although the density of the SSBs is not very high, the highest concentration of MSGLs and elongated drumlins (>5:1) occurs there. The CSRs in Þistilfjörður are, however, located further west in the valley, surrounded by a small cluster of large bedrock-cored SSBs with a rather low elongation ratio (<5:1). The ice streaming in Þistilfjörður is therefore suggested to have migrated over time, as also supported by the variation in morphology of the SSBs within the flow-set. The SSBs with a high elongation ratio at the eastern margin suggest that the active streaming was concentrated there but shifted towards the western side during the ice-stream shutdown when the CSRs were formed. The two clusters of SSBs in Bakkaflói, with areas of CSRs either down-ice or to their side, might suggest two centers of ice streaming within this flow-set (Fig. 4.5).

The ribbed moraines within the Vopnafjörður-Jökuldalsheiði flow-set and the CSRs within the Þistilfjörður and Bakkaflói flow-sets are considered to indicate the shutdown of ice streaming (e.g. Stokes et al., 2008; Evans et al., 2016). Due to the varying processes and locations in which the bedforms are formed, these bedforms are a clear indicator of diverse ice dynamics. The ribbed moraines are suggested to be formed due to dynamic instabilities and velocity changes (Raunholm et al., 2003; Finlayson and Bradwell, 2008; Stokes et al., 2008) under the lateral shear margins, marking the lateral boundary of the ice stream during the time of their formation (e.g. Vérité et al., 2021). The CSRs are depositional bedforms that are formed further down ice or close to the ice margin (e.g. Evans and Rea, 2003). The difference in the morphology of the bedforms between the areas can further be used to infer how ice dynamics and stress regimes vary within the ice streams. The linear CSRs in Bakkaflói are considered to have formed further upstream where extensional forces parallel to ice flow dominated, whereas the reticular CSRs in Þistilfjörður are more indicative of transverse and longitudinal forces near the terminal zone (Evans et al., 2016; Kurjanski et al., 2019).

Another explanation for the presence of CSRs could be surging behaviour during deglaciation, as has been suggested elsewhere (e.g. Ingólfsson et al., 2016; Farnsworth et al., 2016; Delaney et al., 2018; Benn, 2021). However, this could not be concluded as no evidence for cyclic readvances was observed but high-resolution bathymetric data might reveal different aspects of this matter. Dynamic instabilities during the deglaciation of the IIS have been implied before based on oscillating ice margins in west Iceland during the Early YD period (Sigfúsdóttir and Benediktsson, 2020) but not with emphasis on subglacial bedforms or ice-stream shutdown. The descriptions of CSRs and ribbed moraines in northeast Iceland therefore have important implications for the dynamic deglaciation history of the IIS.

5.3 Glacial history

Incomplete geomorphological and chronological records from northeast Iceland have hampered reliable reconstructions on palaeo-ice streams and ice sheet extent (Benediktsson et al. 2022a). Fundamental studies, such as geomorphological mapping, must be conducted before applying absolute dating methods on specific landforms or areas to constrain the glacial history. Therefore, the emphasis of this study was on determining the relative age of the different palaeo-ice stream flow-sets and the landforms within them and correlating those findings with previous studies on the glacial history in the area. The distribution and morphology of the landforms, such as the CSRs, can be used to roughly reconstruct the ice margins in the absence of chronological constraints or geomorphological data from the sea floor (Fig. 4.5). While the lack of chronological data may limit the interpretation of the results, it also offers more freedom in analyzing the findings and paves the way for future research.

The hypothesized configuration of the palaeo-ice stream flow-sets during several stages of glacier advance and retreat are presented on Figure 5.3. The stages are not confined to specific chronozones due to the lack of absolute ages, but the relative timing of the formation of the landforms is discussed below.

A) *Maximum glaciation and subsequent deglaciation* – The SSBs are formed during active ice streaming and are suggested to have formed during the LGM and the subsequent deglaciation, when the palaeo-ice streams extended out onto the shelf (e.g. Norðdahl and Pétursson, 2005; Patton et al., 2017). The cross-cutting of the flow sets (Figs 4.2 & 5.3) suggests that the ice flow was unconstrained by topography during the maximum flow (orange arrows) but topographically constrained during the subsequent deglaciation (blue arrows). During the maximum flow, an E-W orientated ice divided was most likely located over the present Vatnajökull ice cap (see Fig. 1.1) but migrated above the mountain range west of the study area when the ice sheet had become thinner. The variable morphometry of SSBs within the northward trending flow-sets is likely the result of longer and variable periods of ice streaming from maximum glaciation to deglaciation.

B) *Deglaciation I* – Bustarfell, Hauksstaðaheiði, and surrounding areas are suggested to have become ice-free during the deglaciation following the maximum glaciation, based on the extent of glaciofluvial sediments. Meltwater was released from the ice margin during the retreat, proglacial sediments were deposited in basins and minor outwash fans formed on Bustarfell (Fig. 4.3). This might have occurred during the Bølling-Allerød interstadial when the ice sheet retreated to an unknown position inside the present coast (Ingólfsson and Norðdahl, 2001; Norðdahl and Ingólfsson, 2015; Patton et al., 2017; Benediktsson et

al., 2023b, c). There is no evidence for this deglaciation stage in the other areas, but they have been suggested to be ice-free during that time based on numerical modelling (Patton et al., 2017) and volcanic formations in north Iceland (Liccardi et al., 2007).

C) *Glacier readvances* – Ice is suggested to have extended from the highlands into Vopnafjörður based on the subglacial traction till overlaying the glaciofluvial sediments in the drumlins on Bustarfell and the ribbed moraines on Hauksstaðaheiði (Figs 4.3 & 4.6). This agrees with the readvance of the ice sheet during the Late Glacial that has been observed at several locations around Iceland, as reported in various studies and associated with the YD period (e.g. Norðdahl et al., 2008, 2019; Benediktsson et al., 2023c). In northeast Iceland, the ice margin has been estimated to extend down to the coast in Vopnafjörður (Sæmundsson, 1995) and further out into the fjords of Bakkaflói and Þistilfjörður (Fig. 4.5; Norðdahl and Hjort, 1993) during the YD based on chronological data and cross-cutting relationship of glacial landforms, sediments, and raised beaches (Fig. 5.3). In contrast, ice did not reach the coast in Bakkakflói and Þistilfjörður in the modelling experiments by Patton et al. (2017).

The uniform size and shape of the drumlins within the well-developed drumlin fields on Bustarfell, Tunguheiði, and Kverkártunga (see Fig. 2.1 for location), all associated with northeasterly flow, are considered the results of only one generation of ice streaming under relatively stable glaciological condition. As these areas were likely covered with ice during the YD readvance, it is proposed that these drumlins were formed then, which is also supported by the internal architecture of the drumlins on Bustarfell, as previously mentioned. It is unlikely that the CSRs in Bakkaflói and Þistilfjörður and the ribbed moraines in Vopnafjörður, would be preserved if they formed prior to the YD, as they would have been overridden by the readvancing ice (Norðdahl and Hjort, 1993; Sæmundsson, 1995). The readvance during the Early PB (Fig. 5.3) is not considered to have affected these bedforms considering the location of the ice margin associated with the CSRs and ribbed moraines (Norðdahl and Hjort, 1993; Sæmundsson, 1995). Consequently, it is suggested that the CSRs and ribbed moraines were also formed during the termination of the Late Glacial readvance associated with the YD period. Therefore, ice streams are suggested to have continued to operate in Þistilfjörður, Bakkaflói, and Vopnafjörður during the YD readvance.

D) *Deglaciation II* – Several identified ice-marginal positions on Jökuldalsheiði and transverse ice-marginal channels incised into the drumlins, are the main indication of the deglaciation inside the inferred YD and PB extents (Figs 4.3, 4.6 & 5.3). The generally well-preserved bedforms formed during the Late Glacial suggest that the retreat was passive although the ice-marginal moraines and channels indicate short lived readvances or stillstands during the Early Holocene deglaciation.

Figure 5.3 (next page) A-D shows the hypothesized configuration of palaeo-ice streams within the IIS at several stages during the last glaciation without absolute age constraints. Explanations of the stages are in the text where the age is discussed. The yellow circles and boxes indicate the locations of data used to constrain the ice margin during the YD (1) and PB (2) from Norðdahl and Hjort (1993) and Sæmundsson (1995). The ice margins are marked with dashed lines to indicate that their positions are speculated between the mapped landforms and/or data from previous studies. On B) and D), the ice margin in Þistilfjörður and Bakkaflói have no constraints. The areas with no indications of the ice extent are marked with question marks.

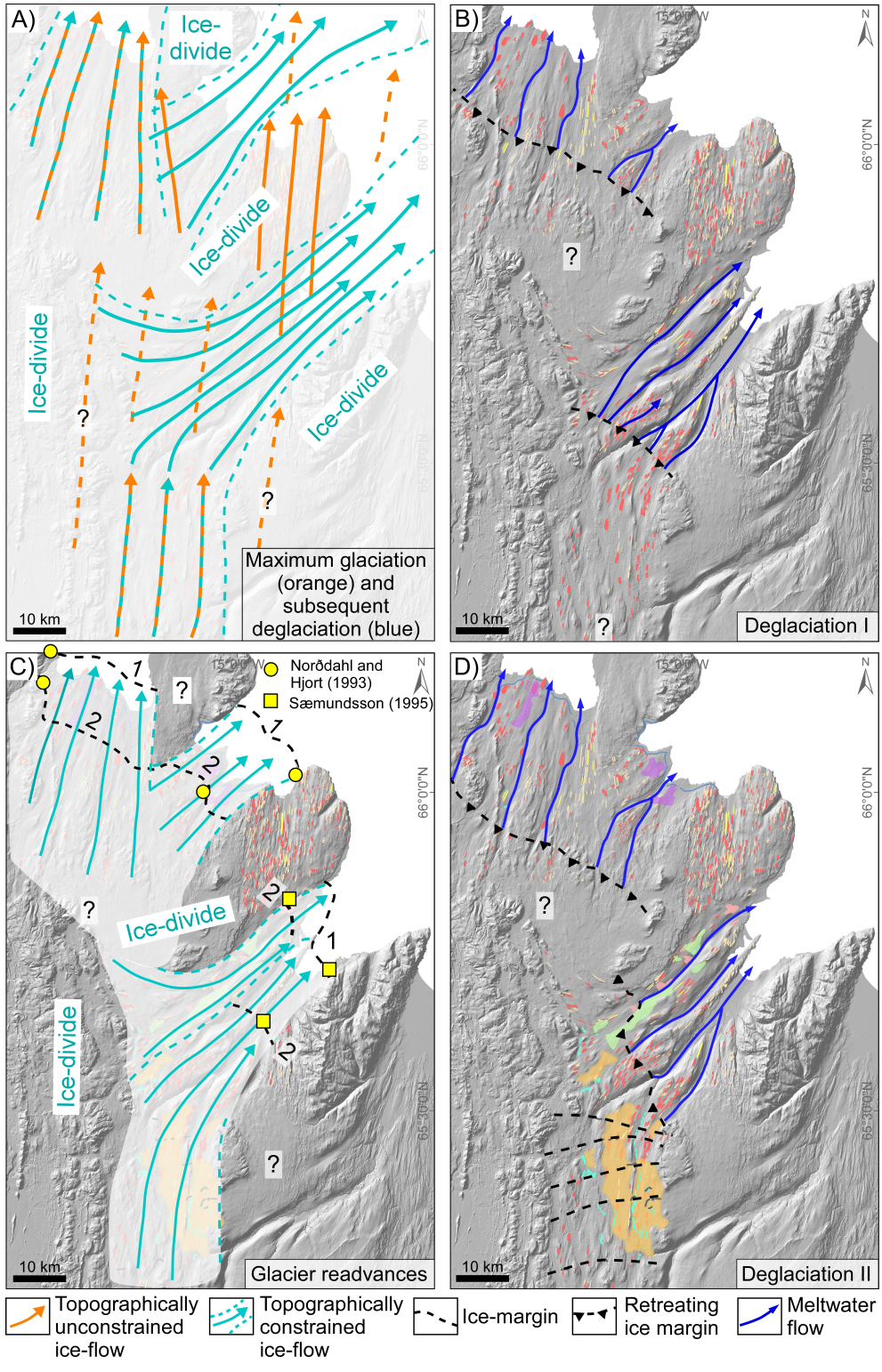
A)
Ice-divide
Ice-divide
Ice-divide
Ice-divide
?
?
Maximum glaciation (orange) and subsequent deglaciation (blue)
10 km
B)
15°0'0" W
66°0'0" N
65°30'0" N
?
?
10 km
Deglaciation I
C)
Norðdahl and Hjort (1993)
Sæmundsson (1995)
1
2
?
Ice-divide
Ice-divide
10 km
Glacier readvances
D)
?
10 km
Deglaciation II
Topographically unconstrained ice-flow
Topographically constrained ice-flow
Ice-margin
Retreating ice margin
Meltwater flow

6 Conclusion

The distribution, morphology, and internal architecture of glacial landforms in northeast Iceland are presented in this thesis based on geomorphological mapping and sedimentological investigations. The findings are important for the reconstruction of the configuration and dynamics of palaeo-ice streams within the IIS during the LGM and Late Glacial. The main conclusions are:

- The distribution and orientation of SSBs in northeast Iceland reveal four cross-cutting flow-sets of palaeo-ice streams; the Þistilfjörður, Bakkaflói, Bakkaheiði and Vopnafjörður-Jökuldalsheiði flow-sets.
- A conceptual landsystem model of palaeo-ice streams is presented, highlighting the ice dynamics and distribution of landforms. It consists of SSBs, CSRs, ribbed moraines, eskers, hummocky terrain, ice-marginal landforms, and raised shorelines.
- Northward trending SSBs suggest an older generation of ice streaming during a maximum glaciation in the area, with flow independent of the underlying topography. Due to ice sheet thinning during deglaciation, the ice streams became confined to valleys and fjords. This is supported by cross-cutting SSBs.
- CSRs are restricted to corridors within the Þistilfjörður and Bakkaflói flow-sets. This is the first time they are described in the palaeo record in Iceland and are considered to have formed during ice-stream shutdown.
- Ribbed moraines are described for the first time in Iceland within the Vopnafjörður-Jökuldalsheiði flow-set. Based on their distribution and often oblique orientation to former ice flow, they are considered to have formed under the lateral shear margins of the palaeo-ice stream due to velocity gradients during ice-stream shutdown.
- The general stratigraphy of the SSBs, CSRs, and ribbed moraines consists of two subglacial till units that are interbedded with deformed glaciofluvial sediments on Bustarfell and Hauksstaðaheiði.
- No chronological constraint is presented in the thesis and therefore all ages are relative and based on correlation with previous studies. The variance in the morphology and distribution of the landforms between the different flow-sets can be used to help reconstruct the configuration and dynamics of the ice streams.
- The SSBs are formed by active ice streaming, both during the maximum glaciation and the subsequent deglaciation. The CSRs and ribbed moraines are a deglaciation signature and based on the known chronology they are suggested to form during ice-stream shutdown following the YD readvance.
- Well-preserved landforms suggest generally passive retreat during the last deglaciation but ice-marginal landforms imply stepwise retreat in some areas.
- Geomorphological mapping is an essential prerequisite for future chronological studies to constrain and reconstruct the glacial history of northeast Iceland. This study has implications for modern and palaeo-ice sheet behaviour during deglaciation under climate warming.

7 Future perspectives

This study is the first to investigate in detail the geomorphology of glacial landforms in northeast Iceland and creates the foundation for continued work regarding the glacial history in the area. A holistic approach is fundamental in glacial geology and various approaches are recommended here for future research.

- Chronological constraints are necessary to get an absolute age of the mapped landforms and ice-stream flow-sets. However, direct dating of glacial landforms in Iceland can be challenging as datable material such as organic matter and tephra, is often lacking. Cosmogenic exposure dating has been used to improve glacial reconstructions in Iceland (e.g. Licciardi et al., 2007; Brynjólfsson et al., 2015). A project focusing on constraining the deglaciation history with exposure ages and tephrochronology has already been initiated (Benediktsson et al., 2024b) and the mapping of landforms and delineation of flow-sets boundaries are valuable when deciding sample locations.
- Lake sediment records are important for better understanding the glacial and climate history in formerly glaciated areas such as Iceland (e.g. Geirsdóttir et al., 2009; Striberger et al., 2012). Several lakes have already been cored in the study area (Farnsworth et al., 2023) offering opportunities for further analyses of the regional glacial history.
- High-resolution mapping in the marine environment is essential to obtain holistic views of the configuration of the flow-sets and to connect the on- and offshore records. Bathymetric data from Þistilfjörður and Bakkaflói, where CSRs are hypothesized in the marine environment (Paper III), are of high importance to test the proposed Late Glacial ice margin in the fjords (see Fig. 4.5) and reconstruct the deglacial history. Recent mapping of the shelf in north Iceland revealed glacial landforms that indicate ice streams extending further out on the shelf than previously thought (Höfer, 2019; OConnell, 2020). Those findings are encouraging for future collection of bathymetric data in northeast Iceland and elsewhere.
- The mapping conducted within this study is of great value for future modelling of the IIS, especially when combined with the ongoing work on constraining the deglaciation history. Furthermore, well-developed models from the IIS, especially during the deglaciation, can serve as an analog for the ongoing deglaciation of contemporary marine-based ice sheets and ice streams (WAIS and GIS; Hugonnet et al., 2021).
- The GPR method has its limitations and various factors can affect the data such as the use of different parameters, infrastructure, and characteristics of the sediments (Jol and Bristow, 2003; Spagnolo et al., 2014). As disturbance from infrastructure and vegetation cover are less problematic in Iceland than in many other countries, further use of GPR is therefore recommended including experiments with suitable acquisition parameters.

- The landforms produced during the deglacial stages were outside the main scope of this thesis (e.g. meltwater channels, moraines, etc.). These landforms should be thoroughly mapped and combined with the results of this thesis in a composite glacial geomorphological map of northeast Iceland to document full deglaciation history.
- Lastly, for a comprehensive reconstruction of the IIS and its dynamics, glacial geomorphological investigation for all of Iceland needs to be conducted and combined with the results from this study.

References

Aðalsteinsson, B. (1985). Skessugarður. Náttúrufræðingurinn 55(2), 82.

Aðalsteinsson, B. (1987). Jökulhörfun á Brúaröræfum. Í Jarðfræðafélag Íslands: Ísaldarlok á Íslandi. Geological Society of Iceland spring conference, Reykjavík, 28th of April 1987.

Alley, R.B., Anandakrishnan, S., Dupont, T.K., & Parizek, B.R. (2004). Ice streams – fast, and faster? Comptes Rendus Physique 5, 723-734.

Alley, R.B., Clark, P.U., Huybrechts, P., & Joughin, I. (2005). Ice-sheet and sea-level changes. Science 310, 456-460.

Andrés, N., Palacios, D., Sæmundsson, Þ., Brynjólfsson, S., & Fernández-Fernández, J.M. (2019). The rapid deglaciation of the Skagafjörður fjord, northern Iceland. Boreas, 48(1), 92-106.

Andrews, J.T. (2008). The role of the Iceland Ice Sheet in the North Atlantic during the late Quaternary: a review and evidence from Denmark Strait. Journal of Quaternary Science 23, 3-20.

Andrews, J.T., Harðardóttir, J., Helgadóttir, G., Jennings, A.E., Geirsdóttir, Á., Sveinbjörnsdóttir, Á.E., Schoolfield, S., Kristjánsdóttir, G.B., Smith, L.M., Thors, K., & Syvitski, J.P.M. (2000). The N and W Iceland Shelf: insights into Last Glacial Maximum ice extent and deglaciation based on acoustic stratigraphy and basal radiocarbon AMS dates. Quaternary Science Reviews 19, 619-631.

Arnardóttir, S. (2022). Streamlined subglacial bedforms in Bárðardalur, northern Iceland: a signature of palaeo-ice streams within the Iceland Ice Sheet. Master's thesis, Faculty of Earth Sciences, University of Iceland. 80 p.

Barchyn, T.E., Dowling, T.P., Stokes, C.R., & Hugenholtz, C.H. (2016). Subglacial bed form morphology controlled by ice speed and sediment thickness. Geophysical Research Letters, 43(14), 7572-7580.

Benediktsson, Í.Ö., Brynjólfsson, S., & Ásbjörnsdóttir, L. (2022a). Chapter 12 - Glacial landscapes of Iceland. Editors: Palacios, D., Hughes, P.D., García-Ruiz, J.M., Andrés, N., European Glacial Landscapes: Maximum Extent of Glaciations. Elsevier, pp. 95-101.

Benediktsson, Í.Ö., Brynjólfsson, S., & Ásbjörnsdóttir, L. (2022b). Chapter 55 – Iceland: glacial landforms from the Last Glacial Maximum. Editors: Palacios, D., Hughes, P., García-Ruiz, J.M., Andrés, N., European Glacial Landscapes: Maximum Extent of Glaciations. Elsevier, pp. 427-434.

Benediktsson, Í.Ö., Brynjólfsson, S., & Ásbjörnsdóttir, L. (2023a). Chapter 17 - Iceland: glacial landforms during deglaciation. Editors: Palacios, D., Hughes, P., García-Ruiz, J.M., Andrés, N., European Glacial Landscapes. Elsevier, pp. 149-155.

Benediktsson, Í.Ö., Brynjólfsson, S., & Ásbjörnsdóttir, L. (2023b). Chapter 34 - Iceland: glacial landforms from the Bølling-Allerød interstadial. Editors: Palacios, D., Hughes, P., García-Ruiz, J.M., Andrés, N., European Glacial Landscapes. Chennai: Elsevier, pp. 331-339.

Benediktsson, Í.Ö., Brynjólfsson, S., & Ásbjörnsdóttir, L. (2023c). Chapter 52 – Iceland: glacial landforms of Iceland from the Younger Dryas Stadial. Editors: Palacios, D., Hughes, P., García-Ruiz, J.M., Andrés, N., European Glacial Landscapes, Elsevier, pp. 497-507.

Benediktsson, Í.Ö., Brynjólfsson, S., Ásbjörnsdóttir, L., & Farnsworth, W. (2024a). Chapter 12 – Holocene glacial history and landforms of Iceland. Editors: Palacios, D., Hughes, P., García-Ruiz, J.M., Andrés, N., European Glacial Landscapes, Elsevier, pp. 193-224.

Benediktsson, Í.Ö. Licciardi, J.M., Brynjólfsson, S., Principato, S., Aradóttir, N., Guðmundsdóttir, E.R., & Farnsworth, W (2024b). Early Holocene deglaciation of eastern Iceland constrained by cosmogenic ^{36}Cl exposure ages and tephrochronology. 36th Nordic Geological Winter Meeting, Gothenburg University, 10-12 January 2024b

Benediktsson, Í.Ö., Jónsson, S.A., Schomacker, A., Johnson, M.D., Ingólfsson, Ó., Zoet, L., Iverson, N.R., & Stötter, J. (2016). Progressive formation of modern drumlins at Múlajökull, Iceland: stratigraphical and morphological evidence. Boreas 45, 567-583.

Benjamínsdóttir, M.M. (2021) Ribbed moraine ridges in Bakkaflói, NE-Iceland: Morphometry, sedimentology and formation. Master's thesis, Faculty of Earth Sciences, University of Iceland. 67 p. Available from: http://hdl.handle.net/1946/38501

Benn, D.I. (2021). Surging glaciers in Scotland. Scottish Geographical Journal, 137(1-4), 1-40.

Benn, D. I., & Ballantyne, C. K. (1993). The description and representation of particle shape. Earth Surface Processes and Landforms 18, 665–672.

Benn, D.I., & Evans, D.J.A., 2010. Glaciers and Glaciation. 802 pp. Hodder Education, London.

Bennett, M.R. (2003). Ice stream as the arteries of an ice sheet; their mechanics, stability and significance. Earth-Science Reviews 61, 309-339.

Briner, J.P. (2007). Supporting evidence from the New York drumlin field that elongate subglacial bedforms indicate fast ice flow. Boreas 36, 143-147.

Brynjólfsson, S., Schomacker, A., Ingólfsson, Ó., & Keiding, J.K. (2015). Cosmogenic 36Cl exposure ages reveal a 9.3 ka BP glacier advance and the Late Weichselian-Early Holocene glacial history of the Drangajökull region, northwest Iceland. Quaternary Science Reviews, 126, 140-157.

Boulton, G.S. (1987). A theory of drumlin formation by subglacial sediment deformation. In Drumlin symposium. (pp. 25-86). AA Balkema Publishers.

Bourgeois, O., Dauteuil, O., & Van Vliet-Lanoë, B. (1998). Pleistocene subglacial volcanism in Iceland: tectonic implications. Earth and Planetary Science Letters, 164(1-2), 165-178.

Bourgeois, O., Dauteuil, O., & Van Vliet-Lanoë, B. (2000). Geothermal control on flow patterns in the last glacial maximum ice sheet of Iceland. Earth Surface Processes and Landforms 25, 59-76.

Carr, S.J., & Rose, J. (2003). Till fabric patterns and significance: particle response to subglacial stress. Quaternary Science Reviews, 22(14), 1415-1426.

Carr, J.R., Vieli, A., & Stokes, C. (2013). Influence of sea ice decline, atmospheric warming, and glacier width on marine-terminating outlet glacier behavior in northwest Greenland at seasonal to interannual timescales. Journal of Geophysical Research: Earth Surface, 118(3), 1210-1226.

Chandler, B.M.P., Lovell, H., Boston, C.M., Lukas, S., Barr, I.D., Benediktsson, Í.Ö., Benn, D.I., Clark, C.R., Darvill, C.M., Evans, D.J.A., Ewertowski, M.W., Loibl, D., Margold, M., Otto, J-C., Roberts, D., Stokes, C.R., Storrar, R.D., & Stroeven, A.P. (2018). Glacial geomorphological mapping: A review of approaches and frameworks for best practice. Earth-Science Reviews, 185, 806-846.

Clark, C.D. (1993). Mega-scale glacial lineations and cross-cutting ice-flow landforms. Earth Surface Processes and Landforms 18, 1-29.

Clark, C.D., & Spagnolo, M. (2016). Glacially eroded cross-shelf troughs surrounding Iceland from Olex data. In: Dowdeswell, J.A., Canals, M., Jakobsson, M., Todd, B.J., Dowdeswell, E.K., Hogan, K.A. (Eds.). Atlas of Submarine Glacial Landforms: Modern, Quaternary and Ancient. Geological Society, London, Memoirs 46, 165-166. Geological Society of London.

De Angelis, H., & Kleman, J. (2008). Palaeo-ice-stream onsets: examples from the north-eastern Laurentide Ice Sheet. Earth Surface Processes and Landforms 33, 560-572.
Delaney, C.A., McCarron, S., & Davis, S. (2018). Irish Ice Sheet dynamics during deglaciation of the central Irish Midlands: Evidence of ice streaming and surging from airborne LiDAR. Geomorphology, 306, 235-253.
Dunlop, P., & Clark, C.D. (2006). The morphological characteristics of ribbed moraine. Quaternary Science Reviews, 25(13-14), 1668-1691.
Evans, D.J.A., & Benn, D.I. (Eds.). (2004). A practical guide to the study of glacial sediments. pp. 83-87 & 97-107. Arnold, London.
Evans, D.J.A., & Rea, B.R. (1999). Geomorphology and sedimentology of surging glaciers: a land-systems approach. Annals of Glaciology, 28, 75-82.
Evans, D.J.A., & Rea, B.R. (2003). Surging glacier landsystem. In Glacial landsystems (pp. 259-288). Taylor and Francis.
Evans, D.J.A, Clark, C.D., & Rea, B.R. (2008). Landform and sediment imprints of fast glacier flow in the southwest Laurentide Ice Sheet. Journal of Quaternary Science: Published for the Quaternary Research Association, 23(3), 249-272.
Evans, D.J., Storrar, R.D., & Rea, B.R. (2016). Crevasse-squeeze ridge corridors: diagnostic features of late-stage palaeo-ice stream activity. Geomorphology, 258, 40-50.
Eiríksson, J., Knudsen, K.L., Haflidason, H., & Henriksen, P. (2000). Late-glacial and Holocene palaeoceanography of the North Icelandic shelf. Journal of Quaternary Science 15, 23-42.
Ely J.C., Clark, C.D., Spagnolo, M., Stokes, C.R., Greenwood, S.L., Hughes, A., Dunlop, P., & Hess, D. (2016). Do subglacial bedforms comprise a size and shape continuum? Geomorphology 257, 108-119.
Eyles, N., Moreno, L.A., & Sookhan, S. (2018). Ice streams of the Late Wisconsin Cordilleran Ice Sheet in western North America. Quaternary Science Reviews, 179, 87-122.
Eyles, N., Putkinen, N., Sookhan, S., & Arbelez-Moreno, L. (2016). Erosional origin of drumlins and megaridges. Sedimentary Geology 338, 2-23.
Farnsworth, W.R., Ingólfsson, Ó., Retelle, M., & Schomacker, A. (2016). Over 400 previously undocumented Svalbard surge-type glaciers identified. Geomorphology, 264, 52–60.
Farnsworth, W.R., Jackson, R., Aradóttir, N., Benediktsson, Í.Ö., Brynjólfsson, S., Erlendsson, E., Guðmundsdóttir, E.R., Ingólfsson, Ó., Kjær, K.H., & Larsen, N.K. (2023). Tephra constrains natural and anthropogenic changes in postglacial Icelandic sediments. The 4th International PalaeoARC Conference 2023, Akureyri, Iceland.
Finlayson, A.G., & Bradwell, T. (2008). Morphological characteristics, formation and glaciological significance of Rogen moraine in northern Scotland. Geomorphology, 101(4), 607-617.
Fowler, A.C. (2000). An instability mechanism for drumlin formation. Geological Society, London, Special Publications, 176(1), 307-319.
Fowler, A.C., & Chapwanya, M. (2014). An instability theory for the formation of ribbed moraine, drumlins and mega-scale glacial lineations. Proceedings of the Royal Society A: Mathematical, Physical and Engineering Sciences, 470(2171), 20140185.
Geirsdóttir, Á. (2011). Pliocene and Pleistocene glaciations of Iceland: A brief overview of the glacial history. Developments in Quaternary Sciences, 15, 199-210.
Geirsdóttir, Á., Miller, G.H., Axford, Y., & Ólafsdóttir, S. (2009). Holocene and latest Pleistocene climate and glacier fluctuations in Iceland. Quaternary Science Reviews, 28(21-22), 2107-2118.

Greenwood, S.L., & Clark, C.D. 2009. Reconstructing the last Irish Ice Sheet 1: changing flow geometries and ice flow dynamics deciphered from the glacial landform record. Quaternary Science Reviews 28, 3085-3100.

Hättestrand, C., & Kleman, J. (1999). Ribbed moraine formation. Quaternary Science Reviews, 18(1), 43-61.

Hart, J.K. (1997). The relationship between drumlins and other forms of subglacial glaciotectonic deformation. Quaternary Science Reviews, 16(1), 93-107.

Helgadóttir, E.G. (2020). Ribbed moraines in the Vopnafjörður region, Iceland. Master's thesis, Faculty of Earth Sciences, University of Iceland. 104 p. Available from: http://hdl.handle.net/1946/35879

Hillier, J.K., Smith, M.J., Armugam, R., Barr, I., Boston, C.M., Clark, C.D., Ely, J., Frank, A., Greenwood, S.L., Gosselin, L., Hättestrand, C., Hogan, K., Hughes, A.L.C., Livingstone, S.J., Lovell, H., McHenry, M., Munoz, Y., Pellicer, X.M., Pellitero, R., Robb, C., Roberson, S., Ruther, D., Spagnolo, M., Standell, M., Stokes, C.R., Storrar, R., Tate, N.J., & Wooldridge, K. (2015). Manual mapping of drumlins in synthetic landscapes to assess operator effectiveness. Journal of Maps, 11(5), 719-729.

Hindmarsh, R.C. (1998). Drumlinization and drumlin-forming instabilities: viscous till mechanisms. Journal of Glaciology, 44(147), 293-314.

Hjartardóttir, Á.R., Einarsson, P., & Brandsdóttir, B. (2010). The Kerlingar fault, Northeast Iceland: A Holocene normal fault east of the divergent plate boundary. Jökull 60, 103-116.

Hjartarson, Á., & Sæmundsson, K. (2014). Geological map of Iceland. Bedrock 1:600.000. Iceland GeoSurvey.

Hubbard, A., Sugden, J., Dugmore, A., Norðdahl, H., & Pétursson, H.G. (2006). A modelling insight into the Icelandic Late Glacial Maximum ice sheet. Quaternary Science Reviews 25, 2283-2296.

Hughes, A.L.C., Clark. C.D., & Jordan, C.J. (2010). Subglacial bedforms of the last British Ice Sheet. Journal of Maps, 6:1, 543-563.

Hugonnet, R., McNabb, R., Berthier, E., Menounos, B., Nuth, C., Girod, L., Farinotti, D., Huss, M., Dussaillant, I., Brun, F., & Kääb, A. (2021). Accelerated global glacier mass loss in the early twenty-first century. Nature 592, 726-731.

Höfer, P. (2019). Morphodynamic Features of Palaeo Ice Streams offshore N-Iceland based on Multibeam Bathymetric and High Resolution Chirp Seismic Data. Master's thesis, Faculty of Earth Sciences, University of Iceland. 71 p. Available from: https://skemman.is/handle/1946/34505

Ingólfsson, Ó., & Norðdahl, H. (2001). High relative sea-level during the Bølling interstadial in W Iceland: a reflection of ice-sheet collapse and extremely rapid glacial unloading. Arctic, Antarctic and Alpine Research 33, 231-243.

Ingólfsson, Ó., Benediktsson, Í. Ö., Schomacker, A., Kjær, K. H., Brynjólfsson, S., Jónsson, S. A., Korsgaard, N.J., & Johnson, M. D. (2016). Glacial geological studies of surge-type glaciers in Iceland—Research status and future challenges. Earth-Science Reviews, 152, 37-69.

Iverson, N.R., McCracken, R.G., Zoet, L., Benediktsson, Í.Ö., Schomacker, A., Johnson, M.D., & Woodard, J. 2017. A theoretical model of drumlin formation based on observations at Múlajökull, Iceland. Journal of Geophysical Research Earth Surface 122.

Jol, H.M., & Bristow, C.S. (2003). GPR in sediments: advice on data collection, basic processing and interpretation, a good practice guide. Geological Society, London, Special Publications, 211(1), 9-27.

Joughin, I., Alley, R.B., & Holland, D.M. (2012). Ice-sheet response to oceanic forcing. Science, 338(6111), 1172-1176.

Joughin, I., Smith, B. E., & Medley, B. (2014). Marine ice sheet collapse potentially under way for the Thwaites Glacier Basin, West Antarctica. Science, 344(6185), 735-738.

Jóhannesson, H., & Sæmundsson, K. (2009). Geological map of Iceland. 1:500.000. Bedrock (1st edition). Icelandic Institute of Natural History. Reykjavík.

Kamb, B. (2001). Basal zone of the West Antarctic ice streams and its role in lubrication of their rapid motion. The West Antarctic ice sheet: behavior and environment, 77, 157-199.

King, E., Hindmarch, R.C.A., & Stokes, C.R. (2009). Formation of mega-scale glacial lineations observed beneath a West Antarctic ice stream. Nature Geoscience 2, 585-588.

Kjær, K.H., Houmark-Nielsen, M., & Richardt, N. (2003). Ice-flow patterns and dispersal of erratics at the southwestern margin of the last Scandinavian Ice Sheet: signature of palaeo-ice streams. Boreas, 32(1), 130-148.

Kjær, K.H., & Krüeger, J. (1998). Does clast size influence fabric strength?. Journal of Sedimentary Research, 68(5), 746-749.

Kjær, K.H., Sultan, L., Krüger, J., & Schomacker, A. (2004). Architecture and sedimentation of outwash fans in front of the Mýrdalsjökull ice cap, Iceland. Sedimentary Geology, 172(1-2), 139-163.

Krüger, J., & Kjær, K.H. (1999). A data chart for field description and genetic interpretation of glacial diamicts and associated sediments - with examples from Greenland, Iceland, and Denmark. Boreas, 28(3), 386-402.

Kurjanski, B., Rea, B.R., Spagnolo, M., Winsborrow, M., Cornwell, D.G., Andreassen, K., & Howell, J. (2019). Morphological evidence for marine ice stream shutdown, central Barents Sea. Marine Geology, 414, 64-76.

Larsen, D.J., Miller, G.H., Geirsdóttir, Á., & Ólafsdóttir, S. (2012). Non-linear Holocene climate evolution in the North Atlantic: a high-resolution, multi-proxy record of glacier activity and environmental change from Hvítárvatn, central Iceland. Quaternary Science Reviews, 39, 14-25.

Lawson, D.E. (1979). A comparison of the pebble orientations in ice and deposits of the Matanuska Glacier, Alaska. The Journal of Geology, 87(6), 629-645.

Licciardi, J.M., Kurz, M.D., & Curtice, J.M. (2007). Glacial and volcanic history of Icelandic table mountains from cosmogenic 3He exposure ages. Quaternary Science Reviews, 26(11-12), 1529-1546.

Livingstone, S.J., Cofaigh, C.Ó., Stokes, C.R., Hillenbrand, C., Vieli, A., & Jamieson, S.S.R. (2012). Antarctic palaeo-ice streams. Earth-Science Reviews, 111(1-2), 90-128.

Lukas, S., Benn, D.I., Boston, C.M., Brook, M., Coray, S., Evans, D.J., Graf, A., Kellerer-Pirklbauer, A., Kirkbride, M.P., Krabbendam, M., Lovell, H., Machiedo, M., Mills, S.C., Nye, K., Reinardy, B.T.T., Ross, F.H., & Signer, M. (2013). Clast shape analysis and clast transport paths in glacial environments: A critical review of methods and the role of lithology. Earth-Science Reviews, 121, 96-116.

Maclachlan, J.C., & Eyles, C.H. (2013). Quantitative geomorphological analysis of drumlins in the Peterborough drumlin field, Ontario, Canada. Geografiska Annaler: Series A, Physical Geography, 95(2), 125-144.

McCracken, R.G., Iverson, N.R., Benediktsson, Í.Ö., Schomacker, A., Zoet, L.K., Johnson, M. D., Hooyer, T.S., & Ingólfsson, Ó. (2016). Origin of the active drumlin field at Múlajökull, Iceland: new insights from till shear and consolidation patterns. Quaternary Science Reviews, 148, 243-260.

McKenzie, M.A., Principato, S.M., & Benediktsson, Í.Ö. (2017). Geomorphic evidence for a palaeo-ice stream near Bárðardalur, north Iceland. GSA Annual Meeting, Seattle, WA, USA, 22-25 October 2017.

Menzies, J. (1979). A review of the literature on the formation and location of drumlins. Earth-Science Reviews, 14(4), 315-359.

Margold, M., Stokes, C.R., & Clark, C.D. (2015). Ice streams in the Laurentide Ice Sheet: Identification, characteristics and comparison to modern ice sheets. Earth-Science Reviews 143, 117-146.
Napieralski, J., & Nalepa, N. (2010). The application of control charts to determine the effect of grid cell size on landform morphometry. Computers & Geosciences 36, 222-230.
Norðdahl, H. (1991). A review of the glaciation maximum concept and the deglaciation of Eyjafjörður, north Iceland. In: Maizels, J.K. and Caseldine, C. (Eds.). Environmental change in Iceland: Past and Present. Netherlands, Kluwer Academic Publishers, pp. 31-47.
Norðdahl, H., & Hjort, C. (1993). Lateglacial raised beaches and glacier recession in the Þistilfjörður-Bakkaflói area. Jökull 43, 32-44.
Norðdahl, H., & Ingólfsson, Ó. (2015). Collapse of the Icelandic ice sheet controlled by sea-level rise? Arktos 1, 1-18.
Norðdahl, H., Ingólfsson, Ó., Pétursson, H.G., & Hallsdóttir, M. (2008). Late Weichselian and Holocene environmental history of Iceland. Jökull, 58, 343-364.
Norðdahl, H., Ingólfsson, Ó., Vogler, E.D., Steingrímsson, B.Ó., & Hjartarson, Á. (2019). Glacio-isostatic age modelling and Late Weichselian deglaciation of the Lögurinn basin, East Iceland. Boreas, 48(3), 563-580.
Norðdahl, H., & Pétursson, H.G. (2005). Relative sea-level changes in Iceland. New aspects of the Weichselian deglaciation of Iceland. In: Caseldine C, Russel A, Harðardóttir J, Knudsen Ó (Eds.), Iceland – modern processes and past environments. Elsevier, Amsterdam, pp. 25-78.
OConnell, B. (2020). Marine terminating ice-stream retreat within the Eyjafjarðaráll basin, North Iceland; documented by multibeam bathymetric and high-resolution Chirp reflection data. Master's thesis, Faculty of Earth Sciences, University of Iceland. 85 p. Available from: https://skemman.is/handle/1946/35954
Ó Cofaigh, C., Dowdeswell, J.A., Evans, J., & Larter, R.D. (2008). Geological constraints on Antarctic palaeo-ice-stream retreat. Earth Surface Processes and Landforms: The Journal of the British Geomorphological Research Group, 33(4), 513-525.
Ó Cofaigh, C., & Stokes, C.R. (2008). Reconstructing ice-sheet dynamics from subglacial sediments and landforms: introduction and overview. Earth Surface Processes and Landforms, 33(4).
Ó Cofaigh, C., Stokes, C.R., Lian, O.B., Clark, C.D., & Tulacyzk, S. (2013). Formation of mega-scale glacial lineations on the Dubawnt Lake Ice Stream bed: 2. Sedimentology and stratigraphy. Quaternary science reviews, 77, 210-227.
Paterson, W.S.B. (1994). Physics of glaciers. Butterworth-Heinemann, 480 pp.
Patton, H., Hubbard, A., Bradwell, T., & Schomacker, A. (2017). The configuration, sensitivity and rapid retreat of the Late Weichselian Icelandic ice sheet. Earth-Science Reviews 166, 223-245.
Porter, Claire; Morin, Paul; Howat, Ian; Noh, Myoung-Jon; Bates, Brian; Peterman, Kenneth; Keesey, Scott; Schlenk, Matthew; Gardiner, Judith; Tomko, Karen; Willis, Michael; Kelleher, Cole; Cloutier, Michael; Husby, Eric; Foga, Steven; Nakamura, Hitomi; Platson, Melisa; Wethington, Michael, Jr.; Williamson, Cathleen; Bauer, Gregory; Enos, Jeremy; Arnold, Galen; Kramer, William; Becker, Peter; Doshi, Abhijit; D'Souza, Cristelle; Cummens, Pat; Laurier, Fabien; Bojesen, Mikkel, (2018), "ArcticDEM",
Powers, M.C. (1953). A new roundness scale for sedimentary particles. Journal of Sedimentary Research, 23(2), 117-119.
Principato, S.M., Moyer, A.N., Hampsch, A.G., & Ipsen, H.A. (2016). Using GIS and streamlined landforms to interpret palaeo-ice flow in northern Iceland. Boreas 45, 470-482.
Raunholm, S., Sejrup, H.P., & Larsen, E. (2003). Lateglacial landform associations at Jæren (SW Norway) and their glaci-dynamic implications. Boreas, 32(3), 462-475.

Sharp, M. (1985) “Crevasse-fill” ridges-a landform type characteristic of surging glaciers? Geografisker Annaler, Series a, Physical Geography, 67(3–4), 213–220.
Shaw, J. (2002). The meltwater hypothesis for subglacial bedforms. Quaternary International, 90(1), 5-22.
Sigfúsdóttir, T., & Benediktsson, Í.Ö. (2020). Refining the history of Younger Dryas and Early Holocene glacier oscillations in the Borgarfjörður region, western Iceland. Boreas, 49(2), 296-314.
Smalley, I.J., & Unwin, D.J. (1968). The formation and shape of drumlins and their distribution and orientation in drumlin fields. Journal of Glaciology, 7(51), 377-390.
Smith, A.M., Anker., P.G.F., Nicholls., K.W., Makinson, K., Murray, T., Rios-Costas, S., Brisbourne. A.M., Hodgson, D.A., Schlegel., R., & Anandakrishnan, S. (2021). Ice stream subglacial access for ice-sheet history and fast ice flow: the BEAMISH Project on Rutford Ice Stream, West Antarctica and initial results on basal conditions. Annals of Glaciology 62(85-86), 203–211.
Smith., M.J., & Clark, C.D. (2005). Methods for the visualization of digital elevation models for landform mapping. Earth Surface Processes and Landforms, 30(7).
Smith., M.J., & Wise, S.M. (2007). Problems of bias in mapping linear landforms from satellite imagery 9(1).
Spagnolo, M., & Clark C.D. (2009). A geomorphological overview of glacial landforms on the Icelandic continental shelf. Journal of Maps, 2009, 37-52.
Spagnolo, M., Clark, C.D., Ely, J.C., Stokes, C.R., Anderson, J.B., Andreassen, K., Graham, A.G.C., & King, E.C. (2014). Size, shape and spatial arrangement of mega-scale glacial lineations from a large and diverse dataset. Earth Surface Processes and Landforms, 39(11), 1432-1448.
Stokes, C.R. (2018). Geomorphology under ice streams: Moving from form to process. Earth Surfaces Processes and Landforms 43, 85-123.
Stokes, C.R., & Clark. C.D. (1999). Geomorphological criteria for identifying Pleistocene ice streams. Annals of Glaciology 28, 67-74.
Stokes, C.R., & Clark, C.D. (2001). Palaeo-ice streams. Quaternary Science Reviews 20, 1437-1457.
Stokes, C.R., Clark, C.D., Lian, O.B., & Tulaczyk, S. (2006). Geomorphological map of ribbed moraines on the Dubawnt Lake Palaeo-Ice stream bed: a signature of ice stream shut-down?.Journal of Maps,2(1), 1-9.
Stokes, C.R., Clark, C.D., Lian, O.B., & Tulaczyk, S. (2007). Ice stream sticky spots: a review of their identification and influence beneath contemporary and palaeo-ice streams. Earth-Science Reviews,81(3-4), 217-249.
Stokes, C.R., Fowler, A.C., Clark, C.D., Hindmarsh, R.C., & Spagnolo, M. (2013b). The instability theory of drumlin formation and its explanation of their varied composition and internal structure. Quaternary Science Reviews,62, 77-96.
Stokes, C.R., Lian, O.B., Tulaczyk, S., & Clark, C. D. (2008). Superimposition of ribbed moraines on a palaeo-ice-stream bed: implications for ice stream dynamics and shutdown. Earth Surface Processes and Landforms: The Journal of the British Geomorphological Research Group,33(4), 593-609.
Stokes, C., Margold, M., Clark, C., & Tarasov, L. (2016). Ice stream activity scaled to ice sheet volume during Laurentide Ice Sheet deglaciation. Nature 530, 322–326.
Stokes, C.R., Spagnolo, M., & Clark, C.D. (2011). The composition and internal structure of drumlins: complexity, commonality, and implications for a unifying theory of their formation. Earth-Science Reviews,107(3-4), 398-422.
Stokes, C.R., Spagnolo, M., Clark, C.D. Ó Cofaigh, C. Lian, O.B., & Dunstone, R.B. (2013a). Formation of mega-scale glacial lineations on the Dubwant Lake Ice Stream bed 1: size,

shape and spacing from a large remote sensing dataset. Quaternary Science Reviews 77, 210-227.
Sookhan, S., Eyles, N., & Bukhari, S. (2022). Drumlins and mega-scale glacial lineations as a continuum of subglacial shear marks: A LiDAR based morphometric study of streamlined surfaces on the bed of a Canadian paleo-ice stream. Quaternary Science Reviews, 292, 107679.
Sookhan, S., Eyles, N., Bukhari, S., & Paulen, R.C. (2021). LiDAR-based quantitative assessment of drumlin to mega-scale glacial lineation continuums and flow of the paleo Seneca-Cayuga paleo-ice stream. Quaternary Science Reviews, 263, 107003.
Sookhan, S., Eyles, N., & Putkinen, N. (2016). LiDAR-based volume assessment of the origin of the Wadena drumlin field, Minnesota, USA. Sedimentary Geology 338, 72-83.
Striberger, J., Björck, S., Holmgren, S., & Hamerlík, L. (2012). The sediments of Lake Lögurinn–A unique proxy record of Holocene glacial meltwater variability in eastern Iceland. Quaternary Science Reviews, 38, 76-88.
Syvitski, J.P., Jennings, A.E., & Andrews, J.T. (1999). High-resolution seismic evidence for multiple glaciations across the southwest Iceland shelf. Arctic, Antarctic and Alpine Research 31, 50-57.
Sæmundsson, K. (1977). Geological Map of Iceland, Sheet 7, NE-Iceland. 1:250.000. Icelandic Institute of Natural History and National Land Survey of Iceland, Reykjavik.
Sæmundsson, Th. (1995). Deglaciation and shoreline displacement in Vopnafjörður, northeastern Iceland. LUNDQUA thesis 33,1-106. Department of Quaternary Geology, Lund University.
Vérité, J., Ravier, É., Bourgeois, O., Pochat, S., Lelandais, T., Mourgues, R., Clark, C.D., Bessin, P., Peigné, D., & Atkinson, N. (2021). Formation of ribbed bedforms below shear margins and lobes of palaeo-ice streams. The Cryosphere, 15(6), 2889-2916.
Winsborrow, M.C., Clark, C.D., & Stokes, C.R. (2010). What controls the location of ice streams?. Earth-Science Reviews, 103(1-2), 45-59.
Woodard, J., Zoet, L., Benediktsson, Í.Ö., Iversson, N., & Finlayson, A. (2020). Insight into drumlin development from ground-penetrating radar at Múlajökull, Iceland, a surge-type glacier. Journal of Glaciology, 66(259), 822-830.
Yu, P., Eyles, N., & Sookhan, S. (2015). Automated drumlin shape and volume estimation using high resolution LiDAR imagery (Curvature Based Relief Separation): A test from the Wadena Drumlin Field, Minnesota. Geomorphology, 246, 589-601.

Paper I

Geomorphology 396 (2022) 108009

Contents lists available at ScienceDirect

Geomorphology

journal homepage: www.elsevier.com/locate/geomorph

Cross-cutting palaeo-ice streams in NE-Iceland reveal shifting Iceland Ice Sheet dynamics

Ívar Örn Benediktsson [a,*], Nína Aradóttir [a], Ólafur Ingólfsson [a], Skafti Brynjólfsson [b]

[a] Institute of Earth Sciences, University of Iceland, Iceland
[b] Icelandic Institute of Natural History, Iceland

ARTICLE INFO

Article history:
Received 21 June 2021
Received in revised form 20 October 2021
Accepted 20 October 2021
Available online 25 October 2021

Keywords:
Iceland Ice Sheet
Palaeo-ice streams
Streamlined subglacial bedforms (drumlins and megascale glacial lineations)
Ice-sheet dynamics and ice divide migration

ABSTRACT

Ice streams are thought to have regulated the past Iceland Ice Sheet (IIS) during and following the Last Glacial Maximum (LGM) by discharging ice and sediment from the interior of the ice sheet towards the shelf edge. Previous assessments of ice streams within the IIS have produced contradictory reconstructions of ice sheet dynamics and location of ice divides. Here, we reconstruct palaeo-ice streams in NE-Iceland based on detailed mapping of streamlined subglacial bedforms (SSBs) and other glacial lineations. The morphometrics, distribution and orientation of the SSBs indicate the flow-sets of several cross-cutting palaeo-ice streams and the location and migration of ice divides, while high density and packing of SSBs possibly suggest the axial zones of the ice streams. North-trending flow-sets suggest that during maximum glaciation and ice-sheet thickness, ice flow within the study area was largely unaffected by underlying topography allowing ice to flow northwards across valleys and fjords. This ice flow direction correlates with the orientation of previously identified troughs on the north-eastern shelf and indicates that an E-W orientated ice divide was located to the south of the study area. During deglaciation and ice sheet thinning, a N-S orientated ice divide was located to the west of the study area, and palaeo-ice streams became confined to valleys and fjords, so that associated flow-sets crosscut the older ones. The absolute ages of these flow-sets are uncertain, but the simplest interpretation is that the older ones pertain to the LGM and the younger ones to the following deglaciation. This study sheds light on the dynamics and evolution of palaeo-ice streams within the IIS and highlights the importance of further efforts to understand the subglacial processes responsible for the formation of the streamlined subglacial bedforms as well as to constrain the evolution of shelf glaciation and chronology of ice stream retreat.

© 2021 Published by Elsevier B.V.

1. Introduction

Ice streams are corridors of fast-flowing ice that have long been recognized as the main regulators of ice sheet discharge and sediment flux (e.g. Bennett, 2003; Briner, 2016; Eyles and Ross, 2016; Stokes et al., 2016). Their vulnerability to climate and sea-level changes, their temporal behaviour, and mechanism of fast flow, are poorly understood (e.g. Bennett, 2003; Alley et al., 2004, 2005), and it is uncertain how ice stream drainage networks evolve and regulate rates of mass loss over longer timescales (Larter et al., 2019). Modern ice streams are present within the Antarctic and Greenland ice sheets (Bennett, 2003; Alley et al., 2004) and palaeo-ice stream landsystems have been reported from former ice sheets (Stokes and Clark, 2001). Their geomorphological imprint is characterized by streamlined terrain consisting of highly elongated drumlins or mega-scale glacial lineations (MSGL), geomorphologically heterogeneous onset zones, and abrupt shear margins to more sluggish ice (e.g. Briner, 2007; De Angelis and Kleman, 2008; King et al., 2009; Margold et al., 2015; Stokes, 2018). Ice streams are thought to have regulated the Iceland Ice Sheet (IIS) during and following the Last Glacial Maximum (LGM) by discharging ice and sediment from the ice sheet interior towards the shelf edge (Bourgeois et al., 2000; Stokes and Clark, 2001; Norðdahl and Pétursson, 2005; Hubbard et al., 2006; Spagnolo and Clark, 2009; Clark and Spagnolo, 2016; Patton et al., 2017). The location of ice streams within the IIS has been projected on the basis of large-scale topography, streamlined subglacial bedforms and glacial striae, often resulting in contradictory reconstructions of ice divides (Bourgeois et al., 2000; Hubbard et al., 2006; Fig. 1A). Norðdahl (1991) depicted major ice streams in the main fjords of central North Iceland whereas Bourgeois et al. (2000) reconstructed flow patterns across entire Iceland with topographic ice streams located in all major fjords, and ice divides over mountainous regions in between these fjords. Spagnolo and Clark et al. (2009) concluded that major troughs and streamlined ridges on the Iceland shelf were imprints of palaeo-ice streams, and Clark and Spagnolo (2016)

* Corresponding author.
E-mail address: ivarben@hi.is (Í.Ö. Benediktsson).

https://doi.org/10.1016/j.geomorph.2021.108009
0169-555X/© 2021 Published by Elsevier B.V.

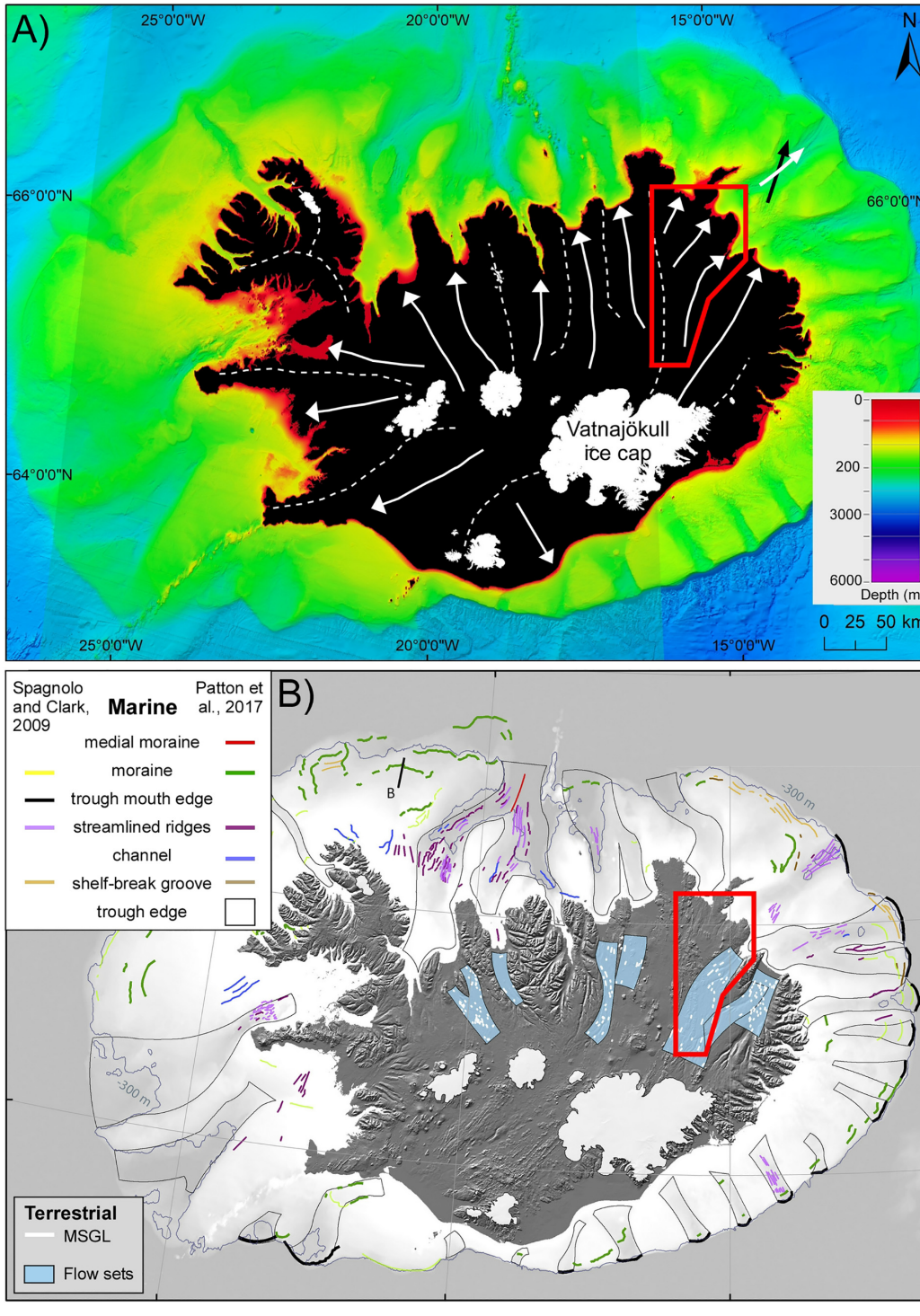

Fig. 1. (A) Iceland with a bathymetric DEM of the Iceland shelf. Bathymetry from GEBCO. Arrows indicate previously hypothesized major ice streams according to Bourgeois et al. (2000), Stokes and Clark (2001), and Principato et al. (2016). Black and white arrows on the north-eastern shelf indicate cross-cutting troughs identified by Clark and Spagnolo (2016). (B) Glacial geomorphology of the Iceland continental shelf based on Spagnolo and Clark et al. (2009) and Patton et al. (2017). The blue polygons indicate terrestrial palaeo-ice stream flow sets in N- and NE-Iceland as outlined by Patton et al. (2017). Modified from Patton et al. (2017). The red box in A and B indicates the study area (Fig. 2).

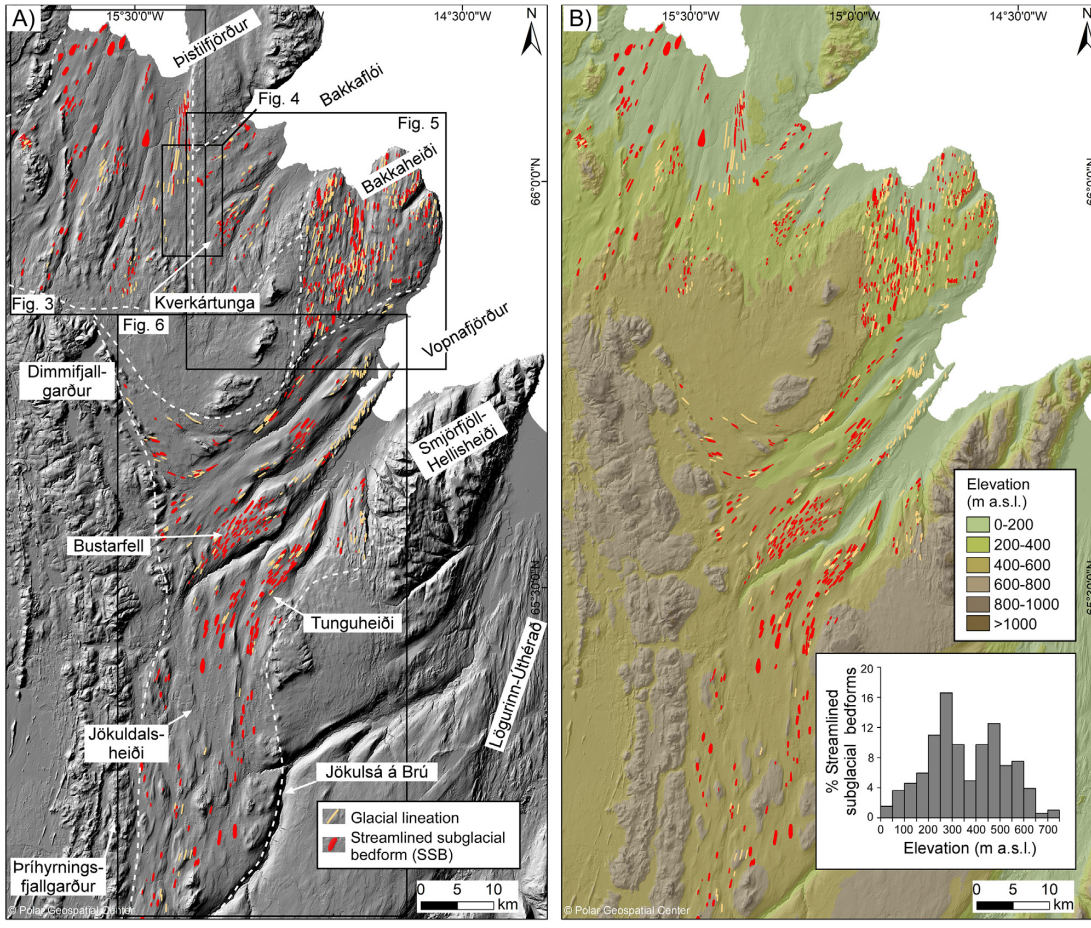

Fig. 2. (A) Overview map of streamlined subglacial bedforms and glacial lineations in NE-Iceland. The white dashed lines indicate boundaries between the study areas of Þistilfjörður, Bakkaflói, Bakkaheiði, and Vopnafjörður-Jökuldalsheiði. The locations of Figs. 3-6 are indicated with black squares. Map base layer: Hillshade of the ArcticDEM (Porter et al., 2018). (B) Altitudinal distribution of streamlined subglacial bedforms. The inset histogram shows that 15% of all bedforms occur below 200 m a.s.l. but that 79% are situated at 200–600 m a.s.l.

identified cross-cutting troughs indicative of multiple phases of shelf glaciation (Fig. 1A). A significant step in the study of palaeo-ice streams in Iceland was made by Principato et al. (2016) who mapped and quantified the properties of streamlined subglacial bedforms with spatial analysis, supporting the presence of palaeo-ice streams in NW-Iceland. Despite these important previous efforts, the configuration and cross-cutting relationships of palaeo-ice streams in Iceland are still relatively poorly understood, compared to many other regions that were occupied by past ice streams (e.g. Kjær et al., 2003; Greenwood and Clark, 2009a; Margold et al., 2015).

Our aim is to clarify the configuration, dynamics, and geomorphological imprint of palaeo-ice streams in NE-Iceland by mapping and analyzing streamlined subglacial bedforms (SSBs) in the Þistilfjörður, Bakkaflói, Bakkaheiði, Vopnafjörður, and Jökuldalsheiði areas (Figs. 1 and 2). Previous studies of glacial history in this region are rare and have mainly focused on the last deglaciation and associated shoreline displacement after the Younger Dryas (YD) (Norðdahl and Hjort, 1993; Sæmundsson, 1995; Richardsson, 1997; Norðdahl et al., 2019). Patton et al. (2017) modelled a rapid marine deglaciation in this region from 21.8–15 ka BP (GS-2c throughout GS-2a[1]) with rates of mass loss comparable to the contemporary West Antarctic Ice Sheet (WAIS) (Hugonnet et al., 2021). According to their model, abrupt warming during the Bølling Interstadial (14.7–14.1 ka BP; GI-1e[1]) forced a dramatic collapse of the IIS onshore, consistent with what had been previously suggested by Ingólfsson and Norðdahl (2001) and Norðdahl and Ingólfsson (2015). Patton et al. (2017) modelling suggests that this collapse was analogous to contemporary rates of mass loss in Greenland and the Amundsen Basin in the WAIS (Rignot et al., 2011; Feldmann and Levermann, 2015; Hugonnet et al., 2021), with the coastal areas of NE-Iceland ice free from c. 17 ka BP. According to their model, the ice margin retreated far inland at 13.2 ka BP but readvanced to the coast in Vopnafjörður, but not elsewhere in this region, at 11.7 ka BP (YD; GS-1[1]). Norðdahl et al. (2019) studied the glacial history of Fljótsdalshérað (Fig. 2A) and concluded that it was occupied by a fast-flowing ice stream during the LGM, and deglaciated between 14.7 and 13.2 cal. ka BP at the earliest.

2. Setting

The study area covers the northeastern part of Iceland, from Þistilfjörður in the north to Vopnafjörður and Jökuldalsheiði in the south (Fig. 1). The bedrock in this region consists primarily of Miocene and Pliocene (>3.3–0.8 myr) plateau basalts with intercalated sediment horizons. It generally becomes progressively younger towards the west. In general, the basalts have a northward strike and are heavily

[1] According to Lowe et al. (2008).

intersected by N-S trending dykes, especially in the Bakkaheiði area (Sæmundsson, 1977; Jóhannesson and Sæmundsson, 2009). The study area is delineated to the west by an arcuate chain of Middle Pliocene (0.12–0.8 Ma) hyaloclastite ridges that stretch from the Vatnajökull ice cap in the south towards the northern coast and separate the area from the currently active northern volcanic rift zone (Fig. 2; Hjartardóttir et al., 2010; Hjartarson and Sæmundsson, 2014). Hence, basal ice flow within the study area was not directly affected by volcanic activity and glacial landforms are not obscured by post-glacial lavas. To the south and southeast, the study area is delimited by the deep channel/valley of the Jökulsá á Brú glacial river and the Smjörfjöll-Hellisheiði massif. The analysis of SSBs is focused on the three, major valley-fjord systems that dominate the coastal areas, and associated uplands and plateaus to the south or south-west of these systems (Fig. 2A). These valley-fjord systems are the result of frequent glaciations since the onset of the Quaternary (Benediktsson et al., 2021a). Þistilfjörður is the widest valley (~18–33 km) whereas the Vopnafjörður catchment is characterized by three narrow valleys (~1–6 km), which are carved into the highland plateau. The Bakkaflói area in between comprises restricted lowlands, shallower valleys, and lower plateaus. These areas exhibit glacially streamlined terrain with bedforms that have not been previously mapped, although glacial striations are indicated on older maps (Sæmundsson, 1977). Besides, Patton et al. (2017) presented a rough estimate of a flow set extending from Jökuldalsheiði in the highlands to the coast in Vopnafjörður (Fig. 1B).

3. Methods

The principal data source used for mapping and analyzing the SSBs was the Arctic Digital Elevation Model (ArcticDEM) with a 2 m vertical and < 1 m horizontal resolution (Porter et al., 2018). The data has been corrected and mosaicked by the National Land Survey of Iceland (NLSI), the Icelandic Met Office, and the Polar Geospatial Center (Porter et al., 2018). Additionally, infrared Spot satellite images with 2.5 m resolution from NLSI and aerial images from Loftmyndir ehf., were used to facilitate the mapping. The mapping was ground verified by field checking selected areas within the study area.

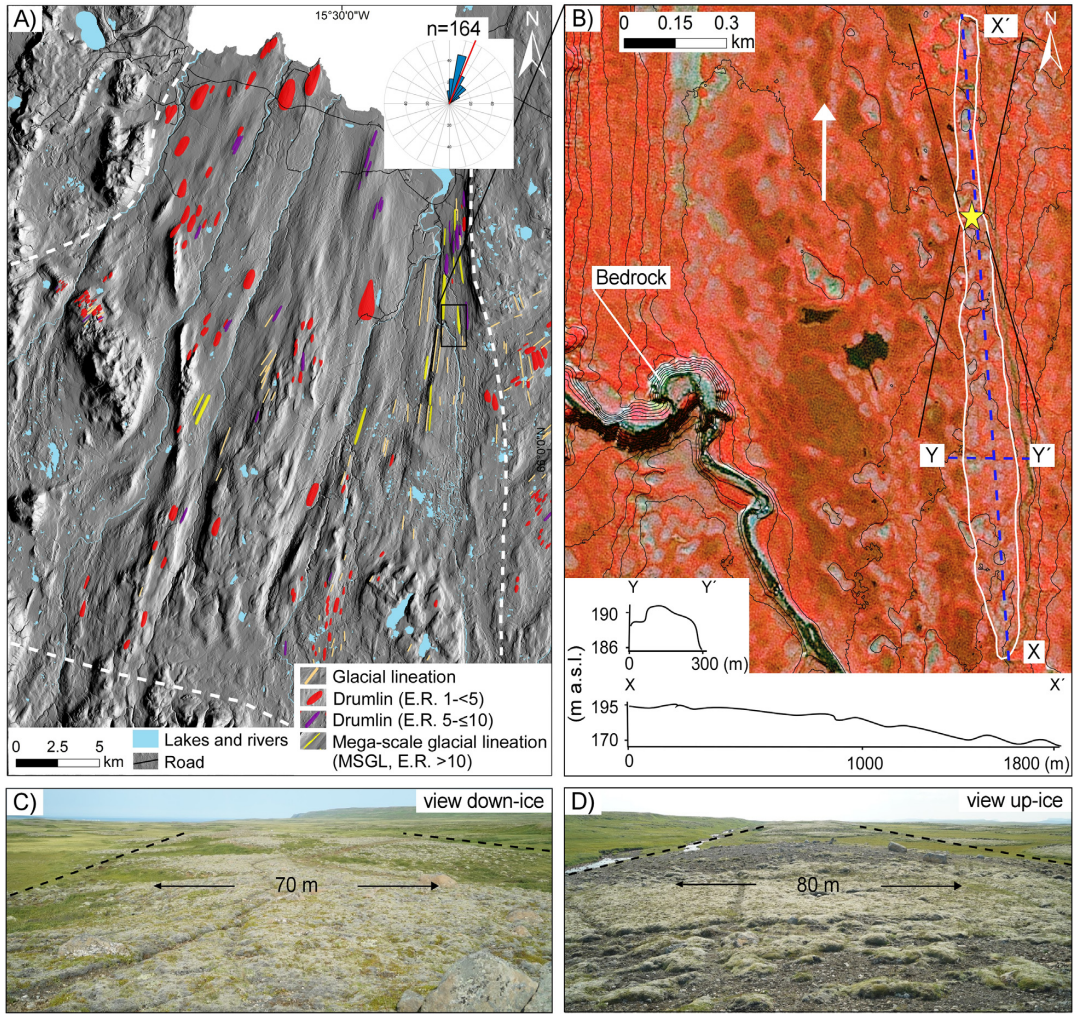

Fig. 3. (A) Streamlined subglacial bedforms and glacial lineations in the Þistilfjörður subarea. See Fig. 2 for location. Rose diagram indicates the orientation of the bedforms. Location of bedforms shown on B—D is indicated. (B) Example of a segmented MSGL with inset long (X-X') and cross (Y-Y') terrain profiles. Contour lines are 5 m. (C—D) Downglacier and upglacier view along the MSGL in B.

Geomorphological mapping of the SSBs was undertaken following the guidelines of Chandler et al. (2018), by combining the interpretation of remotely sensed data and field data. Analysis of the data and mapping was conducted in ESRI ArcGIS 10.4 and finalized in Canvas X. The identification and mapping of the SSBs were carried out at a scale of 1:3000. All data were handled in the Lambert Conformal Conic reference system, and elevations are in meters above sea level. Hillshaded relief models of the ArcticDEM were produced and used as a basis for the mapping. To avoid azimuth bias (Smith and Clark, 2005; Smith and Wise, 2007), the hillshades were illuminated from four different azimuths, 0°, 45°, 90° and 315°, selected according to the orientation of the bedforms, and one with the solar angle at 90° (i.e. overhead). The hillshades were vertically exaggerated by three to five with a solar angle of 25° to enhance subtle features. A slope map and 2-m contour lines were generated from the ArcticDEM to help delineating the bedforms. To minimize the influence of user bias, strict criteria were followed during the mapping (Smith and Clark, 2005; Hillier et al., 2015). For SSBs to be mapped, they had to show a clear orientation of elongation, be upstanding from the landscape in both axes, and have a clear break of slope. Mapping was therefore carried out using a combination of the hillshades with different azimuths, satellite and aerial images, slope map and contour lines. A polygon was drawn at the break of slope of each bedform. Although automated mapping techniques are increasingly being applied in glacial geomorphology, especially in areas with large numbers of similar features (>1000 to >10,000; Yu et al., 2015; Sookhan et al., 2016; Chandler et al., 2018), the bedforms here were manually digitized due to the geospatial resolution and the relatively small number (<800). The SSBs are classified into drumlins and mega-scale glacial lineation (MSGL), with the latter having elongation ratios of >10:1 (Stokes and Clark, 1999). We do however acknowledge that drumlins and MSGLs are a part of a morphological continuum and that this strict boundary is up for debate (Spagnolo et al., 2014; Ely et al., 2016). Therefore, in Figs. 3, 5 and 6, drumlins with elongation ratios <5:1 and 5–10:1 are separated for better visualization of the E.R. spectrum. If bedforms could not be delineated due to undiscernible break of slope but streamlining of the landscape was nonetheless clear, polylines were used to indicate the streamlining and mapped as glacial lineations. Despite the possibility that the streamlining of bedrock with negligible till cover may be the cumulative result of several ice sheet cycles (Hughes et al., 2010), we include streamlined bedrock in our mapping because of the difficulty in distinguishing separate glacial cycles in such areas.

To investigate the morphology of the SSBs, the length of the long axis, the width orthogonal to the long axis and the orientation of the long axis were measured for each bedform using the minimum bounding geometry tool in ArcGIS, as described by Napieralski and Nalepa (2010), although other approaches may also be useful depending on the bedforms' planar shape and elongation ratio (Jorge and Brennand, 2017). The elongation ratio (E.R.) is found by dividing the length with the width. The orientation of the bedforms was compiled in rose diagrams for each selected subarea. A point was created in the center of each bedform and the density calculated by counting the number of bedforms within each 4 km^2 grid cell. The packing of bedforms, i.e. the surface area of bedforms per 4 km^2, was calculated with the Point Density tool in ArcToolbox with bedform area as the population field. This cell size turned out to be the most effective one for visualizing bedform density and packing considering both bedform dimensions and map scale, similar to other studies (e.g. Rice et al., 2020).

4. Results

Streamlined subglacial bedforms (SSBs) and glacial lineations in NE-Iceland are distributed within the Þistilfjörður, Bakkaflói and Vopnafjörður fjord-valley systems and associated plateaus, such as Jökuldalsheiði and Bakkaheiði (Fig. 2A). The SSBs are more abundant on the highland plateaus (above ~400 m a.s.l.) and elevated terrain near the coast (above ~200 m a.s.l.), except in Þistilfjörður where they mainly occur in the lowlands below 300–400 m a.s.l. (Fig. 2B). Mapping revealed 797 SSBs within the entire study area, as well as additional 417 glacial lineations, which were mapped to further indicate palaeo-ice flow direction.

4.1. Þistilfjörður

The Þistilfjörður area is characterized by sparse and generally widely spaced SSBs ($n = 164$) and glacial lineations, with 7% ($n = 12$) classifying as MSGLs (Fig. 3A). Although the range in SSB length stretches from 101 m to 2694 m, the median is 576 m while the mean is 717 m (Table 1). Shorter landforms are mainly focused on the coastal, western, and southern parts whereas longer and more elongate landforms are concentrated in the eastern part where glacial lineations, drumlins

Table 1
Morphometrics of streamlined subglacial bedforms in NE-Iceland.

		Þistilfjörður	Bakkaflói	Bakkaheiði	Vopnafjörður-Jökuldalsheiði	All
n		164	77	246	310	797
	Median	576	451	530	749	623
	Mean	717	501	649	827	719
	Max	2694	1095	3841	2905	3841
	Min	101	135	154	200	101
	10%	219	292	265	387	291
	90%	1322	799	1120	1345	1253
Length (m)	Stdew	495	210	426	423	442
	Median	151	154	147	192	163
	Mean	179	167	161	208	185
	Max	942	347	459	666	942
	Min	36	61	51	43	36
	10%	72	92	88	108	86
	90%	309	253	262	315	299
Width (m)	Stdew	136	67	72	96	104
	Median	3.2	2.9	3.6	3.7	3.5
	Mean	4.4	3.1	4	4.1	4.0
	Max	16.8	8.3	14.4	12.8	16.8
	Min	1.9	1.9	2	1.9	1.9
	10%	2.4	2.2	2.5	2.8	2.5
	90%	8.0	4.1	5.6	6.0	5.9
E.R.	Stdew	2.8	1.1	1.9	1.7	2
Orientation(°)		23	35	6	38	–
Area (km^2)		1400	550	500	2300	2300
MSGLs		12	0	9	11	32

and MSGLs are juxtaposed (Fig. 3A). The width of the SSBs has a median of 151 m (range:36–942 m) a, and the median elongation ratio is 3.2:1 (range: 1.9:1–16.8:1; Table 1). In the southeastern part of this area, a complicated network of hummocky and transverse ridges appears to superimpose highly elongate SSBs, presumably MSGLs, which are thus very difficult to map. Many of these highly elongate bedforms underlying the hummocky and transverse ridges appear to be segmented (Fig. 3B-D). The SSBs show a mean orientation of 23° (SSW-NNE) (Fig. 3A; Table 1). Most of the largest bedforms in Þistilfjörður appear to be streamlined bedrock hills.

4.2. Þistilfjörður-Bakkaflói transition zone

On the eastern margin of the Þistilfjörður area, a transition to the Bakkaflói area occurs within a 2.5–4.5 km wide zone. This zone is morphologically complicated but seems to comprise ribbed moraine with individual ridges of various orientation and highly streamlined but segmented glacial bedforms with S—N orientation. These segmented bedforms appear to be superimposed by generally SW-NE orientated SSBs and lineations pertaining to the Bakkaflói area (Fig. 4). This superimposition is indicated by some of the S—N orientated bedforms (black lines and polygons on Fig. 4) in that the sediment within them appears to be smeared-out towards the northeast. Sediments within SW-NE orientated bedforms do not seem to be smeared out in the same way to the north. Thus, these cross-cutting relationships suggest that ice flow in this area was initially towards the north and subsequently towards the north-east (Fig. 4). Unfortunately, suitable bedrock outcrops containing striations that could potentially verify these crosscutting relationships are absent in this area. However, about 5 km north of this area, striations with an orientation towards the north have been reported (Sæmundsson, 1977; Norðdahl and Hjort, 1993).

4.3. Bakkaflói area

In the Bakkaflói area, the main cluster of SSBs and glacial lineations occurs within a relatively well-developed drumlin field that is



Fig. 4. Overview of the transistion zone between the Þistilfjörður and Bakkaflói areas showing cross-cutting ice flow indicators. N-S orientated and SW-NE orientated streamlined subglacial bedforms and lineations and reconstructed ice flow are indicated in black and white, respectively. Ovals indicate mapped SSBs, and solid and dashed lines indicated mapped glacial lineations. The N-S streamlining on the western (Þistilfjörður) side appears to be superimposed by the SW-NE streamlining on the eastern (Bakkaflói) side.

located on the Kverkártunga plateau between two shallow valleys (Fig. 5A). Several similar features occur just to the south, east, and north of this plateau. A total of 77 SSBs were mapped within the Bakkaflói area. Their length and width are rather uniform; the length has a median of 451 m (range:135–1095 m), and the width a median of 154 m (range: from 61 to 347 m). The median elongation ratio of the SSBs in the Bakkaflói area is 2.9:1, within a range of 1.9:1–8.3:1 (Table 1). The SSBs and glacial lineations in this area are mainly orientated SW-NE (35°) (Fig. 5A, E-F), although a few in the southern part of this area are orientated N-S suggesting a curvature in the former ice flow direction within this area (Fig. 5A).

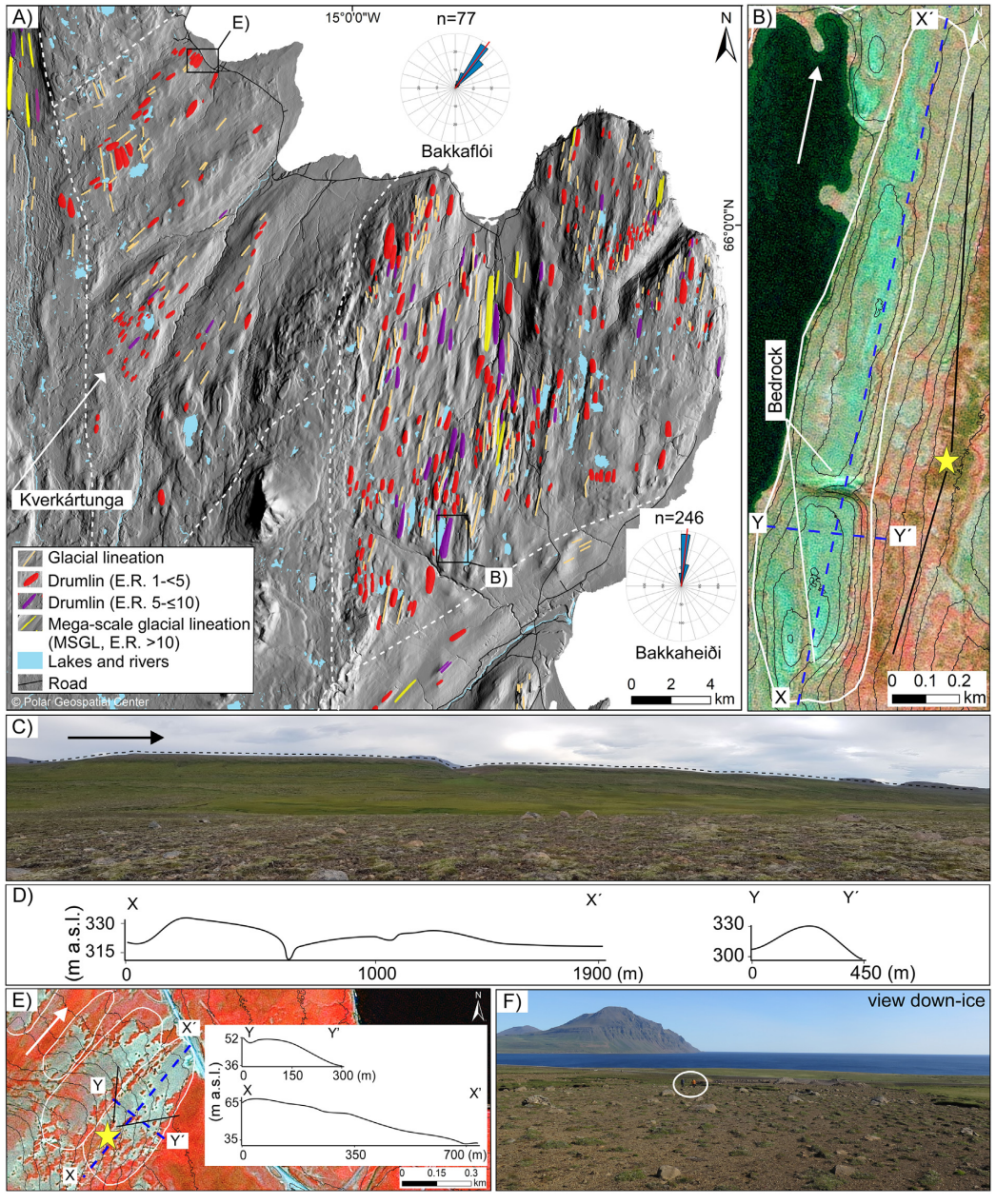

Fig. 5. (A) Streamlined subglacial bedforms and glacial lineations in the Bakkaflói and Bakkaheiði subareas. See Fig. 2 for location. Rose diagrams indicate SSBs orientation. Location of bedforms shown on B and D is indicated. (B) An example of a SSB on Bakkaheiði with long (X-X') and cross (Y-Y′) terrain profiles indicated by blue dashed lines. Contour lines are 5 m. (C) A panorama view of the SSB shown in B with black, dashed line outlining the bedform surface profile. (D) Terrain long and cross profiles of the bedform shown in B and C. (E) Example of a SSB in the Bakkaflói area. Long (X-X') and cross (Y-Y′) terrain profiles indicated by blue dashed lines and shown on the inset diagram. Contour lines are 5 m. (F) Down-ice view along the subtle bedform shown in E. Persons for scale encircled.

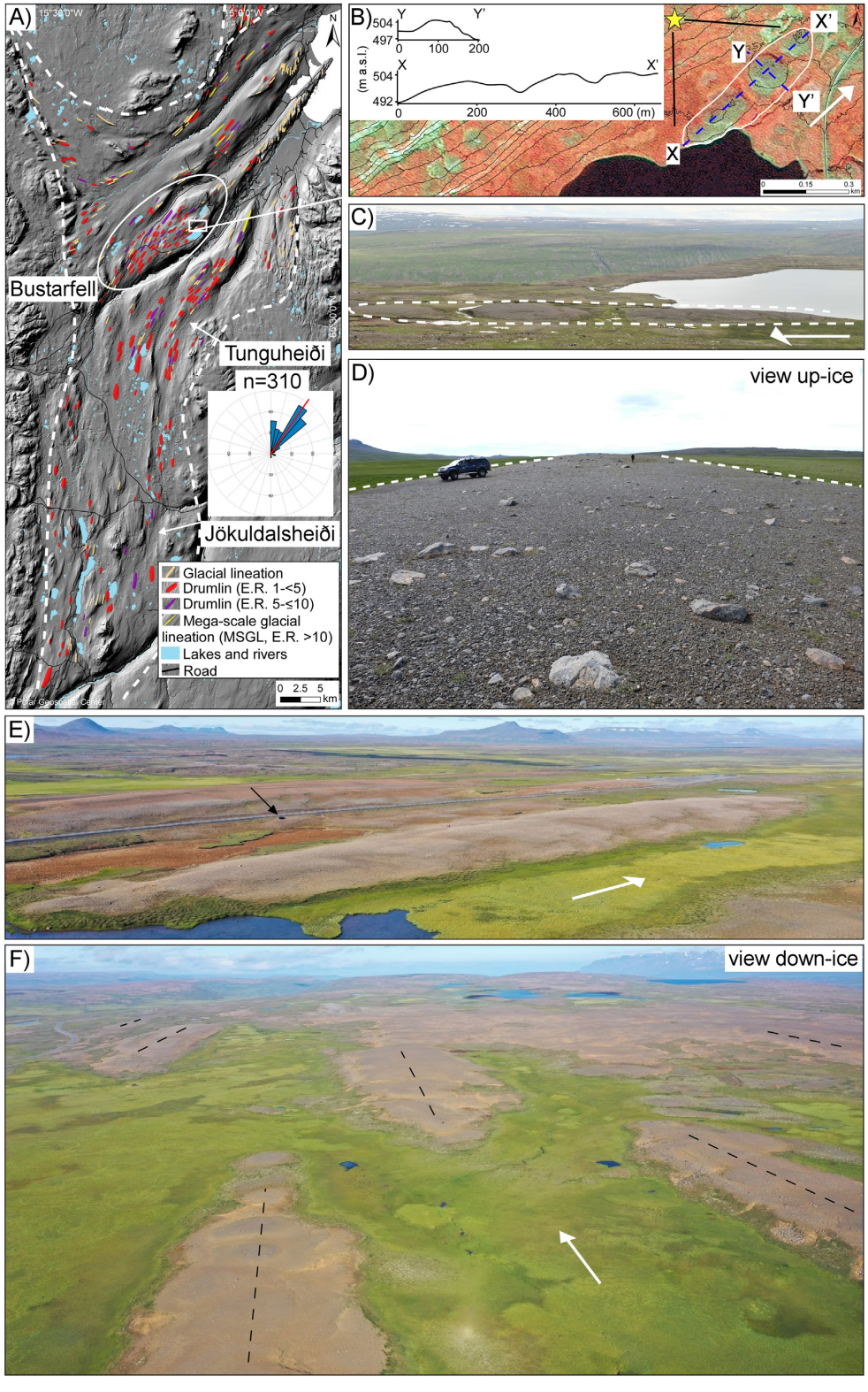
A)
19°30'0"W
19°0'0"W
N
Bustarfell
Tunguheiði
n=310
Jökuldalsheiði
Glacial lineation
Drumlin (E.R. 1-<5)
Drumlin (E.R. 5-≤10)
Mega-scale glacial lineation (MSGL, E.R. >10)
Lakes and rivers
Road
0 2.5 5 km
B)
Y
Y'
504
497
0
100
200
X
X'
504
492
0
200
400
600 (m)
(m a.s.l.)
X'
Y
Y'
X
0 0.15 0.3 km
C)
D)
view up-ice
E)
F)
view down-ice

4.4. The Bakkaheiði plateau

The Bakkaheiði plateau reveals a dense population ($n = 246$) of closely spaced drumlins, MSGLs and glacial lineations that are orientated S—N (Fig. 5A. Only about 4% ($n = 9$) of the SSBs classify as MSGL (Table 1). The median length, width, and elongation ratio of the SSBs on Bakkaheiði are 530 m (range: 154–3841 m), 147 m (range: 51–459 m), and 3.6:1 (range: 2–14.4:1), respectively, with the longest bedform being nearly 4 km long and a maximum elongation ratio of 14.4 (Table 1). The Bakkaheiði population has an abrupt boundary to the west where SSBs and glacial lineations become totally absent above 750 m a.s.l. (Fig. 2B), and to the south where it appears to be truncated by SW-NE orientated bedforms and lineations pertaining to the Vopnafjörður system (Fig. 5A). The bedrock strata in Bakkaheiði mainly have a southward strike (dip towards west) along a monoclinic flexure zone, although an opposite strike and dip also occurs just east of this zone (Icelandic Institute of Natural History, 2019). These strata frequently crop out on the surface in the form of low, elongate bedrock ridges. Thus, glacial lineations and streamlined bedforms with a bedrock core are common and occur juxtaposed with sedimentary bedforms (Fig. 5B-C). The bedrock crops out in a few places but tends to be much weathered; hence, striations are rare but those reported have an orientation towards the NNE (Sæmundsson, 1977; Norðdahl and Pétursson, 2005).

4.5. The Vopnafjörður-Jökuldalsheiði area

The Vopnafjörður system just south of Bakkaheiði includes three SW-NE orientated valleys in the outer part and the Jökuldalsheiði plateau that stretches southwards into the highlands north of the present Vatnajökull ice cap (Figs. 1 and 2). Collectively, this system contains a total of 310 SSBs with a median length of 749 m (range: 200–2905 m), median width of 192 m (range: 43–666 m), and elongation ratios with a median of 3.7 (range 1.9:1–12.8:1) (Table 1). A large majority of these bedforms classify as drumlins (~96%) as only a few MSGLs were observed ($n = 11$) (Fig. 6A). In the outer part of the valleys, elevated bedrock separating the three valleys contains glacial lineations with predominantly S—N orientation, which correlates with the SSBs on Bakkaheiði and indicates an older palaeo-ice flow direction towards the north. On the Bustarfell and Tunguheiði plateaus, dense clusters of sedimentary drumlins form well-defined drumlin fields with rather consistent drumlin sizes and shapes (Fig. 6A-F). These drumlins are often cross-cut by transverse channels that may be of ice-marginal origin (Fig. B—C). Bedforms on the Jökuldalsheiði plateau are rather sparse and have more variable morphometrics (Fig. 6A). The bedforms within the Vopnafjörður system reveal a converging pattern with variable orientations in the highlands but largely parallel the trend of the fjord-valley in the central part with more constant SW-NE orientations (Fig. 6A). This is consistent with the orientation of a few striations previously reported from this area (Sæmundsson, 1995; Norðdahl and Pétursson, 2005). On the northern side of this system, near the mouth of the fjord, this orientation clearly crosscuts the N-S orientation of the bedforms within the Bakkaheiði subarea (Fig. 6A), indicating that ice flow within the Vopnafjörður system may have been active for a longer period.

4.6. Statistics of the streamlined subglacial bedforms

In total, 797 SSBs and 417 glacial lineations have been identified and mapped in our study area in NE-Iceland. For the SSBs identified, 765 (96%) classify as drumlins and 32 (4%) as MSGL. The morphometrics are summarized in Table 1 and illustrated with histograms on Fig. 7. Collectively for all the bedforms, the median length is 623 m with a range of 101–3841 m (mode: 300–500 m), and the median width is 163 m with a range of 36–942 m (mode: 100–150 m). The median elongation ratio for the entire dataset is 3.5:1 with a range of 1.9:1–16.8:1 (mode: 3:1–4:1). For drumlins and MSGLs separately, the mean elongation ratios are 3.8:1 and 11.7:1, respectively. The histograms all demonstrate a unimodal distribution with positive skews, similar to other studies of SSBs morphometrics in both Pleistocene and modern glacial environments (e.g. Clark et al., 2009; Stokes et al., 2013; Principato et al., 2016; Benediktsson et al., 2016; Hillier et al., 2018), and the box plots show that 50% of the bedforms are between 414 and 915 m long, 119–225 m wide and with an elongation ratio between 2.9 and 4.7:1 (Fig. 7). This also suggests that the dimensions at which drumlin formation is initiated are seldom below the 100 m magnitude, which may imply that few small bedforms are generated (Hillier et al., 2018). A linear regression between length and width reveals a moderately strong relationship between these two variables ($r^2 = 0.47$) with less than half of the variance in width explained by the variance in length (Fig. 8A). This may reflect a variable degree of bedform maturity, influenced by residence time beneath the ice (duration of ice flow), but moreover indicates that the length-to-width ratio is also influenced by other factors, such as substrate structure and composition, and subglacial hydrological and glaciological processes (Clark et al., 2009; Benediktsson et al., 2016). The linear regression between the length and elongation ratio reveals a weak relationship ($r^2 = 0.27$) with less than a third of the variance in elongation ratio explained by the variance in length, (Fig. 8B). In contrast, a linear relationship between width and elongation ratio is not identified although the plot on Fig. 8C demonstrates that the largest elongation ratios (from ~8:1 to 16.8:1) occur for the narrowest bedforms and that the far widest bedforms have low elongation ratios (Fig. 8C). These morphometrics suggest that the SSBs in NE-Iceland comprise a continuum from stubby bedforms to highly elongated bedforms as the low- and high-end members, respectively (Ely et al., 2016). Bedforms with an elongation ratio > 10 classify as MSGLs and represent only 4% of the dataset ($n = 32$; Table 1), which is somewhat lower than reported from NW Iceland (Principato et al., 2016). The MSGL are most frequent on the Bakkaheiði plateau, in the eastern part of Þistilfjörður, and on the plateaus and slopes above the Vopnafjörður valleys (Figs. 2, 3, 5, 6).

Analysis of the density and packing of the SSBs reveals that bedforms are most scattered in Þistilfjörður and Jökuldalsheiði and most clustered in specific areas of Bakkaflói, Bakkaheiði and Vopnafjörður where 4–9 SSBs per 4 km^2 grid cell is quite common. More specifically, the highest density of SSBs occurs within the drumlin fields of Bustarfell and Kverkártunga as well as on the Bakkaheiði plateau, where 7–9 and even up to 18 SSBs occur, respectively, per 4 km^2. These bedforms are all relatively small, which partly explains their high density (Fig. 9A). The packing of the SSBs shows similar pattern to the overall density, with prominent areas of high packing on plateaus and slopes above the Vopnafjörður valleys as well as on the Bakkaheiði plateau (Fig. 9B).

5. Discussion

5.1. SSB morphometry and implications for processes of formation

The morphometry of the SSBs within our study area is quite variable, which probably indicates diverse composition and internal structure, maturity, as well as subglacial processes responsible for their formation

Fig. 6. (A) Streamlined subglacial bedforms and glacial lineations in the Vopnafjörður-Jökuldalsheiði area. Rose diagram shows their orientation. The Bustarfell drumlin field is encircled. (B) Drumlin Thury as an example of a drumlin within the Bustarfell drumlin field. Blue dashed lines indicate the long (X-X') and cross (Y-Y') profiles shown on the inset. Contour lines are 5 m. Overview photograph of drumlin Thury from the viewpoint (yellow star) indicated on B. Note the two transverse channels that cut across the drumlin. (D) Ground view from a SSB on Tunguheiði. (E and F) Drumlins within the Bustarfell drumlin field where ice flow was towards the northeast (white arrows). Note the car (black arrow) for scale on E. Dashed lines on F indicate the long axes of the most obvious drumlins in this view.

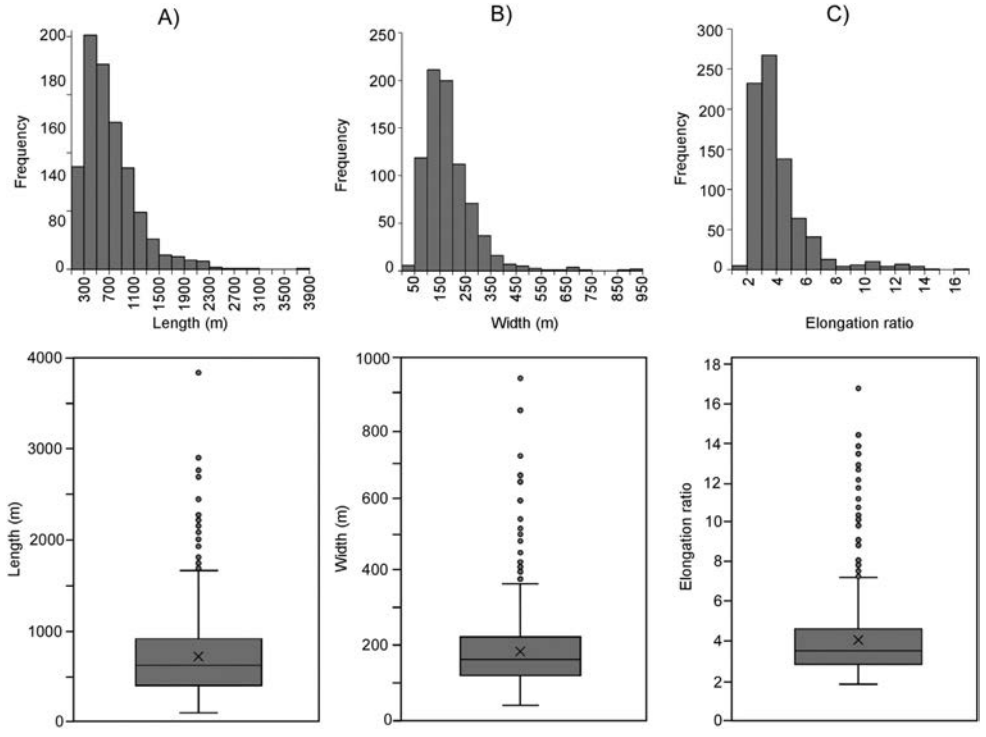

Fig. 7. Size-frequency distribution of the morphometrics of the streamlined subglacial bedforms presented with histograms and boxplots. A) Length. B) Width. C) Elongation ratio. The median and average of the datasets are denoted by the horizontal line and the 'x', respectively, within the box plots. Half (50%) of the values occur within the boxes and the other half outside. The dots are outliers.

(Krüger, 1987; Clark et al., 2009; Stokes et al., 2011; Dowling et al., 2015). The mean length, width, and elongation ratio of our SSBs are similar to those of both Pleistocene (Clark et al., 2009; Dowling et al., 2015) and modern drumlin fields (Krüger, 1987; Jónsson et al., 2016; Hillier et al., 2018) indicating that the SSBs have been formed through the streamlining of pre-existing landscape and that few if any small drumlins are produced (Figs. 7 and 8). Our study area includes well-developed drumlin fields, such as in Kverkártunga, Bustarfell, and Tunguheiði, with SSBs of relatively uniform size and shape within each field (Figs. 5 and 6). This implies that the substrate from which the bedforms develop in these fields is rather homogenous and that the processes under which they formed were persistent (Dowling et al., 2015; Benediktsson et al., 2016; Iverson et al., 2017). Therefore, these areas may also be considered as indicating the axial zones of ice streaming where relatively high ice-flow velocities persisted for a long time, either during maximum glaciation or deglaciation, or both. Although the SSBs in these fields appear to be primarily sedimentary, it is difficult to determine exactly which subglacial processes contributed to their formation without data on their internal structure and composition. A potential suitable modern analogue exists at Múlajökull, Iceland, where drumlins of similar dimensions consist primarily of till layers and were formed through a combination of erosion and deposition during successive surge cycles (Johnson et al., 2010; Benediktsson et al., 2016). Controlled by the distribution of effective stress on the bed, net till aggradation over the entire bed during surging and net erosion on drumlin heads, flanks and inter-drumlin areas during quiescent

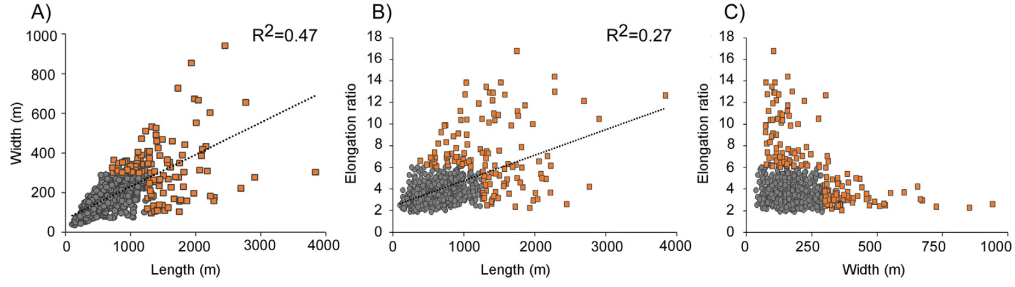

Fig. 8. Relationships between SSB length and width (A), length and elongation ratio (B), and width and elongation ratio (C). Values within the 90th percentile are represented by gray circles and the remaining 10% by orange squares.

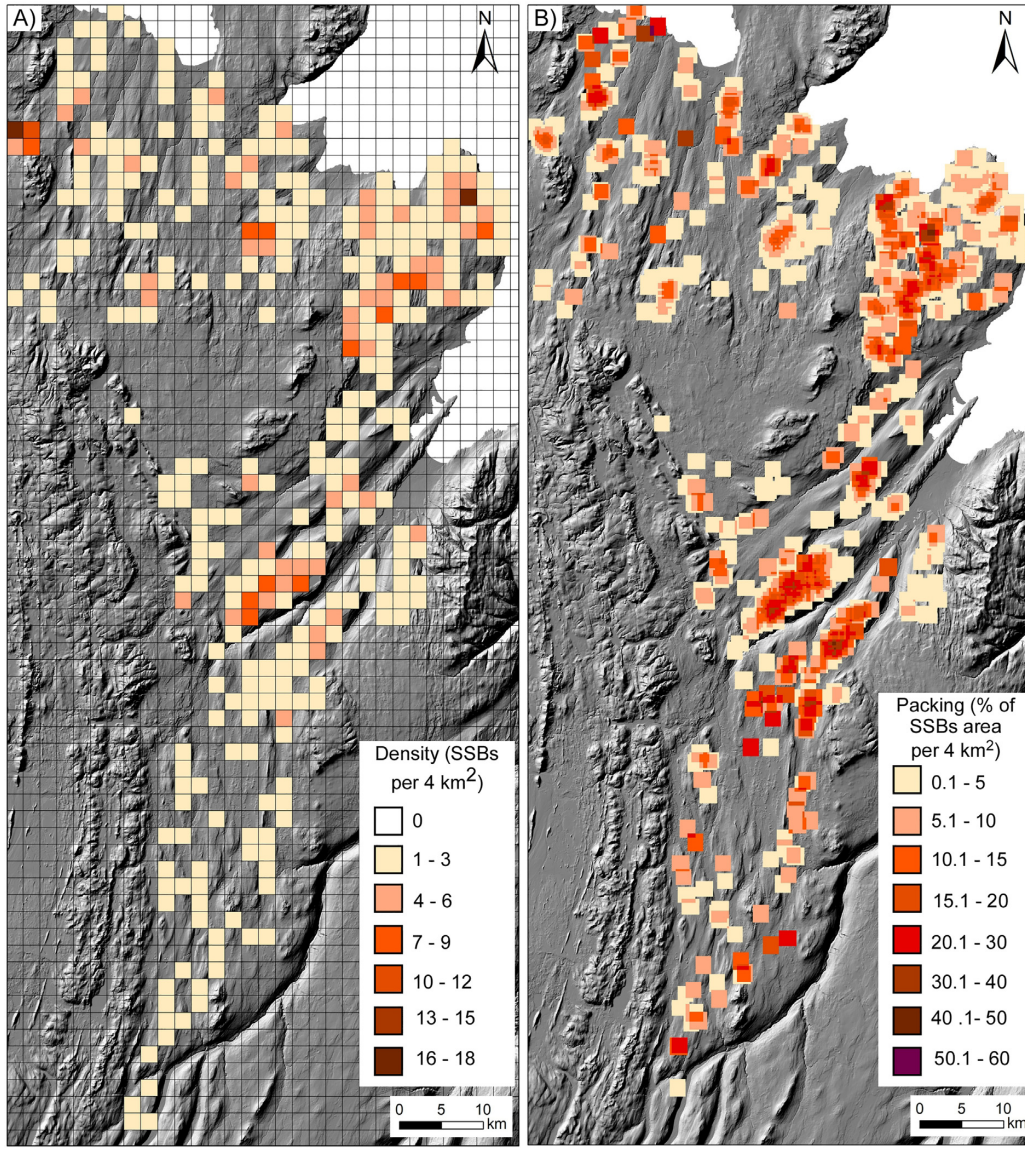

Fig. 9. A) Density of SSBs per 4 km^2. B) Packing of SSBs per 4 km^2.

flow caused the drumlins to grow rapidly in relief and elongation and migrate downglacier (Benediktsson et al., 2016; Iverson et al., 2017). If the drumlins within these drumlin fields in NE-Iceland were formed under fluctuating ice-flow velocities (e.g. periodic slow-down or shut-down), this model predicts that they consist of multiple till layers with unconfomities below the uppermost till at drumlin heads and flanks (Benediktsson et al., 2016; Iverson et al., 2017). In the absence of fast flow (surging), the drumlins would have formed through erosion only (Iverson et al., 2017), causing lowering of the bed and leaving no substantial stratigraphic record except a layer of deforming subglacial debris that eroded into antecedent sediments or bedrock (Eyles et al., 2016; Sookhan et al., 2016). This could possibly apply to the SSBs on Bakkaheiði, in Þistilfjörður and on Jökuldalsheiði that are apparently bedrock cored with a veneer of till. Consequently, it raises the question if these SSBs are formed initially under sluggish ice and if the erosion of the bed is a means to create a streamlined, low-friction surface that ultimately allows faster ice flow and ice streaming (Eyles et al., 2016). Additional studies of the SSBs in NE-Iceland should aim at deciphering their internal architecture and compositions in order to better determine which processes contributed to fast ice flow and the formation of the streamlined terrain.

5.2. Configuration and cross-cutting flow-sets of palaeo-ice streams

The mapped streamlined subglacial bedforms (SSBs) show a pattern that we interpret as different flow-sets of several palaeo-ice streams in NE-Iceland. The SSBs in Þistilfjörður suggest a slightly convergent flow from the highlands to the lowlands, indicating funneling of ice towards

the Þistilfjörður fjord and trough beyond (Fig. 3A; Spagnolo and Clark, 2009). The SSBs and glacial lineations in this area are of variable dimensions from small and less elongated drumlins to large bedrock forms and highly elongated MSGLs. This possibly indicates different generations of SSBs and superimposed flow sets, which, however, share a common, dominant flow direction to the north during full glaciation and deglaciation phases and thus, do not reveal any obvious cross-cutting relationships. An exception to this occurs within a narrow zone at 150–250 m a.s.l. between the Þistilfjörður and Bakkaflói areas where subtle elongated and often segmented bedforms crosscut at almost right angles (Fig. 4). We interpret this as the superimposition of two different flow-sets: an older one with ice flow towards the north and a younger one with ice flow to the northeast and east off the elevated ground between the two areas. In the Bakkaflói and Bakkaheiði area, the SSBs clearly represent two generations of palaeo-ice streaming with the S—N orientated flow-set on the Bakkaheiði plateau predating the SW-NE flow-set in Kverkártunga and adjacent areas in Bakkaflói (Figs. 5 and 10). The Bakkaheiði flow-set with SSBs orientated S—N also clearly pre-dates and is cross-cut by the SW-NE flow-set in Vopnafjörður (Figs. 2 and 5). Although some of the SSBs within the Bakkaheiði flow-set appear to be sedimentary in composition, most of them are bedrock-cored with a relatively thin sediment cover (Fig. 5B-C). This is also true for the southernmost part of this flow set on the narrow peninsula that extrudes from the coast in Vopnafjörður. Because the location, morphology, and formation of bedrock-cored SSBs along structural geological lineaments tend to be controlled by the bedrock characteristics (Newton et al., 2018), it is worth considering if the SSBs within this flow-set truly reflect the palaeo-ice stream flow direction or if they are merely a result of the attenuation of S—N orientated bedrock forms by obliquely overriding ice. Our data reveal no oblique superimposition by SSBs or remolding of bedrock lineaments in this area, as reported from many other palaeo-ice stream beds (e.g. Hughes et al., 2010; Evans et al., 2020), that could support cross-cutting flow-sets in this area. Consequently, we interpret the bedrock-cored SSBs within the Bakkaheiði flow-set as representing long-term, cumulative palaeo-ice streaming towards the north (Krabbendam et al., 2016). This resembles the Lögurinn-Úthérað lowland area 40–50 km southeast of Bakkaheiði (Fig. 2) where remolded bedrock, crag-and-tails, and drumlins parallel or sub-parallel the northward bedrock strike but nevertheless represent the flow direction of a palaeo-ice stream during the LGM and the deglaciation (Norðdahl et al., 2019).

The abrupt cross-cutting of the Bakkaheiði flow-set by the SW-NE orientated SSBs immediately to the south indicates the flow-set of a relatively younger, northeastward flowing palaeo-ice stream in the

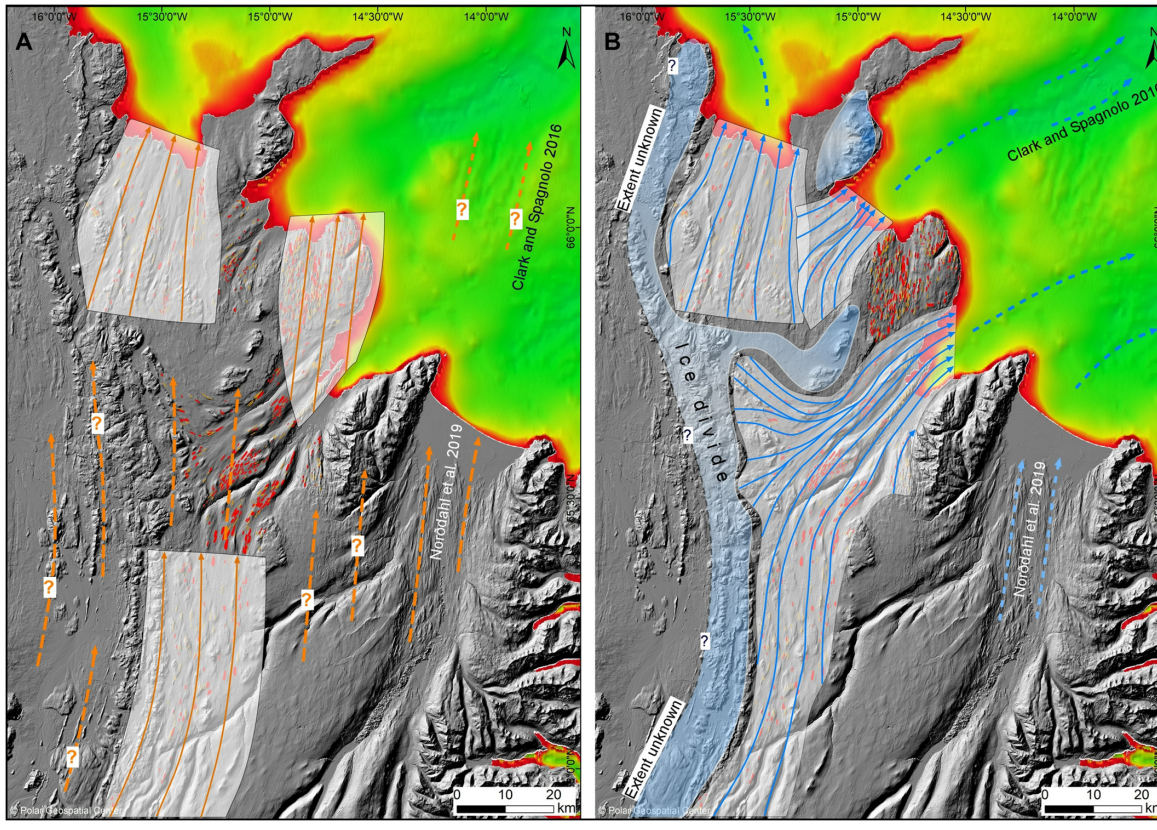

Fig. 10. Hypothesized flow sets of cross-cutting palaeo-ice streams in NE-Iceland. A) Flow-sets related to a maximum phase of glaciation during which ice flow was predominantly towards north independent of underlying topography. A major E-W orientated ice divide was located near or above the present Vatnajökull ice cap (south of this map; see Fig. 1). This northward ice flow corresponds to a NNE trending shallow trough on the shelf. B) Flow-sets related to deglaciation when the ice sheet had become thinner and ice streams were topographically controlled. A major ice divide was located above the mountain range to the west of the study area and in the highland area between Þistilfjörður and Vopnafjörður. Converging palaeo-ice stream flow characterized the areas of Jökuldalsheiði-Vopnafjörður, Bakkaflói, and Þistilfjörður. This convergent flow pattern suggests the onset zones of ice streaming and implies that the trunk flow zones were mainly located within troughs on the shelf (indicated by dashed, blue arrows; described by Spagnolo and Clark, 2009). Note the cross-cutting of the older NNE-trending trough (on A) by the younger NE-trending trough, as identified by Clark and Spagnolo (2016).

Vopnafjörður area (Figs. 5 and 6). This flow-set extends far into the highlands north of the present Vatnajökull ice cap and includes S—N orientated SSBs on the Jökuldalsheiði plateau. Because of the variable dimensions of the SSBs in the Jökuldalsheiði area (upstream of the Vopnafjörður valleys and uplands), it is possible that they represent different generations of palaeo-ice streaming, as in the Þistilfjörður area, with the larger and smaller bedforms resulting from long-term and short-term fast ice flow, respectively (Clark et al., 2009; Benediktsson et al., 2016; Krabbendam et al., 2016; Hillier et al., 2018).

5.3. Palaeo-ice stream dynamics, flow directions and location of ice divides

The SSBs in our study area in NE-Iceland are most common at altitudes between 200 and 650 m a.s.l., signifying that they predominantly occur on upland plateaus rather than in the valleys (Fig. 2B). This is somewhat similar to NW-Iceland where Principato et al. (2016) mapped SSBs mainly above 300–400 m a.s.l., although they also identified indistinct glacial lineations at altitudes down to about 100 m a.s.l. in valleys. Highly streamlined bedforms identified by Bourgeois et al. (2000) in central north Iceland and later mapped by McKenzie et al. (2017) and Benediktsson et al. (2018) also occur mainly at 300–400 m a.s.l. For our study area in NE-Iceland, where the marine limit occurs at altitudes up to 65 m a.s.l. (Norðdahl and Hjort, 1993; Sæmundsson, 1995; Richardsson, 1997), we suggest that the shortage of SSBs at low altitudes indicates that they are, at least partly, obscured by younger marine and glaciofluvial sediments or have been eroded by post-glacial fluvial action. In contrast, the absence of SSBs above 750 m a.s.l. probably indicates low ice-flow velocities and/or a partly frozen bed at or near ice divides – conditions that are generally unfavorable for the formation of SSBs (e.g. Kleman and Hättestrand, 1999; De Angelis and Kleman, 2008; Atkins, 2013; Dubé-Loubert et al., 2021). The overall low density of SSBs at the higher altitudes compared to within ice-stream trunk flow zones (Figs. 2 and 9) also implies that the upper limit of SSB distribution occurs at the onsets of ice streaming (De Angelis and Kleman, 2008). This is consistent with the location of ribbed moraine areas in the uplands of Vopnafjörður that mainly occur upstream of dense SSBs and are considered suggestive of ice stream onsets (Helgadóttir, 2020). A series of transverse ridges in the Bakkaflói area is also tentatively interpreted as ribbed moraine representing a transition zone between slow-flowing ice near ice divides and fast-flowing ice within an ice stream (Benjamínsdóttir, 2021). Consequently, it may be deduced that a major ice divide was at some point located over the mountain range at the western limit of the study area and a minor one over the highland plateau between Þistilfjörður and Vopnafjörður. The latter may have been induced upon ice thinning during late deglaciation whereas the former may possibly have persisted since the early phase of deglaciation. This agrees with previous reconstructions of Lateglacial ice divides in this region based on striations with opposite orientations on the eastern and western side of the mountain range as well as in the highlands between Þistilfjörður and Vopnafjörður (Sæmundsson, 1977; Pétursson, 1991; Norðdahl and Hjort, 1993; Sæmundsson, 1995; Norðdahl and Pétursson, 2005).

The ice flow pattern depicted by the SSBs suggests that all palaeo-ice streams extended beyond the present coast and into troughs on the Iceland shelf, through which they probably reached the shelf edge during maximum glaciation (Spagnolo and Clark, 2009; Patton et al., 2017). The high density and packing of SSBs on Bakkaheiði and in Vopnafjörður (Fig. 9) may suggest that these areas contained the highest ice-flow velocities and acted as the axial zones of ice streaming, and/or signify a mechanism of shutdown during separate phases of glaciation (Clark and Stokes, 2001). While the density and packing of SSBs is likely influenced by sediment availability in many areas, bedrock structure beneath a thin sediment cover may also play a role, as indicated by the bedrock-cored SSBs on Bakkaheiði where the bedrock strike parallels or sub-parallels the former ice-flow direction. Modelling experiments suggest that an *E*-W orientated central ice divide was stable at the time of maximum thickness during the LGM (~1500–2000 m) and throughout the entire glaciation (Patton et al., 2017). In the eastern part of Iceland, this ice divide was probably located near or above the present Vatnajökull ice cap (Bourgeois et al., 2000; Patton et al., 2017). Our data suggest that an ice stream may have flowed northwards from this ice divide and obliquely across but not along the Vopnafjörður valleys (Fig. 10A). This implies that the IIS was thick while this ice stream was active, and that ice flow was independent of underlying topography during maximum glaciation. Similar scenarios are well known from the interior of the Laurentide and Fennoscandian ice sheets, where thick ice streams crossed preglacial valleys (Ross et al., 2009; Putnins and Henriksen, 2017), and from Western Norway where LGM ice flow went right across deep valleys and fjords (Mangerud et al., 2019). Northward flow across the Vopnafjörður valleys conforms to the Bakkaheiði flow-set and implies that the S—N orientations observed on the southern part of the Jökuldalsheiði highland plateau and in the Þistilfjörður area could be the cumulative result of more than one generation of ice streaming (Hughes et al., 2010). Consequently, smaller, and less elongated SSBs would represent a more immature stage of development, possibly due to lower ice flow velocities or shorter duration of flow (Clark et al., 2009; Benediktsson et al., 2016; Iverson et al., 2017; Ely et al., 2018). Similarly, the size of SSBs within the well-defined drumlin fields of Kverkártunga, Bustarfell and Tunguheiði (see Figs. 2, 5, and 6 for locations) is rather uniform, which possibly implies that NE trending flow-sets in general are primarily a result of only one generation of ice streaming under relatively stable conditions – hence, a signature of deglaciation. In contrast, the larger variety of SSB morphometries within S—N orientated flow-sets results from a longer and more variable period of ice streaming from a maximum glaciation to deglaciation. By dating the timing of the formation of SSBs, this hypothesis could be tested. However, datable material within subglacial bedforms tends to be rare and thus, this may have to be tested with ice sheet modelling.

Upon ice thinning during deglaciation, ice stream flow directions became progressively more controlled by the underlying topography with a regional ice divide located over the N-S orientated mountain range (Þríhyrningsfjallgarður-Dimmifjallgarður) that delimits the study area to the west (Figs. 2 and 10B). Previous reconstructions of the IIS have also suggested a regional ice divide in this area either during the LGM (e.g. Bourgeois et al., 2000) or the following deglaciation (e.g. Norðdahl and Hjort, 1993). Local ice divides would also have formed over the Smjörfjöll-Hellisheiði massif and then progressively in elevated terrain between the different flow-sets, such as between Þistilfjörður and Bakkaflói as well as Þistilfjörður and Vopnafjörður (Fig. 10B), as the ice sheet continued to thin. Interestingly, Spagnolo and Clark et al. (2009) and Clark and Spagnolo (2016) identified troughs on the northeastern shelf that overlap at different depths, i.e. a shallower one that is incised in a NNE direction and cross-cut by a deeper one orientated SW-NE. Clark and Spagnolo (2016) suggested these troughs represented different ice flow directions and asynchronous trough excavations during multi-phase glacial evolution of the shelf morphology. Our interpretation of different palaeo-ice stream flow directions and associated migration of ice divides during phases of maximum glaciation and deglaciation is consistent with these cross-cutting relationships on the northeastern shelf (Fig. 10). Collectively, these offshore and onshore data imply that ice-flow directions changed and ice divides migrated significantly during a transition from maximum glaciation to deglaciation due to ice sheet thinning and progressively increased control by underlying topography, as has been described also from larger Pleistocene ice sheets (e.g. McMartin and Henderson, 2004; Hodder et al., 2016). This transition possibly involved competition for ice discharge between the two ice streams on the northeastern shelf and associated piracy of ice drainage basins, which ultimately controlled the switching of ice flow – a mechanism well-known from the marine-based margins of the Laurentide, the Greenland, the British-Irish, and the West Antarctic ice sheets (e.g. Greenwood and Clark, 2009b; Graham et al., 2010; Brouard and Lajeunesses, 2019).

It is difficult to estimate how much thinning or retreat was required for the ice flow to become topographically controlled, but the Vopnafjörður flow-set and its cross-cutting of the Bakkaheiði flow-set demonstrate that topographic control on the ice flow was established before the ice sheet margin retreated up from the troughs and onto land. Estimating the absolute timing of this transition is challenging without chronological data. However, data from the western and northern Iceland shelf, as well as from coastal areas in W- and NE-Iceland suggest that the IIS margin was positioned at the mid-shelf from 18.2 to as late as 15.3 ka BP but had lost a substantial part of its volume and retreated rapidly to a position inside the present coast around 14.6 ka BP (Andrews et al., 2000; Eiríksson et al., 2000; Jennings et al., 2000; Norðdahl and Pétursson, 2005; Norðdahl and Ingólfsson, 2015; Patton et al., 2017; Benediktsson et al., in press). Therefore, it is likely that topographic influence on palaeo-ice streaming in NE-Iceland was established between ca. 18 and 16 ka BP, and certainly before 14.6 ka BP. According to Norðdahl and Ingólfsson (2015), the extremely rapid retreat between 15.3 and 14.6 ka BP caused a draw-down of the ice-sheet surface and acceleration of ice flow within ice streams. It may thus be speculated if the SSBs of the younger flow-sets in our study area, e.g. in Vopnafjörður and Bakkaflói, are the result of increased ice-flow velocities during this phase in the deglaciation of the IIS. This also bears on the overall influence of ice streams on the IIS and if/how it progressively decreased during the deglaciation, as has been shown for large Pleistocene ice sheets (Margold et al., 2015; Stokes et al., 2016).

5.4. Implications for reconstructions of the Iceland Ice Sheet

The glacial geomorphology and chronology of sediments and bedforms on the western, north-western, and northern Iceland shelf indicates that the IIS extended to the shelf edge during the LGM (e.g. Syvitski et al., 1999; Norðdahl and Pétursson, 2005; Andrews, 2008; Benediktsson et al., 2021b). Unfortunately, similar data is largely absent from the north-eastern, eastern, and southern shelf of Iceland, which hampers reliable reconstructions of palaeo-ice streaming and ice sheet extent (Benediktsson et al., 2021b). Thermomechanical modelling experiments suggest that the IIS culminated at the shelf edge around 22.9 ka BP and was characterized by an E-W orientated central ice divide and topographically controlled ice streams (Patton et al., 2017). This broadly corresponds to onshore and offshore records. Our reconstruction of palaeo-ice streams in NE-Iceland and correlation with offshore troughs incised in a NNE direction (Clark and Spagnolo, 2016) supports the presence of an E-W ice divide and an overall northward ice flow in this region. This also implies that ice streaming may have originated in onset zones near the present Vatnajökull ice cap and extended to the northern shelf during maximum glaciation. This region should be mapped in detail in order to test this hypothesis, but it must be acknowledged, however, that onset zones of large ice streams are often rarely preserved because of landscape reshaping during prolonged deglaciation (De Angelis and Kleman, 2008). In contrast, the cross-cutting flow-sets in Bakkaflói and Vopnafjörður suggest that the ice sheet drainage occurred primarily through topographically controlled ice streams during deglaciation, and that onset zones may have shifted as ice divides migrated. These ice streams probably deglaciated rapidly during the collapse of the IIS in the Bølling/Allerød interstadial (Norðdahl and Ingólfsson, 2015), which may explain the preservation of their geomorphological record. However, they may also have been reactivated during Younger Dryas and Preboreal readvances, which terminated several kilometres inland from the present coast (Norðdahl and Hjort, 1993; Sæmundsson, 1995; Norðdahl and Pétursson, 2005; Norðdahl et al., 2019). Based on existing geomorphological and chronological data, it cannot be excluded that the geomorphological imprint of palaeo-ice streaming in our study areas of NE-Iceland results to some degree from the latest regional advances.

While palaeo-ice streams in NW-Iceland appear to have merged on the shelf to feed a larger ice stream that extended to the shelf edge (Principato et al., 2016), our data indicate that each palaeo-ice stream in NE-Iceland drained into its own trough on the shelf. The orientation, dimensions, and extension of these troughs on the NE-Iceland shelf (Spagnolo and Clark, 2009) suggest that these palaeo-ice streams were strong enough to propagate from the shelf break all the way to the ice sheet's interior ice divide . This may also have implications for our notions of turnover rates of the IIS through a glaciation. Future modelling efforts could possibly shed light on the catchment size required to support this kind of ice streaming to the shelf edge and if that corresponds to our empirical geomorphological data and interpretations of the configuration of palaeo-ice streams and location of ice divides.

6. Conclusion

In our study area in NE-Iceland, a total of 797 streamlined subglacial bedforms (SSBs) have been mapped and their orientation and morphometrics measured. The dataset suggests that the SSBs represent the flow-sets of several cross-cutting palaeo-ice streams that drained the north-eastern sector of the Iceland Ice Sheet. Our main conclusions are as follows:

- The majority of the SSBs classify as drumlins (96%). The remaining bedforms are mega-scale glacial lineations (elongation ratio > 1:10), which commonly, albeit not exclusively, occur in areas where bedrock strata with a strike sub-paralleling former ice flow frequently crop out on the surface in the form of low, elongate bedrock ridges.
- The distribution and orientation of the SSBs indicate the flow-sets of palaeo-ice streams and the location of ice divides; both of which migrated over time. Thus, the flow-sets are partly asynchronous and overlap in some areas.
- The density and packing of the SSBs possibly suggests that the Bakkaheiði plateau and the Bustarfell-Tunguheiði drumlin field operated as axial zones of ice streaming during maximum glaciation and deglaciation, respectively.
- During maximum glaciation and ice sheet thickness (~1500–200 m), an E-W orientated ice divide was located to the south of the study area promoting ice flow to the north across NE-trending fjords and valleys. Ice flow during this stage was thus independent of underlying topography. This northward ice flow is evident from S—N orientated SSBs within the Bakkaheiði, Þistilfjörður and Jökuldalsheiði flow-sets, and correlates with a NNE-trending shallow trough offshore.
- During deglaciation, probably between c. 18.2 and 14.6 ka BP, ice flow became progressively more controlled by topography due to ice thinning. Palaeo-ice streams flowed along valleys and fjords towards the north (in Þistilfjörður) and northeast (in Bakkaflói and Vopnafjörður), generating younger flow-sets that crosscut the older ones. This is evident from the Bakkaheiði plateau and the eastern margin of the Þistilfjörður area and corresponds to the NE-trending Bakkaflói trough that crosscuts the older and shallower trough trending NNE.
- Acceleration of topographic ice streams, induced by ice shelf collapse and extremely rapid retreat between c. 15.3 and 14.6 ka BP, may have generated the well-preserved drumlin fields in the axial zones of the younger palaeo-ice stream flow-sets.
- The exact age of these flow-sets is uncertain, but it must be considered most likely that the older flow-sets pertain to the LGM and the younger flow-sets to the following deglaciation. However, this inference must be tested with future research.

The results of this study demonstrate the importance of glacial geomorphological mapping for the reconstruction of palaeo-ice streams and ice divides for understanding the evolution of the IIS. This study increases our understanding of the dynamics of the IIS and provides analogues to other palaeo-ice streams within the IIS as well as guiding future efforts towards constraining the evolution of shelf glaciation and the chronology of ice stream retreat.

Declaration of competing interest

The authors declare no conflict of interests.

Acknowledgements

This project has been funded through grants from the University of Iceland Research Fund (to ÓI), the Icelandic Road and Coastal Administration (to ÍÖB), and the Energy Research Fund of Landsvirkjun (to NA and ÍÖB). We thank our colleagues and graduate students for great company during fieldwork and fruitful discussions over the past few years. Matteo Spagnolo and Martin Ross are gratefully acknowledged for insightful and highly constructive reviews that led to improvements of this paper.

References

Alley, R.B., Anandakrishnan, S., Dupont, T.K., Parizek, B.R., 2004. Ice streams – fast, and faster? C. R. Phys. 5, 723–734.

Alley, R.B., Clark, P.U., Huybrechts, P., Joughin, I., 2005. Ice-sheet and sea-level changes. Science 310, 456–460.

Andrews, J.T., 2008. The role of the Iceland Ice Sheet in the North Atlantic during the late Quaternary: a review and evidence from Denmark Strait. J. Quat. Sci. 23, 3–20.

Andrews, J.T., Harðardóttir, J., Helgadóttir, G., Jennings, A.E., Geirsdóttir, Á., Sveinbjörnsdóttir, Á.E., Schoolfield, S., Kristjánsdóttir, G.B., Smith, L.M., Thors, K., Syvitski, J.P.M., 2000. The N and W Iceland Shelf: insights into last Glacial Maximum ice extent and deglaciation based on acoustic stratigraphy and basal radiocarbon AMS dates. Quat. Sci. Rev. 19, 619–631.

Atkins, C.B., 2013. Geomorphological evidence of cold-based glacier activity in South Victoria Land, Antarctica. In: Hambrey, M.H., Barker, P.F., Barrett, P.J., Bowman, V., Davies, B., Smellie, J.L., Tranter, M. (Eds.), Antarctic Palaeoenvironments and Earth Surface Processes. Geological Society of London Special Publications. 381. https://doi.org/10.1144/SP381.18.

Benediktsson, Í.Ö., Jónsson, S.A., Schomacker, A., Johnson, M.D., Ingólfsson, Ó., Zoet, L., Iverson, N.R., Stötter, J., 2016. Progressive formation of modern drumlins at Múlajökull, Iceland: stratigraphical and morphological evidence. Boreas 45, 567–583.

Benediktsson, Í.Ö., McKenzie, M., Principato, S., 2018. Geomorphological and sedimentological evidence for a palaeo-ice stream in Bárðardalur, North Iceland. 6th International Conference on 'Palaeo-Arctic Spatial and Temporal (PAST) Gateways. Durham University 16-20 April 2018.

Benediktsson, Í.Ö., Brynjólfsson, S., Ásbjörnsdóttir, L., 2021a. Iceland: glacial landscapes of Iceland. In: Palacios, D., Hughes, P., García Ruiz, J.M., Andrés, N. (Eds.), Vol. 1 European Glacial Landscapes: Maximum Extent of Glaciations. Elsevier in press.

Benediktsson, Í.Ö., Brynjólfsson, S., Ásbjörnsdóttir, L., 2021b. Iceland: glacial landforms from the Last Glacial Maximum. In: Palacios, D., Hughes, P., García Ruiz, J.M., Andrés, N. (Eds.), Vol. 1 European Glacial Landscapes: Maximum Extent of Glaciations. Elsevier in press.

Benediktsson, Í.Ö., Brynjólfsson, S., Ásbjörnsdóttir, L., 2022. Iceland: glacial landforms during deglaciation. In: Palacios, D., Hughes, P., García Ruiz, J.M., Andrés, N. (Eds.), Vol. 2 European Glacial Landscapes: Maximum Extent of Glaciations. Elsevier accepted, in press.

Benjamínsdóttir, M.M., 2021. Ribbed Moraine Ridges in Bakkaflói, NE-Iceland: Morphometry, Sedimentology and Formation. Master's thesis, 67 pFaculty of Earth Sciences, University of Iceland. http://hdl.handle.net/1946/38501.

Bennett, M.R., 2003. Ice stream as the arteries of an ice sheet; their mechanics, stability and significance. Earth Sci. Rev. 61, 309–339.

Bourgeois, O., Dauteuil, O., Van Vliet-Lanoë, B., 2000. Geothermal control on flow patterns in the last glacial maximum ice sheet of Iceland. Earth Surf. Process. Landf. 25, 59–76.

Briner, J.P., 2007. Supporting evidence from the New York drumlin field that elongate subglacial bedforms indicate fast ice flow. Boreas 36, 143–147.

Briner, J.P., 2016. Ice streams waned as ice sheets shrank. Nature 530, 287–288.

Brouard, E., Lajeunesses, P., 2019. Ice-stream flow switching by up-ice propagation of instabilities along glacial marginal troughs. Cryosphere 13, 981–996.

Chandler, B.M.P., Lovell, H., Boston, C.M., Lukas, S., Barr, I.D., Benediktsson, Í.Ö., Benn, D.I., Clark, C.R., Darvill, C.M., Evans, D.J.A., Ewertowski, M.W., Loibl, D., Margold, M., Otto, J.-C., Roberts, D., Stokes, C.R., Storrar, R.D., Stroeven, A.P., 2018. Glacial geomorphological mapping: a review of approaches and frameworks for best practice. Earth Sci. Rev. 185, 806–846. https://doi.org/10.1016/j.earscirev.2018.07.015.

Clark, C.D., Spagnolo, M., 2016. Glacially eroded cross-shelf troughs surrounding Iceland from Olex data. In: Dowdeswell, J.A., Canals, M., Jakobsson, M., Todd, B.J., Dowdeswell, E.K., Hogan, K.A. (Eds.), Atlas of Submarine Glacial Landforms: Modern, Quaternary and Ancient. Memoirs46. Geological Society, London, pp. 165–166 Geological Society of London.

Clark, C.D., Stokes, C.R., 2001. Extent and basal characteristics of the M'Clintock Channel Ice Stream. Quat. Int. 86, 81–101.

Clark, C.D., Hughes, A.L.C., Greenwood, S.L., Spagnolo, M., Ng, F.S.L., 2009. Size and shape characteristics of drumlins, derived from a large sample, and associated scaling law. Quat. Sci. Rev. 28, 677–692.

De Angelis, H., Kleman, J., 2008. Palaeo-ice-stream onsets: examples from the north-eastern Laurentide Ice Sheet. Earth Surf. Process. Landf. 33, 560–572.

Dowling, T.P.F., Spagnolo, M., Möller, P., 2015. Morphometry and core type of streamlined bedforms in southern Sweden from high resolution LiDAR. Geomorphology 236, 54–63.

Dubé-Loubert, H., Roy, M., Veillette, J.J., Brouard, E., Schaefer, J.M., Wittmann, H., 2021. The role of glacial dynamics in the development of ice divides and the Horseshoe Intersection Zone of the northeastern Labrador Sector of the Laurentide Ice Sheet. Geomorphology 387, 107777.

Eiríksson, J., Knudsen, K.L., Haflidason, H., Henriksen, P., 2000. Late-glacial and Holocene palaeoceanography of the North Icelandic shelf. J. Quat. Sci. 15, 23–42.

Ely, J.C., Clark, C.D., Spagnolo, M., Stokes, C.R., Greenwood, S.L., Hughes, A., Dunlop, P., Hess, D., 2016. Do subglacial bedforms comprise a size and shape continuum? Geomorphology 257, 108–119.

Ely, J.C., Clark, C.D., Spagnolo, M., Hughes, A., Stokes, C.R., 2018. Using the size and position of drumlins to understand how they grow, interact and evolve. Earth Surf. Process. Landf. 43, 1073–1087.

Evans, D.J.A., Atkinson, N., Phillips, E., 2020. Glacial geomorphology of the Neutral Hills Uplands, Southeast Alberta, Canada: the process-form imprints of dynamic ice streams and suging ice lobes. Geomorphology 350, 106910.

Eyles, N., Ross, M., 2016. Ancient ice streams and their megalineated beds. Sediment. Geol. 338, 1.

Eyles, N., Putkinen, N., Sookhan, S., Arbelez-Moreno, L., 2016. Erosional origin of drumlins and megaridges. Sediment. Geol. 338, 2–23.

Feldmann, J., Levermann, A., 2015. Collapse of the West Antarctic Ice Sheet after local destabilization of the Amundsen Basin. PNAS 112, 14191–14196.

Graham, A.G.C., Larter, R.D., Gohl, K., Dowdeswell, J.A., Hillenbrand, C.-D., Smith, J.A., Evans, J., Kuhn, G., Deen, T., 2010. Flow and retreat of the late Quaternary Pine Island-Thwaites palaeo-ice stream, West Antarctica. J. Geophys. Res. Earth Surf. 115, F03025.

Greenwood, S.L., Clark, C.D., 2009a. Reconstructing the last Irish Ice Sheet 1: changing flow geometries and ice flow dynamics deciphered from the glacial landform record. Quat. Sci. Rev. 28, 3085–3100.

Greenwood, S.L., Clark, C.D., 2009b. Reconstructing the last Irish Ice Sheet 2: a geomorphologically-driven model of ice sheet growth, retreat and dynamics. Quaternary Science Reviews 28, 3101–3123.

Helgadóttir, E.G., 2020. Ribbed moraines in the Vopnafjörður regions, Iceland. Master's thesis, 104 p.Faculty of Earth Sciences, University of Iceland. http://hdl.handle.net/1946/35879.

Hillier, J.K., Smith, M.J., Armugam, R., Barr, I., Boston, C.M., Clark, C.D., Ely, J., Frank, A., Greenwood, S.L., Gosselin, L., Hättestrand, C., Hogan, K., Hughes, A.L.C., Livingstone, S.J., Lovell, H., McHenry, M., Munoz, Y., Pellicer, X.M., Pellitero, R., Robb, C., Roberson, S., Ruther, D., Spagnolo, M., Standell, M., Stokes, C.R., Storrar, R., Tate, N.J., Wooldridge, K., 2015. Manual mapping of drumlins in synthetic landscapes to assess operator effectiveness. J. Maps 11 (5), 719–729.

Hillier, J.K., Benediktsson, Í.Ö., Dowling, T.P.F., Schomacker, A., 2018. Production and preservation of the smallest drumlins. GFF 2018. https://doi.org/10.1080/11035897.2018.1457714.

Hjartardóttir, Á.R., Einarsson, P., Brandsdóttir, B., 2010. The Kerlingar fault, Northeast Iceland: a Holocene normal fault east of the divergent plate boundary. Jökull 60, 103–116.

Hjartarson, Á., Sæmundsson, K., 2014. Geological Map of Iceland. Bedrock 1:600.000. Iceland GeoSurvey.

Hodder, T.J., Ross, M., Menzies, J., 2016. Sedimentary record of ice divide migration and ice streams in the Keewatin core region of the Laurentide Ice Sheet. Sediment. Geol. 338, 97–114.

Hubbard, A., Sugden, J., Dugmore, A., Norðdahl, H., Pétursson, H.G., 2006. A modelling insight into the Icelandic late Glacial Maximum ice sheet. Quat. Sci. Rev. 25, 2283–2296.

Hughes, A.L.C., Clark, C.D., Jordan, C.J., 2010. Subglacial bedforms of the last British Ice Sheet. J. Maps 6 (1), 543–563.

Hugonnet, R., McNabb, R., Berthier, E., Menounos, B., Nuth, C., Girod, L., Farinotti, D., Huss, M., Dussaillant, I., Brun, F., Kääb, A., 2021. Accelerated global glacier mass loss in the early twenty-first century. Nature 592, 726–731.

Icelandic Institute of Natural History, 2019. Geological Map of Iceland. 1st edition. Geology of Iceland, Bedrock (checked 2021-05-07) http://jardfraedikort.ni.is.

Ingólfsson, Ó., Norðdahl, H., 2001. High relative sea-level during the Bølling interstadial in W Iceland: a reflection of ice-sheet collapse and extremely rapid glacial unloading. Arct. Antarct. Alp. Res. 33, 231–243.

Iverson, N.R., McCracken, R.G., Zoet, L., Benediktsson, Í.Ö., Schomacker, A., Johnson, M.D., Woodard, J., 2017. A theoretical model of drumlin formation based on observations at Múlajökull, Iceland. J. Geophys. Res. Earth Surf. 122. https://doi.org/10.1002/2017JF004354.

Jennings, A., Syvitski, J., Gerson, L., Grönvold, K., Geirsdóttir, Á., Harðardóttir, J., Andrews, J., Hagen, S., 2000. Chronology and palaeoenvironments during the late Weichselian deglaciation of the Southwest Iceland shelf. Boreas 29, 167–183.

Jóhannesson, H., Sæmundsson, K., 2009. Geological Map of Iceland. 1:500.000. Bedrock. 1st edition. Icelandic Institute of Natural History, Reykjavík.

Johnson, M.D., Schomacker, A., Benediktsson, Í.Ö., Geiger, A.J., Ferguson, A., Ingólfsson, Ó., 2010. Active drumlin field revealed at the margin of Múlajökull, Iceland: a surge-type glacier. Geology 38, 943–946.

Jónsson, S.A., Benediktsson, Í.Ö., Ingólfsson, Ó., Schomacker, A., Bergsdóttir, H.L., Jacobson Jr., W.R., Linderson Jr., H., 2016. Submarginal drumlin formation and late Holocene history of Fláajökull, southeast Iceland. Ann. Glaciol. 57, 128–141.

Jorge, M.G., Brennand, T.A., 2017. Measuring (subglacial) bedform orientation, length, and longitudinal asymmetry – method assessment. PLoS ONE 12, e0174312.

King, E., Hindmarch, R.C.A., Stokes, C.R., 2009. Formation of mega-scale glacial lineations observed beneath a West Antarctic ice stream. Nat. Geosci. 2, 585–588.

Kjær, K.H., Houmark-Nielsen, M., Richardt, N., 2003. Ice-flow patterns and dispersal of erratics at the southwestern margin of the last Scandinavian Ice Sheet: signature of palaeo-ice streams. Boreas 32, 130–148.
Kleman, J., Hättestrand, C., 1999. Frozen-bed Fennoscandian and Laurentide ice sheets during the last Glacial Maximum. Nature 402, 63–66.. https://www.nature.com/articles/47005.
Krabbendam, M., Eyles, N., Putkinen, N., Bradwell, T., Arbelaez-Moreno, L., 2016. Streamlined hard beds formed by palaeo-ice streams: a review. Sediment. Geol. 338, 24–50.
Krüger, J., 1987. Relationship of drumlin shape and distribution to drumlin stratigraphy and glacial history, Mýrdalsjökull, Iceland. In: Menzies, J., Rose, J. (Eds.), Drumlin Symposium. A.A, Balkema, Rotterdam, pp. 257–266.
Larter, R.D., Hogan, K.A., Hillenbrand, C.-D., Smith, J.A., Batchelor, C.L., Cartigny, M., Tate, A.J., Kirkham, J.D., Roseby, Z.A., Kuhn, G., Graham, A.G.C., Dowdeswell, J.A., 2019. Subglacial hydrological control on flow of an Antarctic Peninsula palaeo-ice stream. Cryosphere 13, 1583–1596.
Lowe, J.J., Rasmusson, S.O., Björck, S., Hoek, W.Z., Steffensen, J.P., Walker, M.J.C., Yu, Z.C., the INTIMATE group, 2008. Synchronisation of palaeoenvironmental events in the North Atlantic region during the last termination: a revised protocol recommended by the INTIMATE group. Quat. Sci. Rev. 27, 6–17.
Mangerud, J., Hughes, A.L.C., Sæle, T.H., Svendsen, J.I., 2019. Ice-flow patterns and precise timing of ice sheet retreat across a dissected fjord landscape in western Norway. Quat. Sci. Rev. 214, 139–163.
Margold, M., Stokes, C.R., Clark, C.D., 2015. Ice streams in the Laurentide Ice Sheet: Identification, characteristics and comparison to modern ice sheets. Earth Sci. Rev. 143, 117–146.
McKenzie, M.A., Principato, S.M., Benediktsson, Í.Ö., 2017. Geomorphic evidence for a palaeo-ice stream near Bárðardalur, north Iceland. GSA Annual Meeting, Seattle, WA, USA, 22-25 October 2017.
McMartin, I., Henderson, P.J., 2004. Evidence from Keewatin (Central Nunavut) for paleo-ice divide migration. Géog. Phys. Quatern. 58, 163–186.
Napieralski, J., Nalepa, N., 2010. The application of control charts to determine the effect of grid cell size on landform morphometry. Comput. Geosci. 36, 222–230.
Newton, M., Evans, D.J.A., Roberts, D.H., Stokes, C.R., 2018. Bedrock mega-grooves in glaciated terrain: a review. Earth Sci. Rev. 185, 57–79.
Norðdahl, H., 1991. A review of the glaciation maximum concept and the deglaciation of Eyjafjörður, north Iceland. In: Maizels, J.K., Caseldine, C. (Eds.), Environmental Change in Iceland: Past and Present. Kluwer Academic Publishers, Netherlands, pp. 31–47.
Norðdahl, H., Hjort, C., 1993. Lateglacial raised beaches and glacier recession in the Þistilfjörður-Bakkaflói area. Jökull 43, 32–44.
Norðdahl, H., Ingólfsson, Ó., 2015. Collapse of the Icelandic ice sheet controlled by sea-level rise? Arktos 1, 1–18.
Norðdahl, H., Pétursson, H.G., 2005. Relative sea-level changes in Iceland. New aspects of the Weichselian deglaciation of Iceland. In: Caseldine, C., Russel, A., Harðardóttir, J., Knudsen, Ó. (Eds.), Iceland – modern processes and past environments. Elsevier, Amsterdam, pp. 25–78.
Norðdahl, H., Ingólfsson, Ó., Vogler, E.D., Steingrímsson, B.Ó., Hjartarson, Á., 2019. Glacio-isostatic age modelling and Late Weichselian deglaciation of the Lögurinn basin, East Iceland. Boreas 48, 563–580.
Patton, H., Hubbard, A., Bradwell, T., Schomacker, A., 2017. The configuration, sensitivity and rapid retreat of the late Weichselian Icelandic ice sheet. Earth Sci. Rev. 166, 223–245.
Pétursson, H.G., 1991. The Weichselian glacial history of west Melrakkaslétta, north-eastern Iceland. In: Maizels, J.M., Caseldine, C. (Eds.), Environmental Changes in Iceland: Past and Present. Kluwer, Dordrecht, pp. 49–65.
Porter, Claire, Morin, Paul, Howat, Ian, Noh, Myoung-Jon, Bates, Brian, Peterman, Kenneth, Keesey, Scott, Schlenk, Matthew, Gardiner, Judith, Tomko, Karen, Willis, Michael, Kelleher, Cole, Cloutier, Michael, Husby, Eric, Foga, Steven, Nakamura, Hitomi, Platson, Melisa, Wethington, Michael Jr., Williamson, Cathleen, Bauer, Gregory, Enos, Jeremy, Arnold, Galen, Kramer, William, Becker, Peter, Doshi, Abhijit, D'Souza, Cristelle, Cummens, Pat, Laurier, Fabien, Bojesen, Mikkel, 2018. "ArcticDEM". V1. Harvard Dataverse. https://doi.org/10.7910/DVN/OHHUKH.
Principato, S.M., Moyer, A.N., Hampsch, A.G., Ipsen, H.A., 2016. Using GIS and streamlined landforms to interpret palaeo-ice flow in northern Iceland. Boreas 45, 470–482.
Putnins, A., Henriksen, M., 2017. Reconstructing the flow pattern evolution in inner region of the Fennoscandian Ice Sheet by glacial landforms from Gausdal Vestfjell area, south-Central Norway. Quat. Sci. Rev. 163, 56–71.
Rice, J.M., Ross, M., Paulen, R.C., Kelley, S.E., Briner, J.P., 2020. A GIS-based multi-proxy analysis of the evolution of subglacial dynamics of the Quebec-Labrador ice dome, northeastern QuebecCanada. 45, 3155–3177.
Richardsson, S.D., 1997. Deglaciation and Shoreline Displacement Adjacent to a Spreading Ridge, N.E. Iceland. Unpublished PhD thesisDepartment of Geography, Royal Holloway, University of London 408 pp.
Rignot, E., Velicogna, I., van den Broeke, M.R., Monoghan, A., Lenaerts, J.T.M., 2011. Acceleration of the contribution of the Greenland and Antarctic ice sheets to sea level rise. Geophys. Res. Lett. 38 (L05503), 2011. https://doi.org/10.1029/2011GL046583.
Ross, M., Campell, J.E., Parent, M., Adams, R.S., 2009. Palaeo-ice streams and the subglacial landscape mosaic of the North American mid-continental prairies. Boreas 38, 421–439.
Sæmundsson, K., 1977. Geological Map of Iceland, Sheet 7, NE-Iceland. 1:250.000. Icelandic Institute of Natural History and National Land Survey of Iceland, Reykjavik.
Sæmundsson, Th., 1995. Deglaciation and Shoreline Displacement in Vopnafjörður, Northeastern Iceland. Department of Quaternary Geology, Lund University, pp. 1–106 LUNDQUA thesis 33.
Smith, M.J., Clark, C.D., 2005. Methods for the visualization of digital elevation models for landform mapping. Earth Surf. Process. Landf. 30 (7), 885–900. https://doi.org/10.1002/esp.1210.
Smith, M.J., Wise, S.M., 2007. Problems of bias in mapping linear landforms from satellite imagery. 9 (1), 65–78. https://doi.org/10.1016/j.jag.2006.07.002.
Sookhan, S., Eyles, N., Putkinen, N., 2016. LiDAR-based volume assessment of the origin of the Wadena drumlin field, Minnesota, USA. Sediment. Geol. 338, 72–83.
Spagnolo, M., Clark, C.D., 2009. A geomorphological overview of glacial landforms on the Icelandic continental shelf. Journal of Maps 2009, 37–52.
Spagnolo, M., Clark, C.D., Ely, J.C., Stokes, C.R., Anderson, J.B., Andreassen, K., Graham, A.G.C., King, E.C., 2014. Size, shape and spatial arrangement of mega-scale glacial lineations from a large and diverse dataset. Earth Surf. Process. Landf. 39 (11), 1432–1448. https://doi.org/10.1002/esp.3532.
Stokes, C.R., 2018. Geomorphology under ice streams: moving from form to process. Earth Surf. Process Landf. 43, 85–123.
Stokes, C.R., Clark, C.D., 1999. Geomorphological criteria for identifying Pleistocene ice streams. Ann. Glaciol. 28, 67–74.
Stokes, C.R., Clark, C.D., 2001. Palaeo-ice streams. Quat. Sci. Rev. 20, 1437–1457.
Stokes, C.R., Spagnolo, M., Clark, C.D., 2011. The composition and internal structure of drumlins: complexity, commonality, and implications for a unifying theory of their formation. Earth Sci. Rev. 107, 398–422.
Stokes, C.R., Spagnolo, M., Clark, C.D.Ó., Cofaigh, C., Lian, O.B., Dunstone, R.B., 2013a. Formation of mega-scale glacial lineations on the Dubwant Lake Ice Stream bed 1: size, shape and spacing from a large remote sensing dataset. Quat. Sci. Rev. 77, 210–227.
Stokes, C.R., Margold, M., Clark, C.D., Tarasov, L., 2016. Ice stream activity scaled to ice sheet volume during Laurentide Ice Sheet deglaciation. Nature 530, 322–326.
Syvitski, J.P., Jennings, A.E., Andrews, J.T., 1999. High-resolution seismic evidence for multiple glaciations across the Southwest Iceland shelf. Arct. Antarct. Alp. Res. 31, 50–57.
Yu, P., Eyles, N., Sookhan, S., 2015. Automated drumlin shape and volume estimation using high resolution LiDAR imagery (Curvature based Relief Separation): a test from the Wadena Drumlin Field, Minnesota. Geomorphology 246, 589–601.

Paper II

 ISSN 0267-8179. DOI: 10.1002/jqs.3481

JQS Journal of Quaternary Science QRA Quaternary Research Association

Drumlin formation within the Bustarfell drumlin field, northeast Iceland: integrating sedimentological and ground-penetrating radar data

NÍNA ARADÓTTIR,[1]* ÍVAR ÖRN BENEDIKTSSON,[1] ÓLAFUR INGÓLFSSON,[1] ERIK STURKELL,[2] SKAFTI BRYNJÓLFSSON,[3] WESLEY R. FARNSWORTH[1,4] and EMRYS PHILLIPS[5]
[1]Institute of Earth Sciences, University of Iceland, Sturlugata 7, Is-102, Reykjavík, Iceland
[2]Department of Earth Sciences, University of Gothenburg, 405 30, Gothenburg, Sweden
[3]Icelandic Institute of Natural History, Borgir við Norðurslóð, 600, Akureyri, Iceland
[4]Globe Institute, University of Copenhagen, Øster Voldgade 5, DK-1350, Copenhagen, Denmark
[5]British Geological Survey, The Lyell Centre, Research Avenue South, Edinburgh, EH14 4AP, UK

Received 12 July 2022; Revised 11 October 2022; Accepted 31 October 2022

ABSTRACT: Drumlins are important bedforms of former glaciated landscapes as they demonstrate past ice-flow directions and elucidate processes that operated at the ice/bed interface. Recently mapped drumlins and other streamlined subglacial bedforms in northeast Iceland reveal the flow-sets of cross-cutting palaeo-ice streams that were active within the Iceland Ice Sheet (IIS) during and following the Last Glacial Maximum. Here we study the Bustarfell drumlin field within the Vopnafjörður–Jökuldalsheiði flow-set. The internal architecture of two drumlins was investigated using sedimentological analysis and ground-penetrating radar (GPR, 50 and 100 MHz) to illuminate subglacial processes that contributed to drumlin formation, as well as the history and dynamics of the IIS. On the stoss side of one of the drumlins, two subglacial traction till units were identified, separated by a thick unit of deformed glaciofluvial sand and gravel. The core of glaciofluvial material suggests that the drumlin formed around well-drained patches (sticky spots) in the subglacial bed that retarded the ice flow locally through increased basal drag and encouraged till deposition. Furthermore, our GPR data indicate a combination of erosional and depositional processes. We suggest that the glaciofluvial sediments were deposited as small ice-marginal fans on the Bustarfell plateau, possibly during the Bølling–Allerød interstadial, and that the drumlins were formed around these fans during a subsequent readvance during the Younger Dryas. © 2022 John Wiley & Sons, Ltd.

KEYWORDS: Bustarfell; drumlin; ground-penetrating radar; Iceland Ice Sheet; subglacial processes

Introduction

Drumlins are subglacial bedforms that have been studied to a great extent for palaeoglaciological reconstructions and as indicators for glacier dynamics (e.g. Menzies, 1979; Stokes, 2018). They commonly occur at palaeo-ice stream beds in conjunction with other streamlined subglacial bedforms (SSBs), such as mega-scale glacial lineations (MSGLs) and mega-flutes (e.g. Clark, 1993; Hart, 1999; Stokes and Clark, 1999, 2002; Briner, 2007) but have also been observed under contemporary ice streams (Smith, 1997; King *et al.*, 2007; Smith *et al.*, 2007) and in recently exposed forefields of retreating glaciers (Johnson *et al.*, 2010; Benediktsson *et al.*, 2016; Jónsson *et al.*, 2016; Allaart *et al.*, 2018). Because direct observations of processes operating under contemporary ice streams are limited to borehole and seismic investigations (King *et al.*, 2007; Stokes, 2018), the geomorphology and composition of palaeo-ice stream beds is critical for our understanding of the formation of SSBs and the dynamics and mechanism of ice streaming (Stokes and Clark, 1999, 2001; Livingstone *et al.*, 2012; Stokes, 2018).

Drumlin composition can vary significantly between and within drumlin fields, as the drumlins can be composed of till, stratified sand and gravel, bedrock, or a combination of all of them (see Stokes *et al.*, 2011). The typical shape of a drumlin is a smooth, streamlined hill (Menzies, 1979), even though recent studies have highlighted more diverse morphologies (Spagnolo *et al.*, 2010; Maclachlan and Eyles, 2013). Drumlins exhibiting a wide range of composition and morphological characteristics have led to several hypotheses of their formation, including deformation of till around more competent cores (Smalley and Unwin, 1968; Boulton, 1987; Hart, 1997), catastrophic meltwater floods (Shaw, 2002) and instabilities at the flat bed causing a rise in the till surface (Hindmarsh, 1998; Fowler, 2000, 2010, 2018; Stokes *et al.*, 2013; Fowler and Chapwanya, 2014). Hart (1997) classified drumlins into three types and suggested that they can be formed by either erosion, deposition or deformation, or a combination of all of them, although others have explained their formation to be solely erosional (Eyles *et al.*, 2016; Hermanowski *et al.*, 2019). The discussion concerning their formation has evolved towards whether their formation can be explained by a unifying theory (Clark, 2010; Stokes *et al.*, 2011) or whether the variety and complexity of drumlin composition indicates that different processes can lead to a similar morphological expression (Möller and Dowling, 2016).

Studies of the internal architecture and composition of SSBs are restricted to open, accessible sections in the field. Thus geophysical instruments, such as ground-penetrating radar (GPR), have increasingly been used to integrate geophysical data with lithostratigraphic and sedimentological data (e.g. Bristow and Jol, 2003; Cassidy *et al.*, 2003; Kjær *et al.*, 2004; Neal, 2004; Benediktsson *et al.*, 2009; Watts *et al.*, 2022). For recent examples, Spagnolo *et al.* (2014) successfully applied GPR on drumlins in Scotland to investigate the relationship between the internal architecture of the drumlins and their substrate and interdrumlin areas, and provided recommendations for future

*Correspondence: Nína Aradóttir, as above.
Email: nia1@hi.is

© 2022 John Wiley & Sons, Ltd.

investigations. Woodard *et al.* (2020) correlated GPR profiles with stratigraphic logs to shed light on drumlin architecture and formation within the recently exposed drumlin field at Múlajökull, Iceland, which supports the previous conclusion that they had formed through both depositional and erosional processes.

Ice streams are considered to have been present within the Iceland Ice Sheet (IIS) during and following the Last Glacial Maximum (LGM). Their existence has to a large extent been based on modelling (Bourgeois *et al.*, 2000; Hubbard *et al.*, 2006; Patton *et al.*, 2017), which has been further supported with onshore and offshore geomorphological mapping of SSBs, glacial striae and large-scale topography (Spagnolo and Clark, 2009; Clark and Spagnolo, 2016; Principato *et al.*, 2016; Norðdahl *et al.*, 2019; Benediktsson *et al.*, 2021b, 2022a; Fig. 1A). Principato *et al.* (2016) mapped and quantified the properties of SSBs in northwest Iceland, significantly improving the understanding of the dynamics and extent of palaeo-ice streams in this region. A recent study by Benediktsson *et al.* (2022a) on SSBs in northeast Iceland revealed a pattern of cross-cutting palaeo-ice streams that reflects shifts in ice-sheet dynamics and the migration of ice divides. Despite this recent effort in investigating drumlins and other SSBs in Iceland, no previous studies have focused on the internal architecture of drumlins formed during the last glaciation/deglaciation.

The aim of this paper is to investigate the internal architecture and composition of drumlins within the Bustarfell drumlin field by integrating sedimentological analysis and GPR profiling. Furthermore, we address the processes leading to regional drumlin formation and enhance our understanding of the glacial history and dynamics of the IIS in northeast Iceland.

Setting

The Bustarfell drumlin field is located on a plateau at 400–550 m a.s.l. between the Hofsárdalur and Vesturárdalur valleys within the Vopnafjörður valley-fjord system in northeast Iceland. The regional bedrock consists primarily of Miocene and Pliocene (>3.3–0.8 million years old) basalt lavas with intercalated sediments, with ages that become progressively younger towards the west. The basalt bedrock strikes gently towards the north (Sæmundsson, 1977; Jóhannesson and Sæmundsson, 2009). The Vopnafjörður fjord and valleys were carved into the bedrock during frequent glaciations during the Quaternary period (Sæmundsson, 1995; Benediktsson *et al.*, 2021a). The valleys are orientated southwest to northeast and are over 30 km long from the coast towards the highlands. The Bustarfell plateau is relatively flat with numerous peat bogs, except for three bedrock hills (Bustarfell, Urðarfell and Kálfafell) (Figs 1B and 2A). Large angular to subangular boulders, up to 4 m in diameter, are common in the drumlin field, especially in the southeast part of the area. Drift thickness in the area has not been mapped but frequent bedrock outcrops suggest discontinuous sediment cover and that the drift is generally thin between the drumlins. The bedrock is frequently glacially scoured and striated, with orientation towards the northeast.

Palaeo-ice stream flow-sets in northeast Iceland were reconstructed based on the mapping of nearly 1000 SSBs (drumlins and MSGLs) which define cross-cutting palaeo-ice streams that operated during and following the LGM. The drumlins from the Vopnafjörður–Jökuldalsheiði flow-set (310 mapped bedforms) exhibit a large-scale converging pattern with variable directions in the highlands that align towards northeast in the central part, parallel to the Vopnafjörður valleys and fjord (Fig. 1B). The Bustarfell drumlin field is situated in the centre of the Vopnafjörður–Jökuldalsheiði palaeo-ice stream flow-set (Benediktsson *et al.* 2022a).

Chronological data on the extent of the IIS in northeast Iceland are limited, but based on thermomechanical modelling experiments by Patton *et al.* (2017), the IIS reached its maximum extent at the shelf edge around 22.9 ka BP and a rapid marine deglaciation began at around 21.8 ka BP. The abrupt warming at the Bølling Interstadial (14.7–14.1 cal. ka BP) during the deglaciation resulted in a collapse of the ice sheet offshore (Ingólfsson and Norðdahl, 2001; Norðdahl and Ingólfsson, 2015). Subsequently, two readvances occurred, during the Younger Dryas period (YD) (12.9–11.7 cal. ka BP) and Early Preboreal (10.3–9.0 cal. ka BP). Previous studies in northeast Iceland have mainly focused on the deglaciation and

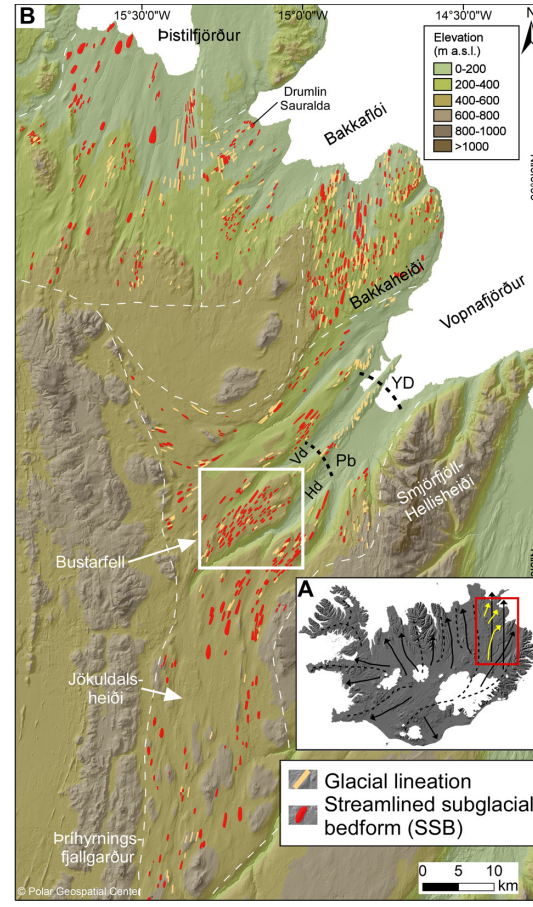

Figure 1. (A) Major ice streams of the Iceland Ice Sheet according to Bourgeois *et al.* (2000), Stokes and Clark (2001) and Principato *et al.* (2016). In northeast Iceland the black arrows indicate an older generation of ice flow during maximum glaciation while the yellow arrows represent a younger generation during deglaciation (Benediktsson *et al.*, 2022a). Fig. 1B is outlined in red on Fig. 1A. (B) Overview map of glacial lineations and streamlined subglacial bedforms (SSBs) in northeast Iceland (modified from Benediktsson *et al.* 2022a). The white dashed lines indicate boundaries between flow-sets; Þistilfjörður, Bakkaflói, Bakkaheiði and Vopnafjörður–Jökuldalsheiði with Vesturárdalur (Vd) and Hofsárdalur (Hd) marked. The present study area, the Bustarfell drumlin field, is located within the white box. Ice-marginal positions during the Younger Dryas (YD) and the Preboreal (Pb) are indicated within the Vopnafjörður valley-fjord based on Sæmundsson (1995). Map base layer: Hillshade of the ArcticDEM (PGC, 2018). [Color figure can be viewed at wileyonlinelibrary.com]

© 2022 John Wiley & Sons, Ltd.

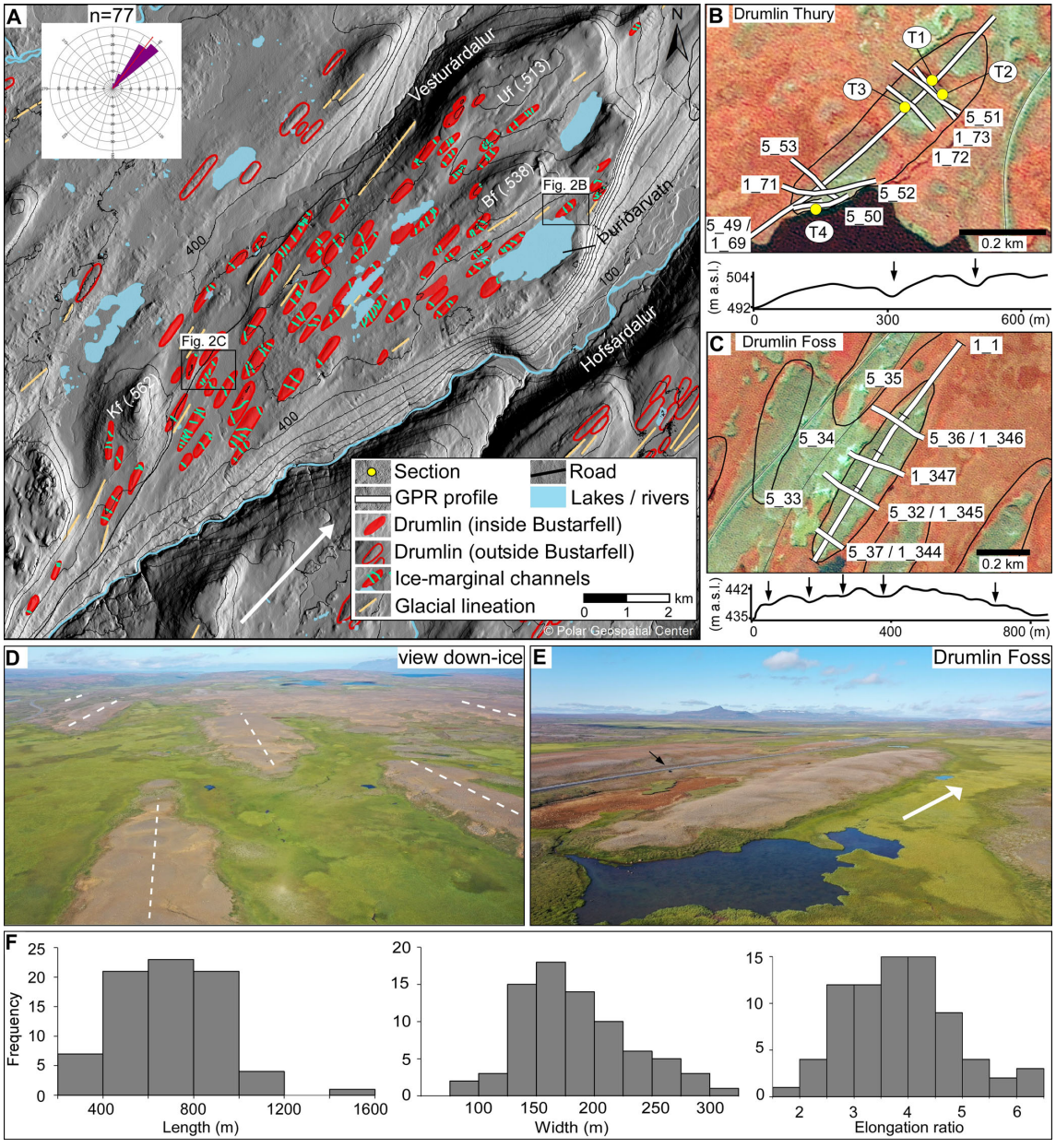

Figure 2. (A) The Bustarfell drumlin field within the Vopnafjörður–Jökuldalsheiði flow-set. The rose diagram shows the orientation of the 77 drumlins that have been mapped. Place names referred to in the text are marked and their altitude a.s.l. indicated (Kf – Kálfafell, Bf – Bustarfell, Uf – Urðarfell). The hillshade is from the ArcticDEM with solar angle from the north at 30° and three times exaggeration. Contour intervals are 50 m. The legend applies to A–C. (B) Drumlin Thury. (C) Drumlin Foss. Cross profiles are shown below them with arrows pointing at ice-marginal channels. The white lines on B and C indicate the locations of the GPR profiles and the numbers in front of them represent the respective frequencies (5:50 MHz, 1:100 MHz). Background data are infrared satellite images from National Land Survey of Iceland. (D) Drone image of several drumlins within the Bustarfell drumlin field. The dashed lines indicate the long axes of the most obvious drumlins. (E) Drone image of drumlin Foss with a car for scale (black arrow). Note how well-defined the drumlins are within the peat bogs and high groundwater table in the interdrumlin areas. The white arrows indicate the general ice-flow direction. (F) Size-frequency (length, width and elongation ratio) distribution of the morphometrics of the Bustarfell drumlins. [Color figure can be viewed at wileyonlinelibrary.com]

shoreline displacement after the YD (Norðdahl and Hjort, 1993; Sæmundsson, 1995). It has been suggested that the ice margin was situated at the mouth of the Vopnafjörður valley during the YD, but ice-marginal deltas indicate small readvances or stillstands of the ice margin farther up-valley in Vesturárdalur and Hofsárdalur during the Preboreal (Fig. 1B; Sæmundsson, 1995).

Methods

Geomorphological mapping and morphological analysis

The geomorphological mapping (Figs 1B and 2A–C) of the drumlins at Bustarfell was initially performed by Benediktsson *et al.* (2022a) but reviewed and refined for this study. The

© 2022 John Wiley & Sons, Ltd.

mapping was based on the Arctic Digital Elevation Model (ArcticDEM) with a 2 m vertical and <1 m horizontal resolution (Porter et al., 2018; corrected and mosaicked by the National Land Survey of Iceland (NLSI), the Icelandic Met Office and the Polar Geospatial Center). Furthermore, mapping was aided by infrared SPOT satellite images with 2.5 m resolution from NLSI and aerial images from Loftmyndir ehf. Analysis of the data and mapping was conducted in ESRI ArcGIS 10.4-7 and finalised in Canvas X. In addition, channels incising through the drumlins were mapped for this study using the criteria from Greenwood *et al.* (2007). To investigate the morphology of the drumlins, the length of the long axis, the width orthogonal to the long axis, and the orientation of the long axis were measured for each bedform using the minimum bounding geometry tool in ArcGIS, as described by Napieralski and Nalepa (2010).

Sedimentology

Natural sections through drumlins in the area are rare and only one natural coastal section could be cleaned by hand and studied (T4); that on the flank of drumlin Thury. An excavator was used to dig three pits (T1–3) in drumlin Thury, all located in dry transverse channels (Fig. 2B). Sediments exposed in the sections were documented at a scale of 1:20, using the data chart by Krüger and Kjær (1999) for glacial sediments, and the strike and dip of beds/structures were measured. Clast fabric measurements were collected from a 25 × 25 cm surface at each site, where the dip and dip direction were measured for at least 25 elongated clasts (*a*:*b* ratio >1.5:1) with an *a*-axis ranging in length from 0.6 to 6 cm (Kjær and Krüger, 1998). The measurements were then plotted and analysed in the software Stereonet and the eigenvectors (S_1 and S_3) and eigenvalues (V_1) calculated. If the eigenvalue of the principal eigenvector was higher than 0.54, the clasts were considered to show preferred orientation (Lawson, 1979). All compass measurements were corrected for the regional negative declination of 10° (in 2020). The sections and additional data were illustrated in Canvas X.

Grain-size analyses of diamict units were carried out using standard sieving methods, starting by washing out materials finer than 0.063 mm (fines; clay and silt), followed by dry sieving to separate the sand and gravel fractions. To examine the clast morphology, 50 clasts, with an *a*-axis between 1.5 and 10 cm, were collected from 25 × 25 cm surfaces. The *a*- (long), *b*- (intermediate) and *c*- (short) axes were measured and plotted in a ternary diagram (Evans and Benn, 2004). In addition, the roundness and texture of the clast was estimated (Powers, 1953; Evans and Benn, 2004). The clast shape is presented as the C_{40} index (percentage of clasts with *c*:*a* axis ratio ≤0.4) and the clast roundness as the RA index (percentage of angular and very angular clasts) (Benn and Ballantyne, 1993).

Ground-penetrating radar

GPR profiles were acquired on two drumlins, Thury and Foss (Fig. 2B–C), with a Malå Ramac/GPR CUII using both 50 and 100 MHz antennas, and antenna separation of 4 and 0.6 m, respectively. Surveys were made with a step size ranging from 0.02 to 0.5 m (Table 1). The data collection window was 0–715 ns for 50 MHz and 0–218 ns for 100 MHz and the sampling frequency was approximately 10 times the antenna frequency. In total, 20 profiles were acquired with a total length of 6437 m, transverse, longitudinal and diagonal, across the targets (Table 1). Some of the profiles from drumlin Thury were collected along the sections (Fig. 2B) in order to facilitate correlation between the GPR profiles and the sections. Data were processed with ReflexW 8.0 Sandmeier software, a GPR and seismic processing software, and topographic data from the ArcticDEM were used to rectify the profile elevation. The processing steps were done in this order (when deemed beneficial): dewowing, move start time, energy decay, background removal and elevation correction (see supplementary data). A velocity of 0.084 m/ns was used for depth conversion

Table 1. Information on the GPR profiles acquired. The highlighted profiles are considered representative for the GPR dataset and discussed in the manuscript. The additional profiles can be made available upon request.

Drumlin	Profile ID	Antenna (MHz)	Antenna separation (m)	Step size (m)	Length (m)	Direction	Start point		End point		Geometry
							Longitude	Latitude	Longitude	Latitude	
	5_49	50	4	0.4	800	SW–NE	492528	7276296	493123	7276762	Longitudinal
	5_51	50	4	0.5	215	NW–SE	495882	7276671	493026	7276553	Transversal
	5_53	50	4	0.4	159	NW–SE	492633	7276468	492734	7276369	Transversal
	5_50	50	4	0.4	76	W–E	492632	7276354	492698	7276367	Diagonal
Thury	5_52	50	4	0.4	105	W–NNE	492662	7276360	492759	7276377	Diagonal
	1_69	100	0.6	0.25	691	SW–NE	492608	7276336	493119	7276761	Longitudinal
	1_73	100	0.6	0.25	150	NW–SE	492932	7276657	493018	7276537	Transversal
	1_72	100	0.6	0.25	149	NW–SE	492867	7276616	492967	7276513	Transversal
	1_71	100	0.6	0.25	221	W–E	492611	7276404	492823	7276404	Diagonal
	5_33	50	4	0.02	672	SSW–NNE	484089	7272929	484423	7273416	Longitudinal
	5_34	50	4	0.02	142	SSW–NNE	484258	7273173	484332	7273285	Longitudinal
	5_35	50	4	0.4	631	SSW–NNE	484433	7273286	484700	7273737	Longitudinal
	5_36	50	4	0.4	250	WNW–ESE	484345	7273516	484533	7273380	Transversal
	5_32	50	4	0.02	265	WNW–ESE	484144	7273266	484341	7273118	Transversal
Foss	**5_37**	50	4	0.25	148	WNW–ESE	484195	7272969	484107	7273045	Transversal
	1_1	100	0.6	0.05	884	SSW–NNE	484100	7272947	484587	7273622	Longitudinal
	1_344	100	0.6	0.05	134	WNW–ESE	484108	7273064	484199	7272972	Transversal
	1_345	100	0.6	0.05	251	WNW–ESE	484138	7273267	484339	7273121	Transversal
	1_346	100	0.6	0.05	246	WNW–ESE	484340	7273512	484529	7273361	Transversal
	1_347	100	0.6	0.05	237	WNW–ESE	484245	7273344	484452	7273241	Transversal

© 2022 John Wiley & Sons, Ltd.

of the recorded two-way travel time based on common mid-point measurements on drumlin Sauralda in Bakkaflói (Fig. 1B). This value is similar to other glacial sediments in Iceland (Cassidy *et al.*, 2003; Kjær *et al.*, 2004; Benediktsson *et al.*, 2009; Woodard *et al.*, 2020) and to the tabulated range of 0.06–0.1 m/ns for saturated and damp sand (Jol and Bristow, 2003).

Results

Morphology of the drumlins

In total, 77 drumlins occur within the Bustarfell drumlin field, an area of ~100 km^2. The mean orientation of the drumlins is southwest to northeast (36°), the mean length is 696 m with a range of 319–1438 m and the mean width is 183 m with a range of 86–301 m. The mean elongation ratio (ER) is 3.8:1 with a range of 1.8:1–6.5:1 (Table 2). The histograms all demonstrate a unimodal distribution, similar to the entire data set of SSBs in northeast Iceland (Benediktsson *et al.*, 2022a). However, the histograms for the Bustarfell drumlins do not have such clear positive skews and indicate rather consistent morphometry, with little to no difference between the mean and median values (Fig. 2F; Table 2). Compared with the mapped drumlins in northeast Iceland, the Bustarfell drumlin field is well-defined with a relatively high density of 7–9 drumlins per 4 km^2 (Benediktsson *et al.*, 2022a). Peat bogs are common in the interdrumlin areas and occasionally link with seasonal drainage channels. Often these drainage channels correspond to transverse depressions cutting perpendicular through the drumlins (Fig. 2A, D, E). Given the morphology and re-occurring interval of the transverse channels (Fig. 2A, D, E), we associate these features with ice-marginal positions and meltwater incision during stepwise glacial retreat and drumlin exposure from under the ice (cf. Greenwood *et al.*, 2007).

Two drumlins within the Bustarfell drumlin field were investigated in detail: drumlin Thury and drumlin Foss. Drumlin Thury is in the northeastern part of the drumlin field and is orientated southwest to northeast (46°). The drumlin is around 600 m long, 160 m wide and up to 12 m high with an ER of 3.6:1. The longitudinal profile of the drumlin is asymmetric, with a reversed shape (lee side higher than the stoss side) and has been subdivided by two large, transverse meltwater channels, each over 50 m in width and around 3–4 m deep with ~180 m spacing between them (Fig. 2A, B). Drumlin Foss is located within the western part of the drumlin field, northeast of Kálfafell, and is orientated south-southwest to north-northeast (32°). It is around 840 m long, 175 m wide and up to 8 m high with an ER of 4.8:1. The longitudinal profile of the drumlin is nearly symmetrical. Five transverse, shallow (<2 m deep) meltwater channels can be identified in the surface of drumlin Foss with incision either half-way or completely through the drumlin. The spacing between the channels varies from 70 to 180 m (Fig. 2A, C).

Sedimentology

Four sections were logged in drumlin Thury (T1–T4; Figs 2B, 3 and 4) with six lithofacies identified: (f1) clayey-gravelly, grey diamict; (f2) silty-sandy, dark/blue-grey diamict; (f3) sand and gravel; (f4) silt, sand and gravel; (f5) soil; (f6) gravelly, brownish diamict. Lithofacies codes are according to Krüger and Kjær (1999) (Fig. 3).

F1, clayey-gravelly, grey diamict [Dm/h/b/M/F(m_{1-3})2–4]. The main deposit in sections T1–3 in drumlin Thury is a grey, firm, moderate to clast-rich diamict with clayey to gravelly matrix. It is generally homogeneous, but areas of banded and heterogeneous matrix appear. The clast content generally decreases in the lower part of the sections and the matrix becomes firmer. Examination of clasts in the field and the clast morphology show that they are to a large extent blocky and subrounded to subangular (C_{40} = 0–16 and RA = 0–2). Occasional bullet-shaped and striated clasts occur (18–26%). Based on three grain-size analyses from two sections (T2 and T3) the matrix ranges are: 32–54% fines, 30–35% sand and 16–35% gravel. The grain-size analysis of f1 does not show any significant change between the sections, although section T2 has greater content of fines than the other sections and T3 slightly more gravel. Poorly developed fissility was observed sporadically. Lenses and bands of stratified sand and gravel (f4), often showing signs of deformation, commonly occur within the lithofacies (Figs 3B, B and 6A–D). F1 is interpreted as subglacial traction till deposited by a combination of deformation and lodgment, based on its characteristics, fissility, clast morphology, fabric and deformed inclusions (Krüger and Kjær, 1999; Evans *et al.*, 2006).

F2, silty-sandy, dark/blue-grey diamict [DmM(m_2)3]. This lithofacies is a massive, homogeneous, matrix-supported diamict with a silty-sandy matrix and a moderate clast content, and is only observed in section T4 (Figs 4B and 5). It is firm and rather difficult to excavate. The colour of the lithofacies is dark/blue-grey, which differentiates it from f1. Based on the grain-size distribution it contains 31% fines, 46% sand and 22% gravel and the clasts are usually blocky and subrounded to subangular (C_{40} = 5 and RA = 2) and below 15 cm in diameter. Larger boulders (<30 cm in diameter) do also occur. No structures were observed in the diamict but a few lenses of laminated/rippled sand (f4) occur within it (Figs 4B and 6F). Based on its characteristics and the presence of sand lenses within it, f2 is interpreted as subglacial traction till (Krüger and Kjær, 1999; Evans *et al.*, 2006).

F3, sand and gravel [S/G/m/h/p]. This lithofacies represents layers (~5–100 cm thick) of sorted sand and gravel that are observed in sections T1 and T4 (Figs 6C–D and 5). It appears as either massive, horizontally laminated or cross-bedded with visible deformation structures. The clasts in the gravel layers are mostly subrounded (<3 cm in diameter). We interpret f3 as glaciofluvial outwash deposits (Evans *et al.*, 2006).

F4, silt, sand and gravel [F/S/G/m/h/p]. This lithofacies describes lenses or thin layers (<3 cm thick) of silt, sand and gravel, which were observed in all of the sections in f1 and f2. F4 appears as massive or horizontally laminated, with occasional vague ripples and deformation structures (Fig. 6A, D). The sand lenses are very compact, and most of the lenses are dipping towards the northeast, parallel to the drumlin's long axis. The gravel is mostly subrounded, although subangular clasts are also present. F4 is interpreted to represent the infilling of smaller subglacial meltwater streams or ponds (Evans *et al.*, 2006).

F5, soil [Fm]. In the upper part of sections T1–3 in drumlin Thury is a 25–200 cm thick unit of fine-grained brownish soil. Lenses of sand and gravel can be found within this lithofacies as well as dark and light-coloured, fine-grained tephra layers

Table 2. Morphometrics of drumlins within the Bustarfell drumlin field.

n = 77	Mean	Median	Max	Min	SD	10%	90%
Length (m)	696	689	1438	319	229	409	962
Width (m)	183	176	301	86	49	130	262
Elongation ratio	3.8	3.8	6.5	1.9	1	2.8	5.1
Orientation (°)	36	37	52	3	9	27	46

© 2022 John Wiley & Sons, Ltd.

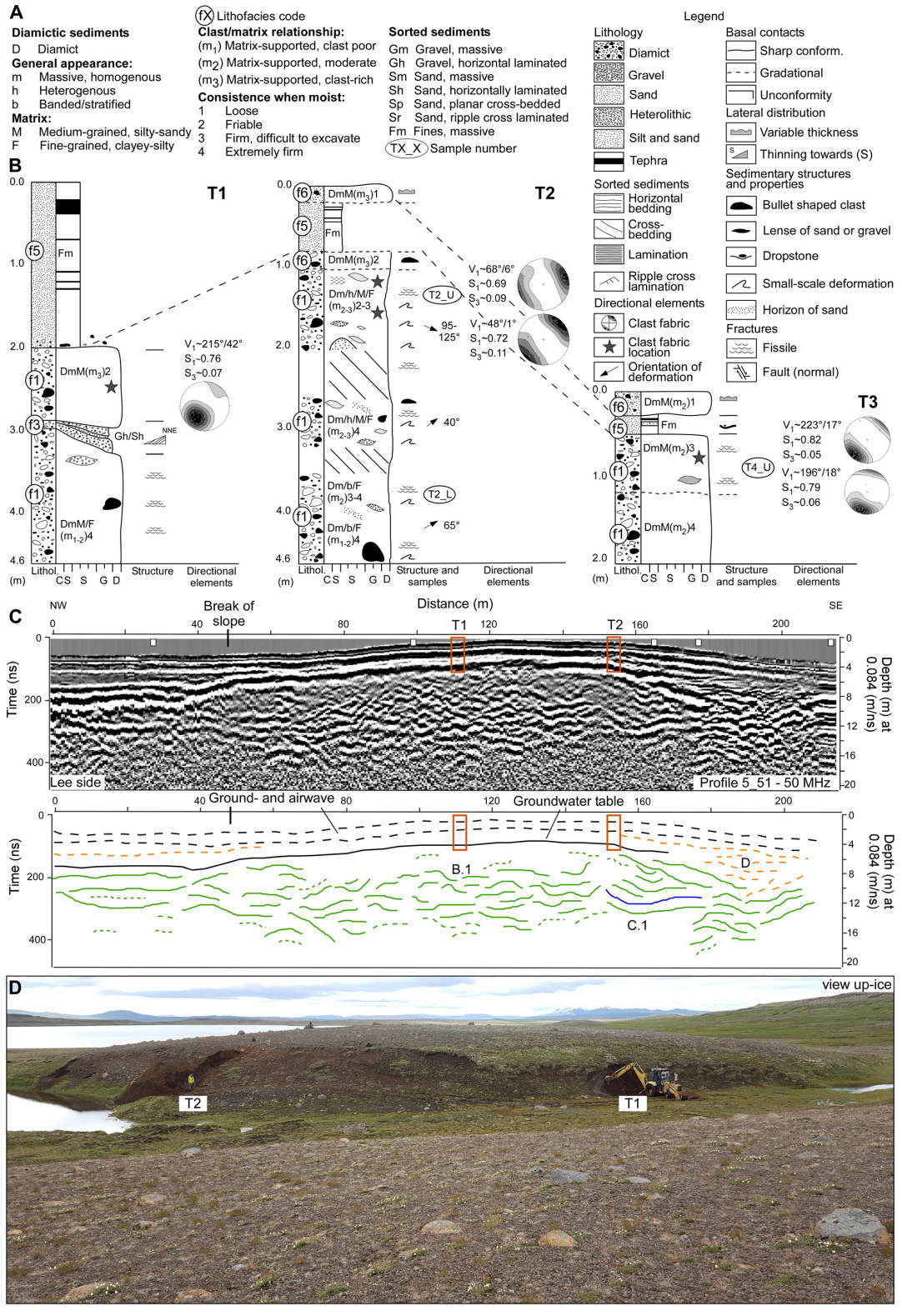

Figure 3. (A) Legend with symbols and lithofacies codes used here and for other logs in the paper, following Krüger and Kjær (1999). (B) Stratigraphical logs from sections T1, 2 and 3. The dashed lines show the correlation between the different units as made in the field. (C) The processed and interpreted GPR profile 5_51 (50 MHz). The location of sections T1 and T2 are marked. The profiles are exaggerated ×2 vertically. (D) View up-ice of drumlin Thury during the opening of the sections T1–2 with the excavator. [Color figure can be viewed at wileyonlinelibrary.com]

© 2022 John Wiley & Sons, Ltd.

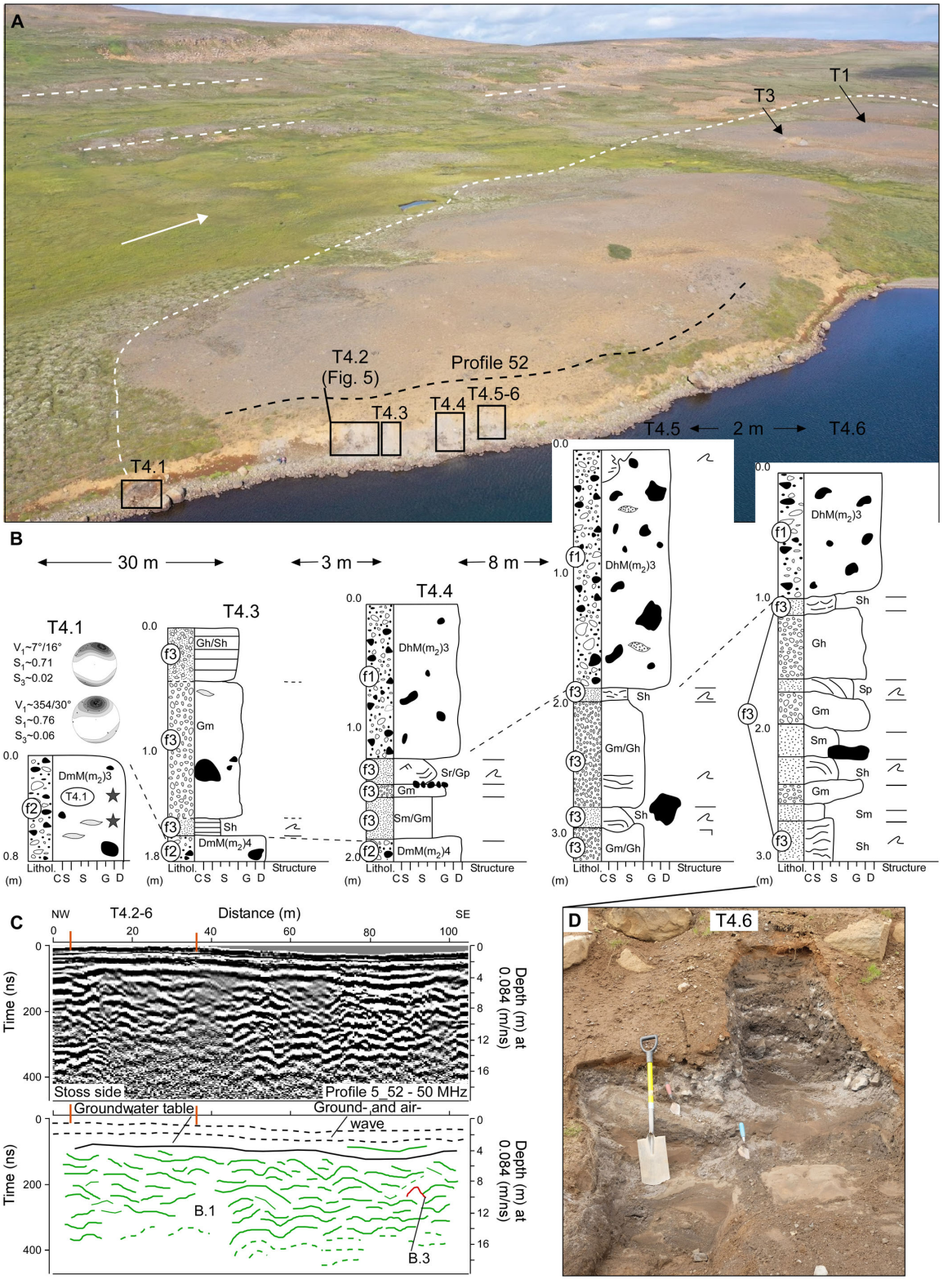

FIGURE 4 Continued.

© 2022 John Wiley & Sons, Ltd.

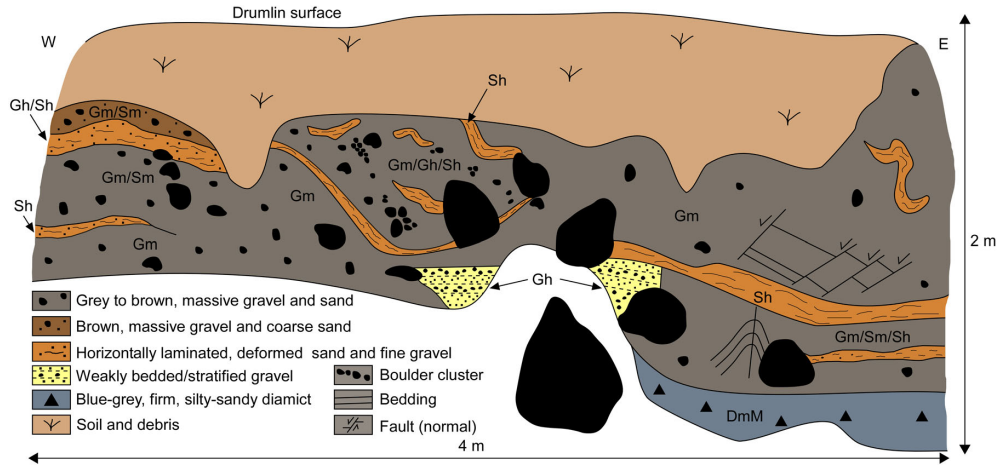

Figure 5. Section T4.2 in drumlin Thury. [Color figure can be viewed at wileyonlinelibrary.com]

(Fig. 6A, C). The tephra layers are usually 1–5 cm thick except for a layer in the upper part of T1 that is around 10 cm thick. The tephra was transported as air-fall from various Icelandic volcanoes and deposited on the Bustarfell plateau. Although we do not have any constraint on the origin or age of the tephra layers, the ash distribution maps of the area indicate that the light-coloured layers might be Hekla 3 (3000 cal. yr BP) and 4 (4200 cal. yr BP) (Guðmundsdóttir *et al.*, 2011). The dark layers are most likely of unknown origin from the Late Holocene.

F6, brownish, gravelly diamict [DmM(m_{2-3})1]. Brownish, massive diamict with a silty to gravelly matrix is observed at the top of sections T2 and T3 and right below the soil (f5) in T2 (Fig. 6A and C). It can be distinguished from f1 by the brownish colour and higher content of gravel and no boulders (>3 cm in diameter). No structures can be found within the lithofacies. F6 is interpreted as cryoturbated diamict because of its location above and below the soil (f5), structureless characteristics and the different clast content from f2.

Stratigraphy

Section T1 is located in a dry transverse ice-marginal channel at the down-ice side of drumlin Thury, close to the long-itudinal axis of the drumlin (Fig. 2B and D). The section is orientated southeast to northwest, and is 4.6 m high with four lithofacies observed. Groundwater was present at the base of the section (Fig. 6C). The lowermost part of the section (3.0–4.6 m) is composed of grey massive, till with clayey to sandy matrix (f1) with lenses of sand (f4). Very delicate fissile structures were observed in the matrix. At ~3 m depth, the till is dissected by interbedded, stratified sand to coarse gravel (<5 cm in diameter) (f3). The layer is 0.5–0.2 m thick, thickening towards the north-northeast and coarsening down-wards. F1 appears again overlying the gravel with a sharp boundary (2.0–2.8 m). The upper till has a coarser matrix (sandy to gravelly) and higher clast content than the till below and is less compact. Clast fabric in the upper part of the till (sampled at 2.5 m depth) shows preferred orientation roughly parallel to the orientation of the bedform (southwest to northeast), dipping towards the southwest (up-ice) (V_1 = 215°/42°, S_1 = 0.76) (Fig. 3B). There is a sharp conformable contact up to the uppermost 2 m of the section, which are composed of brown soil (f5) with five light and dark tephra layers. A few outsized clasts (<1 cm in diameter) occur in the lowermost part of the soil (Figs 3B and 6C).

Section T2 is ~40 m south-southwest of section T1 in the same transverse channel, southeast of the long axis and is orientated north-northwest to south-southeast (Fig. 2B and D). The section is 4.6 m high with four lithofacies identified. The section is mostly composed of subglacial traction till (1.1–4.6 m: f1) with silt, sand and gravel lenses (f4). Fissile and small-scale ductile deformation structures appear throughout the section, with apparent dip towards the northeast. Clast fabrics in the upper part of the till (sampled at 1.3 and 1.6 m depth) show preferred orientation parallel and oblique to the bedform long axis, southwest to northeast, where clasts are dipping down-ice (V_1 = 48°/1° and 68°/6°, S_1 = 0.69 and 0.72). Above the till is a gradual boundary to f6, where there is a transition zone about 0.2–0.3 m thick between clean soil and diamict. There is an abrupt change in colour between f6 and the underlying till (f1) from brown to grey. Cryoturbated diamict (f6) is at the top of the section (0–0.2 m), with gradational boundary to f5, a 0.6 m thick soil with four thin (<1 cm), cryoturbated tephra layers (Figs 3B and 6A).

Section T3 is located ~90 m southwest of section T1, in the transverse channel that cuts through the middle of the drumlin (Fig. 2B). The section is orientated southeast to northwest and west-southwest to east-northeast. In total, four lithofacies were identified in the 2 m high section. Most of the section (0.6–2 m) is composed of massive, silty-sandy till (f1) that becomes less compact in the uppermost part of the section. Vague fissility and laminated sand lenses (f4) are identified in the upper part of the section (Fig. 6B). Two clast fabrics were examined in this section. One of them (sampled at 0.8 m depth) shows a preferred orientation parallel to the bedform,

Figure 4. (A) Drone image of drumlin Thury with view to the north. The different parts of section T4 that have been logged are marked (T4.1–6) together with GPR profile 52. Sections T1 and 2 that are located further down-ice are marked as well. The drumlin and glacial lineations are indicated with white dashed lines to enhance their appearance. The white arrow indicates the general ice-flow direction. (B) Stratigraphical logs from section T4. The key to the logs is in Fig. 3A. The dashed lines show the correlation between the different units. (C) The processed and interpreted GPR profile 5_52 (50 MHz). The location of sections T4.2–6 are marked. The profile is exaggerated ×2 vertically. (D) Section T4.6. Note the deformation of the sorted sediments in the lower part.

© 2022 John Wiley & Sons, Ltd.

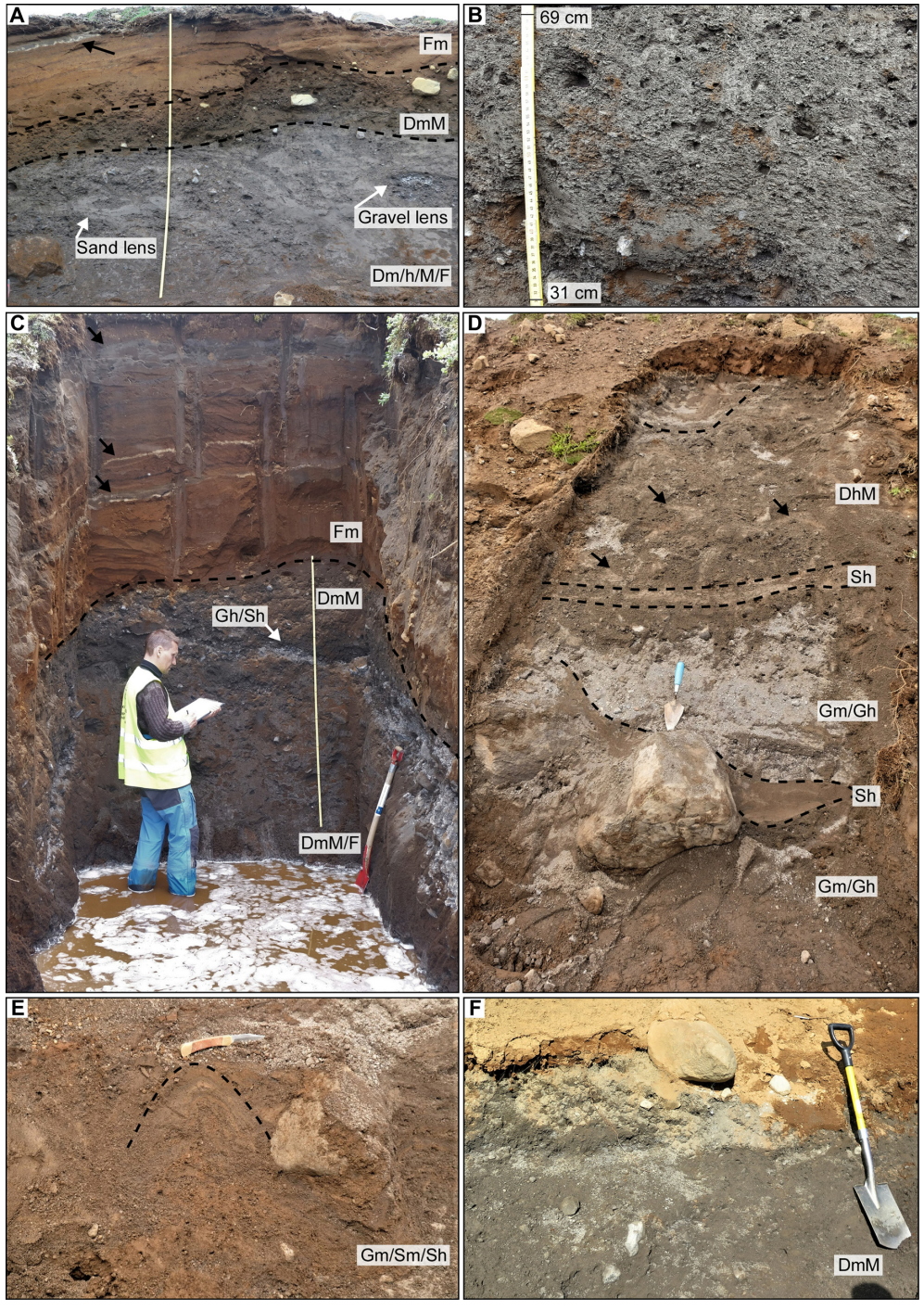

Figure 6. (A) The top of section T2. Note the deformed sand and gravel lenses and the cryoturbated soil (DmM) between the till (Dm/h/M/F) and the soil (Fm). The ruler is 2 m long. (B) A close-up of the fissile structure in subglacial traction till in section T3. (C) Section T1 with groundwater at the base (4.6 m depth). Note the stratified gravel and sand layer (Gh/Sh) that intersects the till layers. Note also the tephra layers (black arrows) in the soil (Fm). The ruler is 2 m long. (D) Section T4.5 is composed of deformed, massive and stratified sand and gravel layers with heterogeneous till with sand and silt lenses (black arrows) on top. (E) A close-up of a tight, upright fold in sand and gravel in section T4.2. (F) Section T4.1 is composed of massive, dark grey till. [Color figure can be viewed at wileyonlinelibrary.com]

© 2022 John Wiley & Sons, Ltd.

southwest to northeast, with clasts dipping towards southwest/south-southwest (up-ice) (V_1 = 223°/17°, S_1 = 0.82), whereas the other one (sampled at 0.9 m depth) showed preferred orientation oblique to the long axis of the bedform (V_1 = 196°/18°, S_1 = 0.79). The upper part of the section is composed of brownish soil (0.25–0.6 m: f5) with few tephra layers and cryoturbated diamict (0–0.25 m: f6) is at the top. The contact between all the lithofacies is sharp (Fig. 3B).

Section T4 is located by the lake at the stoss side of drumlin Thury and is orientated west to east, i.e. obliquely to the drumlin's long axis. In total, the section is around 40 m long and was documented in five stratigraphical logs and one diagram, in which four lithofacies were identified (Figs 2B, 4A, B and 5; T4.1–6). T4.1 is located at the western end of the section at the break of slope of the drumlin and is only 0.8 m high. It consists of silty-sandy, massive, dark-grey till (f2) with small lenses of sand (f4) (Fig. 6F). Two fabric analyses (sampled at 0.3 and 0.5 m depth) show preferred orientation towards the north (V_1 = 7°/16° and 354°/30°, S_1 = 0.71 and 0.76) (Fig. 4B). T4.2 is located ~25 m east of T4.1 and is illustrated on Fig. 5. The section is up to 2 m high and massive, compact, blue-grey till (f2) is observed partly at the base (<0.25 m thick). Most of the section above is composed of blue-grey to brown, massive sand to gravel (f3), with deformed layers and lenses of laminated gravel, sand and silt (f4). Small-scale normal faults and an upright fold were also observed, indicative of both brittle and ductile deformation (Figs 5 and 6E). Smaller cobbles (5–15 cm in diameter) and larger boulders (>30 cm in diameter) are embedded in the till. Slightly further to the east are sections T4.3 and T4.4, which show similar stratigraphy to T4.2, although T4.4 does have over 1 m of subglacial traction till (f1) at the top with a sharp boundary to the sand and gravel below (f3). Sections T4.5–6 are ~8–10 m farther to the east with similar stratigraphy as the sections to the west. Interbedded, laminated, rippled, cross-bedded to massive sand and gravel beds, showing signs of deformation (f3), make up the lowermost part of the sections (1.2–2 m thick). Large boulders (>20 cm in diameter) are lodged in the sorted sediments. The boundary is sharp with the overlying subglacial traction till (f1; 1–1.9 m thick). Occasional sand lenses (f4) are found within the subglacial traction till (Figs 4B, D and 6D).

Ground-penetrating radar

Twenty GPR profiles were collected with 50 and 100 MHz antennas (Fig. 2B and C; Table 1). Here, we show six transverse profiles that are considered to be representative of the drumlin architecture and the remaining profiles. The different radar facies and structures that are identified within the profiles are described and labelled in Table 3.

Drumlin internal architecture

On the 50 MHz profiles, the interior of the drumlins can be described in general as wavy with moderately continuous to discontinuous reflections (radar facies B.1) that can be traced down to a maximum depth of ~16 m. On the 100 MHz profiles, one radar facies (B.2) could also be identified; chaotic, moderately continuous to discontinuous reflections (Table 3; Figs 3C, 4C and 7). Although the reflection pattern between the two frequencies varies slightly as they have a different resolution, we interpret the radar facies in a similar manner, based on their characteristics and correlation with the stratigraphical logs (Figs 3B, C and 4B, C). Radar facies B.1 and B.2 are interpreted as subglacial traction till with interbedded glaciofluvial material of various thicknesses.

Table 3. Radar facies description and interpretation.

Facies/structures antenna	Example	Description	Lithology	Sedimentological interpretation
A (Structure) 50 MHz		Planar to wavy, moderately continuous reflections	Bedrock contact	Upper boundary of the bedrock (plateau basalts)
B.1 (Facies) 50 MHz	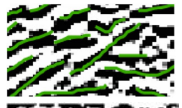	Wavy, moderately continuous to discontinuous reflections	Diamict and sorted sediments	Subglacial traction till and glaciofluvial material
B.2 (Facies) 100 MHz		Chaotic, moderately continuous to discontinuous reflections	Diamict and sorted sediments	Subglacial traction till and glaciofluvial material
B.3 (Structure) 50 and 100 MHz	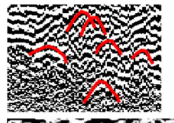	Hyperbolas	Boulder cluster	Boulder or boulder clusters in diamict
C.1 (Structure) 50 MHz		Concave and convex reflections	Gravel and sand layers	Channel infillings
C.2 (Structure) 100 MHz		Concave, subparallel reflections	Gravel and sand layers	Channel infillings
D (Facies) 50 and 100 MHz		Parallel, (vague) reflections that range from being continuous to discontinuous	Mixed finer grained sediments	Post-glacial sediments

© 2022 John Wiley & Sons, Ltd.

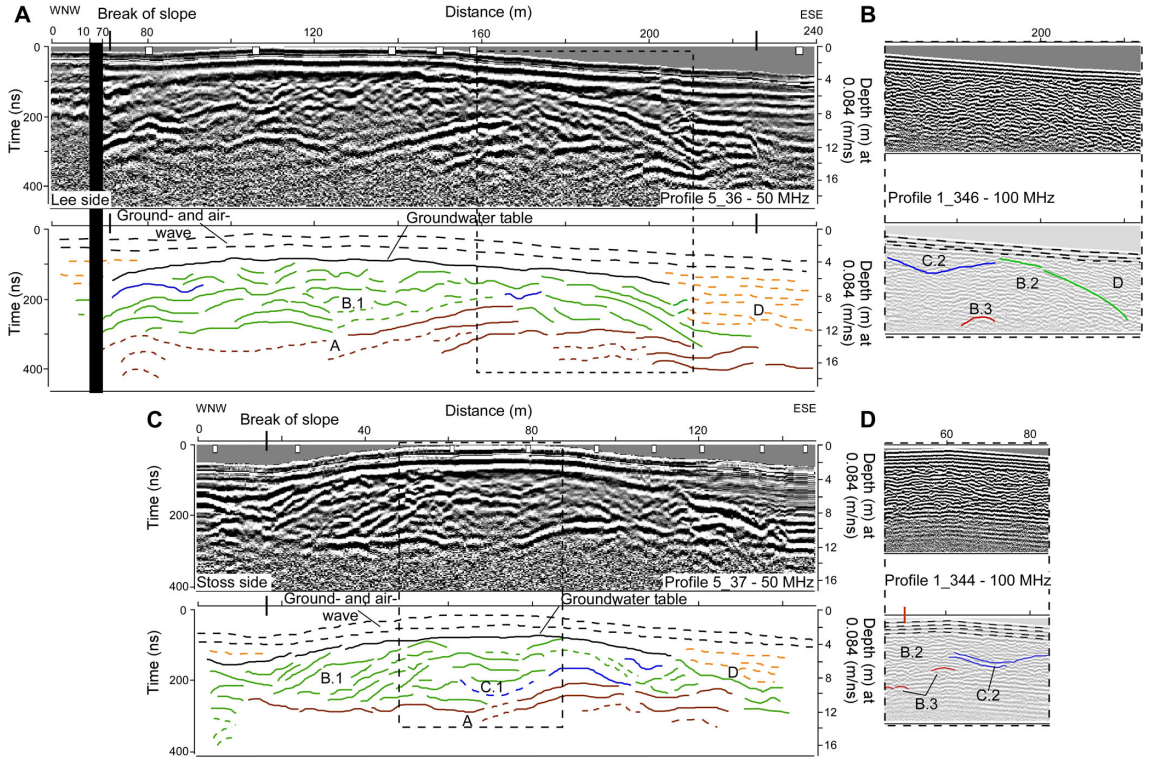

Figure 7. GPR profiles from drumlin Foss (see location on Fig. 2C). (A) Profile 5_36, 50 MHz, from the lee side. The black line represents a 60 cm gap that was cut out from the profile. (B) A close up of profile 1_346, 100 MHz. (C) Profile 5_37, 50 MHz, from the stoss side. The dashed boxes indicate the location of the 100 MHz profiles compared with the 50 MHz ones. (D) A close-up of profile 1_344, 100 MHz. Note the correlation of structures between the profiles. Due to the chaotic reflections in radar facies B.2 on the 100 MHz profiles, individual reflections are not drawn but the transparent profile is displayed instead. [Color figure can be viewed at wileyonlinelibrary.com]

Different structures are identified within the radar facies, such as concave and convex structures and occasional hyperbolas (Table 3; Figs 3C, 4C and 7A, C). The hyperbolas (B.3) are interpreted as larger boulders or boulder clusters in the till and the concave and convex structures as channel infillings (C.1 and C.2) (Neal, 2004). The chaotic structure might represent the deformation of the sediments that was observed in the sections (Neal, 2004; Watts *et al.*, 2022), and explain why it is challenging to distinguish between the till and the glaciofluvial material. The direct air- and ground-waves in the 50 MHz profiles appear as strong arrivals at the top, followed by another strong arrival that we interpret to be the groundwater table, as it correlates with the depth of the groundwater table (at 4–5 m) observed in section T1 (Fig. 6C). These strong arrivals hamper a straightforward correlation with the excavated sections.

Three general patterns can be detected from the transverse profiles. 1) Profiles from both drumlins show outward-dipping, long reflections that are conformable with the surface of the drumlins (Figs 3C and 7). 2) On one or both flanks of drumlins Thury and Foss, the outward-dipping reflections cut either shallower-dipping or inward-dipping, shorter reflections below. This is visible from both the lee side on drumlin Thury (Fig. 3C) and the stoss side on drumlin Foss (Fig. 7C). However, due to the interference of the air- and ground wave and the groundwater table in the upper part of the profiles (3–4 m), the extent of patterns no. 1 and 2 are not entirely understood. 3) The general appearance of the reflections is slightly stronger and less chaotic on the stoss side and at the base of the profiles (Figs 3C and 7). Other studies have interpreted stronger and more prominent reflections as a higher concentration of sorted material (e.g. Stokes *et al.*, 2008; Woodard *et al.*, 2020).

Boundary to the substratum

In a part of the 50 MHz profiles from drumlin Foss, strong reflections (radar structure A) are identified below radar facies B.1. The radar structure is planar to wavy and moderately continuous. In drumlin Foss the reflection generally occurs at 10–12 m depth, with little to no difference between the stoss and the lee side but is curved up towards the east-southeast on the transverse profiles. No coherent radar returns are beneath radar structure A (Fig. 7A and C; Table 3). This structure is interpreted to be the surface of the bedrock in the area, similar to other studies on drumlins' internal architecture with GPR (Spagnolo *et al.*, 2014). Based on its (strong reflective) characteristics and wavy structure, it is suggested that the bedrock has been sculpted by ice. No bedrock outcrops are seen in close proximity to the investigated drumlins; however, the general appearance of bedrock exposures in the area is supportive of our interpretation. There are several potential reasons why the strong reflection is not seen in drumlin Thury, such as the thickness or the characteristics of the sediment (e.g. higher clay content) preventing deeper penetration, or lower data resolution (Jol and Bristow, 2003; Spagnolo *et al.*, 2014).

Interdrumlin areas

Most of the GPR profiles extend beyond the break of slope of the drumlins (Fig. 2B and C) and indicate that the drumlin form

© 2022 John Wiley & Sons, Ltd.

extends below on-lapping sediments in the interdrumlin areas. These areas are characterised by radar facies D, which comprises numerous parallel (vague) reflections that range from being continuous to discontinuous (Table 3; Figs 3C, 7A and C). This facies is interpreted to be post-glacial sediments with thickness up to 8 m. Based on field observations, the uppermost part of the facies can be classified as peat bog (Fig. 2D and E). The peat bog extenuates the original morphology of the drumlins, especially their height (Spagnolo *et al.*, 2012, 2014; Finlayson, 2013; Benediktsson *et al.*, 2016).

Correlation between sections and GPR profiles

Although the GPR profiles were surveyed in the vicinity of the sections, a precise correlation between them was challenging, most likely due to sediment deformation and the lack of radar structures or facies that could be used as markers. The ground- and air-waves and the groundwater table interfere with the upper 3–4 m of the profiles, thus affecting the precise correlation of the GPR data to the stratigraphical logs. However, without the sections in drumlin Thury, the interpretation of the GPR profiles would have been more demanding as the radar facies interpretation is to a great extent based on the sections. We do therefore assume that the sections are representative of the drumlin composition at greater depth, as no clear boundaries or different units could be identified on the GPR profiles. Certain structures correlated well between the 50 and 100 MHz antennas from drumlin Foss as illustrated in Fig. 7.

Discussion

Internal architecture

The investigated drumlins on Bustarfell can be classified as part till, part sorted sediment drumlins (type 4 in Stokes *et al.*, 2011). Although the boundary to the underlying bedrock could probably be detected with the GPR on drumlin Foss, the drumlins do not comprise an actual bedrock core but rather seem to rest on the bedrock surface. The sections at the lee side and in the middle of drumlin Thury (sections T1–3) are composed of subglacial traction till, interbedded with lenses or layers of glaciofluvial material, showing signs of deformation. At the stoss side (section T4), thick, deformed glaciofluvial material appears between two tills. Our GPR profiles show slightly more prominent reflections at the stoss side, which supports the view that the glaciofluvial material is more abundant at the stoss side than the lee side (e.g. Stokes *et al.*, 2008; Woodard *et al.*, 2020). The deformation in drumlin Thury is generally more intense and extensive at the stoss side with most deformation structures classified as ductile and compressional, except for a few small normal faults indicating minor extensional deformation. The general orientation of the deformation structures indicates stress from the southwest. Although individual deformational structures could not be identified on the GPR profiles, the generally chaotic pattern is considered to be representative of intensive deformation (Neal, 2004). Based on the sedimentological data alone, there is no evidence for unconformities between the subglacial traction till and glaciofluvial material. Nor do the data reveal multiple till units that would suggest depositional processes during the drumlin formation (Benediktsson *et al.*, 2016). GPR data from other drumlin fields (Spagnolo *et al.*, 2014; Woodard *et al.*, 2020) have demonstrated erosional unconformities at the stoss side and flanks, and down-ice dipping reflections on the lee side indicating deposition. Our data do not exhibit the same clear evidence of depositional or erosional processes; however, minor unconformities seem to occur on one or both flanks of drumlin Thury and Foss where shorter internal reflections are truncated by the outward-dipping reflections conforming to the drumlin shape (Figs 3C and 7C). This suggests that both erosional and depositional processes are involved in the drumlin formation (Woodard *et al.*, 2020). According to Iverson *et al.* (2017), such cross-cutting relationships within drumlins reflect till deposition during active flow, and erosion by regelation infiltration or meltwater in subglacial channels during quiescence or slow flow. The architecture and cross-cutting relationships in the two investigated drumlins on Bustarfell may, therefore, indicate separate phases of erosion and deposition related to glacier flow dynamics.

The clast fabrics in lithofacies 1 in sections T1–3 in drumlin Thury all show unimodal and clustered fabric shapes with preferred orientation (S_1 = 0.69–0.82). Three out of the five clast fabric measurements are roughly parallel to the drumlin long axis, dipping either up-ice or down-ice, and the other two are oblique to the orientation of the drumlin. A systematic pattern of preferred orientation cannot be detected from the number or location of the clast fabrics in sections T1–3 (Fig. 3). However, the clast fabrics in lithofacies 2 in section T4.1, is orientated towards the north (353° and 7°) rather than the northeast. Benediktsson *et al.* (2022a) suggested that the regional ice flow during a phase of maximum glaciation was towards the north, independent of underlying topography. Thus, it may be speculated whether the northward-orientated clast fabrics in the lowermost till might result from this phase. This could be further supported by the location of the till unit in T4.1 at the edge of the drumlin's stoss side, which may suggest that it was not influenced during the drumlin-forming process, and that its sedimentological characteristics are different from the overlying till units which certainly constitute parts of the drumlin.

Formation of the drumlins and conceptual model

Sticky spots on the beds of glaciers are well-drained patches where the resistance to basal sliding is higher than in well-lubricated, low-strength areas around them, generating strain gradients across the bed (e.g. Boulton, 1987; Alley, 1993; Piotrowski *et al.*, 2004; Stokes *et al.*, 2007). Boulton (1987) attributes drumlins to strain gradients that lead to accretion on their top and downstream end but erosion along their periphery. The sticky spot model has thus been used to explain the formation of drumlins, e.g. under non-surging and surging glaciers in southeast Iceland (Boulton, 1987; Evans and Twigg, 2002; Waller *et al.*, 2008; Jónsson *et al.*, 2016) as well as on palaeo-ice stream beds elsewhere (e.g. Menzies and Brand, 2007; Evans *et al.*, 2015; Menzies *et al.* 2016). The glaciofluvial material in the core of drumlin Thury suggests a pre-existing obstacle in the substratum that acted as a sticky spot and facilitated the formation of the drumlin. The unimodal shape of the Bustarfell drumlins, their high density and similar morphometry (Fig. 2A–F; Table 2) does suggest to us that they were all formed by similar processes. However, we acknowledge that our data are spatially limited within the Bustarfell drumlin field and stress that this inference could be tested with more extensive excavations and GPR profiling across the field.

Dowling (2016) demonstrated that pre-existing obstacles, which could serve as drumlin cores, are necessary for the initiation of drumlin formation in areas characterised by thin glacial drift and where bedrock knobs are lacking. If obstacles

© 2022 John Wiley & Sons, Ltd.

like glaciofluvial outwash exist, then drumlin formation is initiated through differential flow over and around them (Boulton, 1987). Further growth and shaping are then dependent on the physical characteristics of the substratum, till accretion and rheology, hydrology and ice, and the subsequent architecture of the drumlin is the result of the interplay between deposition, erosion and deformation (Hart, 1997; Möller and Dowling, 2016). Recent investigation of a modern drumlin field at Múlajökull, central Iceland, suggests that lower effective stresses occur on drumlins than between them, resulting in till accretion on their top and lee slope during surge events but erosion on drumlin heads and flanks during quiescent flow (Benediktsson *et al.*, 2016; McCracken *et al.*, 2016; Iverson *et al.*, 2017). These drumlins are thus mostly composed of multiple till units with erosional unconformities. This model may be partly applicable to the drumlins at Bustarfell, but it cannot explain the initiation of their formation, which we consider to be related to pre-existing glaciofluvial material.

Based on our observations of two drumlins within the Bustarfell drumlin field, we propose the following conceptual model for their formation (Fig. 8):

(A) During a maximum glaciation, subglacial traction till was deposited on Bustarfell, possibly during a phase of northward flow across the site, as discussed by Benediktsson *et al.* (2022a) and indicated by the clast fabrics in the lowermost till unit at drumlin Thury.
(B) The ice sheet margin retreated onshore and inland during the deglaciation with meltwater being released from the glacier margin. We surmise that the glaciofluvial sediment observed within drumlin Thury was deposited proglacially during episodic retreat of the ice margin. Possibly, a sandur formed across the entire plateau with extensive braid bars that later acted as sticky spots during drumlin formation. However, due to the regional topography, we assume that the main volume of the meltwater went down the valleys on each side of Bustarfell and less water was released up on the plateau. Hence, we consider it more likely that the

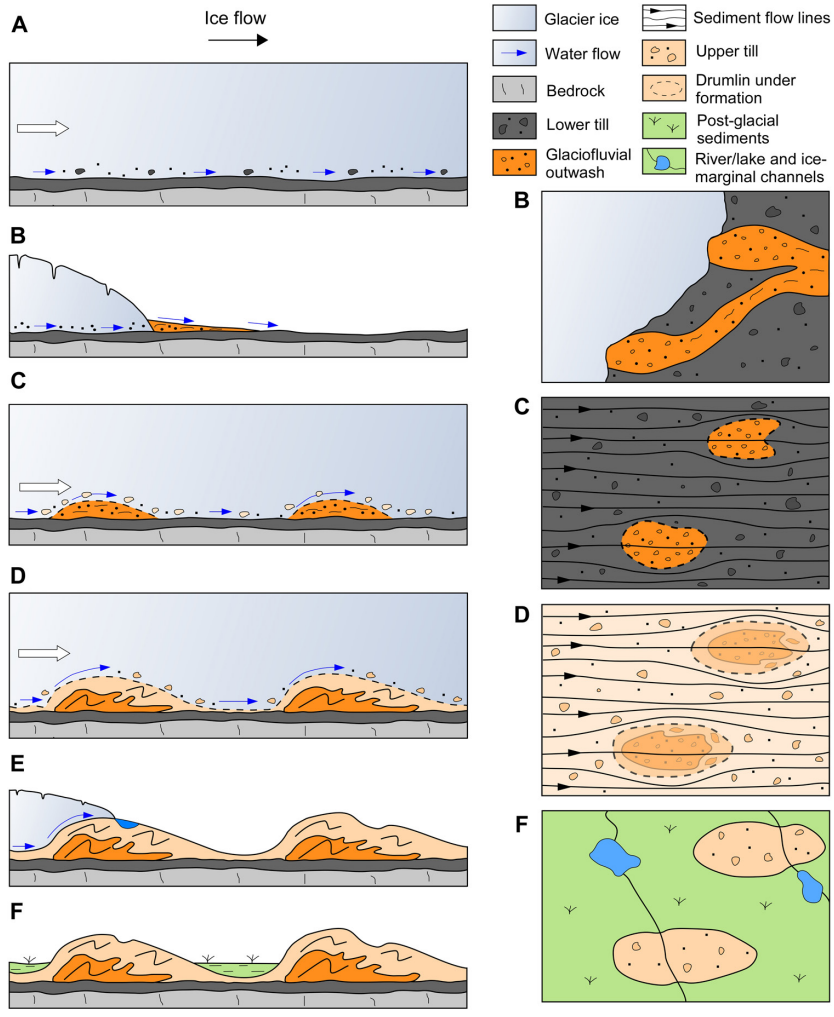

Figure 8. A conceptual model of the formation of the investigated drumlins. (A) Maximum glaciation. Deposition of subglacial traction till. (B) Deglaciation. Ice-marginal outwash fans are deposited. (C) Glacier readvance. The coarser grained glaciofluvial material acts as sticky spots and initiates the drumlin formation. (D) Drumlin formation. Deformation of the glaciofluvial core and subglacial traction till is draped around it followed by drumlinisation of the landscape. (E) Deglaciation. The ice retreat is stepwise and ice-marginal channels are formed during the retreat. (F) Post-glacial sediments are deposited with time in the interdrumlin areas. The scale is non-proportional.

© 2022 John Wiley & Sons, Ltd.

glaciofluvial material represents minor outwash fans deposited in front of small meltwater outlets in the retreating ice margin.

(C) During a glacial readvance, the small outwash fans obstructed glacier flow and acted as sticky spots for the initiation of drumlin formation. That, together with the heterogeneous surface, caused velocity and strain gradients around the sticky spots, resulting in the deposition and deformation of subglacial traction till around the core.

(D) Till was deposited down-glacier from the core due to low pressure shadow while erosion was effective at the periphery of the drumlin (Boulton, 1987; Hart, 1997). During the drumlin formation process, the glaciofluvial core was deformed together with the till. The deformation within both the upper till and the glaciofluvial core suggests that the drumlins were formed by subglacial deformation around a relatively weak core (Hart, 1995). The approximate alignment of the clast fabrics and deformation structures with the drumlin orientation and the conformation of the upper till with the drumlin shape suggests that the upper till accreted during, rather than prior to, the drumlin formation. The deformation and lenses of glaciofluvial material in the subglacial traction till, especially at the lee side of the drumlin, possibly indicates fluctuating water pressures and phases of coupling and decoupling at the ice/bed interface (Boulton *et al.*, 2001; Kjær *et al.*, 2006).

(E) The drumlins were exposed during the final deglaciation and transverse ice-marginal channels incised the drumlin surface during a stepwise retreat of a passive terminus (Greenwood *et al.*, 2007).

(F) Post-glacial sediments have been and are deposited in the interdrumlin areas, reducing the apparent drumlin relief (Spagnolo *et al.* 2012; Finlayson, 2013; Benediktsson *et al.*, 2016).

Glacial history

Based on the present understanding of the glacial history of the Vopnafjörður area together with the conceptual model for the drumlin formation, the timing of the formation is speculated. During the LGM, the ice sheet extended all the way to the shelf edge (Spagnolo and Clark, 2009; Patton *et al.*, 2017; Benediktsson *et al.*, 2021b), with an ice stream draining northwards independent of topography from an east-to-west-orientated ice divide over the present Vatnajökull ice cap (Benediktsson *et al.*, 2022a; Fig. 1A). The northward fabric measured in the lowermost till at the stoss side of drumlin Thury could possibly be a result of the earlier northward ice flow. Ice-sheet thinning during the following deglaciation caused a shift in the ice-sheet dynamics so that the ice flow became controlled by the topography with an ice stream flowing along the Vopnafjörður valley-fjord system towards the northeast (Benediktsson *et al.*, 2022a). During the Bølling–Allerød interstadial, the ice sheet retreated onshore and inland to an unknown position in the eastern highlands of Iceland (Norðdahl and Pétursson, 2005; Hubbard *et al.*, 2006; Norðdahl *et al.*, 2008, 2012; Patton *et al.*, 2017; Benediktsson *et al.*, 2022b). Our data support the theory that Bustarfell became ice-free at that time, signified by the glaciofluvial material that we consider to have been deposited subaerially on top of the lower till. There is evidence for glacier readvances during the YD period from numerous sites around Iceland (Norðdahl *et al.*, 2008, 2019; Benediktsson *et al.*, 2022c) and Sæmundsson (1995) suggested that the readvance during the YD extended to the mouth of the Vopnafjörður valley (~17 km northeast of Bustarfell). In correlation with our conceptual model (Fig. 8), we consider the ice-contact glaciofluvial material deposition during the deglaciation to be crucial for the initiation of the drumlin formation. Consequently, we suggest that the drumlins were formed during the YD when the ice sheet readvanced and streamed across the glaciofluvial outwash. The ice-marginal channels incising the drumlins represent the final glacier retreat on Bustarfell. By assuming that they formed annually and considering their distribution and spacing, we roughly estimate that the ice margin retreated 70–180 m/year over the drumlin field. During the Preboreal, glaciers readvanced into the Vopnafjörður valleys, resulting in the formation of ice-marginal deltas and dead-ice fields (Sæmundsson, 1995; Fig. 1B). During this less extensive phase of glacier expansion, ice did not cover Bustarfell nor affect the drumlin, protected by the (~300 m) prominence of the plateau from the valley floor.

Conclusions

- The investigated drumlin Thury within the Bustarfell drumlin field is composed of two units of subglacial traction till with interbedded glaciofluvial sediments. The volume of glaciofluvial material is greater at the stoss side than the lee side, suggesting a core of glaciofluvial outwash. The upper till and the glaciofluvial sediments are clearly deformed.
- The boundary to the underlying bedrock was implied at ~10–12 m depth, based on the GPR data. There is no evidence of a bedrock core in the drumlins.
- The interdrumlin areas are composed of post-glacial sediments, up to 8 m thick. This sediment infill extenuates the original morphology of the drumlins, especially its height.
- The formation of the investigated drumlins is best explained by the sticky spot hypothesis where glaciofluvial outwash near the stoss side (essentially the drumlin core) retarded basal sliding and promoted deformation and accretion of subglacial traction till around the core and towards the drumlin tail. Our data indicate that the bedforms developed from a combination of erosional and depositional processes together with subglacial deformation.
- The unimodal shape, high spatial density and similar morphometry of the drumlins within the Bustarfell drumlin field suggest a similar formation process.
- Correlation of the drumlin formation to the glacial history in northeast Iceland indicates that they were formed during a YD readvance. Glaciofluvial material, which accumulated on the Bustarfell plateau during deglaciation after the LGM, makes up the core of the drumlins.
- The sedimentological and GPR data are complimentary, although the deformation and lack of trace layers made the interpretation of the GPR profiles challenging. Integrating GPR data with sedimentological data in glacial environments in Iceland can be useful to investigate the internal architecture of glacial bedforms and learn about processes operating at the beds of advancing glaciers and ice sheets.

Acknowledgements. This project has been funded through grants from the University of Iceland Research Fund (to ÓI), the Energy Research Fund of Landsvirkjun (to NA and ÍÖB) and the Icelandic Road and Coastal Administration (to ÍÖB). We would like to thank all our colleagues and graduate students for their great company during fieldwork, constructive discussions and helpful feedback during the project, especially for the help collecting the GPR data. Bragi Vagnsson, farmer at Bustarfell, kindly gave us the permission to excavate in drumlin Thury. The authors thank Adam Booth and an anonymous reviewer for their constructive comments, which improved the manuscript.

© 2022 John Wiley & Sons, Ltd.

Data availability statement

The data that support the findings of this study are available from the corresponding author upon reasonable request.

Author contributions—**Nína Aradóttir**: Investigation; Writing - original draft; Funding acquisition; Software; Visualization; Conceptualization; Formal analysis. **Ívar Örn Benediktsson**: Supervision; Writing - review & editing; Investigation; Funding acquisition; Conceptualization; Project administration; Resources. **Ólafur Ingólfsson**: Supervision; Writing - review & editing; Investigation; Funding acquisition; Resources. **Erik Sturkell**: Writing - review & editing; Software; Resources. **Skafti Brynjólfsson**: Investigation; Writing - review & editing; Resources. **Wesley R Farnsworth**: Writing - review & editing; Investigation. **Emrys Phillips**: Investigation.

Supporting information

Additional supporting information can be found in the online version of this article.

References

Allaart L, Friis N, Ingólfsson Ó et al. 2018. Drumlins in the Nordenskiöldbreen forefield, Svalbard. *Gff* **140**(2): 170–188. https://doi.org/10.1080/11035897.2018.1466832

Alley RB. 1993. In search of ice-stream sticky spots. *Journal of Glaciology* **39**: 447–454.

Benn DI, Ballantyne CK. 1993. The description and representation of particle shape. *Earth Surface Processes and Landforms* **18**: 665–672.

Benediktsson ÍÖ, Ingólfsson Ó, Schomacker A et al. 2009. Formation of submarginal and proglacial end moraines: implications of ice-flow mechanism during the 1963–64 surge of Brúarjökull, Iceland. *Boreas* **38**(3): 440–457. https://doi.org/10.1111/j.1502-3885.2008.00077.x

Benediktsson ÍÖ, Jónsson SA, Schomacker A et al. 2016. Progressive formation of modern drumlins at Múlajökull, Iceland: stratigraphical and morphological evidence. *Boreas* **45**: 567–583. https://doi.org/10.1111/bor.12195

Benediktsson ÍÖ, Brynjólfsson S, Ásbjörnsdóttir L. 2021a. Iceland: glacial landscapes of Iceland, *Palacios, Hughes, García-Ruiz, Andrés: Vol. 1 European Glacial Landscapes: Maximum Extent of Glaciations*. Elsevier.

Benediktsson ÍÖ, Brynjólfsson S, Ásbjörnsdóttir L. 2021b. Iceland: glacial landforms from the Last Glacial Maximum, *Palacios, Hughes, García-Ruiz, Andrés: Vol. 1 European Glacial Landscapes: Maximum Extent of Glaciations*. Elsevier.

Benediktsson ÍÖ, Aradóttir N, Ingólfsson Ó et al. 2022a. Cross-cutting palaeo-ice streams in NE-Iceland reveal shifting Iceland Ice Sheet dynamics. *Geomorphology* **396**: 108009. https://doi.org/10.1016/j.geomorph.2021.108009

Benediktsson ÍÖ, Brynjólfsson S, Ásbjörnsdóttir L. 2022b. Iceland: glacial landforms from the Bølling-Allerød interstadial. In *European Glacial Landscapes*, Palacios D, Hughes P, García-Ruiz JM, Andrés N (Eds.). Elsevier, in press.

Benediktsson ÍÖ, Brynjólfsson S, Ásbjörnsdóttir L. 2022c. Glacial landscapes of Iceland from the Younger Dryas. In *European Glacial Landscapes*, Palacios D, Hughes P, García-Ruiz JM, Andrés N (Eds.). Elsevier, in press.

Briner JP. 2007. Supporting evidence from the New York drumlin field that elongate subglacial bedforms indicate fast ice flow. *Boreas* **36**: 143–147. https://doi.org/10.1111/j.1502-3885.2007.tb01188.x

Boulton GS. 1987. A theory of drumlin formation by subglacial sediment, *Drumlin Symposium*. Balkema: Rotterdam.

Boulton GS, Dobbie KE, Zatsepin S. 2001. Sediment deformation beneath glaciers and its coupling to the subglacial hydraulic system. *Quaternary International* **86**(1): 3–28.

Bourgeois O, Dauteuil O, Van Vliet-Lanoë B. 2000. Geothermal control on flow patterns in the last glacial maximum ice sheet of Iceland. *Earth Surface Processes and Landforms* **25**: 59–76. https://doi.org/10.1002/(SICI)1096-9837(200001)25:1<59::AID-ESP48>3.0.CO;2-T

Bristow CS, Jol HM (Eds.). 2003. *Ground penetrating radar in sediments*. Geological Society of London.

Cassidy NJ, Russell AJ, Marren PM et al. 2003. GPR derived architecture of November 1996 jökulhlaup deposits, Skeiðarársandur, Iceland. *Geological Society, London, Special Publications* **211**(1): 153–166. https://doi.org/10.1144/GSL.SP.2001.211.01.13

Clark CD. 1993. Mega-scale glacial lineations and cross-cutting ice-flow landforms. *Earth surface processes and landforms* **18**(1): 1–29.

Clark C. 2010. Emergent drumlins and their clones: From till dilatancy to flow instabilities. *Journal of Glaciology* **56**(200): 1011–1025. https://doi.org/10.3189/002214311796406068

Clark CD, Spagnolo M. 2016. Glacially eroded cross-shelf troughs surrounding Iceland from Olex data. In *Atlas of Submarine Glacial Landforms: Modern, Quaternary and Ancient. Geological Society, London, Memoirs*, Dowdeswell JA, Canals M, Jakobsson M, Todd BJ, Dowdeswell EK, Hogan KA (Eds.) (**46**). Geological Society of London, 165–166. https://doi.org/10.1144/M46.86; https://doi.org/10.1016/j.geomorph.2015.02.018

Dowling T. 2016. *The drumlin problem: streamlined subglacial bedforms in southern Sweden*. Lund University.

Evans DJA, Twigg DR. 2002. The active temperate glacial landsystem: a model based on Breiðamerkurjökull and Fjallsjökull, Iceland. *Quaternary science reviews* **21**(20-22): 2143–2177. https://doi.org/10.1016/S0277-3791(02)00019-7

Evans DJA, Phillips ER, Hiemstra JF et al. 2006. Subglacial till: formation, sedimentary characteristics and classification. *Earth-Science Reviews* **78**(1-2): 115–176. https://doi.org/10.1016/j.earscirev.2006.04.001

Evans DJA, Benn DI (Eds.) 2004. *A practical guide to the study of glacial sediments* (**83-87**). Arnold: London; 97–107.

Evans DJA, Roberts DH, Cofaigh CÓ. 2015. Drumlin sedimentology in a hard-bed, lowland setting, Connemara, western Ireland: implications for subglacial bedform generation in areas of sparse till cover. *Journal of Quaternary Science* **30**(6): 537–557. https://doi.org/10.1002/jqs.2801

Eyles N, Putkinen N, Sookhan S et al. 2016. Erosional origin of drumlins and megaridges. *Sedimentary Geology* **338**: 2–23. https://doi.org/10.1016/j.sedgeo.2016.01.006

Finlayson A. 2013. Digital surface models are not always representative of former glacier beds: palaeoglaciological and geomorphological implications. *Geomorphology* **194**: 25–33. https://doi.org/10.1016/j.geomorph.2013.03.026

Fowler AC. 2000. An instability mechanism for drumlin formation, *Geological Society, London, Special Publications*. **176**(1): 307–319.

Fowler AC 2010. The instability theory of drumlin formation applied to Newtonian viscous ice of finite depth. Proceedings of the Royal Society A: Mathematical, Physical and Engineering Sciences, **466**(2121), 2673-2694. https://doi.org/10.1098/rspa.2010.0017

Fowler AC. 2018. The philosopher in the kitchen: the role of mathematical modelling in explaining drumlin formation. *GFF* **140**(2): 93–105. https://doi.org/10.1080/11035897.2018.1444671

Fowler AC, Chapwanya M. 2014. An instability theory for the formation of ribbed moraine, drumlins and mega-scale glacial lineations. *Proceedings of the Royal Society A: Mathematical, Physical and Engineering Sciences* **470**(2171): 20140185. https://doi.org/10.1098/rspa.2014.0185

Greenwood SL, Clark CD, Hughes AL. 2007. Formalising an inversion methodology for reconstructing ice-sheet retreat patterns from meltwater channels: application to the British Ice Sheet. *Journal of Quaternary Science: Published for the Quaternary Research Association* **22**(6): 637–645. https://doi.org/10.1002/jqs.1083

Guðmundsdóttir ER, Eiríksson J, Larsen G. 2011. Identification and definition of primary and reworked tephra in Late Glacial and Holocene marine shelf sediments off North Iceland. *Journal of Quaternary Science* **26**(6): 589–602. https://doi.org/10.1002/jqs.1474

Hart JK. 1997. The relationship between drumlins and other forms of subglacial glaciotectonic deformation. *Quaternary Science Reviews* **16**(1): 93–107. https://doi.org/10.1016/S0277-3791(96)00023-6

© 2022 John Wiley & Sons, Ltd.

Hart JK. 1999. Identifying fast ice flow from landform assemblages in the geological record: a discussion. *Annals of Glaciology* **28**: 59–66. https://doi.org/10.3189/172756499781821887

Hermanowski P, Piotrowski JA, Szuman I. 2019. An erosional origin for drumlins of northwest Poland. *Earth Surface Processes and Landforms* **44**(10): 2030–2050. https://doi.org/10.1002/esp.4630

Hindmarsh R. 1998. Drumlinization and drumlin-forming instabilities: Viscous till mechanisms. *Journal of Glaciology* **44**(147): 293–314. https://doi.org/10.3189/S002214300000263X

Hubbard A, Sugden J, Dugmore A et al. 2006. A modelling insight into the Icelandic Late Glacial Maximum ice sheet. *Quaternary Science Reviews* **25**(17-18): 2283–2296. https://doi.org/10.1016/j.quascirev.2006.04.001

Ingólfsson Ó, Norðdahl H. 2001. High relative sea-level during the Bølling interstadial in W Iceland: a reflection of ice-sheet collapse and extremely rapid glacial unloading. *Arctic, Antarctic and Alpine Research* **33**: 231–243. https://doi.org/10.1080/15230430.2001.12003426

Iverson NR, McCracken RG, Zoet L et al. 2017. A theoretical model of drumlin formation based on observations at Múlajökull, Iceland. *Journal of Geophysical Research Earth Surface* **122**: 2302-2323. https://doi.org/10.1002/2017JF004354

Johnson MD, Schomacker A, Benediktsson ÍÖ et al. 2010. Active drumlin field revealed at the margin of Múlajökull, Iceland: a surge-type glacier. *Geology* **38**: 943–946. https://doi.org/10.1130/G31371.1

Jóhannesson H, Sæmundsson K. 2009. *Geological map of Iceland. 1:500.000. Bedrock*. 1st edition. Icelandic Institute of Natural History: Reykjavík.

Jol HM, Bristow CS. 2003. GPR in sediments: advice on data collection, basic processing and interpretation, a good practice guide. *SPECIAL PUBLICATION-GEOLOGICAL SOCIETY OF LONDON* **211**: 9–28.

Jónsson SA, Benediktsson ÍÖ, Ingólfsson Ó et al. 2016. Submarginal drumlin formation and late Holocene history of Fláajökull, southeast Iceland. *Annals of Glaciology* **57**(72): 128–141. https://doi.org/10.1017/aog.2016.4

King E, Woodward J, Smith A. 2007. Seismic and radar observations of subglacial bed forms beneath the onset zone of Rutford Ice Stream, Antarctica. *Journal of Glaciology* **53**(183): 665–672. https://doi.org/10.3189/002214307784409216

Kjær KH, Krüger J. 1998. Does clast size influence fabric strength? *Journal of Sedimentary Research* **68**(5): 746–749. https://doi.org/10.2110/jsr.68.746

Kjær KH, Sultan L, Krüger J et al. 2004. Architecture and sedimentation of outwash fans in front of the Mýrdalsjökull ice cap, Iceland. *Sedimentary Geology* **172**(1-2): 139–163. https://doi.org/10.1016/j.sedgeo.2004.08.002

Kjær KH, Larsen E, van der Meer J et al. 2006. Subglacial decoupling at the sediment/bedrock interface: a new mechanism for rapid flowing ice. *Quaternary Science Reviews* **25**(21-22): 2704–2712.

Krüger J, Kjær KH. 1999. A data chart for field description and genetic interpretation of glacial diamicts and associated sediments - with examples from Greenland, Iceland, and Denmark. *Boreas* **28**(3): 386–402. https://doi.org/10.1111/j.1502-3885.1999.tb00228.x

Lawson DE. 1979. A comparison of the pebble orientations in ice and deposits of the Matanuska Glacier, Alaska. *The Journal of Geology* **87**(6): 629–645.

Livingstone SJ, Cofaigh CÓ, Stokes CR et al. 2012. Antarctic palaeo-ice streams. *Earth-Science Reviews* **111**(1-2): 90–128. https://doi.org/10.1016/j.earscirev.2011.10.003

Maclachlan JC, Eyles CH. 2013. Quantitative geomorphological analysis of drumlins in the Peterborough drumlin field, Ontario, Canada. *Geografiska Annaler: Series A, Physical Geography* **95**(2): 125–144. https://doi.org/10.1111/geoa.12005

McCracken RG, Iverson NR, Benediktsson ÍÖ et al. 2016. Origin of the active drumlin field at Múlajökull, Iceland: new insights from till shear and consolidation patterns. *Quaternary Science Reviews* **148**: 243–260. https://doi.org/10.1016/j.quascirev.2016.07.008

Menzies J. 1979. A review of the literature on the formation and location of drumlins. *Earth-Science Reviews* **14**(4): 315–359.

Menzies J, Brand U. 2007. The internal sediment architecture of a drumlin, Port Byron, New York State, USA. *Quaternary Science Reviews* **26**(3-4): 322–335. https://doi.org/10.1016/j.quascirev.2006.07.003

Menzies J, Hess DP, Rice JM et al. 2016. A case study in the New York Drumlin Field, an investigation using microsedimentology, resulting in the refinement of a theory of drumlin formation. *Sedimentary Geology* **338**: 84–96.

Möller P, Dowling TP. 2016. Streamlined subglacial bedforms on the Närke plain, south-central Sweden–areal distribution, morphometrics, internal architecture and formation. *Quaternary Science Reviews* **146**: 182–215. https://doi.org/10.1016/j.quascirev.2016.04.007

Napieralski J, Nalepa N. 2010. The application of control charts to determine the effect of grid cell size on landform morphometry. *Computers & Geosciences* **36**: 222–230.

Neal A. 2004. Ground-penetrating radar and its use in sedimentology: principles, problems and progress. *Earth-science reviews* **66**(3-4): 261–330. https://doi.org/10.1016/j.earscirev.2004.01.004

Norðdahl H, Hjort C. 1993. Lateglacial raised beaches and glacier recession in the Þistilfjörður-Bakkaflói area. *Jökull* **43**: 32–44.

Norðdahl H, Pétursson HG. 2005. Relative sea-level changes in Iceland. New aspects of the Weichselian deglaciation of Iceland. In *Iceland – modern processes and past environments*, Caseldine C, Russel A, Harðardóttir J, Knudsen Ó (Eds.). Elsevier: Amsterdam; 25–78.

Norðdahl H, Ingólfsson Ó, Pétursson HG et al. 2008. Late Weichselian and Holocene environmental history of Iceland. *Jökull* **58**: 343–364.

Norðdahl H, Ingólfsson Ó. 2015. Collapse of the Icelandic ice sheet controlled by sea-level rise? *Arktos* **1**: 1–18. https://doi.org/10.1007/s41063-015-0020-x

Norðdahl H, Ingólfsson Ó, Vogler ED et al. 2019. Glacio-isostatic age modelling and Late Weichselian deglaciation of the Lögurinn basin, East Iceland. *Boreas* **48**(3): 563–580. https://doi.org/10.1111/bor.12366

Patton H, Hubbard A, Bradwell T et al. 2017. The configuration, sensitivity and rapid retreat of the Late Weichselian Icelandic ice sheet. *Earth-Science Reviews* **166**: 223–245. https://doi.org/10.1016/j.earscirev.2017.02.001

Piotrowski JA, Larsen NK, Junge FW. 2004. Reflections on soft subglacial beds as a mosaic of deforming and stable spots. *Quaternary Science Reviews* **23**(9-10): 993–1000. https://doi.org/10.1016/j.quascirev.2004.01.006

Porter C, Morin P, Howat I et al. 2018. "ArcticDEM". https://doi.org/10.7910/DVN/OHHUKHHarvard Dataverse, V1.

Powers MC. 1953. A new roundness scale for sedimentary particles. *Journal of Sedimentary Research* **23**(2): 117–119.

Principato SM, Moyer AN, Hampsch AG et al. 2016. Using GIS and streamlined landforms to interpret palaeo-ice flow in northern Iceland. *Boreas* **45**: 470–482. https://doi.org/10.1111/bor.12164

Shaw J. 2002. The meltwater hypothesis for subglacial bedforms. *Quaternary International* **90**(1): 5–22. https://doi.org/10.1016/S1040-6182(01)00089-1

Smalley I, Unwin D. 1968. The Formation and Shape of Drumlins and their Distribution and Orientation in Drumlin Fields. *Journal of Glaciology* **7**(51): 377–390. https://doi.org/10.3189/S0022143000020591

Smith AM. 1997. Basal conditions on Rutford ice stream, West Antarctica, from seismic observations. *Journal of Geophysical Research: Solid Earth* **102**(B1): 543–552.

Smith AM, Murray T, Nicholls KW et al 2007. Rapid erosion, drumlin formation, and changing hydrology beneath an Antarctic ice stream. *Geology* **35**(2): 127–130. https://doi.org/10.1130/G23036A.1

Spagnolo M, Clark CD. 2009. A geomorphological overview of glacial landforms on the Icelandic continental shelf. *Journal of Maps* **2009**: 37–52. https://doi.org/10.4113/jom.2009.1049

Spagnolo M, Clark CD, Hughes AL et al. 2010. The planar shape of drumlins. *Sedimentary Geology* **232**(3-4): 119–129. https://doi.org/10.1016/j.sedgeo.2010.01.008

Spagnolo M, Clark CD, Hughes AL. 2012. Drumlin relief. *Geomorphology* **153**: 179–191. https://doi.org/10.1016/j.geomorph.2012.02.023

© 2022 John Wiley & Sons, Ltd.

Spagnolo M, King EC, Ashmore DW et al 2014. Looking through drumlins: testing the application of ground-penetrating radar. *Journal of Glaciology* **60**(224): 1126–1134. https://doi.org/10.3189/2014JoG14J110

Stokes CR, Clark CD. 1999. Geomorphological criteria for identifying Pleistocene ice streams. *Annals of Glaciology* **28**: 67–74. https://doi.org/10.3189/172756499781821625

Stokes CR, Clark CD. 2001. Palaeo-ice streams. *Quaternary Science Reviews* **20**: 1437–1457. https://doi.org/10.1016/S0277-3791(01)00003-8

Stokes CR, Clark CD. 2002. Are long subglacial bedforms indicative of fast ice flow? *Boreas* **31**(3): 239–249.

Stokes CR, Clark CD, Lian OB et al. 2007. Ice stream sticky spots: a review of their identification and influence beneath contemporary and palaeo-ice streams. *Earth-Science Reviews* **81**(3-4): 217–249. https://doi.org/10.1016/j.earscirev.2007.01.002

Stokes CR, Lian OB, Tulaczyk S et al. 2008. Superimposition of ribbed moraines on a palaeo-ice-stream bed: implications for ice stream dynamics and shutdown. *Earth Surface Processes and Landforms: The Journal of the British Geomorphological Research Group* **33**(4): 593–609. https://doi.org/10.1002/esp.1671

Stokes CR, Spagnolo M, Clark CD. 2011. The composition and internal structure of drumlins: complexity, commonality, and implications for a unifying theory of their formation. *Earth-Science Reviews* **107**(3-4): 398–422. https://doi.org/10.1016/j.earscirev.2011.05.001

Stokes CR, Fowler AC, Clark CD et al. 2013. The instability theory of drumlin formation and its explanation of their varied composition and internal structure. *Quaternary Science Reviews* **62**: 77–96. https://doi.org/10.1016/j.quascirev.2012.11.011

Stokes CR. 2018. Geomorphology under ice streams: Moving from form to process. *Earth Surfaces Processes and Landforms* **43**: 85–123. https://doi.org/10.1002/esp.4259

Sæmundsson K. 1977. Geological Map of Iceland, Sheet 7, NE-Iceland. 1:250.000. Icelandic Institute of Natural History and National Land Survey of Iceland, Reykjavik.

Sæmundsson Th. 1995. Deglaciation and shoreline displacement in Vopnafjörður, northeastern Iceland. LUNDQUA thesis 33,1-106. Department of Quaternary Geology, Lund University.

Waller RI, Van Dijk TA, Knudsen O. 2008. Subglacial bedforms and conditions associated with the 1991 surge of Skeiðarárjökull, Iceland. *Boreas* **37**(2): 179–194. https://doi.org/10.1111/j.1502-3885.2007.00017.x

Watts H, Booth AD, Reinardy BT et al. 2022. An Assessment of Geophysical Survey Techniques for Characterising the Subsurface Around Glacier Margins, and Recommendations for Future Applications. *Frontiers in Earth Science* **10**: Article 734682. https://doi.org/10.3389/feart.2022.734682

Woodard JB, Zoet LK, Benediktsson ÍÖ et al. 2020. Insights into drumlin development from ground-penetrating radar at Múlajökull, Iceland, a surge-type glacier. *Journal of Glaciology* **66**: 822–830. https://doi.org/10.1017/jog.2020.50

© 2022 John Wiley & Sons, Ltd.

Paper III

Received: 7 February 2023 | Revised: 18 May 2023 | Accepted: 19 May 2023

DOI: 10.1002/esp.5636

CASE STUDY

ESPL WILEY

Ice-stream shutdown during deglaciation: Evidence from crevasse-squeeze ridges of the Iceland Ice Sheet

Nína Aradóttir[1] | Ívar Örn Benediktsson[1] | Ólafur Ingólfsson[1] | Skafti Brynjólfsson[2] | Wesley R. Farnsworth[1,3] | Margrét Mjöll Benjamínsdóttir[1] | Lena Björg Ríkharðsdóttir[1]

[1]Institute of Earth Sciences, University of Iceland, Reykjavík, Iceland

[2]Icelandic Institute of Natural History, Akureyri, Iceland

[3]Globe Institute, University of Copenhagen, Copenhagen, Denmark

Correspondence
Nína Aradóttir, Institute of Earth Sciences, University of Iceland, Sturlugata 7, Is-102 Reykjavík, Iceland.
Email: nia1@hi.is

Funding information
University of Iceland Research Fund, Grant/Award Number: 80844; Icelandic research fund, Grant/Award Number: 228321-051; Energy Research Fund of Landsvirkjun; Icelandic Road and Coastal Administration

Abstract

Both modern and palaeo-ice streams experience shutdown, which has critical implications for their mass balance and influence on relative sea level. Reconstructions of palaeo-ice streams have mainly focused on their phase of active flow and thus less is understood of their shutdown and style of deglaciation. Mapping of streamlined subglacial bedforms (SSBs), including drumlins and mega-scale glacial lineations, in northeast Iceland reveals cross-cutting flow-sets of palaeo-ice streams within the Iceland Ice Sheet (IIS) during and following the last glacial maximum (LGM). Here we map geometrical ridges (linear and reticular) within the Bakkaflói and Þistilfjörður flow-sets and combine the morphological data with sedimentological analyses to increase our understanding of the dynamics of the IIS during deglaciation in northeast Iceland. We interpret the ridges as crevasse-squeeze ridges (CSRs), based on their interconnected network, primary orientation transverse and/or oblique to former ice flow and internal composition of homogenous subglacial till. In both areas, the CSRs are superimposed on the SSBs, indicating that they post-date the SSBs and signify the waning stage of ice streaming associated with the readvance of the IIS during the Younger Dryas period. The preservation of the CSRs suggests ice stagnation following the readvance and ice-stream shutdown. The morphological difference of the CSRs between the flow-sets is taken to indicate different kinematic setting within the ice streams; the linear CSRs in Bakkaflói formed further upstream where extensional forces parallel to ice flow were dominant, whereas the reticular CSRs in Þistilfjörður are more indicative of transverse and longitudinal forces near the terminal zone. Future research reconstructing past ice-sheet behaviour and ice-stream dynamics would benefit from high-resolution bathymetric data from the adjoining shelf as well as enhanced geochronological constraints.

KEYWORDS
crevasse-squeeze ridges, deglaciation, glacial landforms, Iceland Ice Sheet, ice-sheet dynamics, ice-stream shutdown, palaeo-ice stream

1 | INTRODUCTION

Ice streams and their dynamics are critical for regulating ice sheet stability and mass balance through ice and sediment discharge (Bennett, 2003). Their sensitivity to sea level and climate change is currently of great concern (Alley et al., 2005; Briner, 2016), highlighting the importance of understanding ice-stream development during deglaciation (Franke et al., 2022; Robel & Tziperman, 2016; Stokes et al., 2016). Direct observations of the bed of contemporary ice streams are limited to boreholes and seismic investigations (Bennett, 2003; Kamb, 2001; Smith et al., 2021). As a result, numerous factors concerning ice-stream behaviour, such as the mechanism

 © 2023 John Wiley & Sons Ltd.

of fast flow, temporal and spatial behaviour, and their effect on ice-sheet mass balance, remain poorly understood (e.g., Alley et al., 2004; Bennett, 2003; Bingham et al., 2017). Understanding the geomorphological fingerprinting of palaeo-ice stream beds is therefore important for our perception of the behaviour of ice streams, as the formation of bedforms can be a window into the processes at the ice/bed interface (Livingstone et al., 2012; Stokes, 2018; Stokes & Clark, 1999, 2001). Furthermore, data from palaeo-ice stream beds are essential for the reconstruction and modelling of past ice sheets and ice streams (Greenwood & Clark, 2009; Stokes & Clark, 2001).

Surge-type glacier landsystems serve as analogues for palaeo-ice streams and surging lobes; thus, research within both settings can enhance knowledge of glacier behaviour in modern and palaeo environments (Evans & Rea, 1999; Ingólfsson et al., 2016). Crevasse-squeeze ridges (CSRs) are one key bedform characterizing the forefield of surge-type glaciers which has been extensively studied in modern settings and used to infer past glacier dynamics (Evans & Rea, 1999, 2003; Sharp, 1985). Recently, CSRs have been described from palaeo-settings in relation to ice stream or surging lobe shutdown, in both terrestrial (Ankerstjerne et al., 2015; Benn, 2021; Cline et al., 2015; Delaney et al., 2018; Evans et al., 2016; Evans & Rea, 1999; Lamsters et al., 2021; Öhrling et al., 2020; Sutherland et al., 2019) and marine (Andreassen et al., 2014; Bjarnadóttir et al., 2014; Greenwood et al., 2017, 2018; Klages et al., 2013, 2015; Kurjanski et al., 2019; Newton & Huuse, 2017) environments. Descriptions of CSRs associated with palaeo-ice stream beds imply similar instabilities between surge-type glaciers and ice streams, which has implications for our understanding of ice streams and their dynamics.

The Iceland Ice Sheet (IIS) reached its maximum extent, most likely at the shelf edge, around 22.9 ka BP, followed by a rapid deglaciation of the marine sector that initiated at around 21.8 ka BP (e.g., Benediktsson et al., 2023a; Benediktsson, Brynjólfsson, & Ásbjörnsdóttir, 2022; Norðdahl & Ingólfsson, 2015; Norðdahl & Pétursson, 2005). Ice streams within the IIS during the last glacial maximum (LGM) and the subsequent deglaciation (Figure 1a) have been proposed based on large-scale geomorphology and glacial striae (e.g., Benediktsson, Aradóttir, et al., 2022; Benediktsson, Brynjólfsson, & Ásbjörnsdóttir, 2022; Bourgeois et al., 2000; Norðdahl et al., 2019; Norðdahl & Pétursson, 2005; Principato et al., 2016; Spagnolo & Clark, 2009) and numerical modelling (Bourgeois et al., 2000; Hubbard et al., 2006; Patton et al., 2017). Recent investigations have focused on streamlined subglacial bedforms (SSBs; such as drumlins and mega-scale glacial lineations, MSGLs), their cross-cutting relationships and formation (Aradóttir et al., 2023; Benediktsson, Aradóttir, et al., 2022; Principato et al., 2016).

Here we present detailed mapping, morphological and spatial analyses as well as sedimentological investigations of linear and reticular ridge networks that we interpret as CSRs within the previously identified ice-stream flow-sets in Bakkaflói and Þistilfjörður, northeast Iceland. Furthermore, we combine previous studies on glacial bedforms in the area in a geomorphological map to enhance our understanding of the relative timing of CSRs formation and the glacial history and dynamics of the IIS during deglaciation in northeast Iceland.

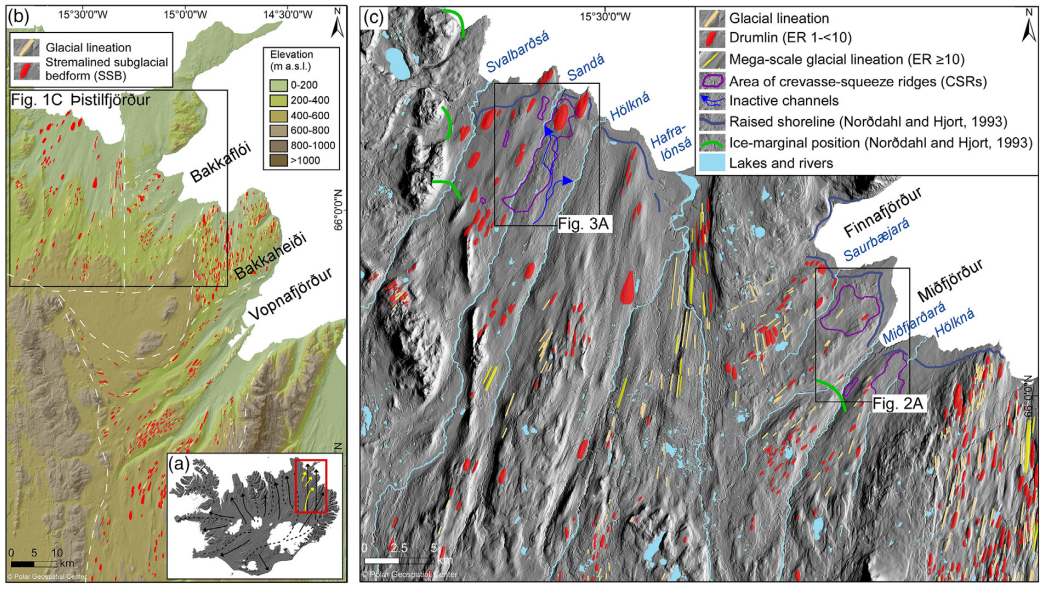

FIGURE 1 (a) Major ice streams of the Iceland ice sheet represented by arrows (Benediktsson, Aradóttir, et al., 2022; Bourgeois et al., 2000; Principato et al., 2016; Stokes & Clark, 2001). Figure 1b is outlined in red. Within the red box the black arrows indicate an older generation of ice flow during maximum glaciation while the yellow arrows represent a younger generation of flow during deglaciation (Benediktsson, Aradóttir, et al., 2022). (b) Overview map of glacial lineations and SSBs in Northeast Iceland (modified from Benediktsson, Aradóttir, et al., 2022). The white dashed lines indicate boundaries between flow-sets; Þistilfjörður, Bakkaflói, Bakkaheiði, and Vopnafjörður-Jökuldalsheiði. The study areas, Bakkaflói and Þistilfjörður, are located within the black box (Figure 1c). (c) Geomorphological map of Bakkaflói and Þistilfjörður. Shorelines and ice-marginal positions within the area are from Norðdahl & Hjort (1993). Place names referred to in the text are marked. The map legend applies to Figures 2a and 3a as well. The map without annotation is in supplementary data (Figure S1).

2 | SITES AND METHODS

2.1 | Study sites

The study area is within the Bakkaflói and Þistilfjörður fjord-valley systems in northeast Iceland (Figure 1b,c). The Bakkaflói area (~600 km^2) is comprised of restricted lowlands, shallow valleys and low plateaus (<500 m a.s.l.). The fjord opens towards the northeast with two coastal embayments, Finnafjörður and Miðfjörður. Several rivers, Miðfjarðará, Hölkná and Saurbæjará, drain from the highlands down to Bakkaflói (Figures 1c and 2a). The Þistilfjörður area (~1100 km^2) is a broad low-lying valley, trending towards north-northeast, extending gradually inland to low plateaus (<500 m a.s.l.). The area is subdivided by five main rivers, Svalbarðsá, Sandá, Hölkná, Hafralónsá and Kverká, running

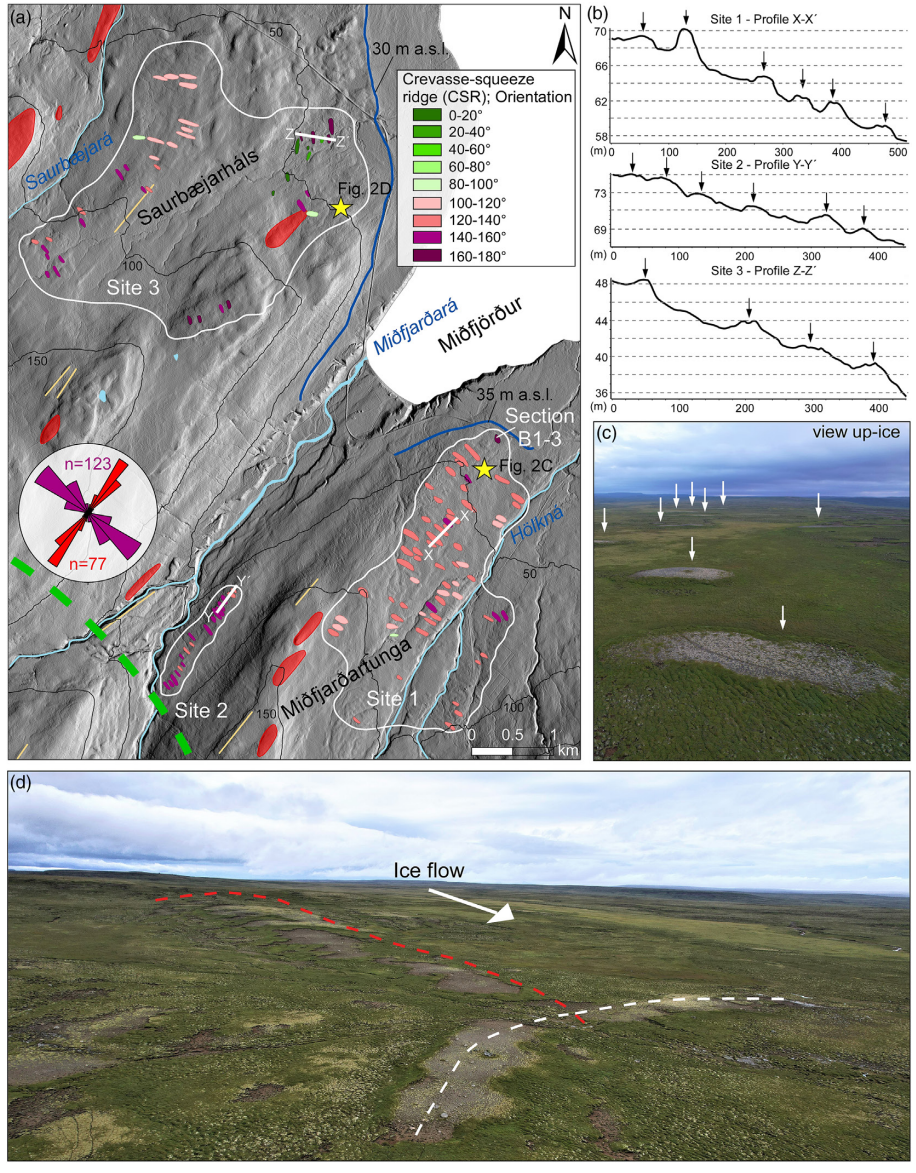

FIGURE 2 (a) Map of crevasse-squeeze ridges (CSRs) in Bakkaflói highlighting their orientation. The rose diagram shows the orientation of the mapped 123 CSRs (purple; median 132°-312°) and the 77 SSBs (red; median 217°-37°) within the Bakkaflói flow-set. The CSRs are divided into three sites. The green dashed line represents the mapped ice-marginal position from Norðdahl & Hjort (1993) and is considered to represent the readvance during the Pb. The stars mark the location of the photos in Figures 1c,d. Contour intervals are 50 m. (b) Three terrain cross profiles from sites 1–3 with the arrows pointing at the CSRs. The profiles are marked in Figure 1a. The CSRs are usually between 0.5 and 2 m in relief with symmetrical cross profiles and flat-crests. (c) Transverse linear CSRs at site 1 with a consistent dominant orientation southeast to northwest, or transverse to former ice flow. The arrows point at the ridges. (d) CSRs (white) superimposed on the lee side of a drumlin (red) on Saurbæjarháls at site 3. CSRs are orientated transverse and oblique to former ice-flow (northeast). The map without annotation is in the supporting information (Figure S2).

from the highlands (Figures 1c and 3a). The eastern margin of the area is delimited by the boundary between the Pliocene and Pleistocene bed-rock, which also marks the boundary to Bakkaflói. In both areas, the bed-rock in the lowlands consists primarily of Miocene and Lower Pliocene (>3.3 million years old) basic and intermediate extrusive rocks with intercalated sediments. Younger basalt lavas (3.3–0.8 million years old) are found further inland, up on the plateaus and at the boundary between the two areas, extending out to the Langanes Peninsula. Hyaloclastite ridges (<0.8 million years old) delimit the western and southern boundary in Þistilfjörður (Jóhannesson & Sæmundsson, 2009; Sæmundsson, 1977). The bed-rock is frequently exposed in river sections, which together with glacially sculptured bed-rock outcrops suggest discontinuous sediment cover in the area. Heathland commonly surrounds the bedforms and bed-rock, but peatland is also present with typical soil thickness of >2–3 m, as observed during fieldwork (Figures 2c,d and 4a,b).

Bakkaflói and Þistilfjörður comprise cross-cutting palaeo-ice stream flow-sets reconstructed from the mapping of SSBs in northeast Iceland (Figure 1b; Benediktsson, Aradóttir, et al., 2022). The drumlins within the Bakkaflói flow-set are mainly orientated towards the northeast, although a few in the southern part are orientated to the north, suggesting two generations of flow-sets in the area. The older generation orientated towards north represents maximum glaciation, with flow independent of underlying topography, while the younger one orientated towards northeast signifies deglaciation and ice sheet thinning when the flow was more controlled by the topography (Figure 2a; Benediktsson, Aradóttir, et al., 2022). Glacial striae also indicate general ice flow towards northeast (Norðdahl & Hjort, 1993; Sæmundsson, 1977). Within the Þistilfjörður flow-set, the general ice-flow direction was towards the north-northeast (Figure 3a; Sæmundsson, 1977; Norðdahl & Hjort, 1993; Benediktsson, Aradóttir, et al., 2022). While recent efforts have mainly focused on mapping the SSBs and analysing their cross-cutting relationships, the ridges in Bakkaflói were examined by Benjamínsdóttir (2021) and findings are synthesized in this study.

Earlier investigations within the area mainly focused on the deglaciation history by surveying shoreline displacement after the Younger Dryas (YD) period. Three sets of raised shorelines have been identified. The two higher limits at ~65 m a.s.l. and ~50–45 m a.s.l. are restricted to two locations in the eastern part of Bakkaflói and the western part of Þistilfjörður. The lowest shoreline at ~30 m a.s.l. is much more distinct and continuous (Figure 1c; Norðdahl & Hjort, 1993). Several ice-marginal positions were also inferred by Norðdahl & Hjort (1993) in Þistilfjörður and Bakkaflói (Figure 1c). Although age constraints for these landforms are sparse, Norðdahl & Hjort (1993) connect the lower shoreline and ice-marginal positions to the Preboreal (Pb) period and the upper shoreline to the YD period, based on available data in the neighboring areas.

2.2 | Geomorphological mapping

The geomorphological mapping was based on the Arctic digital elevation model (ArcticDEM) with a 2 m vertical and <1 m horizontal resolution (Porter et al., 2018; corrected and mosaicked by the National Land Survey of Iceland [NLSI], the Icelandic Met Office, and the Polar Geospatial Center). Mapping was aided by infrared Spot satellite images with 2.5-m resolution from NLSI and aerial images from Loftmyndir ehf. The mapping was done by the combination of field work and remote sensing. Analysis of the data and mapping was conducted in ESRI ArcGIS 10.5–8 and finalized in Canvas X. The ridges in Bakkaflói and Þistilfjörður were mapped in detail (i.e., 1:3000). Inactive channels intersecting the area of ridges were additionally mapped. The raised shorelines and ice-marginal positions mapped by Norðdahl & Hjort (1993) were digitized.

2.3 | Morphological and spatial analyses

To investigate the morphology of the ridges, the length of the long axis, the width orthogonal to the long axis and the orientation of the long axis were measured using the minimum bounding geometry tool in ArcGIS, as described by Napieralski & Nalepa (2010). The ridge prominence and their symmetry were examined with the 3D profile tool in ArcGIS as well as the spacing between the ridges was measured using the average nearest neighbour tool in ArcGIS. To calculate the density of the bedforms a point was created in the centre of each bedform and the number of ridges within each km^2 grid cell calculated.

2.4 | Sedimentology

There are no natural sections exposing the sediments in the ridge networks and therefore an excavator was used to dig trenches through one ridge in Bakkaflói (B1-3) and two ridges in Þistilfjörður (Th1 and Th2) (Figures 2a and 3a). Sediments exposed in the sections were documented at a scale of 1:20, using the data chart by Krüger & Kjær (1999) for glacial sediments, and the strike and dip of beds/structures were measured. Clast fabric measurements were collected from a 25 × 25-cm surface, where the dip and dip direction were measured for at least 25 elongated clasts (a:b ratio >1.5:1) ranging from 0.6 to 6 cm in diameter (Kjær & Krüger, 1998). In the Þistilfjörður sections, clast fabric measurements proved to be infeasible because of the dearth of elongate clasts. The measurements were then plotted and analysed in the software Stereonet and the eigenvectors (V_1) and eigenvalues (S_1 and S_3) calculated. If the eigenvalue of the principal eigenvector was higher than 0.54, the clasts were considered to show preferred orientation (Lawson, 1979). In addition, the mean dip of the measured clasts was calculated. All compass measurements were corrected for the regional negative declination of 10° (in 2020). Grain-size analyses on diamict units were carried out using standard sieving methods, starting by washing out material finer than 0.063 mm (fines; clay and silt), followed by dry sieving to separate sand and gravel fractions. To examine the clast morphology, a minimum of 50 clasts with an *a*-axis between 1.5 and 10 cm were collected from a 25 × 25-cm surface. The *a* (long)-, *b* (intermediate)- and *c* (short)-axis were measured (Evans & Benn, 2004) and plotted in a ternary diagram. In addition, the roundness and texture of the clast was estimated (Evans & Benn, 2004; Powers, 1953). The clast morphology and roundness are displayed with C_{40} index (percentage of clasts with *c*:*a* axis ratio ≤0.4) and RA index (percentage of angular and very angular clasts) (Benn & Ballantyne, 1993). The sections and additional data were illustrated in Canvas X.

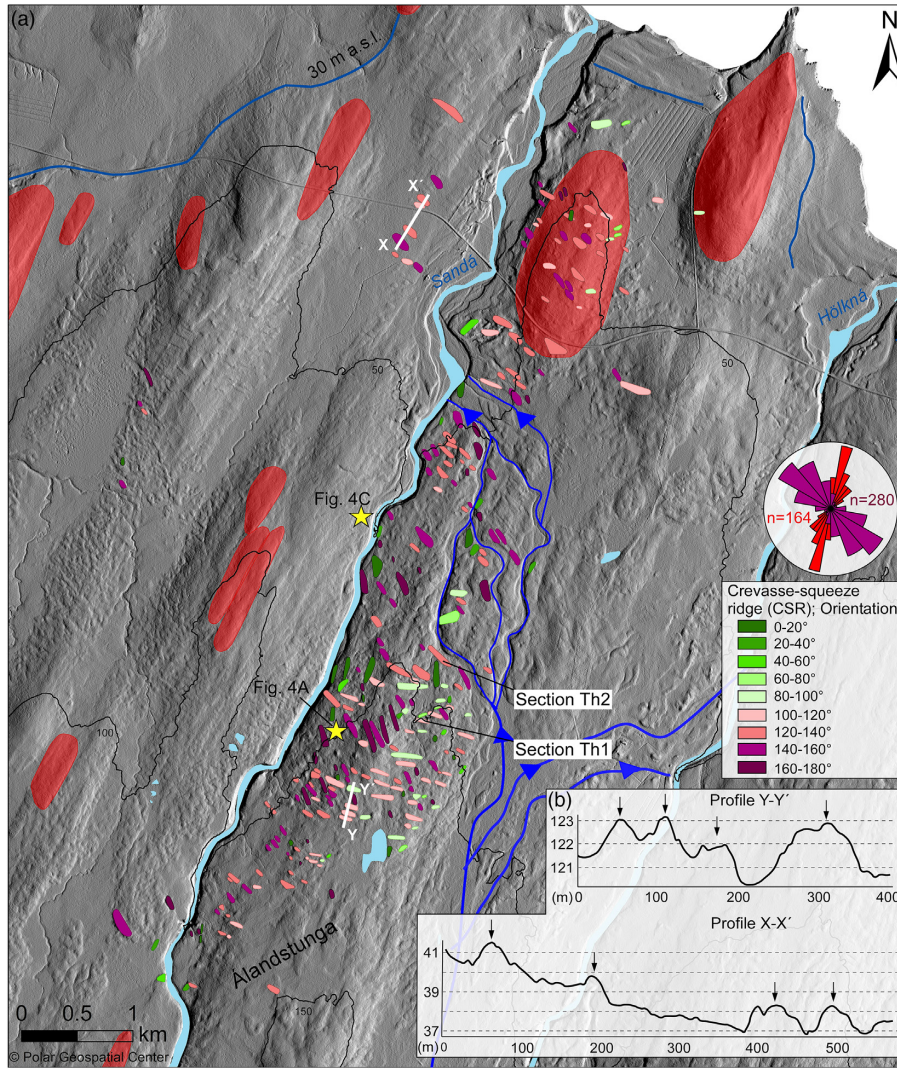

FIGURE 3 (a) Map of crevasse-squeeze ridges (CSRs) in Álandstunga in Þistilfjörður, highlighting their variable orientation. The rose diagram shows the orientation of the 280 CSRs (purple; median 130°–310°) and the 164 SSBs (red; median 199°–19°) mapped within the Þistilfjörður flow-set. The stars mark the location of the photos in Figure 4. Contour intervals are 50 m. (b) Two terrain cross profiles with the ridges indicated by arrows. The profiles are marked in Figure 3a. The CSRs are usually between 0.5 and 3 m in relief with symmetrical cross profiles and flat-crests. The map without annotation is in the supporting information (Figure S3).

3 | RESULTS

The results are divided into four parts. The morphology, cross-cutting relationships to other bedforms and sedimentology of the ridges is described separately for the two areas, Bakkaflói and Þistilfjörður. In the final section, bedforms are compared from the two sites.

3.1 | Morphology of the ridges

3.1.1 | Bakkaflói

In total, 123 ridges were mapped in Bakkaflói where their distribution is restricted to three sites (1–3), from 35 m a.s.l. up to 136 m a.s.l., with ~75% of the ridges occurring between 45 and 90 m a.s.l. (Figures 2a and 5). Two of the sites are located up from Miðfjörður, with a network of 63 ridges on Miðfjarðartunga (site 1) and 18 ridges next to Miðfjarðará (site 2). The remaining 42 ridges are located to the northwest of sites 1 and 2, up on Saurbæjarháls (site 3) (Figures 1c and 2a). The ridges are characterized as linear, rather uniform in shape within an interconnected network (Figure 2a,c). The median length is 132 m with a range of 55–273 m and the median width is 50 m with a range of 28–90 m. The median elongation ratio is 2.6:1 with a range from 1.4–5.9:1 (Table 1 and Figure 5). The ridges are generally low in relief, between 0.5 and 2 m (Figure 2b). The median ridge orientation, of the three sites in Bakkaflói, is southeast to northwest (132°–312°) with a range of 1°–178° (Figure 2 and Table 1). The ridges are clustered with an observed average crest-to-crest distance of 131 m, with

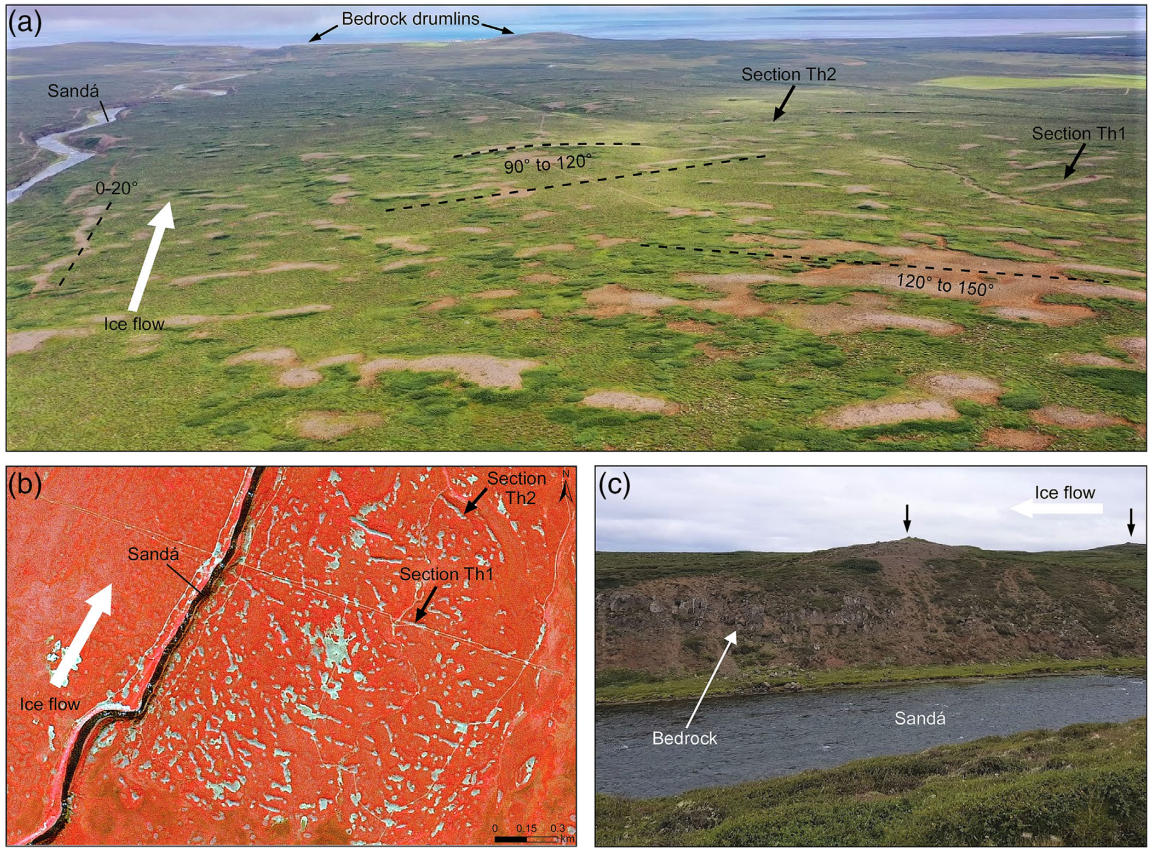

FIGURE 4 (a) Drone image from Þistilfjörður with a downglacier view over the corridor with the highest density of crevasse-squeeze ridges (CSRs) (43 CSRs per km^2). The difference in orientation of the CSRs is highlighted. The black arrows point at the sections and large bedrock drumlins by the coast. (b) Infrared satellite image from National Land Survey of Iceland (NLSI) emphasizing the reticular CSR pattern and how they stand out from the vegetation in Þistilfjörður. Note the interconnected network and segmented CSRs and how the ridges are mostly absent on the southwest of the corridor and west of Sandá. (C) A river cut through a CSRs by Sandá in Þistilfjörður. The bedrock is frequently exposed in the river cut, sometimes only <0.5 m under the surface. The black arrows point at the visible CSRs.

a symmetrical cross profile and are typically flat-crested (Figure 2b). The mean density of ridges is 0.98 ridges per km^2 with maximum density of 21 ridges per km^2 (Table 1).

The ridges at site 1 are the most prominent and easy to distinguish, both in the field and through remote sensing. They have a clear dominant orientation, 129°–309° (range: 94°–167°), roughly the same as the median orientation for all the ridges in Bakkaflói (Figure 2a,c). The average spacing between the ridges is 148 m, with consistent crest-to-crest spacing (Figure 2b). Site 2 contains closely spaced (74 m in average), low-relief ridges (<1 m) within a narrow SW–NE trending corridor. Their orientation is slightly more southerly (median: 145°–325°; range: 123°–153°) than the regional median orientation (Figure 2a,b). The ridges at site 3 are the least prominent from aerial- and satellite images, but in the field, they are outstanding from the surrounding vegetation (Figure 2d). The ridges exhibit similar relief as site 2 (<1 m). The deviation in orientation of the ridges is greater (range: 1°–178°) although the median orientation (129°–309°) conforms within the whole regional data set. The orientation of the ridges closer to the coast appears to coincide with the contour lines or essentially the bed-rock topography to some extent. The ridges at site 3 are more dispersed compared to the other areas, and the average crest-to-crest spacing between the ridges is 130 m (Figure 2a,b).

3.1.2 | Þistilfjörður

In Þistilfjörður, 280 ridge segments have been mapped in Álandstunga. Majority of the ridges (262) occur within a narrow corridor (<2 km wide), confined by the Sandá river on the western side and abrupt margin on the eastern side. The corridor extends over 10 km in length, from 30 m a.s.l. up to 148 m a.s.l., with ∼50% of the ridges above 90 m a.s.l. The remainder of the ridges are distributed on the western side of Sandá, mostly below 70 m a.s.l. (Figures 1c, 3a and 5). The Þistilfjörður ridge network is characterized as a reticular ridge complex, with discontinuous ridge segments in an interconnected network. The median length is 97 m with a range of 34–343 m and the median width is 39 m with a range of 19–111 m. The median elongation ratio is 2.5:1 with a range from 1.2–6.8:1. The ridges are clustered with an observed average distance of 114 m (Figures 3, 4a,b

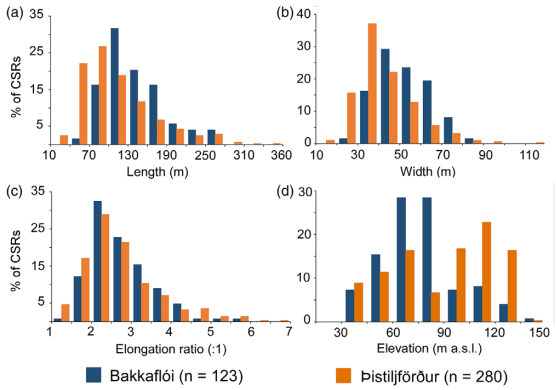

FIGURE 5 Size-frequency (a) length, (b) width, (c) elongation ratio and (d) elevation distribution of the morphometrics of the CSRs in Bakkaflói and Þistilfjörður.

and 5 and Table 1). The relief of the ridges varies, from <0.5 to 8 m high, although most of the ridges are between 0.5 and 3 m high. The cross profile of the ridges is generally symmetrical and examples of both flat- or sharp-crested ridges occur (Figure 3b). The mean density is 2.97 ridges per km^2 with maximum of 43 (Table 1).

The orientation of the ridges can be divided into two main sectors (120° to 140°, 140° to 160°), with the median orientation southeast to northwest (130°–310°, range: 0°–179°). No systematic pattern between the orientation of the ridges and their distribution can be detected (Figures 3a and 4a and Table 1). Spacing and size distribution is variable with the highest density of ridges and longer and higher ridges located just south of the corridor's centre. Those ridges are also the most prominent (Figures 3a and 4a,b).

3.2 | Cross-cutting relationship with other bedforms

3.2.1 | Bakkaflói

The drumlins in Bakkaflói are located up-ice from the ridge networks at all sites and to the northwest of site 3 (Benediktsson, Aradóttir, et al., 2022). The only example of a drumlin adjacent to the ridges is at site 3 (Figures 1c and 2a). There, two ridges are superimposed on the drumlin's lee side. That drumlin, and other drumlins in proximity to the coast, have a visible bed-rock core or are located on the lee side of bed-rock hills (Figure 2a,b). The drumlins further inland appear to be more sedimentary in composition. All SSBs mapped have an elongation ratio <10:1, and therefore are classified as drumlins, not MSGLs (Benediktsson, Aradóttir, et al., 2022). The meadian orientation of the mapped ridges is predominantly 98° offset from the general orientation of the drumlins (SW–NE), that is, transverse to the former ice-flow direction (Figures 1c and 2a). No ridges were observed below the raised shoreline at 30–35 m a.s.l. in the area, investigated by Norðdahl & Hjort (1993), but sites 1 and 3 are situated right above the shoreline (Figures 2a and 5). The ice-marginal position in Kverkártunga (Norðdahl & Hjort, 1993) is located just to the southwest or up-ice of site 2 (Figures 1c and 2a).

TABLE 1 Morphometrics of CSRs in Bakkaflói and Þistilfjörður.

		Bakkaflói	Þistilfjörður
n		123	280
Length (m)	Median	132	97
	Mean	141	114
	Min	55	34
	Max	273	343
	Q_1	110	70
	Q_3	164	144
Width (m)	Median	50	39
	Mean	52	42
	Min	28	19
	Max	90	111
	Q_1	42	32
	Q_3	62	49
Elongation ratio (:1)	Median	2.6	2.5
	Mean	2.8	2.7
	Min	1.4	1.2
	Max	5.9	6.8
	Q_1	2.2	2.1
	Q_3	3.2	3.1
Orientation (°)	Median	132	130
	Mean	128	119
	Min	1	0
	Max	178	179
	Q_1	121	107
	Q_3	144	147
Density (no. of CSR/km^2)	Mean	0.98	2.97
	Max	21	43
	Min	1	1
Area of CSRs (km^2)		~15	~18
Width of the fjord (km)		~15	~22

3.2.2 | Þistilfjörður

The drumlins in Þistilfjörður are mostly located further inland and west of the ridges. At the eastern side of Þistilfjörður a cluster of MSGLs occurs (Figure 1c; Benediktsson, Aradóttir, et al., 2022). The larger drumlins in proximity to the mapped ridges can be classified as bed-rock drumlins. One large bed-rock drumlin is located at the north-eastern end of the ridge corridor with the ridges superimposed on the drumlin. The median orientation of the ridges (NW-SE) is oblique to the general orientation of the drumlins (NNE–SSW) or with a 73° offset. There is no obvious connection between the topography and the orientation of the ridges, although the highest concentration of ridges is situated on a bed-rock high (Figures 1c and 3a). All the ridges are located above the highest raised shoreline in the region (30 m a.s.l.) mapped by Norðdahl & Hjort (1993) (Figures 1c and 5). The three inferred ice-marginal positions in Þistilfjörður (Norðdahl & Hjort, 1993) are located to the west and southwest of the ridge corridor (Figure 1c).

Former meltwater channels occur within the ridge corridor (Figures 1c and 3a). The largest channels are over 300 m wide and up

to 10 m deep. They generally run parallel to the valley and present-day rivers, except when they turn to the west and merge with Sandá. In most cases their cross profile can be described as U-shaped. Some of the ridges appear to be truncated at channel margins and may thus have been eroded by meltwater activity (Figures 3a and 4c).

3.3 | Sedimentology of the ridges

3.3.1 | Bakkaflói

The internal architecture of the ridges in Bakkaflói was studied in three trenches (B1-3) that were excavated along the cross profile in the northeastern most ridge at site 1, one kilometre from the coast in Miðfjörður (Figures 2a and 6a,b). The ridge is 116 m long, 65 m wide and between 1.5 and 3 m prominent. The ridge is orientated south-east to northwest (142°–322°) with a maximum elevation of 39 m a.s.l. In total, the sections investigated are over 26 m long and are all orientated transverse to the ridge (Figure 6a,b). Five lithofacies were identified in the three sections: (f1) grey, matrix-supported subglacial traction till; (f2) brown, matrix-supported subglacial traction till; (f3) cryoturbated soil, (f4) water-laid sediments (f5) soil. Those are described and interpreted in Table 2.

Section B1 is located on the proximal (SW) side of the ridge. The section is 10.4 m in length with a maximum height of 2.6 m (Figure 6a,b). Most of the section (0.8–2.6 m) is composed of lithofacies

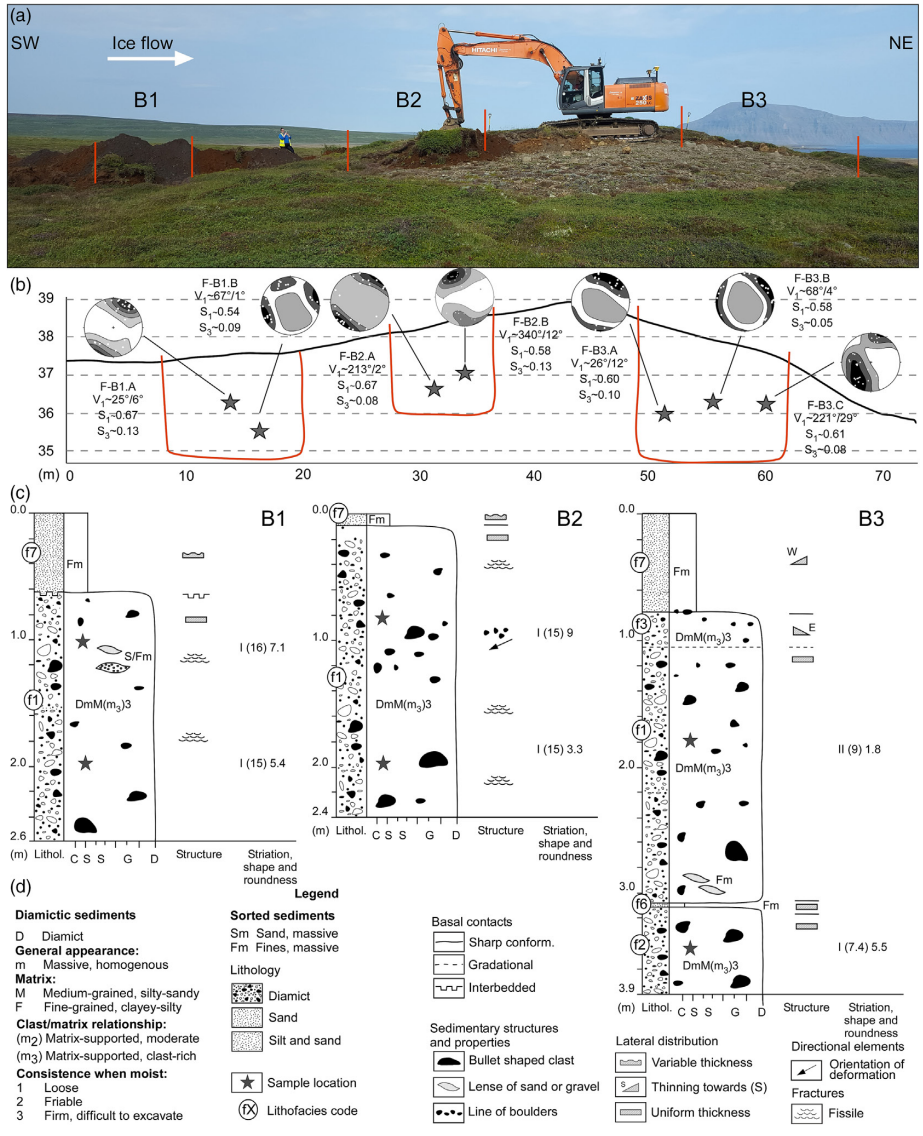

FIGURE 6 (a) An excavator digging sections B1-3 in a crevasse-squeeze ridge (CSR) close to the coast in Miðfjörður in Bakkaflói. The general direction of ice flow in the area is from southwest to northeast. (b) Cross profile of the CSR showing the location of the sections and the clast fabric analysis. (c) Stratigraphical logs from sections B1-3. Here the stars indicate the location of the samples for grain-size analyses and clast morphology. (d) Legend with symbols and lithofacies codes used here and for other logs in the paper, following Krüger & Kjær (1999).

TABLE 2 Lithofacies identified in CSRs in Bakkaflói and Þistilfjörður. Lithofacies codes are according to Krüger & Kjær (1999).

Lithofacies no. and code	Location and description	Interpretation	References
1 - DmM(m_3)3	Sections B1-3 • 1.8–2.2 m thick units • Massive, medium-grained, matrix supported, firm diamict • Grey in colour • Clast-rich, dominated by subangular to subrounded, blocky pebbles and boulders • Occasional sand and silt lenses (f4) • Vague fissile structure and line of boulders • Moderate clast-fabric, generally oblique to the general ice flow direction, with a gentle to steep plunge down- and upglacier	Subglacial traction till • Deposited beneath the active ice • The sand and silt lenses (f4) indicate fluctuating water pressure • The clast-fabric indicates upward squeezing of sediments	Krüger and Kjær (1999); Evans et al. (2006)
2 - DmM(m_3)3	Section B3 • 0.7 m thick unit • Massive, medium-grained, matrix supported, firm diamict • Brown in colour • Clast-rich, dominated by subangular to subrounded, blocky pebbles and boulders	Subglacial traction till • Deposited beneath the active ice	Krüger and Kjær (1999); Evans et al. (2006)
3 - DmM(m_3)2	Section B3 • 0.2 m thick unit • Massive, medium-grained, matrix supported, friable diamict • Grey in colour • High content of coarse gravel to smaller cobbles (<10 cm) • No structures	Cryoturbated diamict • Formed due to cryoturbation at the boundary between the soil (f5) and the till (f1)	
4 - DmM(m_{2-3})2	Sections Th1.1-3 and Th2 • 2.4–2.8 thick units • Massive, medium-grained, matrix supported, friable diamict • Brown in colour • Moderate to clast-rich, subangular to subrounded, blocky pebbles and boulders • Vague fissile structure	Subglacial traction till • Deposited beneath the active ice	Krüger and Kjær (1999); Evans et al. (2006)
5 - DmM(m_2)1	Sections Th1.1-3 • 0.1–0.8 m thick • Massive, medium-grained, matrix supported, loose diamict • Brown in colour • Moderate-clast content, subangular to subrounded, blocky pebbles and boulders • Vague fissile structure	Subglacial traction till • Deposited beneath the active ice	Krüger and Kjær (1999); Evans et al. (2006)
6 - F/S/m	Section B3 • Light-coloured massive silt to fine sand • Both appears as lenses within f1 and layer (up to 1 cm thick) between f1 and f2	Fluvial fines • Deposited from running water at low flow regime	Evans et al. (2006)
7 - Fm	Sections B1-3, Th1.1-2 and Th2 • 0.1–0.8 m thick units • Massive, brown, fine-grained soil with roots and vegetation on top	Soil	

1 [f1; DmM(m_3)3], interpreted as subglacial traction till (Table 2). Fissile structures appear throughout the unit, with apparent dip towards northeast in the middle of the section but towards southeast in the southwestern part of the section. Lenses of sand and silt [f4; S/Fm] are visible within the upper part of f1. Based on the grain size distribution from two samples at 1.2- and 2.1-m depth, the matrix of f1 contains

35%–38% fines, 32%–35% sand and 30% gravel. The clasts range from 2 to 40 cm in diameter and are mostly blocky (C_{40} = 5.4–7.1) and subrounded to subangular (RA = 15–16) (Figure 6c). Clast fabric sampled at 1.0 m depth (F-B1.A) shows preferred orientation oblique to the cross profile of the ridge (SW–NE) (V_1 = 25°/6°, S_1 = 0.67, mean dip = 21°). The other clast fabric sampled at 1.6-m depth (F-B1.B) shows weak orientation slightly further towards north-northeast than the cross profile of the ridge (V_1 = 67°/1°, S_1 = 0.54, mean dip = 19°) (Figure 6b). The uppermost 80 cm of the section consists of massive, brown, fine-grained soil [f5; Fm] that is interbedded with the till layer below (f1) (Figure 6c).

Section B2 is located in the middle of the three sections. The section is 6.5 m in length and 2.4 m high (Figure 6a,b). Most of the section (0.1–2.4 m) consists of similar subglacial traction till as in B1 [f1; DmM(m_3)3], with a sharp boundary to 10 cm thick soil layer [f5; Fm] at the top (Table 2). At 1.0-m depth there is a clast rich layer, with clasts up to 40 cm in diameter. The layer has an apparent dip towards southwest, or up-ice. The largest clasts above this layer are 15–20 cm in diameter while the largest clasts below this layer are 20–30 cm in diameter. Fissile structures are visible throughout the section (Figures 6c and 8a). The grain size analysis in the upper part of the till (at 0.8-m depth) is similar to the matrix in B1, or 32% fines, 34% sand and 34% gravel. The sample from 1.9-m depth contains slightly less fines and more gravel, or 21% fines, 37% sand and 42% gravel. The clasts from both samples are mostly blocky (C_{40} = 3.3–9) and subrounded to subangular (RA = 15) (Figure 6c). Two clast fabric analyses were done in this section. One of them (sampled at 1.6 m; F-B2.A) shows preferred orientation oblique to the cross profile of the ridge (SW–NE) (V_1 = 213°/2°, S_1 = 0.67, mean dip = 14°), whereas the other one (sampled at 1.2 m; F-B2.B) shows weak orientation along the ridge (SE-NW) and the clasts are predominantly steeply dipping (V_1 = 340°/12°, S_1 = 0.58, mean dip = 27°) (Figure 6b).

Section B3 is located on the distal side of the ridge and is 10.3 m long with a maximum height of 3.9 m (Figure 6a,b). Two units of subglacial traction tills are visible in the section, brown diamict [f2; DmM(m_2)3] from 3.2–3.9 m and grey diamict [f1; DmM(m_2)3] from 1.0–3.2 m. The main difference between the two till units is their colour. They are separated by light-coloured silt layer [f4; Fm] that is inclined towards the centre of the ridge. Lenses of silt [f4; Fm] are visible in the lower part of f1, right above the silt layer that separates the units. No structures are visible in the till units (Table 2 and Figures 6c and 8b,c). Clast and bulk samples were taken from both units, but it was only possible to examine the clast fabric from the upper one. The two units are similar in grain sizes, with slight variations in the sand and gravel content (f1; 33% fines, 26% sand, 41% gravel; f2; 29% fines, 35% sand, 36% gravel). The clast morphology is also similar in lithofacies 1 and 2, or C_{40} = 1.8 and 5.5, RA = 9 and 7.4, respectively (Figure 6c). Three clast fabric analyses were carried out in f1. Two (at 2.2 and 2 m depth) show weak preferred orientation, oblique to the cross profile of the ridge dipping down-ice (V_1 = 68°/4° and 26°/12°, S_1 = 0.58 and 0.60, mean dip = 12° and 18°). The third clast fabric (at 1.3 m depth) conforms roughly to the ridge cross profile but steeply dipping up-ice (V_1 = 221°/29°, S_1 = 0.61, mean dip = 31°) (Figure 6b).Above lithofacies 1 is a gradual boundary to a 20 cm thick cryoturbated diamict [f3; DmM(m_3)2], with higher content of clasts (<10 cm) than f1. At the top of the section is an 0.8 m thick soil layer (Figure 6c).

3.3.2 | Þistilfjörður

In Þistilfjörður, two trenches (Th1 and Th2) were excavated along the cross profiles of two ridges, both located at the eastern side of the ridge corridor, close to the centre (Figure 3a). Sections Th1.1-3 are in a ridge that is 134 m long, 31 m wide and between 1 and 4 m in height with a maximum elevation of 105 m a.s.l. The ridge orientation is east to west (104°–284°) and the orientation of the section is almost perpendicular to the ridge long axes or 24°–204° (Figure 7a,b). Section Th2 is in a ridge that is 228 m long, 50 m wide and between 0.5 to 8 m high with a maximum elevation of 92 m a.s.l. The ridge orientation is south-southeast to north-northwest (159°–339°) and the orientation of the section is close to being perpendicular to the ridge long axes or 49°–229° (Figure 7d,e). Three lithofacies were identified in the two sections: (f4) brown, matrix-supported subglacial traction till; (f5) brown, matrix-supported loose subglacial traction till; (f6) soil. Those are described and interpreted in Table 2.

Section Th1 is in total 7.9 m long with a maximum depth of 3.0 m and visualized in three logs with three observed lithofacies (Figure 7a–c). Logs Th1.1-2 show similar stratigraphy and are 2.8–3.0 m high. Th1.1 is at the distal side of the section and Th1.2 is in the middle of it. At the base, 0.1–0.8 m, is massive, matrix-supported, brown diamict with moderate clast content [f5; DmM(m_2)1]. The diamict is loose, which distinguish it from the unit above but the boundary between the units is gradual. The boundary has an apparent dip towards the northeast at 28°-40°. The diamict unit above [f4; DmM(m_{2-3})2] is very similar to f5, except it is friable. The clast content in the lower part of f4 is similar to f5 but increases higher up in the section. At the top of the section, 0.1–0.2 m, there is a gradual boundary to massive, fine-grained brown soil [f6; Fm] (Figure 7b). Log Th1.3 is at the southern side of the section (Figure 7c). It is 2.4 m high and consists of two lithofacies. Most of the section consist of lithofacies f4, however, a lens of f5 occurs at the base of the section. The boundary between the two units is gradual. Weak fissility was observed throughout the section, typically with apparent dip towards the northeast. Three bulk- and clast samples were collected from log Th1.2 at 2.6, 1.7 and 0.8-m depth. The grain-size analysis did not show any significant difference between the samples (34%–38% fines, 26%–30% sand, 36%–37% gravel). The difference between the clast morphology samples were also minimal, with C_{40} = 3.5–8.3 and RA = 5–16. This is consistent with the other sections, where most of the clasts are sub-angular and blocky, between 2 and 15 cm in diameter, although the largest are up to 30 cm in diameter (Figures 7b and 8d).

Section Th2 is 6 m long and 2.5 m deep and due to its homogeneity, it is visualized in one log (Figure 7d,e). The section is composed of lithofacies f4 [DmM(m_{2-3})2], massive, matrix-supported, brown, friable diamict with moderate clast content. The only change in the section was a line of boulders at 1.5-m depth. Like in section Th1.1-3, vague fissile structures were observed. Two bulk and clast samples were collected at 1.8- and 0.8-m depth, showing similar results to section Th1 and insignificant changes between the samples. Based on the grain-size analysis the diamict is composed of 34%–35% fines, 28% sand and 37%–38% gravel. The clasts are usually blocky (C_{40} = 5–6.7) and subangular (RA = 11–35), between 2 and 10 cm in diameter with the largest up to 20 cm (Figure 7e).

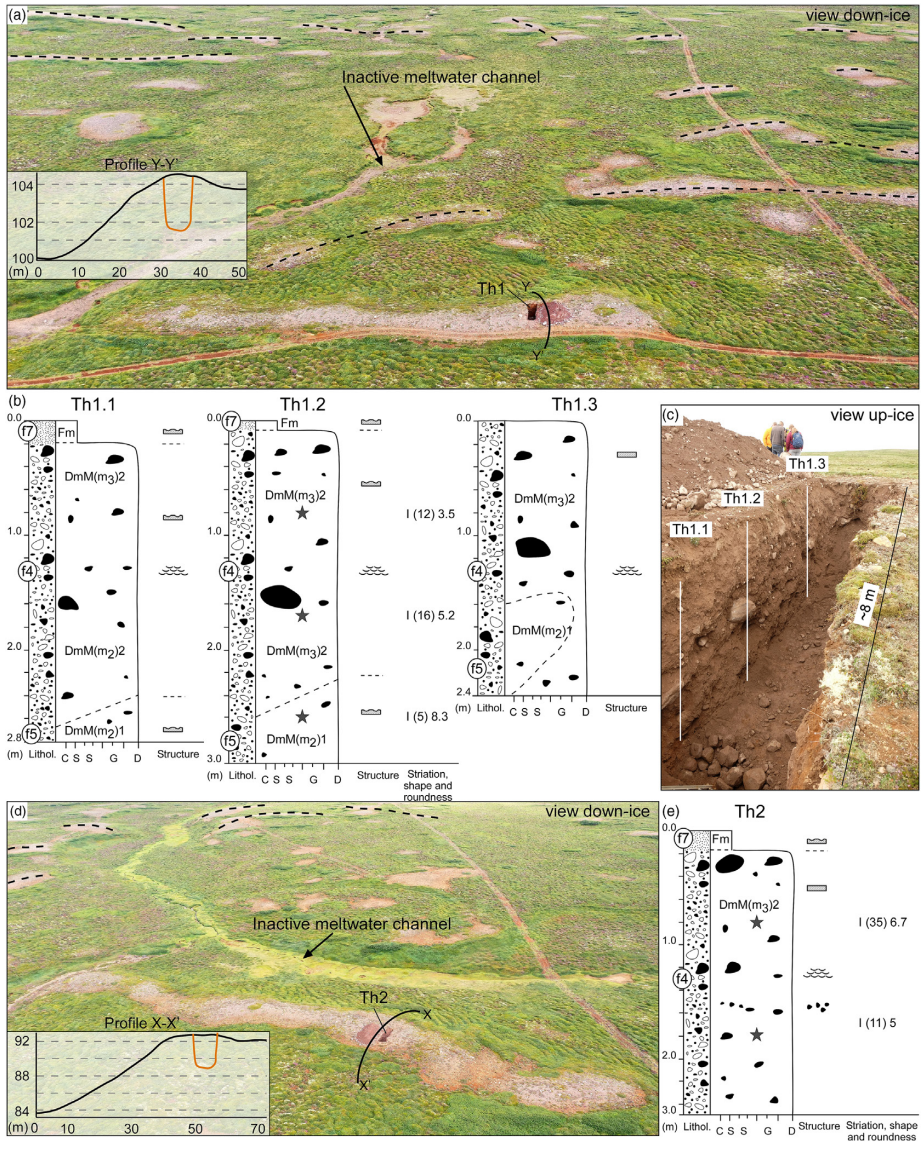

FIGURE 7 (a) Section Th1 in a crevasse-squeeze ridge (CSR) in Álandstunga, Þistilfjörður. Cross profile *Y*-*Y*′ displays symmetric profile that is between 1 and 4 m high. Other CSRs are highlighted with black dashed lines. (b) Stratigraphical logs from sections Th1.1-3. (c) Section Th1 with locations of logs marked. (d) Section Th2 in a CSR in Álandstunga, Þistilfjörður. Cross profile *X*-*X*′ exhibits little prominence on the up-ice side but up to 8 m of relief on the down-ice side, probably due to fluvial erosion, as indicated by the adjacent inactive meltwater channel. Other CSRs are highlighted with black dashed lines. (e) Stratigraphical log from section Th2.

3.4 | Comparison of the areas

In both Bakkaflói and Þistilfjörður the ridges can be described as interconnected network of low-relief ridges that are orientated transverse and/or oblique to the regional former ice flow. Comparing the morphometry of the ridges in the two areas reveals noticeable differences. Firstly, the ridge density in Þistilfjörður is twice as great as in Bakkaflói (Table 1 and Figures 2a and 3a). Secondly, the median length and width of the ridges in Bakkaflói is greater than in Þistilfjörður, although both the longest and widest individual ridges are found in Þistilfjörður. The elongation ratio of the ridges in both areas is similar (Table 1 and Figure 5a–c). The most striking contrast in the morphology of the ridges is their shape and orientation. In Bakkaflói the ridges are regular and linear in shape, while the ridges in Þistilfjörður are more irregular and either linear, arcuate or branched (Figures 2a,c, 3a and 4a,b). While around 85% of the ridges in Bakkaflói are orientated transverse to the former ice flow (±15°), the diversity in Þistilfjörður is much greater with only ~43% orientated transverse to the former ice flow (±15°) but ~47% oblique to it (±15°) and ~10% parallel to it (±15°) (Figures 2a and 3a).

The internal architecture of the ridges within both areas is similar, homogenous subglacial till with weak fissility and sporadic silt/sand

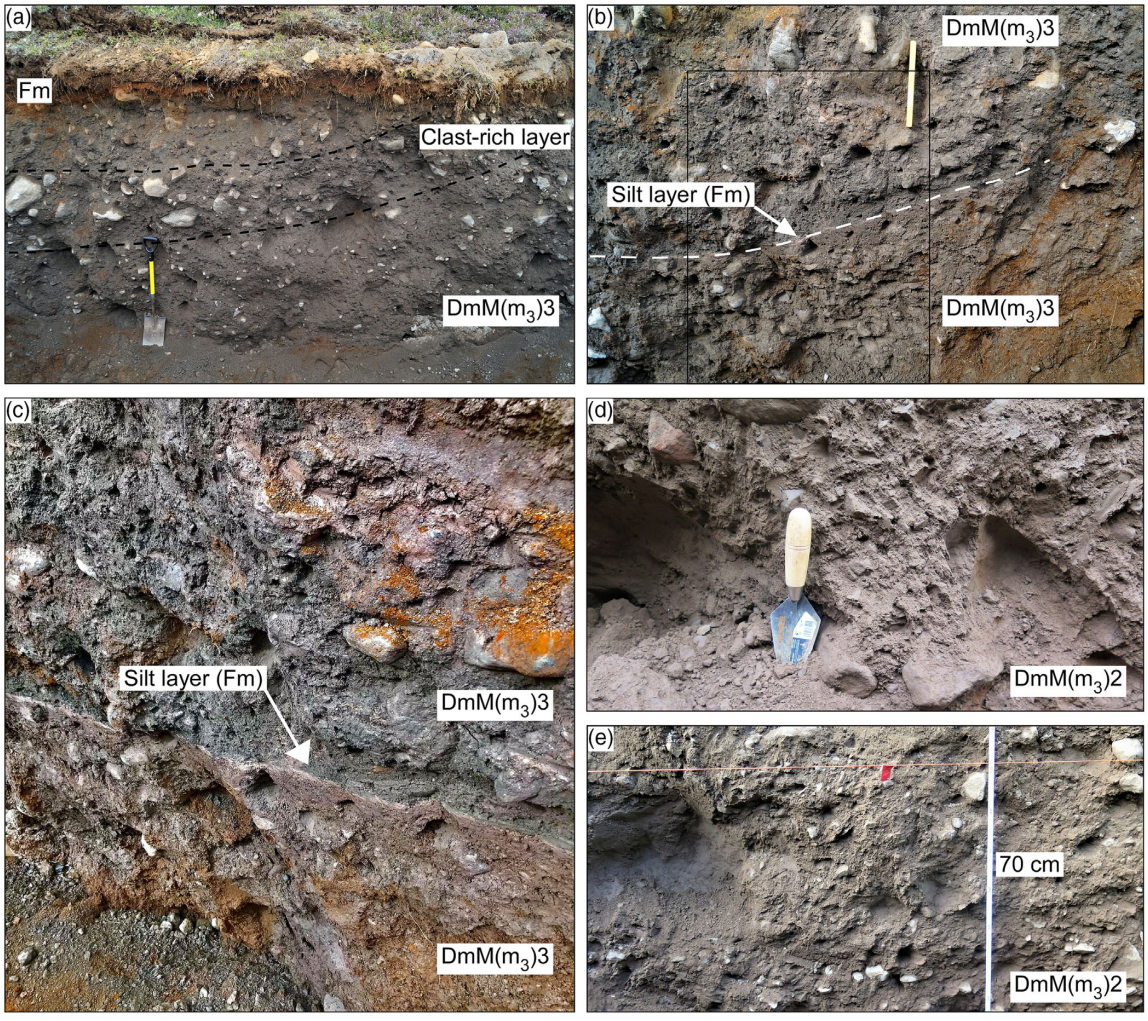

FIGURE 8 (a) Section B2. Note the clast-rich layer in the middle, dipping towards southwest or up-ice. The shovel is 1 m long. (b) Section B3. Two till units, f1 and f2, separated by a light-coloured silt layer that is inclined towards the centre. The till units are very similar, except the upper one is greyish and the lower one brownish. (c) Close-up of the light-coloured silt layer. The colour difference is clearer on this photo. (d) Section Th1.2. Vague fissility was present in the section, typically with apparent dip towards the northeast. (e) Section Th2 in Þistilfjörður is composed of homogenous massive subglacial till, uniform through the whole section.

lenses. Additionally, in Bakkaflói, another homogenous subglacial till was identified at the base, below a silt layer. The main difference between the till units was their colour. The results from the clast fabric measurements from Bakkaflói show generally steeply dipping clasts (average ranging: 12°–31°), both down-glacier and upglacier, predominantly oblique to former ice flow (Figure 9).

4 | DISCUSSION

4.1 | Formation and preservation of the CSRs

The ridges in Bakkaflói were previously interpreted as ribbed moraines associated with increased friction and effective stress at the bed and the formation of transverse basal crevasses during ice-stream shutdown (Benjamínsdóttir, 2021). We agree that the ridges in both Bakkaflói and Þistilfjörður are formed during the ice-stream shutdown as they are superimposed on the drumlins, which are formed during active ice streaming. However, as their linear shape and symmetrical cross profile are not considered typical for ribbed moraines, we discuss other alternatives for their genesis. We exclude the possibility of the ridges being submarginal De Geer moraines formed in subaquatic setting during deglaciation, as they are all situated above the marine limit. Furthermore, the ridges have a symmetrical cross profile and are not composed of deformed marine or glaciofluvial sediments (Bouvier et al., 2015; Lindén & Möller, 2005). Similarly, the symmetric cross profile and lack of compressional deformation structures count against the possibility of recessional or small push moraines (e.g., Bennett, 2001; Chandler et al., 2016). In contrast, we interpret the ridges as CSRs based on their composition of homogenous subglacial till, generally steeply dipping clast fabric, symmetrical cross profiles, interconnected network and reticular pattern (in Þistilfjörður).

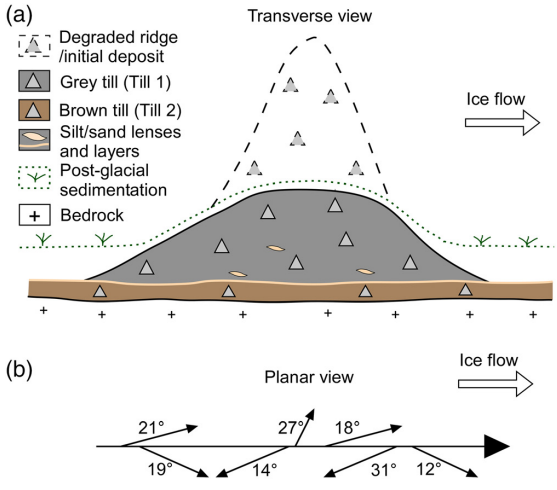

FIGURE 9 (a) Schematic cross-section and cross-profile of crevasse-squeeze ridges (CSRs) in Bakkaflói. The dashed line represents the original profile of the ridge before degradation and the dotted line represents post-glacial sedimentation, which extenuates the present-day CSR relief. The scale is non-proportional. (b) Planar view of the clast fabric orientation in relation to the general ice-flow direction with the mean dip indicated. The illustration highlights the generally steeply dipping clast fabrics with variable orientation, predominantly oblique to the former ice-flow direction.

The ridge networks resemble CSRs previously described from modern surge-type glaciers (e.g., Evans & Rea, 1999, 2003; Kjær et al., 2008; Schomacker et al., 2014; Sharp, 1985) and past ice-stream beds (e.g., Delaney et al., 2018; Evans et al., 2016; Kurjanski et al., 2019; Lamsters et al., 2021).

CSRs have been described in detial from surge-type glacier landsystems (Boulton et al., 1996; Evans & Rea, 1999, 2003; Schomacker et al., 2014; Sharp, 1985, 1988), both in the terrestrial (e.g., Aradóttir et al., 2019; Christoffersen et al., 2005; Evans et al., 2007, 2009; Farnsworth et al., 2016; Kjær et al., 2008; Lovell et al., 2015; Sobota et al., 2016; Waller et al., 2008) and marine settings (e.g., Farnsworth et al., 2017; Flink et al., 2015, 2017; Ottesen et al., 2008; Ottesen & Dowdeswell, 2006). Their formation during surging is connected to short lived acceleration of the ice, usually in phase with a readvance of the ice margin. Ridge preservation is largely a result of the passive retreat when the ice stagnates and melts away in situ and/or floatation (e.g., Kamb et al., 1985; Rea & Evans, 2011; Sharp, 1985). CSR networks form by the squeezing of highly deformable subglacial sediments into basal crevasses that form due to high basal water pressures and extensional forces acting on glacier ice during accelerated flow (Evans & Rea, 1999; Rea & Evans, 2011; Sharp, 1985) and transported englacially within the advancing surge margin (Ankerstjerne et al., 2015; Ben-Yehoshua et al., 2023).

Considering observations of CSRs on palaeo-ice stream beds (e.g., Evans et al., 2016; Kurjanski et al., 2019), we propose that the CSRs in Bakkaflói and Þistilfjörður are formed during the final stages of ice streaming or surging and the preservation of the CSRs indicates that they form immediately prior to ice stagnation. The absence of recessional moraines further supports passive retreat (Aradóttir et al., 2019; Kurjanski et al., 2019; Lamsters et al., 2021). The overall landsystem in Bakkaflói and Þistilfjörður consist of distributed SSBs and restricted corridors of CSRs, raised shorelines at three levels (the lowest one being the most prominent and continuous) and ice-marginal positions. Meltwater channels, both active and inactive, are responsible for erosion of some CSRs. The corridor pattern of CSRs is considered to represent the ice-flow centre lines as suggested by Evans et al. (2016) (Figure 10).

For CSRs to form, the existence of basal or full-depth crevasses is necessary. Such crevasses form when basal water pressures are high enough to initiate hydrofracturing, often in combination with high tensile strain rates (Lovell et al., 2015; Rea & Evans, 2011; van der Veen, 1998). The orientation of CSRs is therefore considered reflective of internal stresses. Sharp (1985) described three principal groups of CSRs classified by their orientation, conforming to our observations in Þistilfjörður. The densely spaced reticular CSRs in Þistilfjörður indicate a dense network of basal crevasses formed by transverse, parallel and oblique tensile stresses while the predominantly transverse CSRs in Bakkaflói suggest mainly longitudinal tensile stress (Figure 10). The correlation between the bed-rock topography and the orientation of CSRs at site 3 in Bakkaflói and the highest concentration of CSRs on a bed-rock high in Þistilfjörður might indicate relatively thin ice around the time of ice-stream shutdown and formation of the ridges. However, as there seems to be no obvious correlation between local topography and CSRs in other locations, we do not consider this to be a major controlling factor in the distribution of the CSRs.

Studies on CSRs in modern settings have highlighted their low preservation potential; newly exposed and sharp-crested ridges collapse as their lateral support is removed during melt out in addition to their susceptibility to erosion by, for example, water and wind (Evans & Rea, 1999, 2003; Kjær et al., 2008; Sharp, 1985). The collapse and reworking of the material results in wider CSRs with lower relief than during initial formation. We suggest the flat-crested topography to be the result of the post-exposure degradation. Furthermore, we would expect that their original height has been extenuated due to the infill of post-glacial sedimentation and soil around the ridges (Figure 9a; Spagnolo et al., 2012; Finlayson, 2013). Inter-bedform thickness was observed as being over 2–3 m in Þistilfjörður and has been recorded up to 8 m around drumlins on Bustarfell in northeast Iceland (Aradóttir et al., 2023). For both reasons, we cannot exclude that additional CSRs remain obscured under the post-glacial sediment cover.

The CSRs in this study are slightly smaller in size to those that have been described from other palaeo-ice stream beds, where some CSRs are up to 2 km long and 200 m wide (Cline et al., 2015; Delaney et al., 2018; Kurjanski et al., 2019; Lamsters et al., 2021), but considerably larger than CSRs in front of modern surge-type glaciers, which are typically tens of metres long and <2 m wide (e.g., Kjær et al., 2008; Lovell et al., 2015; Ben-Yehoshua et al., 2023).

The massive, homogenous macro-scale appearance of the sediment in both areas suggests that the till was well-mixed and far travelled (Phillips et al., 2018). The vague fissile structures indicate that the sediments were slightly sheared while being deposited, supporting the hypothesis that CSRs form prior to ice stagnation (Bjarnadóttir, 2007; Evans et al., 2016; Ben-Yehoshua et al., 2023). Sedimentological work on till within and outside CSRs has not revealed any significant differences between them, except for generally steeper clast fabric within the CSRs, implying common origin (e.g., Sharp, 1985; Christoffersen et al., 2005; Ben-Yehoshua et al., 2023). Therefore, with the available data, we suggest the lower

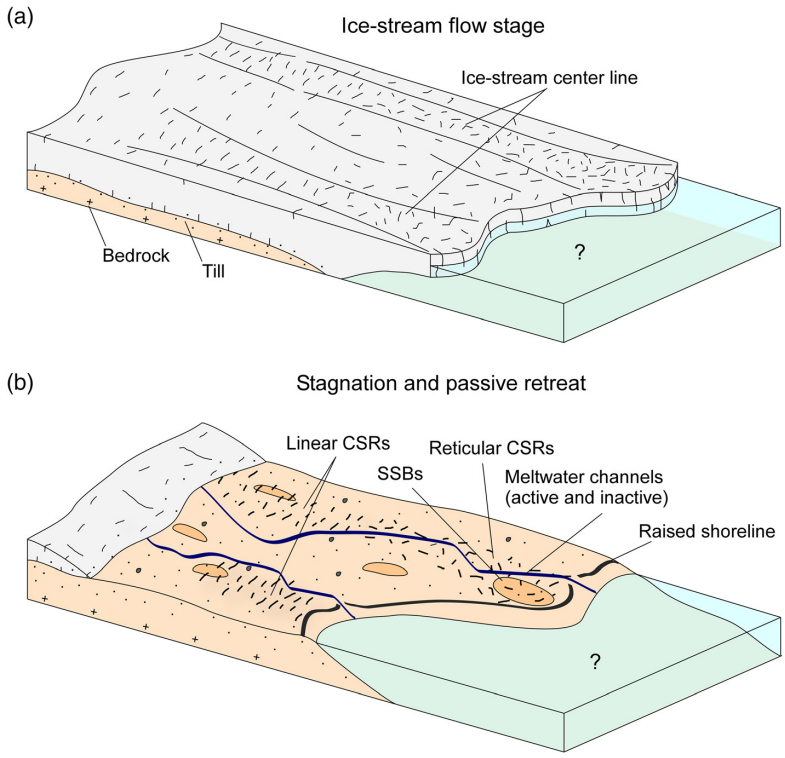

FIGURE 10 Conceptual landsystem model illustrating landforms associated with ice-stream shutdown in terrestrial environment based on observations from Bakkaflói and Þistilfjörður, northeast Iceland. (a) Flow stage of a terrestrial ice stream that extends into the marine environment. Corridors of relatively faster flow within the ice stream generate mainly transverse crevasses in the trunk flow zone due to dominating longitudinal tensile stresses while a combination of longitudinal and lateral stresses near the calving marginal zone generate crevasses with variable orientations. (b) The ice-stream shutdown is followed by stagnation and passive retreat, allowing the preservation of crevasse-squeeze ridges (CSRs) in the terrestrial environment. Their distribution and orientation in the post-glacial landscape reflects the glacial stress regimes around the time of ice-stream shutdown. The question marks indicate that the landsystem in the marine environment is unknown as bathymetric data is lacking.

till (f2) in section B3 in Bakkaflói may have been deposited prior to the formation of the CSRs (Figure 9a).

The low to moderate clast fabrics with generally steeply dipping clasts, both down- and upglacier (Figure 9b), resemble both macro and micro fabric measurements described from CSRs at modern surge-type glaciers in Iceland (Bjarnadóttir, 2007; Gadd, 2016; Sharp, 1985) and elsewhere at beds of past ice streams (Ankerstjerne et al., 2015; Evans et al., 2020; Lamsters et al., 2021), which indicate the intrusion of till into basal crevasses. The upglacier dipping clast rich layer and silt layer in section B2 and B3 in Bakkaflói are further indicative of the upward flow of till. The orientation of the clast fabrics predominantly oblique to the general ice flow direction in the area, in both directions (Figure 9b) is difficult to explain but might reflect the complex flow of till upwards and obliquely into the crevasses. Additionally, this could be influenced by subsequent shearing during post-depositional transport prior to ice stagnation (Ankerstjerne et al., 2015; Gadd, 2016). However, it should be mentioned that the post-glacial degradation of the CSRs (Figure 9a), as previously explained, might affect the clast fabric after its formation, especially on the flanks of the ridges. Therefore the clast fabric should be interpreted with caution. However, the preferred orientation in all samples might suggest that the measurements represent primary clast fabric.

4.2 | Implications for ice dynamics and glacial history

The restricted extent of the CSRs in Þistilfjörður in a narrow corridor is comparable to the CSRs on the bed of the Maskwa palaeo-ice stream (Evans et al., 2016), although of much smaller scale. There, three different types of CSR patterns were classified based on the settings in which they were produced: ice stream, surging glaciers, or active temperate glacier lobes. Based on their study, CSRs associated with ice streams are formed within corridors due to extensional fracturing between the lateral shear zones of flow units moving at different velocities within the ice. CSRs that have been described from other palaeo-ice stream beds exhibit similar corridor patterns (Andreassen et al., 2014; Bjarnadóttir et al., 2014; Delaney et al., 2018; Kurjanski et al., 2019), except in Baltica where Lamsters et al. (2021) did not find any correspondence to the patterns described by Evans et al. (2016). In front of surging glaciers, CSRs are usually displayed in wide arcuate zones but have not been associated with corridor pattern (e.g., Kjær et al., 2008; Schomacker et al., 2014; Evans et al., 2016; Ben-Yehoshua et al., 2023). In Bakkaflói, the corridor pattern is not as clear as in Þistilfjörður but sites 1 and 2 could represent a section of one corridor and site 3 another one (see Figure 2a). It should though be considered, for both Þistilfjörður and Bakkaflói, that we might only see a fraction of the ridges as we do not know how far they extend into the marine environment below the wave-wash. Furthermore, CSRs that formed further upglacier might not be preserved due to glacier overriding (Figure 11).

The variance in the morphology of CSRs between the two areas can further be used to infer how ice dynamics and stress regime varies within the ice streams. Kurjanski et al. (2019) addressed the spatial setting of CSRs based on their morphology within an ice stream in the Barents Sea. They interpreted the linear pattern to represent unidirectional tensile stress regime due to the lateral confining stress of the adjacent slow flowing ice, similar to the reasoning behind the corridor

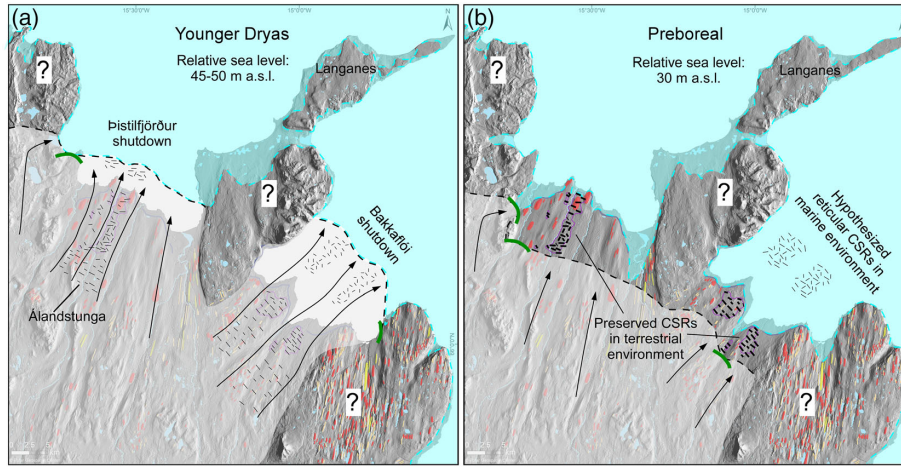

FIGURE 11 Time slices highlighting the glacial history and possible ice-stream configuration and dynamics in Bakkaflói and Þistilfjörður during the (a) YD and (b) Pb periods. The ice-marginal positions from Norðdahl & Hjort (1993) are marked with green and dashed line drawn between them to indicate the possible extent of the ice-margin. As we only focus on the glacial reconstruction within the study area the areas outside are marked with question marks to indicate unknown ice extent.

pattern described from the Laurentide Ice Sheet (Evans et al., 2016). Further down-ice in the Barents Sea, Andreassen et al. (2014) had previously described reticular CSRs that form due to radial extensional stress regime. Additionally, linear CSRs were suggested to form further up ice than the reticular CSRs, highlighting the difference in stress regimes spatially within the ice stream.

Accordingly, we propose that the variable morphology of CSRs suggests difference in stress regime between Bakkaflói and Þistilfjörður. In Þistilfjörður, the prominent corridor represents one flow unit where combination of longitudinal and lateral stresses generated crevasses with variable orientations, which is common near the marginal zone of calving glaciers. In contrast, two flow units could have existed in Bakkaflói with dominating longitudinal tensile stresses due to lateral confinement of slower moving ice. Based on this, we assume that the linear CSR networks in Bakkaflói were formed further upstream (relatively) than the reticular CSRs in Þistilfjörður (Figures 10 and 11). This implies that during the ice-stream shutdown, the margin of the Þistilfjörður ice stream was located near the present coast while the Bakkaflói ice stream extended farther into the marine environment. Hypothetically, reticular CSRs should thus be present at the floor of the Bakkaflói Bay (Figure 11). Studies have highlighted the asynchronous retreat of adjacent ice streams and discussed if it is rather related to internal factors, such as migration of ice divides and local topography, than climate forcing (e.g., Davies et al., 2019; Margold et al., 2015; Stokes et al., 2014). It remains unknown if the ice-stream readvances and the following shutdown were synchronous in northeast Iceland and to address these issues, a better chronological control is needed together with data from the marine environment.

Due to limited age constraints for the ice-marginal features and raised shorelines in the two areas, we can only hypothesize the timing for the formation of the CSRs. The SSBs in Bakkaflói and Þistilfjörður are considered to have mainly formed during the LGM, when the ice sheet extended all the way to the shelf edge, as well as during the deglaciation and subsequent YD and Pb readvance (Aradóttir et al., 2023; Benediktsson, Aradóttir, et al., 2022). Since there are examples in both areas of CSRs that are superimposed on SSBs, it is certain that the CSRs post-date the formation of the SSBs and can thus be associated with the ice-stream shutdown (Figure 10).

During the deglaciation, abrupt warming at the Bølling Interstadial (14.7–14.1 cal. ka BP) resulted in a collapse of the marine-based part of the ice sheet and the formation of marine limit shorelines in western Iceland. This event was followed by crustal rebound and associated regression of sea level (Benediktsson et al., 2023b; Ingólfsson & Norðdahl, 2001; Norðdahl & Ingólfsson, 2015). Subsequently, two readvances occurred, that is, during the YD (12.9–11.7 cal. ka BP) and Preboreal (11.3–10.4 cal. ka BP). These advances depressed the crust to relative sea level rise and the formation of raised shorelines at two different levels. Norðdahl & Hjort (1993) associated the lowest shoreline (at 30–35 m a.s.l.) and the ice-marginal positions in Þistilfjörður and Bakkaflói to the Pb readvance. Therefore, the higher shorelines were considered to have formed during the YD readvance when the ice margin most likely extended outside the present coast (Benediktsson et al., 2023, 2023c; Norðdahl et al., 2008). Based on these correlations, we suggest that the study areas in both Bakkaflói and Þistilfjörður were occupied by ice during the YD, and we consider it unlikely that the CSRs would have been preserved if they were formed prior to that. During the Pb, it is considered unlikely that the ice advanced over the CSRs sites. Consequently, we suggest that the CSRs in both areas are associated with ice-stream shutdown during the YD period (Figure 11). Alternatively, they could be associated with the termination of a surge event; however, their distribution within restricted corridors, similar to other palaeo-ice stream beds, and the lack of evidence of periodic advances, are in favour of ice-stream shutdown (e.g., Evans et al., 2016; Lamsters et al., 2021).

The variety of SSB morphometrics in Þistilfjörður is considered to indicate longer and more variable period of ice streaming than in Bakkaflói, and the cluster of MSGLs at the eastern side indicative of sustained fast flow (Benediktsson, Aradóttir, et al., 2022). In proximity to the CSRs in Þistilfjörður, the SSBs are, however, almost absent.

Thus, we surmise shifting ice dynamics where the ice-stream centerline was concentrated at the eastern margin over a sustained period, and then shifted over to Álandstunga, which probably signifies the later stages of ice streaming in Þistilfjörður.

CSR networks have not been previously described from the IIS, neither from terrestrial nor marine settings. Here we have described CSR networks that are preserved terrestrially in northeast Iceland. Given the lack of high-resolution bathymetric data from the northeastern Icelandic fjords, it is uncertain if CSRs formed and/or remain preserved in the marine environment (Figure 11). Furthermore, marine data may indicate numerous (or cyclical) Late Glacial readvances (e.g., Benn, 2021; Flink et al., 2015; Sigfúsdóttir & Benediktsson, 2020) more suggestive of surge behaviour as opposed to a single shutdown. Such data would provide a holistic understanding of the overall ice-stream landsystem in northeast Iceland and ultimately of the former ice dynamics. We emphasize the importance of a holistic approach, through the integration of both terrestrial and marine data, to best reconstruct past glacial behaviour in northeast Iceland (cf. Aradóttir et al., 2019).

The study of CSRs in northeast Iceland provides the first description of CSRs in palaeo setting in Iceland and adds to the growing investigations of their existence in palaeo settingas evidence for ice-stream shutdown and/or surge termination. Furthermore, it adds to our understanding of ice sheet behaviour during deglaciation which is of importance for ongoing research on modern and future ice stream changes in relation to the current climate change.

5 | CONCLUSION

The ridge networks in Bakkaflói and Þistilfjörður, northeast Iceland, are interpreted as CSR networks based on their linear and reticular, interconnected pattern, symmetric cross profiles, and composition of homogenous subglacial till with generally steeply dipping clast fabrics. The overall landform assemblage in Bakkaflói and Þistilfjörður is interpreted to represent active ice streams within the IIS during the LGM and the following deglaciation, followed by ice-stream shutdown. In addition to the CSRs, the landsystem consists of SSBs, ice-marginal landforms, raised shorelines, and relict meltwater channels. Examples of CSRs superimposed on the SSBs indicate that they post-date the SSBs and signify the final stages of ice-stream shutdown. The preservation of the CSRs suggests ice stagnation and passive melting following ice-stream shutdown. The present CSR morphology (relatively wide and low-relief) reflects post-depositional degradation and post-glacial sedimentation around the ridges. The CSRs are only preserved above the regional marine limit shoreline at 30–35 m a.s.l.

Despite minimal chronological constraints in the area, we surmise that the CSRs were formed during the later stage of ice streaming at the end of the YD. It is unlikely that the CSRs would remain preserved if they formed earlier given the suggested YD age of the ice-marginal features by the present coast. The ice-marginal positions just up-ice from the CSR areas are suggested to have formed during a Pb readvance. While this advance may have overridden other CSRs further up-ice, it did not affect the CSR networks investigated in this study. The variance in the morphology of the CSRs between the flowsets could indicate difference in stress regime and kinematic-setting within the ice streams. Thus, the linear CSRs in Bakkaflói formed further upstream where longitudinal tensile stresses dominated compared to the reticular CSRs in Þistilfjörður which formed where both longitudinal and lateral stresses operated near the calving margin. Therefore, we propose that the ice margin in Bakkaflói might have extended further out into the marine environment at the time of formation of the linear CSRs. Due to the lack of high-resolution bathymetric data from the fjords, it is still unknown if CSRs exist in the marine environment. Such data is crucial for a holistic approach of the palaeo-ice sheet landsystem and enhanced understanding of past ice-sheet dynamics. Our findings highlight the importance of using geomorphological and sedimentological data and analyses to advance our understanding of the dynamics of the IIS during the deglaciation. Furthermore, our study may provide analogues to modern ice-stream and surging lobe shutdown and enhance knowledge of both modern and palaeo-ice sheet behaviour during deglaciation under climate warming.

AUTHOR CONTRIBUTIONS

Nína Aradóttir: Investigation; writing—original draft; funding acquisition; software; visualization; conceptualization; formal analysis. **Ívar Örn Benediktsson:** Supervision; writing—review & editing; investigation; funding acquisition; conceptualization; project administration; resources. **Ólafur Ingólfsson:** Supervision; writing—review & editing; investigation; funding acquisition; resources. **Skafti Brynjólfsson:** Investigation; writing—review & editing; resources. **Wesley R Farnsworth:** Conceptualization; investigation; writing—review & editing. **Margrét Mjöll Benjamínsdóttir:** Investigation; formal analysis; writing—review & editing. **Lena Björg Ríkharðsdóttir:** Investigation; formal analysis; writing—review & editing.

ACKNOWLEDGEMENTS

This project has been supported through grants from the University of Iceland Research Fund (to ÓI), the Icelandic research fund (NA), the Energy Research Fund of Landsvirkjun (to NA and ÍÖB) and the Icelandic Road and Coastal Administration (to ÍÖB). All our colleagues and graduate students are thanked for great company during fieldwork, constructive discussions and helpful feedback during the project. Daniel Ben-Yehoshua is especially thanked for droning the area in Þistilfjörður at the early stage of the project. Thanks are also due to Ólafur B. Vigfússon, farmer at Syðra-Áland, for guidance in the field and giving us the permission to excavate the ridges in Álandstunga in Þistilfjörður and the Icelandic Road and Coastal Administration for excavate the ridge in Bakkaflói. We would like to thank the two anonymous reviewers for their constructive comments that improved the manuscript.

DATA AVAILABILITY STATEMENT

The data that support the findings of this study are available from the corresponding author upon reasonable request.

ORCID

Nína Aradóttir https://orcid.org/0000-0002-6584-8964
Skafti Brynjólfsson https://orcid.org/0000-0002-2792-1964

REFERENCES

Alley, R.B., Anandakrishnan, S., Dupont, T.K. & Parizek, B.R. (2004) Ice streams – fast, and faster? *Comptes Rendus Physique*, 5(7), 723–734. Available from: https://doi.org/10.1016/j.crhy.2004.08.002

Alley, R.B., Clark, P.U., Huybrechts, P. & Joughin, I. (2005) Ice-sheet and sea-level changes. *Science*, 310(5747), 456–460. Available from: https://doi.org/10.1126/science.1114613

Andreassen, K., Winsborrow, M.C., Bjarnadóttir, L.R. & Rüther, D.C. (2014) Ice stream retreat dynamics inferred from an assemblage of landforms in the northern Barents Sea. *Quaternary Science Reviews*, 92, 246–257. Available from: https://doi.org/10.1016/j.quascirev.2013.09.015

Ankerstjerne, S., Iverson, N.R. & Lagroix, F. (2015) Origin of a washboard moraine of the Des Moines lobe inferred from sediment properties. *Geomorphology*, 248, 452–463. Available from: https://doi.org/10.1016/j.geomorph.2015.07.019

Aradóttir, N., Benediktsson, Í.Ö., Ingólfsson, Ó., Sturkell, E., Brynjólfsson, S., Farnsworth, W.R., et al. (2023) Drumlin formation within the Bustarfell drumlin field, Northeast Iceland: Integrating sedimentological and ground-penetrating radar data. *Journal of Quaternary Science*, 38(3), 386–402. Available from: https://doi.org/10.1002/jqs.3481

Aradóttir, N., Ingólfsson, Ó., Noormets, R., Benediktsson, Í.Ö., Ben-Yehoshua, D., Håkansson, L., et al. (2019) Glacial geomorphology of Trygghamna, western Svalbard-integrating terrestrial and submarine archives for a better understanding of past glacial dynamics. *Geomorphology*, 344, 75–89. Available from: https://doi.org/10.1016/j.geomorph.2019.07.007

Benediktsson, Í.Ö., Aradóttir, N., Ingólfsson, Ó. & Brynjólfsson, S. (2022) Cross-cutting palaeo-ice streams in NE-Iceland reveal shifting Iceland ice sheet dynamics. *Geomorphology*, 396, 108009. Available from: https://doi.org/10.1016/j.geomorph.2021.108009

Benediktsson, Í.Ö., Brynjólfsson, S. & Ásbjörnsdóttir, L. (2022) Iceland: Glandforms from the Last Glacial Maximum. In: Palacios, D., Hughes, P., García-Ruiz, J.M. & Andrés, N. (Eds.) *European glacial landscapes: Maximum extent of glaciations*. Chennai: Elsevier, pp. 427–434 https://doi.org/10.1016/B978-0-12-823498-3.00055-8

Benediktsson, Í.Ö., Brynjólfsson, S. & Ásbjörnsdóttir, L. (2023a) Iceland: Glacial landforms during deglaciation. In: Palacios, D., Hughes, P., García-Ruiz, J.M. & Andrés, N. (Eds.) *European Glacial Landscapes*, Vol. 2023a. Chennai: Elsevier, pp. 149–155 https://doi.org/10.1016/B978-0-323-91899-2.00022-X

Benediktsson, Í.Ö., Brynjólfsson, S. & Ásbjörnsdóttir, L. (2023b) Iceland: Glacial landforms from the Bølling-Allerød interstadial. In: Palacios, D., Hughes, P., García-Ruiz, J.M. & Andrés, N. (Eds.) *European Glacial Landscapes*, Vol. 2023b. Chennai: Elsevier, pp. 331–339 https://doi.org/10.1016/B978-0-323-91899-2.00051-6

Benediktsson, Í.Ö., Brynjólfsson, S. & Ásbjörnsdóttir, L. (2023c) Glacial landscapes of Iceland from the Younger Dryas. In: Palacios, D., Hughes, P., García-Ruiz, J.M. & Andrés, N. (Eds.) *European Glacial Landscapes*, Vol. 2023c. Chennai: Elsevier, pp. 497–507 https://doi.org/10.1016/B978-0-323-91899-2.00054-1

Benediktsson, Í.Ö., Brynjólfsson, S., Ásbjörnsdóttir, L. & Farnsworth, W.R. (2023) Glacial landforms from the Holocene. In: Palacios, D., Hughes, P., García-Ruiz, J.M. & Andrés, N. (Eds.) *European glacial landscapes*. Chennai: Elsevier.

Benjamínsdóttir, M.M. (2021) Ribbed moraine ridges in Bakkaflói, NE-Iceland: Morphometry, sedimentology and formation. Master's thesis, Faculty of Earth Sciences, University of Iceland. 67 p. Available from: http://hdl.handle.net/1946/38501

Benn, D.I. (2021) Surging glaciers in Scotland. *Scottish Geographical Journal*, 137(1–4), 1–40. Available from: https://doi.org/10.1080/14702541.2021.1922738

Benn, D.I. & Ballantyne, C.K. (1993) The description and representation of particle shape. *Earth Surface Processes and Landforms*, 18(7), 665–672. Available from: https://doi.org/10.1002/esp.3290180709

Bennett, M.R. (2001) The morphology, structural evolution and significance of push moraines. *Earth-Science Reviews*, 53(3–4), 197–236. Available from: https://doi.org/10.1016/S0012-8252(00)00039-8

Bennett, M.R. (2003) Ice stream as the arteries of an ice sheet; their mechanics, stability and significance. *Earth-Science Reviews*, 61(3-4), 309–339. Available from: https://doi.org/10.1016/S0012-8252(02)00130-7

Ben-Yehoshua, D., Aradóttir, N., Ingólfsson, Ó., Benediktsson, Í.Ö. & Farnsworth, W.R. (2023) Formation of crevasse squeeze ridges—A case study from Trygghamna, Svalbard. *Earth Surface Processes and Landforms*. https://doi.org/10.1002/esp.5631

Bingham, R.G., Vaughan, D.G., King, E.C., Davies, D., Cornford, S.L., Smith, A.M., et al. (2017) Diverse landscapes beneath Pine Island Glacier influence ice flow. *Nature Communications*, 8(1), 1618. Available from: https://doi.org/10.1038/s41467-017-01597-y

Bjarnadóttir, L.R. (2007) Ice-marginal environments of a surge-type glacier: Distribution, formation and morphological evolution of flutes and crevasse cast ridges at Brúarjökull, Iceland. Master's thesis, Faculty of Earth Sciences, University of Iceland. 104 p.

Bjarnadóttir, L.R., Winsborrow, M.C. & Andreassen, K. (2014) Deglaciation of the central Barents Sea. *Quaternary Science Reviews*, 92, 208–226. Available from: https://doi.org/10.1016/j.quascirev.2013.09.012

Boulton, G.S., van de Meer, J.J.M., Harts, J.K., Beets, D.J., Ruegg, G.H.J., van der Wateren, F.M., et al. (1996) Till and moraine emplacement in a deforming bed surge—An example from a marine environment. *Quaternary Science Reviews*, 15(95), 961–987. Available from: https://doi.org/10.1016/0277-3791(95)00091-7

Bourgeois, O., Dauteuil, O. & Van Vliet-Lanoë, B. (2000) Geothermal control on flow patterns in the last glacial maximum ice sheet of Iceland. *Earth Surface Processes and Landforms*, 25(1), 59–76. Available from: https://doi.org/10.1002/(SICI)1096-9837(200001)25:1<59::AID-ESP48>3.0.CO;2-T

Bouvier, V., Johnson, M.D. & Påsse, T. (2015) Distribution, genesis and annual-origin of De Geer moraines in Sweden: Insights revealed by LiDAR. *GFF*, 1-15(4), 319–333. Available from: https://doi.org/10.1080/11035897.2015.1089933

Briner, J.P. (2016) Ice streams waned as ice sheets shrank. *Nature*, 530(7590), 287–288. Available from: https://doi.org/10.1038/530287a

Chandler, B.M.P., Evans, D.J.A. & Roberts, D.H. (2016) Characteristics of recessional moraines at a temperate glacier in SE Iceland: Insights into patterns, rates and drivers of glacier retreat. *Quaternary Science Reviews*, 135, 171–205. Available from: https://doi.org/10.1016/j.quascirev.2016.01.025

Christoffersen, P., Piotrowski, J.A. & Larsen, N.K. (2005) Basal processes beneath an Arctic glacier and their geomorphic imprint after a surge, Elisebreen, Svalbard. *Quaternary Research*, 64(2), 125–137. Available from: https://doi.org/10.1016/j.yqres.2005.05.009

Cline, M.D., Iverson, N.R. & Harding, C. (2015) Origin of washboard moraines of the Des Moines lobe: Spatial analyses with LiDAR data. *Geomorphology*, 246, 570–578. Available from: https://doi.org/10.1016/j.geomorph.2015.07.021

Davies, B.J., Livingstone, S.J., Roberts, D.H., Evans, D.J.A., Gheorghiu, D.M. & Cofaigh, C.Ó. (2019) Dynamic ice stream retreat in the central sector of the last British-Irish ice sheet. *Quaternary Science Reviews*, 225, 105989. Available from: https://doi.org/10.1016/j.quascirev.2019.105989

Delaney, C.A., McCarron, S. & Davis, S. (2018) Irish ice sheet dynamics during deglaciation of the central Irish midlands: Evidence of ice streaming and surging from airborne LiDAR. *Geomorphology*, 306, 235–253. Available from: https://doi.org/10.1016/j.geomorph.2018.01.011

Evans, D.J., Storrar, R.D. & Rea, B.R. (2016) Crevasse-squeeze ridge corridors: Diagnostic features of late-stage palaeo-ice stream activity. *Geomorphology*, 258, 40–50. Available from: https://doi.org/10.1016/j.geomorph.2016.01.017

Evans, D.J.A., Atkinson, N. & Phillips, E. (2020) Glacial geomorphology of the Neutral Hills uplands, Southeast Alberta, Canada: The process-form imprints of dynamic ice streams and surging ice lobes. *Geomorphology*, 350, 106910. Available from: https://doi.org/10.1016/j.geomorph.2019.106910

Evans, D.J.A. & Benn, D.I. (Eds). (2004) *A practical guide to the study of glacial sediments*. 83-87 & 97-107 pp. London: Arnold.

Evans, D.J.A., Phillips, E.R., Hiemstra, J.F. & Auton, C.A. (2006) Subglacial till: Formation, sedimentary characteristics and classification. *Earth-Science Reviews*, 78(1–2), 115–176. Available from: https://doi.org/10.1016/j.earscirev.2006.04.001

Evans, D.J.A. & Rea, B.R. (1999) Geomorphology and sedimentology of surging glaciers: A land-systems approach. *Annals of Glaciology*, 28, 75–82. Available from: https://doi.org/10.3189/172756499781821823

Evans, D.J.A. & Rea, B.R. (2003) Surging glacier landsystem. In: *Glacial landsystems*. London: Taylor and Francis, pp. 259–288.

Evans, D.J.A., Twigg, D.R., Rea, B.R. & Orton, C. (2009) Surging glacier landsystem of Tungnaárjökull, Iceland. *Journal of Maps*, 5(1), 134–151. Available from: https://doi.org/10.4113/jom.2009.1064

Evans, D.J.A., Twigg, D.R., Rea, B.R. & Shand, M. (2007) Surficial geology and geomorphology of the Brúarjökull surging glacier landsystem. *Journal of Maps*, 3(1), 349–367. Available from: https://doi.org/10.1080/jom.2007.9710850

Farnsworth, W.R., Ingólfsson, Ó., Noormets, R., Allaart, L., Alexanderson, H., Henriksen, M., et al. (2017) Dynamic Holocene glacial history of St. Johnsfjorden, Svalbard. *Boreas*, 46(3), 585–603. Available from: https://doi.org/10.1111/bor.12269

Farnsworth, W.R., Ingólfsson, Ó., Retelle, M. & Schomacker, A. (2016) Over 400 previously undocumented Svalbard surge-type glaciers identified. *Geomorphology*, 264, 52–60. Available from: https://doi.org/10.1016/j.geomorph.2016.03.025

Finlayson, A. (2013) Digital surface models are not always representative of former glacier beds: Palaeoglaciological and geomorphological implications. *Geomorphology*, 194, 25–33. Available from: https://doi.org/10.1016/j.geomorph.2013.03.026

Flink, A.E., Noormets, R., Fransner, O., Hogan, K.A., O'Regan, M. & Jakobsson, M. (2017) Past ice flow in Wahlenbergfjorden and its implications for late Quaternary ice sheet dynamics in northeastern Svalbard. *Quaternary Science Reviews*, 163, 162–179. Available from: https://doi.org/10.1016/j.quascirev.2017.03.021

Flink, A.E., Noormets, R., Kirchner, N., Benn, D.I., Luckman, A. & Lovell, H. (2015) The evolution of a submarine landform record following recent and multiple surges of Tunabreen glacier, Svalbard. *Quaternary Science Reviews*, 108, 37–50. Available from: https://doi.org/10.1016/j.quascirev.2014.11.006

Franke, S., Bons, P.D., Westhoff, J., Weikusat, I., Binder, T., Streng, K., et al. (2022) Holocene ice-stream shutdown and drainage basin reconfiguration in Northeast Greenland. *Nature Geoscience*, 15(12), 995–1001. Available from: https://doi.org/10.1038/s41561-022-01082-2

Greenwood, S.L. & Clark, C.D. (2009) Reconstructing the last Irish ice sheet 2: A geomorphologically-driven model of ice sheet growth, retreat and dynamics. *Quaternary Science Reviews*, 28(27-28), 3101–3123. Available from: https://doi.org/10.1016/j.quascirev.2009.09.014

Greenwood, S.L., Clason, C.C., Nyberg, J., Jakobsson, M. & Holmlund, P. (2017) The Bothnian Sea ice stream: Early Holocene retreat dynamics of the south-central Fennoscandian ice sheet. *Boreas*, 46(2), 346–362. Available from: https://doi.org/10.1111/bor.12217

Greenwood, S.L., Simkins, L.M., Halberstadt, A.R.W., Prothro, L.O. & Anderson, J.B. (2018) Holocene reconfiguration and readvance of the East Antarctic Ice Sheet. *Nature Communications*, 9(1), 1–12. Available from: https://doi.org/10.1038/s41467-018-05625-3

Hubbard, A., Sugden, J., Dugmore, A., Norðdahl, H. & Pétursson, H.G. (2006) A modelling insight into the Icelandic late glacial maximum ice sheet. *Quaternary Science Reviews*, 25(17–18), 2283–2296. Available from: https://doi.org/10.1016/j.quascirev.2006.04.001

Ingólfsson, Ó., Benediktsson, Í.Ö., Schomacker, A., Kjær, K.H., Brynjólfsson, S., Jónsson, S.A., et al. (2016) Glacial geological studies of surge-type glaciers in Iceland—Research status and future challenges. *Earth-Science Reviews*, 152, 37–69. Available from: https://doi.org/10.1016/j.earscirev.2015.11.008

Ingólfsson, Ó. & Norðdahl, H. (2001) High relative sea-level during the Bølling interstadial in W Iceland: A reflection of ice-sheet collapse and extremely rapid glacial unloading. *Arctic, Antarctic, and Alpine Research*, 33(2), 231–243. Available from: https://doi.org/10.1080/15230430.2001.12003426

Jóhannesson, H. & Sæmundsson, K. (2009) *Geological map of Iceland. 1: 500.000. Bedrock*, 1st edition. Reykjavík: Icelandic Institute of Natural History.

Kamb, B. (2001) Basal zone of the West Antarctic ice streams and its role in lubrication of their rapid motion. *The West Antarctic Ice Sheet: Behavior and Environment*, 77, 157–199. Available from: https://doi.org/10.1029/AR077p0157

Kamb, B., Raymond, C.F., Harrison, W.D., Engelhardt, H., Echelmeyer, K.A., Humphrey, N., et al. (1985) Glacier surge mechanism: 1982-1983 surge of variegated glacier, Alaska. *Science*, 227(4686), 1982–1983. https://doi.org/10.1126/science.227.4686.469

Kjær, K.H., Korsgaard, N.J. & Schomacker, A. (2008) Impact of multiple glacier surges—A geomorphological map from Brúarjökull, East Iceland. *Journal of Maps*, 4(1), 5–20. Available from: https://doi.org/10.4113/jom.2008.91

Kjær, K.H. & Krüger, J. (1998) Does clast size influence fabric strength? *Journal of Sedimentary Research*, 68(5), 746–749. Available from: https://doi.org/10.2110/jsr.68.746

Klages, J.P., Kuhn, G., Graham, A.G., Hillenbrand, C.D., Smith, J.A., Nitsche, F.O., et al. (2015) Palaeo-ice stream pathways and retreat style in the easternmost Amundsen Sea embayment, West Antarctica, revealed by combined multibeam bathymetric and seismic data. *Geomorphology*, 245, 207–222. Available from: https://doi.org/10.1016/j.geomorph.2015.05.020

Klages, J.P., Kuhn, G., Hillenbrand, C.D., Graham, A.G.C., Smith, J.A., Larter, R.D., et al. (2013) First geomorphological record and glacial history of an inter-ice stream ridge on the West Antarctic continental shelf. *Quaternary Science Reviews*, 61, 47–61. Available from: https://doi.org/10.1016/j.quascirev.2012.11.007

Krüger, J. & Kjær, K.H. (1999) A data chart for field description and genetic interpretation of glacial diamicts and associated sediments—With examples from Greenland, Iceland, and Denmark. *Boreas*, 28(3), 386–402. Available from: https://doi.org/10.1111/j.1502-3885.1999.tb00228.x

Kurjanski, B., Rea, B.R., Spagnolo, M., Winsborrow, M., Cornwell, D.G., Andreassen, K., et al. (2019) Morphological evidence for marine ice stream shutdown, Central Barents Sea. *Marine Geology*, 414, 64–76. Available from: https://doi.org/10.1016/j.margeo.2019.05.001

Lamsters, K., Vītola, Z., Karušs, J. & Džeriņš, P. (2021) Evidence of ice streaming and ice tongue shutdown in western Latvia: Revealed from the mapping of crevasse-squeeze ridges. *Baltica*, 33(1), 1–16. Available from: https://doi.org/10.5200/baltica.2021.1.1

Lawson, D.E. (1979) A comparison of the pebble orientations in ice and deposits of the Matanuska glacier, Alaska. *The Journal of Geology*, 87(6), 629–645. Available from: https://doi.org/10.1086/628457

Lindén, M. & Möller, P. (2005) Marginal formation of De Geer moraines and their implications to the dynamics of grounding-line recession. *Journal of Quaternary Science*, 20(2), 113–133. Available from: https://doi.org/10.1002/jqs.902

Livingstone, S.J., Cofaigh, C.Ó., Stokes, C.R., Hillenbrand, C., Vieli, A. & Jamieson, S.S.R. (2012) Antarctic palaeo-ice streams. *Earth-Science Reviews*, 111(1–2), 90–128. Available from: https://doi.org/10.1016/j.earscirev.2011.10.003

Lovell, H., Fleming, E.J., Benn, D.I., Hubbard, B., Lukas, S., Rea, B.R., et al. (2015) Debris entrainment and landform genesis during tidewater glacier surges. *Journal of Geophysical Research - Earth Surface*, 120(8), 1574–1595. Available from: https://doi.org/10.1002/2015JF003509

Margold, M., Stokes, C.R. & Clark, C.D. (2015) Ice streams in the Laurentide ice sheet: Identification, characteristics and comparison to modern ice sheets. *Earth-Science Reviews*, 143, 117–146. Available from: https://doi.org/10.1016/j.earscirev.2015.01.011

Napieralski, J. & Nalepa, N. (2010) The application of control charts to determine the effect of grid cell size on landform morphometry. *Computers & Geosciences*, 36(2), 222–230. Available from: https://doi.org/10.1016/j.cageo.2009.06.003

Newton, A.M. & Huuse, M. (2017) Glacial geomorphology of the Central Barents Sea: Implications for the dynamic deglaciation of the Barents Sea ice sheet. *Marine Geology*, 387, 114–131. Available from: https://doi.org/10.1016/j.margeo.2017.04.001

Norðdahl, H. & Hjort, C. (1993) Lateglacial raised beaches and glacier recession in the Þistilfjörður-Bakkaflói area. *Jökull*, 43(1), 32–44. Available from: https://doi.org/10.33799/jokull1993.43.033

Norðdahl, H. & Ingólfsson, Ó. (2015) Collapse of the Icelandic ice sheet controlled by sea-level rise? *Arktos*, 1(1), 13. Available from: https://doi.org/10.1007/s41063-015-0020-x

Norðdahl, H., Ingólfsson, Ó., Pétursson, H.G. & Hallsdóttir, M. (2008) Late Weichselian and Holocene environmental history of Iceland. *Jökull*, 58(1), 343–364. Available from: https://doi.org/10.33799/jokull2008.58.343

Norðdahl, H., Ingólfsson, Ó., Vogler, E.D., Steingrímsson, B.Ó. & Hjartarson, Á. (2019) Glacio-isostatic age modelling and late Weichselian deglaciation of the Lögurinn basin, East Iceland. *Boreas*, 48(3), 563–580. Available from: https://doi.org/10.1111/bor.12366

Norðdahl, H. & Pétursson, H.G. (2005) Relative sea-level changes in Iceland. New aspects of the Weichselian deglaciation of Iceland. In: Caseldine, C., Russel, A., Harðardóttir, J. & Knudsen, Ó. (Eds.) *Iceland – modern processes and past environments*. Amsterdam: Elsevier, pp. 25–78 https://doi.org/10.1016/S1571-0866(05)80005-3

Öhrling, C., Peterson, G. & Johnson, M.D. (2020) Glacial geomorphology between Lake Vänern and Lake Vättern, southern Sweden. *Journal of Maps*, 16(2), 776–789. Available from: https://doi.org/10.1080/17445647.2020.1820386

Ottesen, D. & Dowdeswell, J.A. (2006) Assemblages of submarine landforms produced by tidewater glaciers in Svalbard. *Journal of Geophysical Research*, 111(F1), 1–16. Available from: https://doi.org/10.1029/2005JF000330

Ottesen, D., Dowdeswell, J.A., Benn, D.I., Kristensen, L., Christiansen, H.H., Christensen, O., et al. (2008) Submarine landforms characteristic of glacier surges in two Spitsbergen fjords. *Quaternary Science Reviews*, 27(15–16), 1583–1599. Available from: https://doi.org/10.1016/j.quascirev.2008.05.007

Patton, H., Hubbard, A., Bradwell, T. & Schomacker, A. (2017) The configuration, sensitivity and rapid retreat of the late Weichselian Icelandic ice sheet. *Earth-Science Reviews*, 166, 223–245. Available from: https://doi.org/10.1016/j.earscirev.2017.02.001

Phillips, E., Spagnolo, M., Pilmer, A.C., Rea, B.R., Piotrowski, J.A., Ely, J.C., et al. (2018) Progressive ductile shearing during till accretion within the deforming bed of a palaeo-ice stream. *Quaternary Science Reviews*, 193, 1–23. Available from: https://doi.org/10.1016/j.quascirev.2018.06.009

Porter, C., Morin, P., Howat, I., Noh, M.J., Bates, B., Peterman, K., et al. (2018) "ArcticDEM", Harvard Dataverse, V1. Available from: https://doi.org/10.7910/DVN/OHHUKH

Powers, M.C. (1953) A new roundness scale for sedimentary particles. *Journal of Sedimentary Research*, 23(2), 117–119.

Principato, S.M., Moyer, A.N., Hampsch, A.G. & Ipsen, H.A. (2016) Using GIS and streamlined landforms to interpret palaeo-ice flow in northern Iceland. *Boreas*, 45(3), 470–482. Available from: https://doi.org/10.1111/bor.12164

Rea, B.R. & Evans, D.J.A. (2011) An assessment of surge-induced crevassing and the formation of crevasse squeeze ridges. *Journal of Geophysical Research - Earth Surface*, 116(F4), F04005. Available from: https://doi.org/10.1029/2011JF001970

Robel, A.A. & Tziperman, E. (2016) The role of ice stream dynamics in deglaciation. *Journal of Geophysical Research - Earth Surface*, 121(8), 1540–1554. Available from: https://doi.org/10.1002/2016JF003937

Sæmundsson, K. (1977) *Geological map of Iceland, sheet 7, NE-Iceland. 1: 250.000*. Reykjavik: Icelandic Institute of Natural History and National Land Survey of Iceland.

Schomacker, A., Benediktsson, Í.Ö. & Ingólfsson, Ó. (2014) The Eyjabakkajökull glacial landsystem, Iceland: Geomorphic impact of multiple surges. *Geomorphology*, 218, 98–107. Available from: https://doi.org/10.1016/j.geomorph.2013.07.005

Sharp, M. (1985) "Crevasse-fill" ridges-a landform type characteristic of surging glaciers? *Geografisker Annaler, Series a, Physical Geography*, 67(3–4), 213–220. Available from: https://doi.org/10.1080/04353676.1985.11880147

Sharp, M. (1988) Surging glaciers: Geomorphic effects. *Progress in Physical Geography*, 12(4), 533–559. Available from: https://doi.org/10.1177/030913338801200403

Sigfúsdóttir, T. & Benediktsson, Í.Ö. (2020) Refining the history of younger Dryas and Early Holocene glacier oscillations in the Borgarfjörður region, western Iceland. *Boreas*, 49(2), 296–314. Available from: https://doi.org/10.1111/bor.12424

Smith, A.M., Anker, P.G.F., Nicholls, K.W., Makinson, K., Murray, T., Rios-Costas, S., et al. (2021) Ice stream subglacial access for ice-sheet history and fast ice flow: The BEAMISH project on Rutford ice stream, West Antarctica and initial results on basal conditions. *Annals of Glaciology*, 62(85–86), 203–211. Available from: https://doi.org/10.1017/aog.2020.82

Sobota, I., Weckwerth, P. & Nowak, M. (2016) Surge dynamics of Aavatsmarkbreen, Svalbard, inferred from the geomorphological record. *Boreas*, 45(2), 360–376. Available from: https://doi.org/10.1111/bor.12160

Spagnolo, M. & Clark, C.D. (2009) A geomorphological overview of glacial landforms on the Icelandic continental shelf. *Journal of Maps*, 2009(1), 37–52. Available from: https://doi.org/10.4113/jom.2009.1049

Spagnolo, M., Clark, C.D. & Hughes, A.L. (2012) Drumlin relief. *Geomorphology*, 153, 179–191. Available from: https://doi.org/10.1016/j.geomorph.2012.02.023

Stokes, C.R. (2018) Geomorphology under ice streams: Moving from form to process. *Earth Surface Processes and Landforms*, 43(1), 85–123. Available from: https://doi.org/10.1002/esp.4259

Stokes, C.R. & Clark, C.D. (1999) Geomorphological criteria for identifying Pleistocene ice streams. *Annals of Glaciology*, 28, 67–74. Available from: https://doi.org/10.3189/172756499781821625

Stokes, C.R. & Clark, C.D. (2001) Palaeo-ice streams. *Quaternary Science Reviews*, 20(13), 1437–1457. Available from: https://doi.org/10.1016/S0277-3791(01)00003-8

Stokes, C.R., Corner, G.D., Winsborrow, M.C., Husum, K. & Andreassen, K. (2014) Asynchronous response of marine-terminating outlet glaciers during deglaciation of the Fennoscandian ice sheet. *Geology*, 42(5), 455–458. Available from: https://doi.org/10.1130/G35299.1

Stokes, C.R., Margold, M., Clark, C.D. & Tarasov, L. (2016) Ice stream activity scaled to ice sheet volume during Laurentide ice sheet deglaciation. *Nature*, 530(7590), 322–326. Available from: https://doi.org/10.1038/nature16947

Sutherland, J.L., Carrivick, J.L., Evans, D.J., Shulmeister, J. & Quincey, D.J. (2019) The Tekapo glacier, New Zealand, during the last glacial maximum: An active temperate glacier influenced by intermittent surge activity. *Geomorphology*, 343, 183–210. Available from: https://doi.org/10.1016/j.geomorph.2019.07.008

van der Veen, C.J. (1998) Fracture mechanics approach to penetration of bottom crevasses on glaciers. *Cold Regions Science and Technology*, 27(3), 213–223. Available from: https://doi.org/10.1016/S0165-232X(98)00006-8

Waller, R.I., Van Dijk, T.A. & Knudsen, O. (2008) Subglacial bedforms and conditions associated with the 1991 surge of Skeiðarárjökull, Iceland. *Boreas*, 37(2), 179–194. Available from: https://doi.org/10.1111/j.1502-3885.2007.00017.x

Gadd, H.G. (2016) The formation of a rectiliniear ridge network, Múlajökull, Iceland. Master's thesis, Department of Geological and Atmospheric Sciences, Iowa State University, 79 p. Available from: https://www.proquest.com/docview/1808501314?pq-origsite=gscholar&fromopenview=true

SUPPORTING INFORMATION

Additional supporting information can be found online in the Supporting Information section at the end of this article.

How to cite this article: Aradóttir, N., Benediktsson, Ívar Örn, Ingólfsson, Ó., Brynjólfsson, S., Farnsworth, W.R., Benjamínsdóttir, M.M. et al. (2023) Ice-stream shutdown during deglaciation: Evidence from crevasse-squeeze ridges of the Iceland Ice Sheet. *Earth Surface Processes and Landforms*, 1–19. Available from: https://doi.org/10.1002/esp.5636

Paper IV

Ribbed moraines formed during deglaciation of the Iceland Ice Sheet: Implications for ice-stream dynamics

Nína Aradóttir[1] (nia1@hi.is), Ívar Örn Benediktsson[1] (ivarben@hi.is), Erla Guðný Helgadóttir[1] (erlagudny@gmail.com), Ólafur Ingólfsson[1] (oi@hi.is), Skafti Brynjólfsson[2] (skafti@ni.is), Wesley R. Farnsworth[1] (wesleyf@hi.is)

[1]*Institute of Earth Sciences, University of Iceland, Sturlugata 7, Is-102 Reykjavík*
[2]*Icelandic Institute of Natural History, Borgir við Norðurslóð, 600 Akureyri*

Corresponding author: nia1@hi.is (Nína Aradóttir)

Abstract

Geomorphological fingerprints of palaeo-ice streams are essential for our perception of ice-stream behaviour. Cross-cutting flow-sets of palaeo-ice streams, during and following the Last Glacial Maximum, have been suggested in northeast Iceland based on the mapping of streamlined subglacial bedforms (SSBs). To increase our understanding of the dynamics of the Iceland Ice Sheet (IIS) during deglaciation, we investigate transverse ridges, together with glaciofluvial and ice-marginal landforms, within the Vopnafjörður-Jökuldalsheiði flow-set. The main emphasis is on the transverse ridges, which are primarily interpreted as ribbed moraines - the first to be described in Iceland. Morphological data is combined with sedimentological analyses of the ribbed moraines, which are composed of pre-existing material, often exhibiting a base of stratified glaciofluvial sediments draped with subglacial till. Deformation and thrust structures within both units suggest compressional flow during the formation of the ridges. Ribbed moraines are often considered to form at the transition zone between fast and slow ice flow. Our results agree and we suggest the bedforms develop due to velocity gradients under the lateral shear margin of an ice stream based on their distribution and often oblique orientation in relation to SSBs. The ribbed moraines superimpose and thus post-date the SSBs, signifying the waning stage of ice streaming. Correlating the formation of the ribbed moraines with the known glacial history in this region we suppose that the ridges formed during ice-stream shutdown following the YD readvance. Eskers are superimposed on ribbed moraines and frequently terminate at ice-marginal positions on Jökuldalsheiði, implying channelized water drainage during the deglaciation and an active retreat interrupted by short-lived readvances. This study has implications for the style of deglaciation associated with ice streaming in the northeastern part of the IIS. We characterize the role of ribbed moraines within the ice sheet and identify directions for future work.

Keywords: Ribbed moraines; Eskers; Subglacial bedforms; Ice-sheet dynamics; Deglaciation; Iceland Ice Sheet

Manuscript submitted to *Boreas special issue.*

1. Introduction

Ice streams are dynamic constituents of ice sheets that have a substantial effect on their stability and mass balance through the release of ice and sediments. The mechanism controlling their fast flow is complex but is partly governed by processes occurring at the ice-bed interface (e.g. Bennett, 2003; Alley et al., 2004; Stokes et al., 2007). As a result of these processes, distinct and variable subglacial bedforms are formed at the ice-stream bed. After deglaciation, these bedforms can be mapped and used to reconstruct the behaviour of palaeo-ice streams (e.g. Stokes and Clark, 1999, 2001; Bingham et al., 2017). Owing to the complexity of directly monitoring processes operating under ice sheets and ice streams (Kamb, 2001; Bennett, 2003; Smith et al., 2021), glacial geomorphology is essential for our understanding of processes occurring at the ice-bed interface and for palaeoglaciological reconstructions (Livingstone et al., 2012; Stokes, 2018).

Ribbed moraines, also termed Rogen moraines, subglacial ribs, or traction ribs, are clusters of subglacial ridges, formed transverse or oblique to ice flow, often occurring as elongated tracts. They have been considered typical for the core areas of former ice sheets but also occur within the trunk-flow zones of ice streams and in the marginal settings (Lundqvist, 1969, 1989; Aylsworth and Shilts, 1989; Dunlop and Clark, 2006), both related to the ice-stream onset zones and the waning stages of ice streaming (e.g. Dyke et al., 1992; Stokes et al., 2006, 2008). Originally, it was suggested that ribbed moraines formed at the ice margin, explaining their naming (Frödin, 1954; Cowan, 1968), but increased research indicates subglacial origin (e.g. Lundqvist, 1969, Bouchard, 1989; Hättestrand and Kleman, 1999; Vérité et al., 2021). Typically, ribbed moraines are described as closely spaced, straight, or arcuate ridges, transverse to former ice flow (Hättestrand and Kleman, 1999). However, their morphological characteristics can vary significantly, both between and within areas, thus being more complex than previously thought (see Dunlop and Clark, 2006). Their internal composition is also highly variable, ranging from different types of tills to fluvial sediments but they tend to be composed of similar material as found in the surrounding areas. Glaciotectonic structures are common but not always present (e.g. Bouchard, 1989; Hättestrand, 1997; Lundqvist, 1997; Möller, 2006). Drumlins often occur in proximity to ribbed moraines and examples of both ribbed moraines that have undergone drumlinisation and 'ribbed' drumlins are common (e.g. Lundqvist, 1989; Dunlop and Clark, 2006).

The wide range of composition and morphological characteristics has led to several hypotheses of their formation without consensus on whether their formation can be explained by a unifying theory or not (Hättestrand and Kleman, 1999; Dunlop et al., 2008; Chapwanya et al., 2011; Möller and Dowling, 2018). The most prevalent theories invoke fracturing and extension of frozen beds related to extensional stress at transition from warm- to cold-based ice (Hätterstrand, 1997; Hättestrand and Kleman, 1999; Sarala, 2006), modification of pre-existing sediments by overriding ice (Boulton, 1987; Lundqvist, 1989; Möller, 2006), subglacial outburst floods (Fisher and Shaw, 1992) or deformation related to shearing and stacking of subglacial till (Bouchard, 1989; Lindén et al., 2008; Stokes et al., 2008). Those in support of monogenetic origin tend to favor the instability theory for subglacial bedforms, which argues that ribbed moraines are formed by the natural instability formed in the coupled flow of ice and till (e.g. Dunlop et al., 2008; Chapwanya et al., 2011; Fowler and Chapwanya, 2014; Ely et al., 2022). Consequently, correlating ice sheet dynamics

to the formation of ribbed moraines can be challenging due to contradicting hypotheses (Hättestrand and Kleman, 1999). A better comprehension of the formation of ribbed moraines is therefore of utmost significance to increase our insight into ice dynamics (Stokes, 2018).

Ice-stream behaviour within the Icelandic Ice Sheet (IIS) has been reconstructed based on numerical modelling (Bourgeois et al., 2000; Hubbard et al., 2006; Patton et al., 2017), large-scale geomorphology and mapping of certain glacial landforms (e.g. Norðdahl and Pétursson, 2005; Spagnolo and Clark, 2009; Principato et al., 2016; Norðdahl et al., 2019; Benediktsson et al., 2022a). In northeast Iceland, during the Last Glacial Maximum (LGM) and the subsequent deglaciation, mapping of subglacial landforms indicates cross-cutting palaeo-ice streams and ice-stream shutdown during deglaciation (Fig. 1A, B; Benediktsson et al., 2022b; Aradóttir et al., 2023a). Here we continue expanding our knowledge on the ice-stream dynamics during deglaciation of the IIS in northeast Iceland by investigating glacial landforms within the Vopnafjörður-Jökuldalsheiði flow-set with main emphasis on transverse ridges. We present detailed mapping, morphological and spatial analyses on all transverse ridges, and sedimentological investigations of the ridges on Hauksstaðaheiði within the flow-set. The ridges on Hauksstaðaheiði and Jökuldalsheiði are interpreted as ribbed moraines – the first to be described in Iceland. Therefore, the role of ribbed moraines within the IIS has been unknown, highlighting the motivation for this study.

2. Study area

The study area is located within the Vopnafjörður fjord-valley system in northeast Iceland and can be divided into three subareas; the highland plateaus of Jökuldalsheiði and Hauksstaðaheiði, and the Selárdalur valley and its surroundings (Fig. 1B, C). A vast highland plateau, situated mostly between 450 and 600 m a.s.l., extends from the northeast-trending valley, Hofsárdalur, far into the highland interior (Fig. 2A). Most of the plateau is termed Jökuldalsheiði and for simplicity, we use that for the whole plateau. The Hauksstaðaheiði plateau is situated between the Dimmifjallgarður mountain range, Bustarfell drumlin field, Selá river, and Selárdalur and Vesturárdalur valleys. The plateau is relatively flat with elevation ranging between 350-550 m a.s.l., that gradually extends down to sea level in the narrow, northeast-trending valleys of Selárdalur and Vesturárdalur, separated by the Vesturdalsháls ridge (Figs 3A and 4A). Heath- and peatlands characterize the study area and highland lakes are present on both plateaus (Figs 2-4, 6). The Jökuldalsheiði and Hauksstaðaheiði bedrocks consist primarily of basalt lavas (3.3-0.8 million years old) with intercalated sediments and glacially sculptured hyaloclastite ridges. Closer to the coast in Selárdalur, the age of the basalt lavas increases (>3.3 million years old). The mountain range to the west of the area consists of younger hyaloclastite ridges and interglacial basalt lavas with intercalated sediments (<0.8 million years old) (Sæmundsson, 1977; Jóhannesson and Sæmundsson, 2009).

Within the Vopnafjörður-Jökuldalsheiði flow-set, palaeo-ice streams have been reconstructed from the mapping of over 300 streamlined subglacial bedforms (SSBs; drumlins and mega-scale glacial lineations (MSGLs)). The SSBs have a converging pattern with variable orientation in the highlands that align towards the northeast in the central part, parallel to the Vopnafjörður fjord and valley (Fig. 1B, C; Benediktsson et al., 2022b). Most of the drumlins in proximity to the study area are considered to be of sedimentary origin (Benediktsson et al., 2022b; Aradóttir et al., 2023b). The Bustarfell drumlin field is located on a plateau between

Jökuldalsheiði and Hauksstaðaheiði, consisting of well-defined sedimentary drumlins with consistent shapes and sizes and composed of a core of deformed glaciofluvial sediments draped with till (Fig. 1B, C; Aradóttir et al., 2023b). The ribbed moraines on Hauksstaðaheiði were previously investigated by Helgadóttir (2020) and her findings are synthesized in this study.

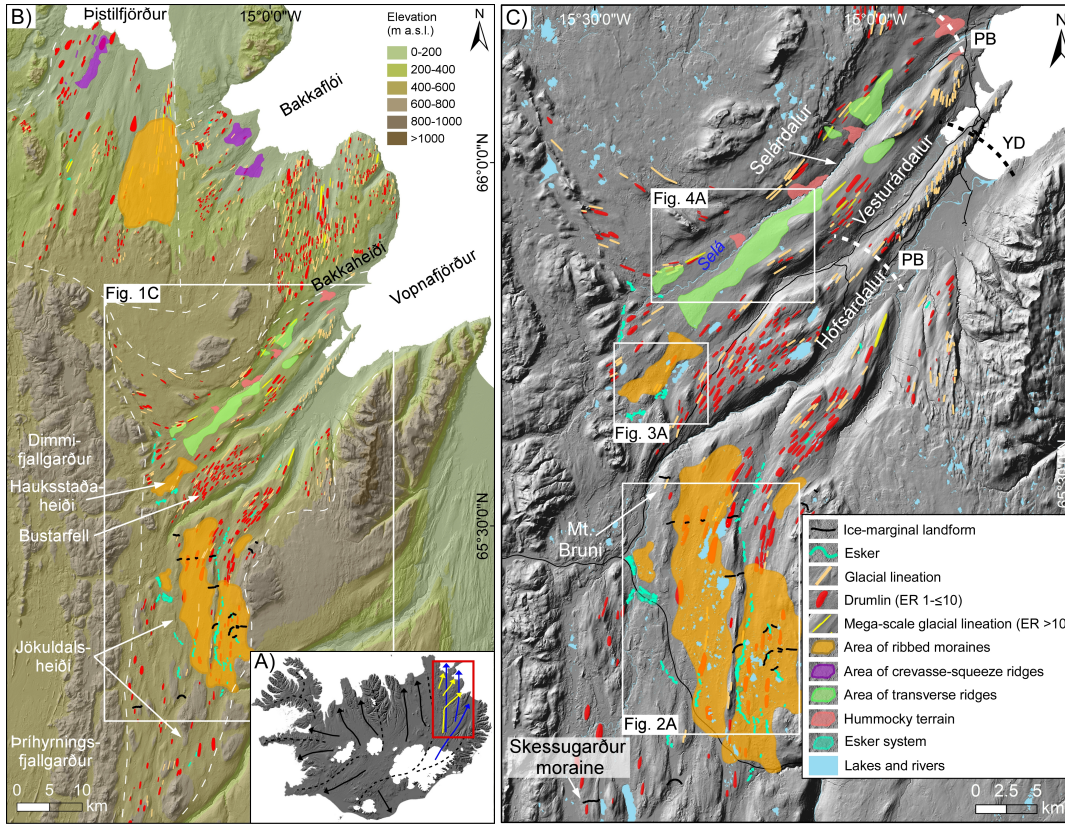

Figure 1. A) Major ice streams of the Iceland Ice Sheet represented by arrows (Bourgeois et al., 2000; Stokes and Clark, 2001; Principato et al., 2016; Benediktsson et al., 2022b). Fig. 1B is outlined in red. Within the red box the blue arrows indicate an older generation of ice flow during maximum glaciation while the yellow arrows represent a younger generation of flow during deglaciation (Benediktsson et al., 2022b). B) Geomorphological map of northeastern Iceland (modified from Benediktsson et al., 2022b and Aradóttir et al., 2023a). The white dashed lines indicate boundaries between three ice-stream flow-sets; 1) Vopnafjörður-Jökuldalsheiði, 2) Bakkaheiði, and 3) Bakkaflói and Þistilfjörður. The study area is located within the white box (Fig. 1C). C) Geomorphological map of the Vopnafjörður-Jökuldalsheiði flow-set. Ice-marginal positions during the Younger Dryas (YD) and Preboreal (PB) are indicated based on Sæmundsson (1995) together with a post-PB stillstand near Mt. Bruni. Place names referred to in the text are marked and the main roads are indicated with a black line. The map legend applies to Fig. 1B, C.

During the LGM the IIS reached its maximum extent, probably extending to the shelf edge, followed by a deglaciation of the marine sector from around 21.8 ka BP (e.g. Norðdahl and Pétursson, 2005; Norðdahl and Ingólfsson, 2015; Benediktsson et al., 2022a, 2023a). Chronological constraints on the deglaciation of the IIS in northeast Iceland are minimal but the abrupt warming during the Bølling-Allerød Interstadial (14.7-14.1 cal. ka BP) caused the collapse of the ice sheet offshore. How far inland the ice sheet retreated is unknown (Ingólfsson and Norðdahl, 2001; Norðdahl and Ingólfsson, 2015; Benediktsson et al., 2023b). Following the deglaciation during the Late Glacial or the Younger Dryas period (YD; 12.9-11.7 cal. ka BP), the IIS began to re-expand (Benediktsson et al., 2023c). The ice margin is considered to have reached the coast in Vopnafjörður based on truncated raised shorelines (Sæmundsson, 1995). Another readvance of the IIS occurred following the termination of the YD period during the Preboreal period (PB; 11.3-10.4 cal. ka BP) in the Early Holocene (Benediktsson et al., 2024a). Ice-marginal deltas in the Vesturárdalur and Hofsárdalur, northeast of Bustarfell, have been associated with that readvance. In Selárdalur, the ice margin during the PB period is suggested to have terminated at the outermost hummocky moraine close to the mouth of the valley (Fig. 1C). Consequently, the ice margin during the YD period is considered to have terminated further out based on correlations of raised shorelines, although no evidence for that has been observed (Sæmundsson, 1995). Several ice-marginal landforms have been mapped inside the suggested PB position and two of them are mapped in Fig. 1C. One is located near Mt. Bruni on the northwestern part of Jökuldalsheiði, just up-ice from the Bustarfell drumlin field (Sæmundsson, 1995) and the Skessugarður end moraine, a prominent ridge consisting solely of 1-3 m high boulders, is located on Jökuldalsheiði southwest of the study area (Aðalsteinsson, 1985, 1987). The latter is part of an ongoing project constraining the deglaciation history in the area from the coast of Vopnafjörður to near the northern margin of Vatnajökull (Benediktsson et al., 2024b).

3. Methods

3.1 Geomorphological mapping

The geomorphological mapping was based on the Arctic digital elevation model (ArcticDEM) with a 2 m vertical and <1 m horizontal resolution (Porter et al., 2018; corrected and mosaicked by the National Land Survey of Iceland (NLSI), the Icelandic Met Office, and the Polar Geospatial Center). Mapping was aided by infrared Spot satellite images with 2.5 m resolution from NLSI and aerial images from Loftmyndir ehf. The geomorphological mapping was done by the combination of fieldwork and remote sensing. Analysis of the data and mapping was conducted in ESRI ArcGIS 10.5-8 and finalized in Canvas X. The transverse ridges (e.g. ribbed moraines), eskers and ice-marginal positions were mapped, with the main emphasis on transverse ridges (i.e. 1:3000). The mapping of SSBs and CSRs was conducted by Benediktsson et al. (2022b) and Aradóttir et al. (2023a) respectively.

3.2 Morphological and spatial analyses

When investigating the morphology of the ribbed moraines and other transverse ridges, characteristics listed in Dunlop and Clark (2006) such as shape, dimensions, spacing, and relation between the ridges and other bedforms, were taken into consideration. The length of the long axis, the width orthogonal to the long axis, and the orientation of the long axis were measured using the minimum bounding geometry tool in ArcGIS, as described by

Napieralski and Nalepa (2010). The ridge prominence and their symmetry were examined with the 3D profile tool in ArcGIS and the spacing between the ridges was measured using the average nearest neighbor tool in ArcGIS. To calculate the density of the ridges a point was created in the center of each bedform and the number of ridges within each km^2 grid cell was calculated. In addition, qualitative descriptions of the ribbed moraines and other transverse ridges and mapped bedforms are presented.

3.3 Sedimentology

Natural sections exposing the sediments in the ribbed moraines were documented at a scale of 1:20, using the data chart by Krüger and Kjær (1999) for glacial sediments, and the strike and dip of beds/structures were measured. To examine the clast morphology, a minimum of fifty clasts with an a-axis between 1.5 and 10 cm, were collected from a 25x25 cm surface. The a (long)-, b (intermediate)- and c (short)-axis were measured (Evans and Benn, 2004) and plotted in a ternary diagram. In addition, the roundness and texture of the clast were estimated (Powers, 1953; Evans and Benn, 2004). The clast morphology and roundness are displayed with C_{40} index (percentage of clasts with c:a axis ratio ≤0.4) and RA index (percentage of angular and very angular clasts) (Benn and Ballantyne, 1993). The sections and additional data were illustrated in Canvas X.

4. Results

The geomorphology of the three subareas, Jökuldalsheiði, Hauksstaðaheiði, and Selárdalur (Figs 1C, 2-4), is described separately with emphasis on the ribbed moraines and other transverse ridges and their surface and cross-cutting relationship with other landforms. Additionally, the sedimentology of the ridges on Hauksstaðaheiði is described.

4.1 Morphology

Jökuldalsheiði

On Jökuldalsheiði, 962 ridge segments were mapped. Their distribution is mostly confined to two flatter areas that are over 20 km long and 5 km wide, orientated south-north, at an elevation from 430 to 660 m a.s.l. They are separated by south-north trending hyaloclastite mountains that are glacially sculptured. The ridges are generally broad, although arcuate ridges also occur and examples of ridges with hummocky appearance are observed in the northwest part of the area. The ridges do though have a fragmented appearance, making them challenging to map (Fig. 2A). Their median length is 127 m with a range of 28 - 657 m, median width is 64 m with a range of 17 - 282 m, and median elongation ratio is 2.0:1 with a range of 1.1:1 - 4.4:1. Further information on the morphology is listed in Fig. 5 and Table 1. The relief of the ridges varies between 0.5 - 15 m, although they are generally between 0.5 - 5 m high and their cross profile appears to be both symmetrical and asymmetrical, generally with a curved crest (Fig. 2C). The median orientation of the ridges is east to west (93° - 273°), or generally transverse or oblique to the mapped SSBs. In the distal part of the area, the ridges are orientated more towards northwest-southeast, which corresponds to changes in the orientation of the SSBs with a more constant southwest-northeast orientation, parallel to the trend of the fjord-valley (Fig. 2A; Table 1). The mean density of ridges is 0.4 ridges per km^2 with a maximum density of 32 ridges per km^2 (Table 1). The highest density of the ridges

occurs in the northwestern part of the area where they are generally smaller in size than the median values (Fig. 2A). Due to the fragmented nature of the ridges, it is difficult to calculate the crest spacing between them but by visual observation, their crest spacing is not considered systematic. Large boulders, up to 3 m in diameter, are common on the surface of the ridges. The boulders are generally blocky and angular to subangular. They are not evenly distributed but appear in clusters, both on the ridges and between them (Fig. 6A, B).

The drumlins in the area are occasionally broken up into transverse ridges and somewhat chaotic transverse ridge fields. Transverse channels, both active and inactive, frequently dissect the drumlins, which might explain some of the segmented drumlins (Figs 2B and 6A). The ridges occasionally occur superimposed on drumlins or in connection with them, especially in the distal part of the area (Fig. 6B). Sinuous and straight ridges made of sorted sediments, with rounded crests that are generally parallel to the SSBs are frequent in the area (Figs 2A, B and 6A). They are interpreted as eskers and usually occur as single ridges but esker systems are also present. Investigations from several gravel pits along the ring road in the southern part of the area reveal that the eskers consist of gravel and sand, recorded up to 5 m in thickness. Usually, the gravel overlies the sand, and horizontal layering was observed in some of the pits (The Icelandic Road and Coastal Administration, 2023). At the eastern side of the hyaloclastite mountains, there are esker segments that are aligned in a row and together they are over 30 km long. At the southwestern margin of the area is a sharp boundary where the ridges abruptly terminate. This boundary coincides with a gentle depression and the river Hárekssta̧akvísl, followed by a slight rise in the elevation up to higher plateaus. In the depression are inactive outwash plains and channels together with esker segments and esker systems. The eskers follow the topography and are orientated parallel to the depression and the present-day river, or towards the northwest to north-northwest (Fig. 2A). Examples of eskers that transform into inactive channels are found in the southwestern part of the area. The eskers occur superimposed on the ridges but large boulders that are frequently on the ridges are never found on top of the eskers (Figs 2A, B and 6A).

Between the two suggested ice-marginal positions of Early Holocene age within the area (Fig. 1C; Aðalsteinsson, 1985, 1987; Sæmundsson, 1995), four additional ice-marginal positions are suggested. They constitute of ridges that are generally more prominent and straighter than the ridges described above, with an asymmetrical cross profile and steeper proximal sides. Inactive channels are often found in connection with the ridges and the eskers sometimes terminate at them. Their surface consists of unsorted sediments and large and angular boulders are also present on them, similar to the ridges described above (Figs 2A-C and 6A). Based on that together with their lateral correlation across the area, the ridges are interpreted as moraines. The distance between the inferred ice-marginal positions ranges from ~1.5 up to 10 km.

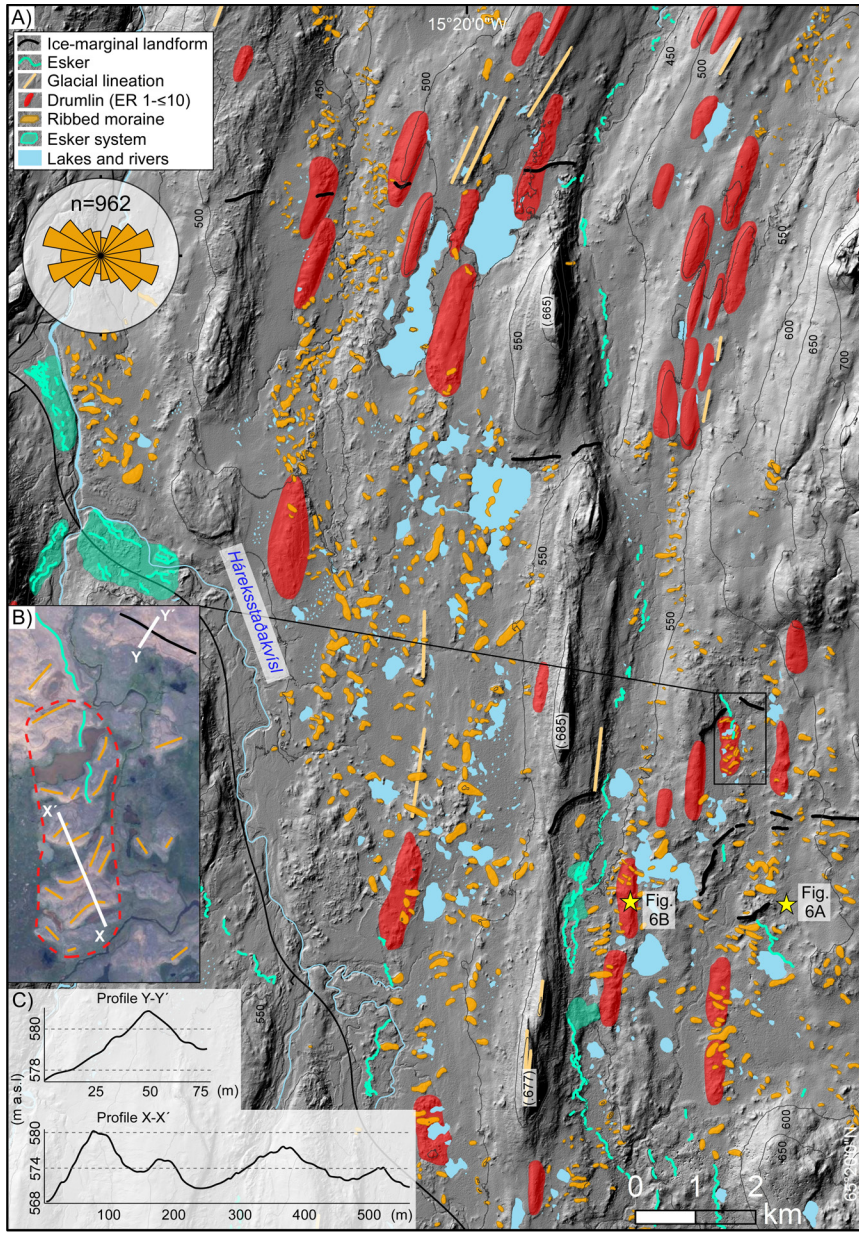

Figure 2. A) Map of glacial landforms on Jökuldalsheiði. The rose diagram shows the orientation of the mapped 962 ribbed moraines (median 93° - 273°). The stars mark the locations where Figs. 6A and B are taken. Contour intervals are 50 m. B) Aerial image of a 'ribbed' drumlin with a superimposed esker. The straight ridge on its distal side is interpreted as an ice-marginal moraine. C) Two terrain cross profiles that are marked in Fig. 2B. The ridges interpreted as ribbed moraines are usually between 0.5 - 5 m in relief with both symmetrical and asymmetrical cross profiles and curved crests. In contrast, the ridge interpreted as an ice-marginal moraine has an asymmetrical cross profile with a steeper proximal side.

Hauksstaðaheiði

On Hauksstaðaheiði, 229 ridge segments were mapped where their distribution is mostly confined within a southwest-northeast shallow basin, Leirvatnskvos, and adjacent hills, at an elevation from 415 to 515 m a.s.l. (Fig. 3A). The ridges are generally broad arcuate or rectangular, but examples of anastomosing ridges also occur (Figs 3A and 6C, D). Their median length is 105 m with a range of 32 - 539 m and the median width is 57 m with a range of 23 - 156 m. Their median elongation ratio is 1.9:1 with a range from 1.0 - 6.1:1 (Fig. 5; Table 1). The relief of the ridges varies between 0.5 - 10 m with generally higher segments in the proximal part of the basin and their cross profile appears to be both symmetrical and asymmetrical (with both steeper distal and proximal sides), generally with a curved crest (Fig. 3B). The median orientation of the ridges is south-southeast to north-northwest (114° - 294°), or generally transverse or oblique to the mapped SSBs. The ridges in the upper part of the basin have a more profound transverse orientation as well as a higher elongation ratio (Fig. 3A; Table 1). The ridges are clustered with an observed average crest-to-crest distance of 115 m, generally increasing down-ice. The mean density of ridges is 2.1 ridges per km^2 with a maximum density of 54 ridges per km^2 (Table 1). Large (up to 2 m in diameter), blocky, and angular to subangular boulders are common on the surface of the ridges, similar to Jökuldalsheiði. The boulders are not evenly distributed and seem to occur in clusters, but only on the ridges (Figs 6A, B and 9A).

The ridges occur superimposed on drumlins and glacial lineations. At the southeastern side of the mapped area, there are examples of ridges that resemble drumlins that have been 'ribbed', similar to Jökuldalsheiði although it is not as prominent (Fig. 3A). Sinuous to straight ridges made of sorted sediments, interpreted as eskers with rounded crests, are observed in two depressions, Skeljungsdalskvos and Möðrudalskvos, southeast of the ridges, and further to the north (Figs 1C and 3A). The direction of the eskers is generally the same as the drumlins in the area (southwest to northeast) or follows the topography. There are no inferred ice-marginal positions within the area.

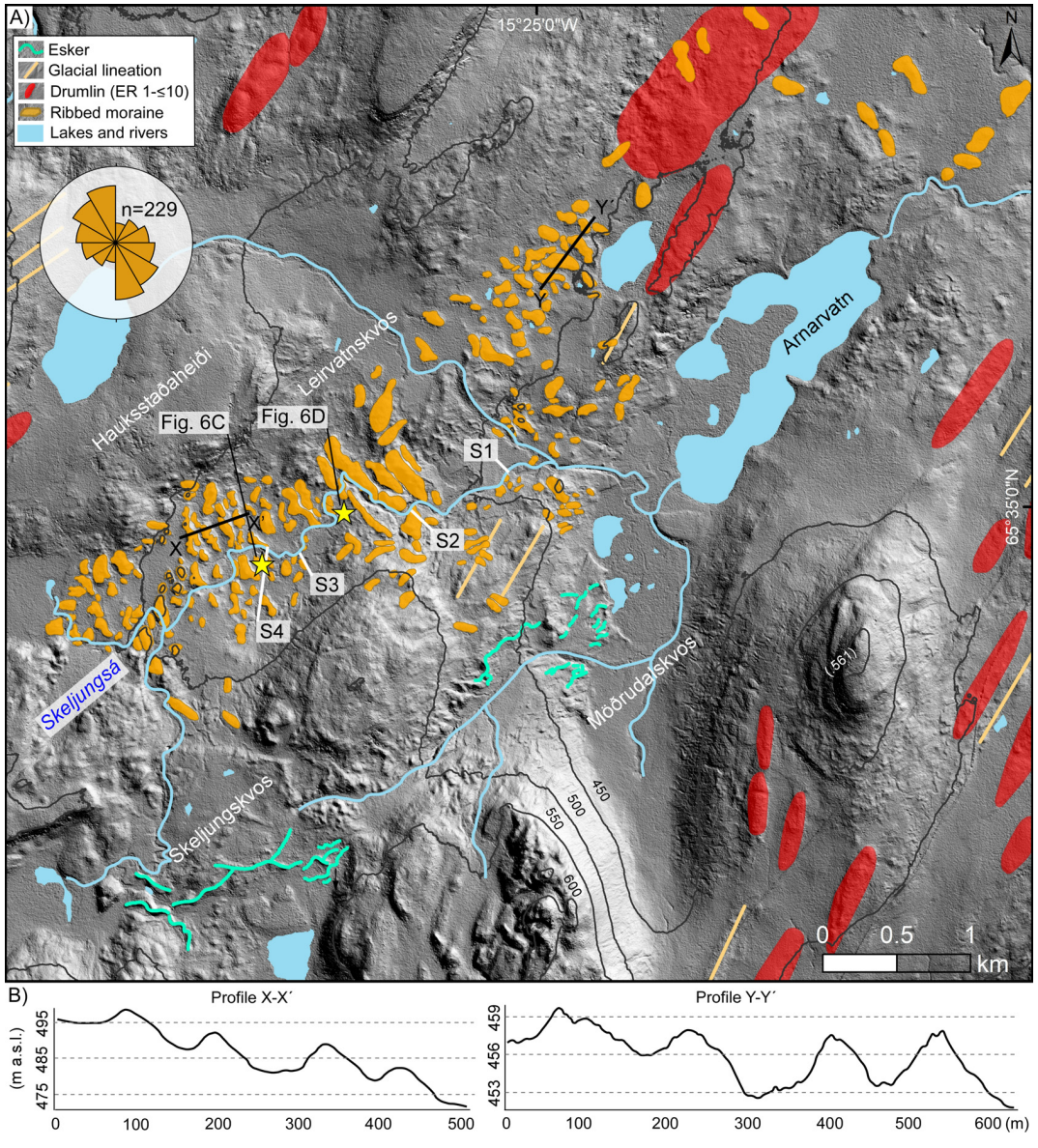

Figure 3. A) Map of glacial landforms on Hauksstaðaheiði. The rose diagram shows the orientation of the mapped 229 ribbed moraines (median 114° - 294°). The location of the sections is marked (S1-4). The stars mark the locations where Figs. 6C and D are taken. Contour intervals are 50 m. B) Two terrain cross profiles that are marked on the map. The ribbed moraines are usually between 0.5 - 10 m in relief with both symmetrical and asymmetrical cross profiles and curved crests.

Selárdalur

In total, 348 ridge segments were mapped in Selárdalur valley and the highlands above at an elevation of 126 - 460 m a.s.l. The ridges are generally linear, especially on Bústaðatungur, and when their distribution is dense enough, they have an interconnected network (Fig. 4A, C). The median length is 70 m with a range of 20 - 220 m and the median width is 33 m with a range of 14 - 78 m. The median elongation ratio is 2.1:1 with a range from 1.0 - 5.6:1 (Fig. 5; Table 1). The ridges are low in relief (<1 m), often only tens of centimeters prominent, and their cross profile appears to be generally symmetrical with a curved crest, although it can be difficult to determine due to their low relief (Fig. 4B). The median ridge orientation is southeast to northwest (128° - 308°), or generally transverse or oblique to the mapped SSBs and the orientation of the valley (Fig. 4A; Table 1). However, the orientation of some segments can be difficult to determine as they have a low elongation ratio and show signs of erosion. The ridges are dispersed within the area, but four clusters occur. Most of the ridges are situated on a gentle slope at the southeastern side of the head of the valley and the highlands above, down-ice from the ribbed moraines on Hauksstaðaheiði. Within the individual clusters of ridges, the orientation is rather constant (Fig. 4A). The mean density of ridges is 2.3 ridges per km^2 with a maximum density of 44 ridges per km^2 and an average crest-to-crest distance of 115 m (Table 1).

On Bústaðatungur, there are examples of ridges superimposed on SSBs and esker segments occur up-ice from those ridges and around Selá (Fig. 4A). The surface of the ridges is composed of diamict, with subangular to subrounded boulders. There are no large angular boulders found on top of the ridges in the valley, distinguishing them from the ridges on Jökuldalsheiði and Hauksstaðaheiði, but further up on the highlands boulders occur both on top of the ridges and surround them. However, the sediment is comparable to sediments on the surface of drumlins on Bustarfell and CSRs in Bakkaflói and Þistilfjörður (Aradóttir et al., 2023a, b). The ridge sediments were investigated briefly in one roadcut and a few gravel pits. They were composed of homogenous matrix-supported diamict and striations were observed on a few clasts (Fig. 4C, D). Based on this data we interpret the ridges to be composed of till, although we acknowledge that our sedimentological data is limited.

Sæmundsson (1995) previously described hummocky moraine close to the mouth of Selárdalur (Fig. 1C). It was interpreted as an ice-marginal position from the Early PB readvance, located just above the 50 m marine limit. Areas with similar hummocky morphology are mapped on four new locations; three within the Selárdalur valley and one on the northern part of Hauksstaðaheiði. The areas within the valley are all located on the northwestern side of Selá and distributed from the center of the valley to its head (Figs 1C and 4A). These areas usually comprise poorly sorted sediments on the surface with subangular to subrounded boulders but sorted sediments were also observed.

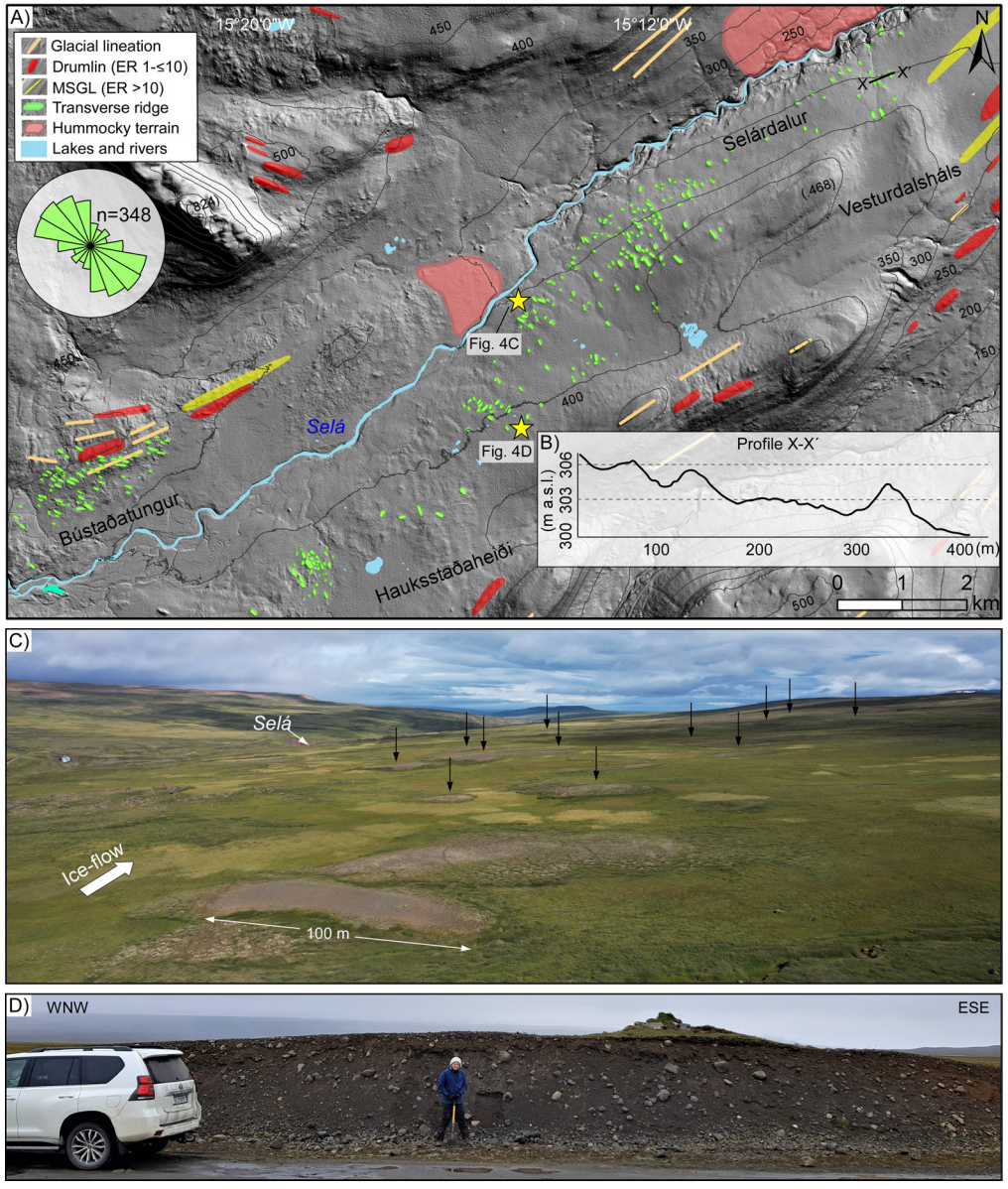

Figure 4. A) Map of glacial landforms in Selárdalur and the highlands above. Note that the map does not cover the whole subarea. The rose diagram shows the orientation of the mapped 348 transverse ridges (median 128° - 308°). The stars mark the locations where Fig. 4C and D were taken. Contour intervals are 50 m. B) A terrain cross profile of the ridges that is marked on the map. The ridges are usually <1 m in relief with symmetrical cross profiles and curved crests. C) Cluster of ridges at the head of Selárdalur. Two ridges are obvious in the foreground and arrows point at other prominent ridges in the distance. D) A roadcut into one of the ridges up on the plateau. The ridge is orientated oblique to the former ice-flow and the section is perpendicular to the ridge. A brief examination of the sediments in the ridge indicates that it is composed of rather homogenous diamict.

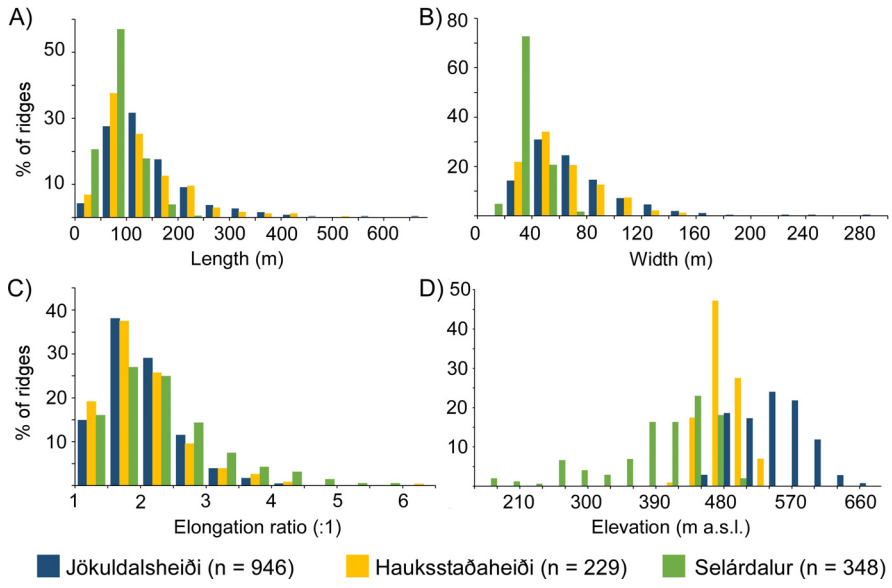

Figure 5. Size-frequency (A) length, B) width, C) elongation ratio, and D) elevation distribution of the morphometrics of the ridges on Jökuldalsheiði and Hauksstaðaheiði and in Selárdalur.

Table 1. Morphometrics of transverse ridges on Jökuldals- and Hauksstaðaheiði and in Selárdalur.

		Jökuldalsheiði	**Hauksstaðaheiði**	**Selárdalur**
n		962	228	348
Length (m)	Median	127	105	70
	Mean	145	131	78
	Min	28	32	20
	Max	657	539	220
	Q_1	90	74	53
	Q_3	181	164	97
Width (m)	Median	64	60	33
	Mean	71	64	34
	Min	17	23	14
	Max	282	156	18
	Q_1	47	44	28
	Q_3	86	78	39
Elongation ratio (:1)	Median	2	1.9	2.1
	Mean	2	2	2.3
	Min	1.1	1	1
	Max	4.4	6	5.6
	Q_1	1.7	1.5	1.7
	Q_3	2.3	2.3	2.7
Orientation (°)	Median	93	114	129
	Mean	92	107	122
	Min	0	0	6
	Max	179	178	179
	Q_1	56	68	107
	Q_3	126	153	151
Density (no. of ridges/km^2)	Mean	0.38	2.1	2.3
	Max	32	54	44


A)
view up-ice
Esker
Ice-marginal ridge
Transverse channel
Inactive channel
B)
Esker
view down-ice
C)
Section 3
Section 4
Skeljungsá
D)
view down-ice
Arnarvatn
Section 2
Skeljungsá

Figure 6. A) Ribbed moraines (white dashed lines) on Jökuldalsheiði at the proximal side of one of the ice-marginal positions where an esker terminates and changes into an inactive channel (up to 15 m wide). Note the 'ribbed' drumlin (red dashed lines). The view is up-ice. B) The lee side of a large drumlin (red dashed line) on Jökuldalsheiði with superimposed and adjacent ribbed moraines (white dashed lines). An esker lies parallel to the drumlin on the western side (left of the image). Note the large and angular boulders on both figures from Jökuldalsheiði and the car for scale at the bottom. C) Ribbed moraines in the upper part of the basin on Hauksstaðaheiði with a view towards the north. Sections 3 and 4 (30 m long) are marked. Note the broad arcuate and rectangular, and anastomosing shape of the ridges. D) Down-ice overview of the ribbed moraines on Hauksstaðaheiði. Section 2 is marked (45 m long) and the most prominent ridges are highlighted with white dashed lines.

4.2 Sedimentology of ribbed moraines

The internal architecture of the transverse ridges on Hauksstaðaheiði was studied in four natural sections (1-4), all cut and exposed by the Skeljungsá river (Fig. 3A). Four units were identified in the four sections: (1) matrix-supported diamict; (2a) interbedded sand and gravel layers; (2b) horizontally laminated silt and fine sand; (3) brown, matrix- to clast-supported diamict; (4) partly stratified, clast-rich, matrix- to clast-supported, firm diamict.

Section 1 is located furthest downstream in Skeljungsá, closest to Lake Arnarvatn. The ridge, in which the section occurs, has been eroded substantially by the river but the remnant of the segment is 40 m long and 30 m wide and trending ~NW-SE (Fig. 3A). The section is in total 20 m long and 9 m high, orientated transverse to the ridge crest (56° - 236°) and two units (2a and 4) are identified within it (Fig. 7A, B). Unit 2a [Gh/m/Sh] is up to 6 m thick and is composed of coarse gravel with interbedded, stratified sand and gravel layers and lenses. The layers within the unit are of variable thickness, 1 - 20 cm. The clasts are mostly blocky (C_{40} = 2) and subrounded to subangular (RA = 7.7) with no striations observed [S1_u2]. Small-scale deformation structures and ripple marks are visible within the sand layers and lenses. Vague fissile structures are observed close to the sharp and conformable boundary to unit 4 [Db/sC(m_3/c)4], a clast-rich matrix-supported to clast-supported, extremely firm diamict (up to 1.5 m thick). The matrix is mostly heterogeneous and stratified, with layers of sand and gravel, but is massive in places. The overall appearance of the unit is chaotic. The clasts are usually blocky (C_{40} = 0), subrounded to angular (RA = 9.3), and striated clasts, facets, and or/bullet-shaped clasts are present [S1_u4]. The largest boulders in both layers are up to 40 cm in diameter and the larger ones are usually more angular. Layers in both units are dipping (6° - 20°) transverse or oblique outwards from the ridge crest (Figs 7B, C and 11A).

Section 2 is located ~700 m upstream from section 1 in a ridge composed of three segments, with a total length of ~950 m, oriented SE-NW (Figs 3A and 6D). The ridge segment containing the section is 180 m long and 170 m wide. The section is 50 m wide and up to 15 m high, aligned transverse to the composite ridge (30° - 210°). Three units were identified within the section (2a, 3, and 4) (Fig. 8A-D). The base of the ridge (< 5 m thick) is composed of unit 2a [G/Sm/h], sorted sand and gravel similar to unit 2a in section 1, although the gravel is more massive and coarser. The clasts are generally between 1 - 10 cm in diameter (largest up to 40 cm in diameter) and are mostly blocky (C_{40} = 0) and subrounded to subangular (RA = 0) [S2_u2]. Occasional ripple marks are observed in the sand layers and lenses. Gravel layers, dipping towards the southwest, at the southwestern part of the unit are truncated by unit 3 [DmM/C(c)4] with an unconformable boundary. Unit 3 is massive, homogenous, clast-supported diamict (< 1 m thick). The clasts are mostly blocky (C_{40} = 0) and subrounded to

subangular (RA = 0) [S2_u3], up to 30 cm in diameter. Gradational boundary separates unit 4 [Db/sC(m_3)4] at the top of the section from units 2a and 3. It has a similar appearance to unit 4 in section 1 and is up ~5 m thick. The clasts are usually blocky (C_{40} = 8) and subrounded to angular (RA = 9.3) [S2_u4]. The layers within unit 4 at the southwestern end are dipping towards the southwest, or down-ice (270°/26° and 280°/15°) (Figs 8B, C and 11B, C).

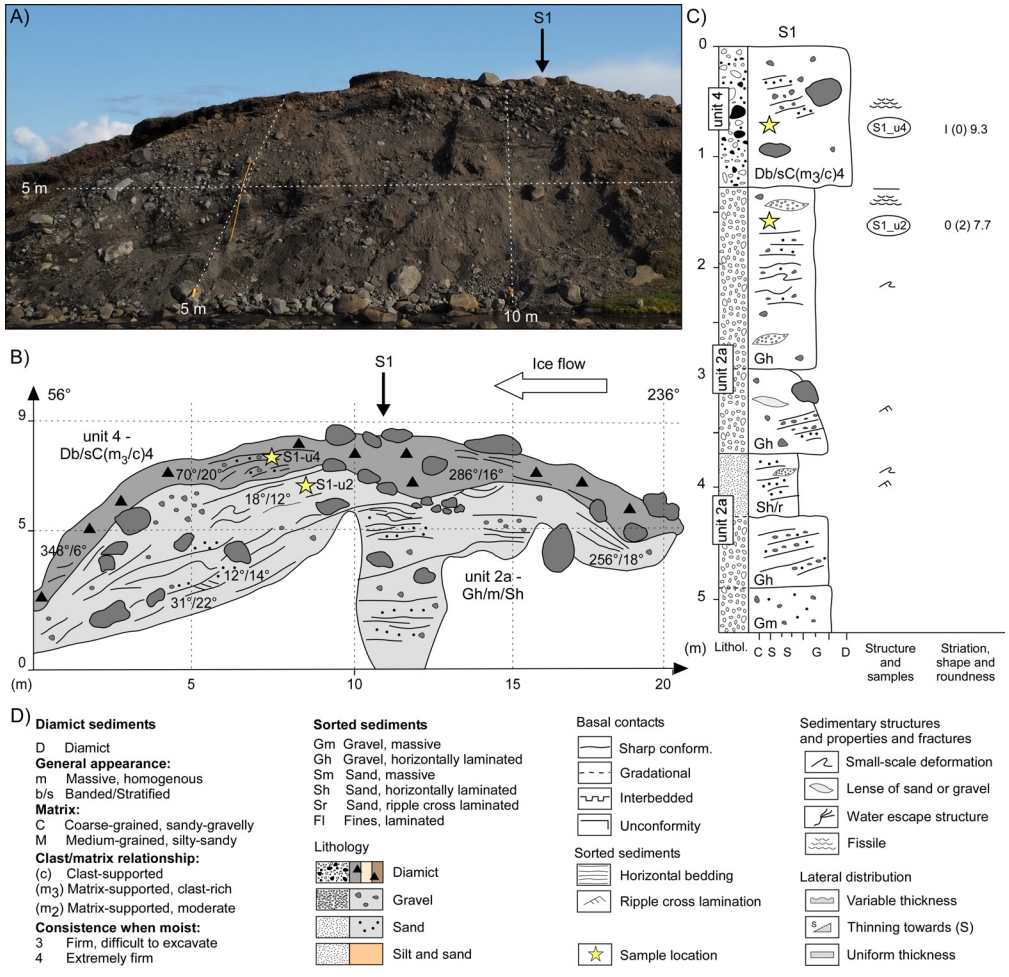

Figure 7. A) Section 1 on Hauksstaðaheiði. Note the dipping of the layers at the distal (left) side of the ridge. B) Diagram of the section. The location of log S1 is marked. The vertical axis is in reverse order compared to the log, with the river as the base. C) Stratigraphical log from S1. D) Legend and lithofacies codes used here and for other logs and diagrams in the paper, following Krüger and Kjær (1999).

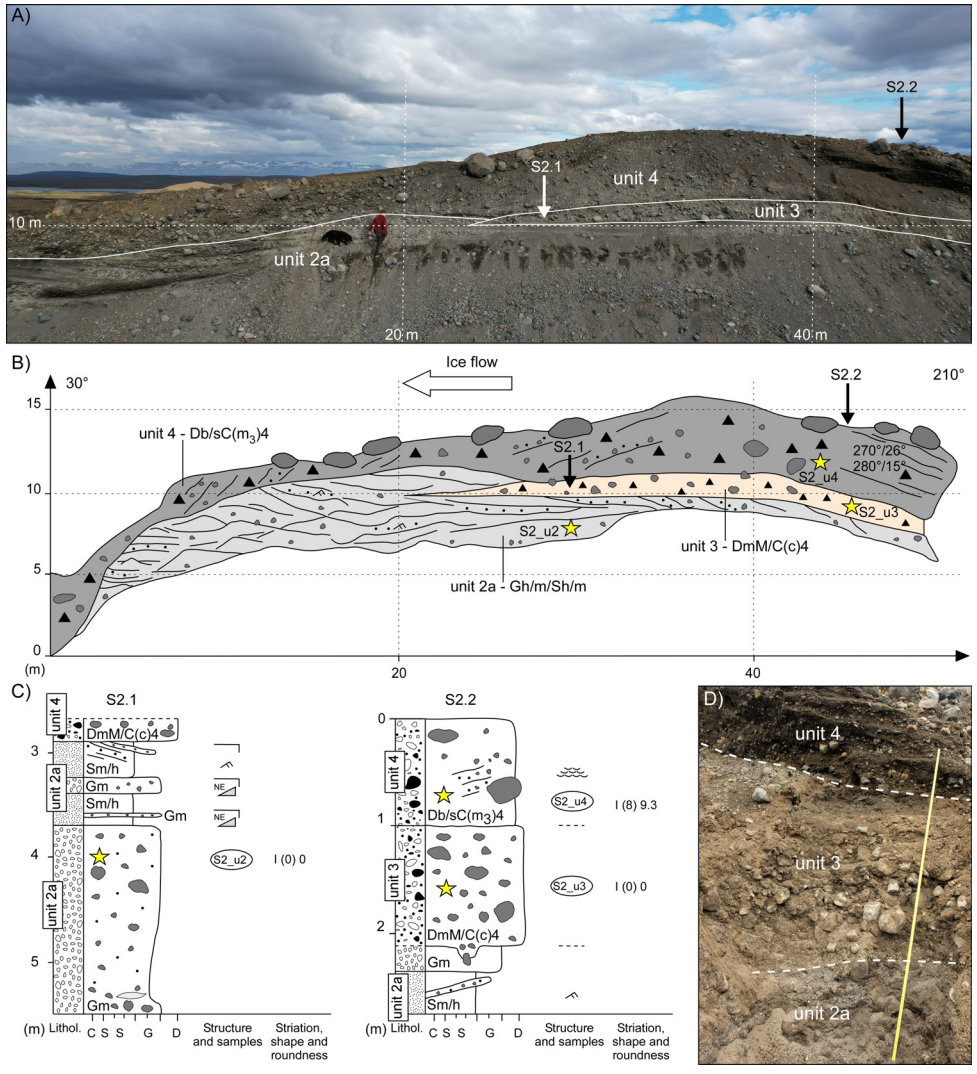

Figure 8. A) Section 2 on Hauksstaðaheiði. Three different units were identified in section 2 that are highlighted. Note the person and dog for scale in the middle of the section. B) Diagram of the section. The location of logs S2.1 and S2.2 are marked. The vertical axis is in reverse order compared to the log, with the river as the base. C) Stratigraphical log from S2.1 and S2.2. D) Part of section S2.2 where all three units (2a, 3, and 4) are observed.

Section 3 is located >1.6 km upstream from section 2. The ridge segment is 116 m long and 50 m wide, orientated SSE-NNW (Fig. 3A). The section is located at the edge of the ridge and is orientated almost parallel to the ridge crest, or 170° - 350°, and is 15 m wide and up to 3 m high. The section has a similar stratigraphy to section 1, composed of units 2a and 4 (Fig 9A, B). At the base is unit 2a, 1.8 m thick, interbedded horizontally laminated gravel and sand layers [Gh/Sh/r]. Ripples are visible both in sand lenses within the gravel and in the sand layers. The clasts are up to 20 cm in diameter and are mostly blocky (C_{40} = 0) and subrounded to angular (RA = 17.3) [S3_u2]. A similar diamict as observed in sections 1 and 2 (unit 4) is at the top of the section [Db/sC(m_3/c)3] (< 3 m thick). A sharp conformable boundary is between

units 2a and 4. Stratified sand vein perpendicular to the general stratification of the diamict, occurs at the up-ice side of the ridge. Clast morphology measurements show mostly blocky clasts (C_{40} = 4) and subrounded to angular (RA = 14.5). Layers in both units generally dip towards the west or southwest, or outwards from the ridge crest (Figs 9B, C and 11D).

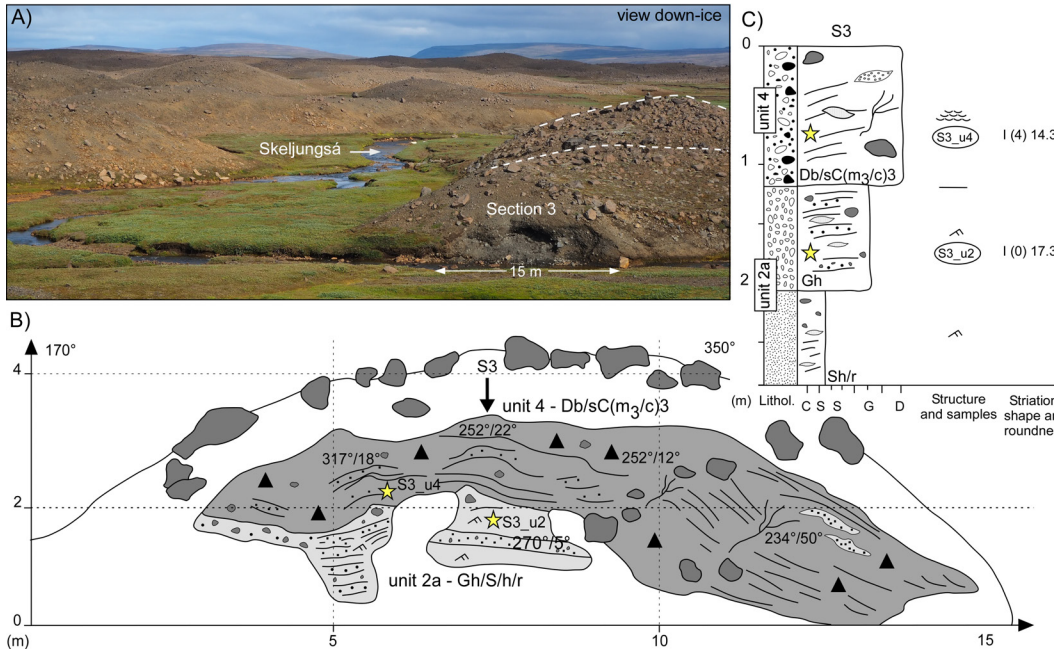

Figure 9. A) Section 3 on Hauksstaðaheiði. The white dotted lines highlight the ridge crest and the adjacent ridge that lies parallel to it. Note the large angular boulders on top of the ridges. B) Diagram of the section. The location of log S3 is marked. C) Stratigraphical log from S3. The vertical axis is in reverse order compared to the log, with the river as the base.

Section 4 is the distal most section, located ~250 m upstream from section 3. The ridge segment is 190 m long and 100 m wide (Fig. 3A). The orientation of the ridge is SSE-NNW and most of the section is orientated 93° - 270°, or oblique to the ridge crest. The orientation of the southeastern part of the section changes to 146° - 326°, almost perpendicular to the ridge crest. The section is 35 wide and up to 19 m high (Fig 10A-C). This section has more complex stratigraphy than the other sections with four units identified. At the base of the section is unit 1, a 1.2 cm layer of matrix-supported, massive diamict with deformed sand and silt lenses and fissile structure [DmM(m_2)3]. Above the diamict is ~1 m of laminated fine/medium sand and silt [Fl/Sh] that have been distorted (unit 2b). A few outsized clasts, up to 3 cm in diameter, are found in the sand and silt. This unit does not continue to the southeast in the section and could therefore be a lens within unit 2a. The most prominent unit in the section is composed of horizontally laminated sand and gravel layers comparable to what was observed in the other sections (unit 2a). The unit is visible through most of the section, over 5 m thick in the middle but thinner at the southeastern side where the log was made. Deformation is more prominent than in the other sections. In general, the unit is grading upwards and ripples are observed in sand lenses within the gravel. Thin silt layers (< 1 cm) separate some of the gravel and sand layers. Clastic dykes are found within the unit. The sand and gravel layers are generally steeply dipping (22° - 69°) towards the north-northeast,

oblique to the ridge crest or down-ice. At the top of the section is unit 4, partly stratified, clast-rich, and firm diamict [Db/sC(m_3)3], similar to the diamict in the upper part of the other sections. The sorted sediments are thrusted into the diamict and lenses of sand and gravel are frequent in the lower part of unit 4. Deformation and fissile structures are visible. Clast samples were not taken here but clasts are usually blocky and angular to subrounded. The unit is up to 4 m thick (Figs 10C, D and 11E, F).

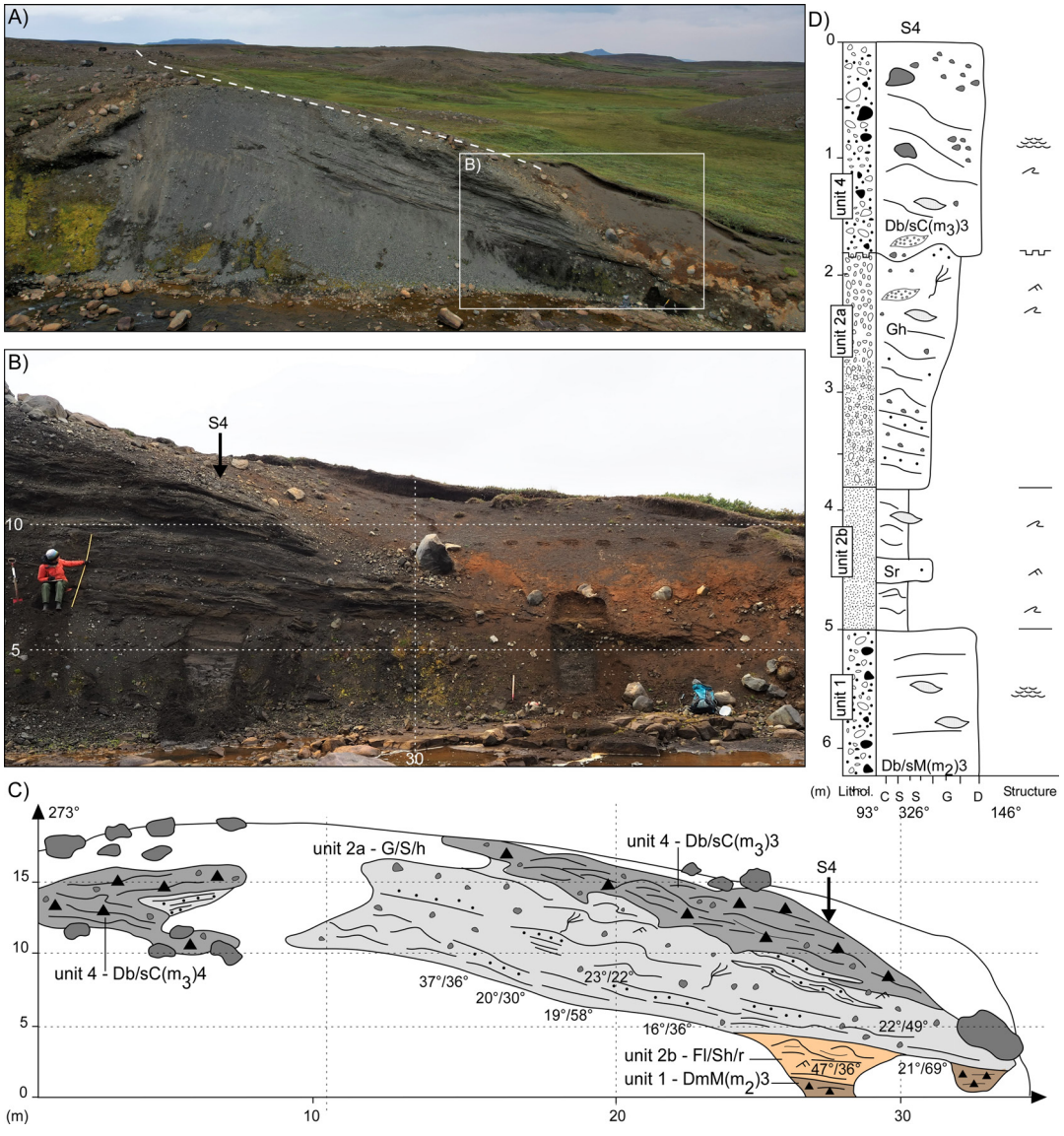

Figure 10. A) Section 4 on Hauksstaðaheiði. The white dashed line highlights the ridge crest. B) The eastern part of the section where the logging was conducted. The orientation of the section changes slightly from W-E to NW-SE. The vertical axis is in reverse order compared to the log, with the river as the base. C) Diagram of the section. The location of log S4 is marked. D) Stratigraphical log from S4.

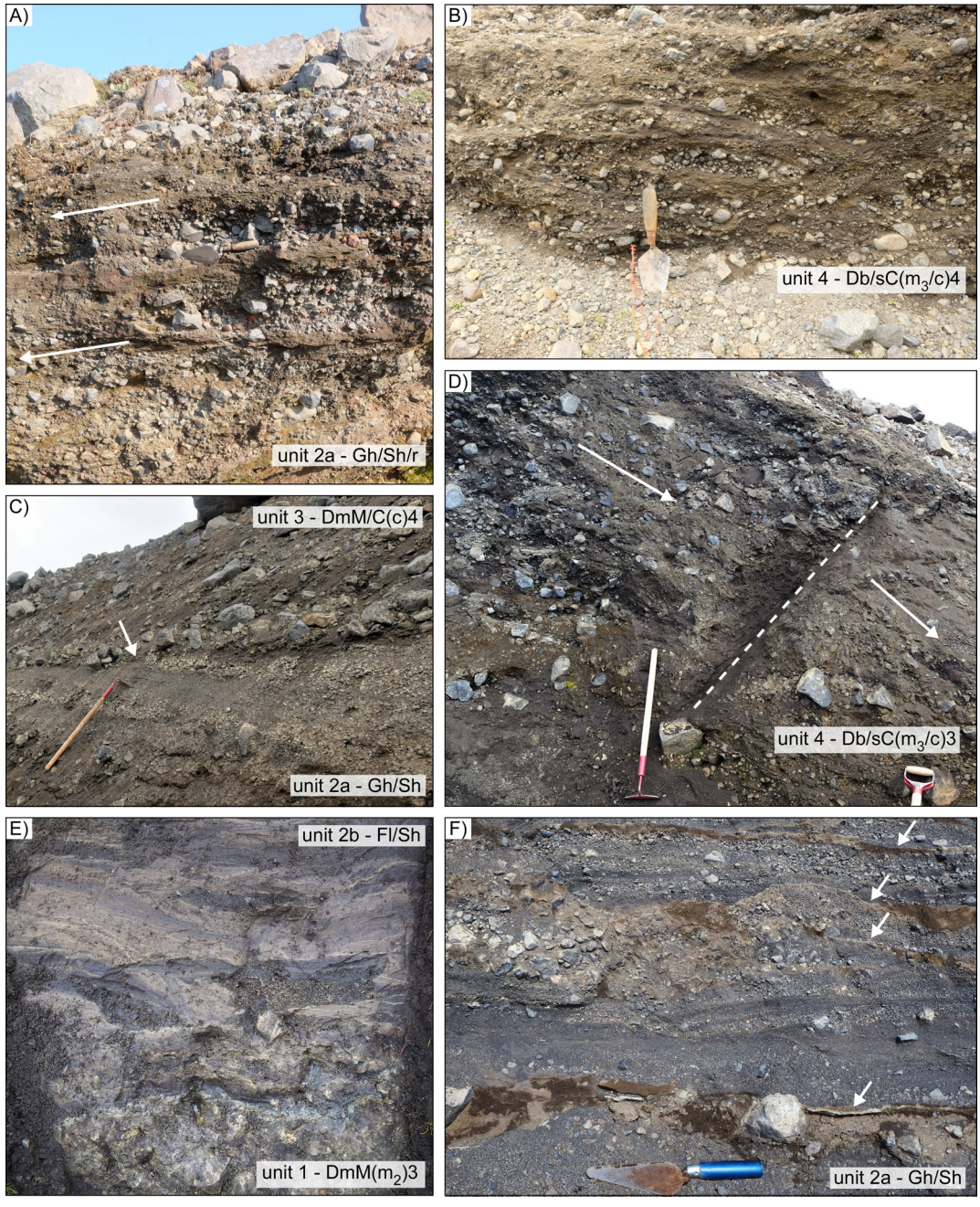

Figure 11. A) Dipping sand and gravel layers towards north-northeast (down-ice), or outwards from the center of the ridge in section 1. Arrows indicate dip direction. B) Stratified diamict in section 2. C) Unconformity (arrow) between units 2a and 3 in section 2. D) Stratified diamict in section 3 dissected with water escape structure (white dashed line). Note the layers dipping towards southwest/south-southwest or up-ice (arrows). E) Deformed laminated silt and fine sand on top of a massive diamict with deformed sand and silt lenses at the base of section 4. F) Laminated sand and gravel in section 3. Note the silt layers between the layers (arrows) with minor deformation structures.

5. Discussion

5.1 Interpretation of transverse ridges

The ridges on Hauksstaðaheiði and Jökuldalsheiði were described by Helgadóttir (2020) who interpreted them as ribbed moraines based on morphological resemblance to a comprehensive analysis of ribbed moraines by Dunlop and Clark (2006). The ridges' appearance on Hauksstaðaheiði is most similar to what Dunlop and Clark (2010) classified as broad arcuate or rectangular ribbed moraines although some can be classified as anastomosing ribbed moraines. On Jökuldalsheiði, a fraction of the ridges shows similarity to the ridges on Hauksstaðaheiði, but the remainder have a hummocky appearance. The median size of the ribbed moraines is similar between the two areas, but they are more closely spaced and have a higher distribution density on Hauksstaðaheiði. The ridges in Selárdalur were also interpreted as ribbed moraines by Helgadóttir (2020), but as they have different morphological characteristics than the ribbed moraines on Hauksstaðaheiði and Jökuldalsheiði, we speculate if they may be of a different origin (Rivers et al., 2023). These ridges appear as linear, interconnected segments with symmetric crests, generally orientated transverse to former ice flow, and show more resemblance to previously described CSRs in Bakkaflói and Þistilfjörður (Aradóttir et al., 2023a). Their linear shape and interconnected network could also suggest that they are recessional moraines (e.g. Bennett, 2001; Chandler et al., 2016). However, their generally symmetric cross profile and lack of other ice-marginal landforms associated with the ridges are rather supportive of CSR origin (e.g. Sharp, 1985; Evans and Rea, 1999, 2003; Rivers et al., 2023). Consequently, that implies deposition during an ice-stream shutdown or a surge-event (e.g. Evans et al., 2016; Kurjanski et al., 2019; Benn, 2021; Lamsters et al., 2021).

Accordingly, we are aware that some of the ridges mapped as ribbed moraines might be recessional moraines as these can be hard to distinguish. This especially applies to Jökuldalsheiði where their fragmented appearance and high frequency, make them more difficult to differentiate. Likewise, it is also possible that some segments of the ice-marginal moraines could be mistaken as ribbed moraines, although ice-marginal channels that are usually associated with the ice-marginal moraines can help distinguish between these two types of ridges. It should also be noted that the primary morphology of ribbed moraines and other transverse ridges has been altered due to post-glacial sedimentation and erosion (Dunlop and Clark, 2006; Finlayson, 2013) and accretion of peat (Aradóttir et al., 2023b).

In general, the sections on Hauksstaðaheiði have similar stratigraphy; core of glaciofluvial sand and gravel (unit 2) draped with massive to stratified, clast-rich diamict (unit 4). The diamict at the base of section 4 (unit 1) was only observed with limited spatial extent. Therefore, it is unclear if it is widespread in the whole basin on Hauksstaðaheiði but the presence of fissility and deformation indicates subglacial origin and is thus interpreted as subglacial till. The sorted sand, gravel, and fines (units 2a and 2b) are interpreted as glaciofluvial sediments deposited in a proglacial setting based on the widespread distribution and thickness. Unit 3, which was only observed in section 2, is interpreted as subglacial till based on the clast morphology and its erosional lower contact with the underlying glaciofluvial sediments. The diamict at the top of all the ridges, unit 4, is interpreted to be subglacial till based on fissility, compactness, clast morphology, and the presence of striated,

bullet-shaped, and faceted clasts. Due to the clast-rich nature of this till, the basal ice is suggested to have been debris-rich. The stratified characteristics of the till and the layers and lenses of sorted sediments within it, indicate the influence of water while being deposited and can at least partly be interpreted as a melt-out till (Evans et al., 2006). The clastic dykes are interpreted as water escape structures that also support subglacial origin and are further indicative of high water pressure at the base of the glacier as they suggest downward intrusion of fluidized sediments (van der Meer et al., 1999). Based on our results we interpret unit 4 as subglacial (melt-out) till, deposited from debris-rich basal ice, with pressurized porewater and reworking of pre-existing sediments. The deformation and thrust structures within both units suggest compressional flow during till deposition due to the overriding of ice (Evans et al., 2006). Fabric measurements were not feasible in the till, and therefore it could not be used to further determine its origin.

The stratigraphy of the ribbed moraines is similar to the drumlins within the adjacent Bustarfell drumlin field where two units of subglacial traction till occur with interbedded glaciofluvial sediments (Aradóttir et al., 2023b). Due to the lack of sections on Jökuldalsheiði, their internal architecture remains unknown but considering the amount of fluvial landforms in the basin, glaciofluvial sediments may exist within some of them. It is, however, unlikely that glaciofluvial sediments would collect on top of the SSBs and therefore make up the core of the ribbed moraines that are superimposed on SSBs in both areas. The internal architecture of ribbed moraines is also variable and generally not considered the cause for their formation (Hättestrand and Kleman, 1997). The ribbed moraines are therefore thought to be formed through the collection of pre-existing sediments, whether it is glaciofluvial sediments and till in the basins or the sediments within the SSBs, as most studies agree on (Hättestrand, 1997; Sarala, 2006; Möller, 2010). The sedimentology of the ribbed moraines in the basin on Hauksstaðaheiði shows a resemblance to ribbed moraines described in Sweden, Norway, Finland, and Scotland, where deformed glaciofluvial sediments and melt-out till have been described (e.g. Lundqvist, 1989, 1997; Raunholm et al., 2003; Möller, 2006, 2010; Sarala, 2006; Finlayson and Bradwell, 2008).

Similar surface of the ridges has been observed by others that have speculated the cause for these large and angular boulders. It is generally agreed that quarrying of bedrock in areas with thin till sheets is the origin of the boulders and that they are transported englacially from nearby bedrock plateaus (Möller, 2006). Sarala (2006) suggested that the freeze-thaw process between the ridges caused quarrying of the bedrock that was subsequently deposited on the next ridge in areas with a thin till sheet based on changes in the lithology of the boulders. As the large and angular boulders are present on the ridges and outside them, although they are more frequent on the ridges, they are not considered to be part of the actual ribbed moraines but deposited after their formation through englacial transport from local bedrock plateaus (Möller, 2006; Sarala, 2006). The higher frequency of boulders in some areas can therefore simply be explained by proximity to bedrock outcrops, but the thicker accumulation of peat might also prevent them from being observed.

5.2 Formation and implication for ice dynamics

The ribbed moraines on Hauksstaðaheiði and Jökuldalsheiði are located upstream from fields of well-defined drumlins and sometimes superimposed on them. On Jökuldalsheiði, the ridges are surrounded by drumlins of various shapes and sizes, some of which can be classified as 'ribbed' drumlins, but there are no examples of ribbed moraines that have undergone

drumlinisation. Based on this cross-cutting relationship and that the ridges have not been overridden by rapidly moving ice, we interpret them to be formed during ice-stream deglaciation rather than in the ice-stream onset zone during ice-stream waxing (e.g. Raunholm et al., 2003; Sarala, 2006; Stokes et al., 2008; Delaney et al., 2023). As we do not see any remolding of pre-existing landforms, besides the 'ribbed' drumlins, we do not consider the ribbed moraines to be formed by modification of pre-existing landforms (Lundqvist, 1989, 1997; Möller, 2006). A ~90° change in flow direction responsible for their formation, as suggested by Boulton (1987), is also highly unlikely in the area based on the inferred flow direction from the mapping of SSBs (Benediktsson et al., 2022b).

The formation of ribbed moraines has generally been associated with compressive ice flow (e.g. Shaw, 1979; Bouchard, 1989, Finlayson and Bradwell, 2008; Stokes et al., 2008; Vérité et al., 2021) or attributed to the fracturing of frozen pre-existing till sheets due to extensional basal ice flow at the boundary between cold- and warm-based conditions (Hättestrand, 1997; Hättestrand and Kleman, 1999; Raunholm et al., 2003; Sarala, 2006). The deformation and thrust structures in the sections on Hauksstaðaheiði support compressive flow, although the lack of large-scale folds or faults does not imply shearing and stacking, as proposed by Lindén et al. (2008) for the formation of ribbed moraines. The general dipping of the layers up- and down-ice, outwards from the ridge crests on Hauksstaðaheiði is difficult to interpret but we surmise that this is the result of compressive flow in line with other deformation structures identified in the sections. Individual ridges in this study do not fit together like a jig-saw puzzle, as would be the case for till sheets that got ripped apart under extensional flow at the transition between warm-based and cold-based ice (Hättestrand, 1997; Hättestrand and Kleman, 1999; Sarala, 2006). In addition, there is no morphological evidence of cold-based ice in this region, thus disputing the fracturing hypothesis for the ribbed moraines in northeast Iceland.

Recent modelling experiments attribute the formation of ribbed moraines to changes in glacial dynamics and soft-bed deformation in areas with high lateral or longitudinal velocity gradients. They are formed in marginal settings due to compression, with transverse ridges below frontal lobes but oblique ridges beneath lateral shear margins (Vérité et al., 2021). Based on the topography and distribution of glacial landforms on Hauksstaðaheiði and Jökuldalsheiði, the ribbed moraines appear to have formed near the shear margins of the ice streams rather than below the frontal lobe, although they occur both transverse and oblique to the former ice flow. However, the orientation of the ridges in the area is affected by the topography and is thus expected to show more variations than modelling experiments on a flat substrate. Other studies have also attributed dynamic instabilities and velocity changes following the deglaciation to the formation of ribbed moraines (Raunholm et al., 2003; Finlayson and Bradwell, 2008; Stokes et al. 2008). Based on all of the above arguments, we consider the most reasonable explanation for the formation of ribbed moraines in northeast Iceland related to changes in ice dynamics and basal processes due to lateral and longitudinal velocity changes within the ice associated with ice stagnation.

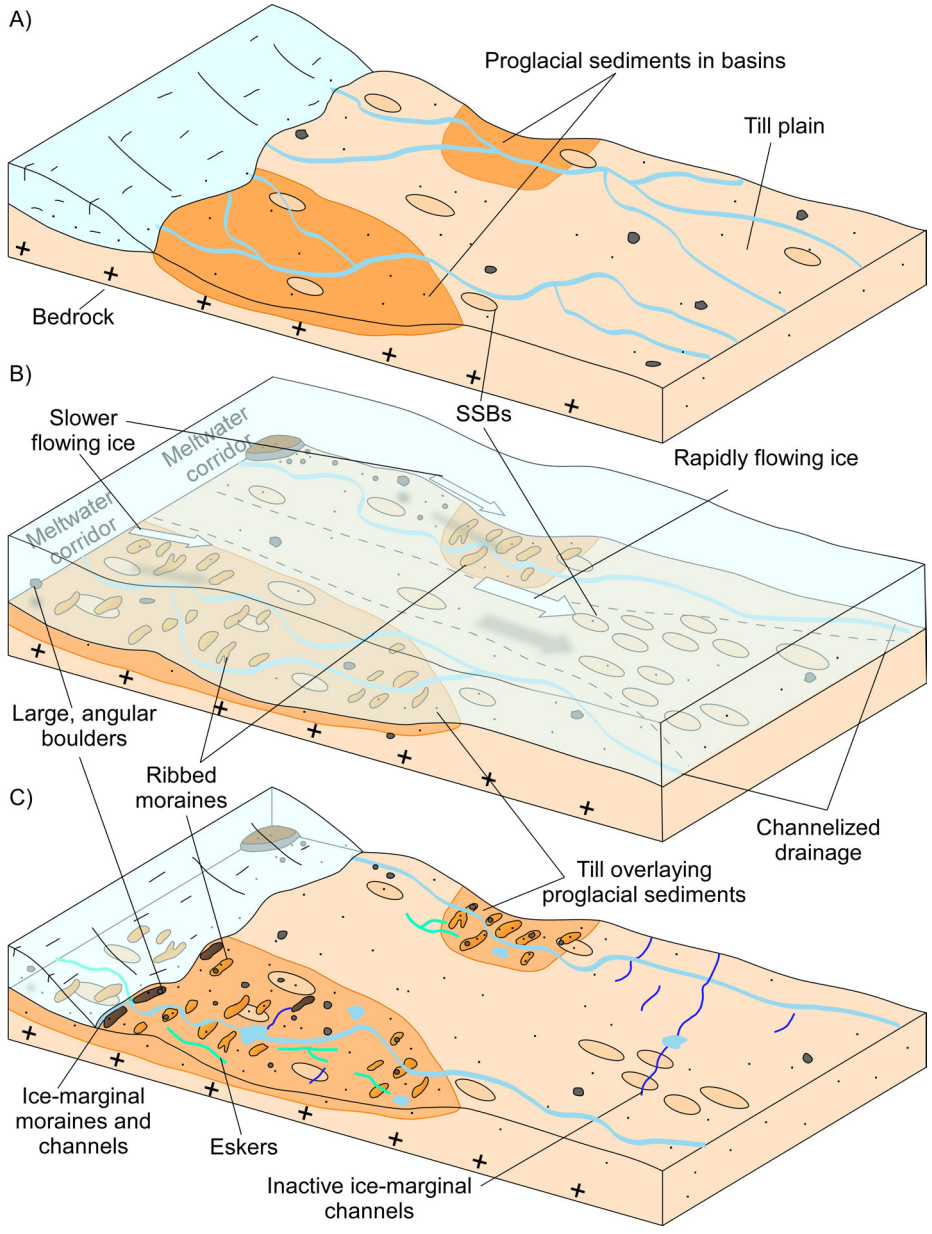

Figure 12. Conceptual landsystem model illustrating ribbed moraines formed within Vopnafjörður-Jökuldalsheiði flow-set, northeast Iceland. A) Deglaciation. SSBs that formed during the last ice advance are exposed and glaciofluvial material is deposited, especially in basins. B) Ice stagnation following glacier readvance. Formation of SSBs continued within the ice-stream trunk during the readvance. Ribbed moraines are formed at the lateral shear margin of the ice stream due to changes in basal processes from the velocity difference within the ice during stagnation. Eskers are formed as the drainage changes from distributed to channelized during deglaciation, enhancing ice-bed coupling and formation of the ribbed moraines. Large and angular boulders are transported englacially from local bedrock outcrops. C) Deglaciation. Ice-marginal positions indicate a stepwise retreat. SSBs are more fragmented due to fluvial erosion around the ribbed moraines due to their locations within or closer to the meltwater corridor.

Subglacial hydrologic modelling highlights the importance of subglacial meltwater corridors for the development of landforms (Vérité et al., 2023). The ribbed moraines in northeast Iceland are likely located within or adjacent to meltwater corridors, as they often occur juxtaposed with eskers. The well-defined drumlins on Bustarfell and further down-ice form Jökuldalsheiði indicate that those areas are outside the main meltwater corridor (Fig. 12B). Eskers described from palaeo-ice sheets are generally interpreted as deglacial landforms, indicating that the water drainage changed from distributed to channelized drainage during the deglaciation. The long and well-organized esker systems on Jökuldalsheiði reflect time transgressive formation during the retreat and that the channelized drainage was rather constant (e.g. Margold et al., 2011; Storrar et al., 2014a, b). This agrees with the model by Vérité et al. (2021) where the formation of ribbed moraines is associated with extensive areas of ice-bed decoupling due to changes in the channelized and effective subglacial drainage (Fig. 12B).

The more fragmented appearance of the ridges and drumlins on Jökuldalsheiði could be explained by a higher amount of fluvial erosion within the corridor on Jökuldalsheiði than on Hauksstaðaheiði, where the ribbed moraines are not as modified by the fluvial erosion. The effect of fluvial erosion should also be considered as a factor for the 'ribbed' drumlins on Jökuldalsheiði. The drumlins on Bustarfell are incised with regular and transverse ice-marginal channels indicating a stepwise retreat (Aradóttir et al. 2023b). Although such regular channels are not observed on Jökuldalsheiði, some of the fragmentation of the drumlins can likely be explained by ice-marginal channeling, again highlighting the challenges in distinguishing between individual ridge segments.

5.2 Glacial history

The chronological constraints on the deglaciation history in the area are limited and therefore the absolute timing for the formation of the ribbed moraines is not known. However, their relative time of formation can be established based on stratigraphic correlation and cross-cutting relationships with other landforms. It has recently been suggested that a lower till unit in the drumlins on Bustarfell represents maximum flow during the LGM, overlain by glaciofluvial sediments that were deposited in proglacial setting during Bølling-Allerød interstadial and that an upper subglacial traction till was deposited by Late Glacial readvance during the YD period when the final formation of the drumlins occurred (Aradóttir et al., 2023b). It is suggested that the glaciofluvial sediments (unit 2) in the ribbed moraines on Hauksstaðaheiði were formed simultaneously with the glaciofluvial sediments in the drumlins on Bustarfell when the ice retreated inland to an unknown position during the Bølling-Allerød interstadial (Fig. 12A). In accordance, the lowermost till (unit 1) observed in the ribbed moraines might be from the LGM, although we acknowledge that the data to support this further is limited. During the Late Glacial readvance, the ice stream overrode and deformed the glaciofluvial sediments and deposited the subglacial (melt-out) till (units 3 and 4). Based on this correlation and that the ribbed moraines are superimposed on the SSBs and not overridden, we suggest that the ribbed moraines were formed during the YD period. Previous studies have associated the formation of ribbed moraines with ice-stream shutdown (e.g Sarala, 2006; Stokes et al., 2008; Delaney et al., 2023) and the proposed formation of ribbed moraines related to dynamic instability due to changes in velocity gradients is in accordance with them being formed during the Late Glacial deglaciation (Fig. 12B).

During the Early PB period, the ice is suggested to have advanced down to the Vopnafjörður valleys, about 15 km beyond the distal part of the ribbed moraine areas (Fig. 1C; Sæmundsson, 1995). Nevertheless, the ribbed moraines, which we suggest having been formed prior to that, are well preserved. Due to the elevation difference between the highlands and the ice-marginal positions (>300 m), we speculate if the ribbed moraines may have been covered with passive ice during this period while active ice was concentrated in the valleys. The preservation of the ridges is further indicative of a generally passive ice retreat. However, the inferred ice-marginal positions on Jökuldalsheiði inside the suggested PB margin signify actively retreating ice margins with minor readvances or stillstands occurring during the deglaciation (Fig. 12C). This is supported by even more pronounced ice-marginal positions and larger moraine, e.g. the Skessugarður moraine, farther inland (Fig. 1C).

The ice margin during the PB period in Selárdalur is suggested to have terminated almost to the outermost hummocky terrain, close to the mouth of the valley. Consequently, the YD ice-marginal position is considered to have been located further out although evidence for that has not been observed (Sæmundsson, 1995). The transverse ridges in Selárdalur, suggested to be either CSRs or recessional moraines, are therefore most likely formed during the deglaciation following the PB. The three hummocky areas inside the outermost moraine suggest stillstands or small readvances during the retreat. It might also be speculated that the landform assemblage of several hummocky areas and CSRs in the valley resemble evidence for repeated cycles, comparable to surge signature, which would offer a new perspective between the style of deglaciation and climate forcing (Benn, 2021). However, we acknowledge that due to their low relief and lack of cross-sections, it was difficult to assess the symmetry of their cross profile and study their internal architecture in detail. Thus, further studies are necessary to test if these ridges in Selárdalur are CSRs or recessional moraines.

This first description of ribbed moraines in Iceland suggests that they are associated with the Late Glacial deglaciation of the IIS. Further investigations of ribbed moraines in Iceland are thus of great importance for advancing our understanding of palaeo-ice stream dynamics during the Late Glacial deglaciation as their distribution provides new insight into subglacial processes occurring during ice-sheet decay.

6. Conclusion

- Broad arcuate or rectangular ridges are mapped in shallow basins on the Hauksstaðaheiði and Jökuldalsheiði plateaus within the Jökuldalsheiði-Vopnafjörður palaeo-ice stream flow-set in northeastern Iceland. The ridges are generally orientated transverse to the former ice flow and interpreted as ribbed moraines, the first to be described in Iceland, based on their morphology and internal architecture.
- The ridges in the Selárdalur valley and the highlands above are more linear and do not resemble ribbed moraines in their morphology but show more similarity to CSRs or recessional moraines. However, further studies are required to confirm their origin.
- The investigated ribbed moraines on Hauksstaðaheiði are composed of glaciofluvial sand and gravel layers draped with partly stratified, clast-rich subglacial (melt-out) till. Both the glaciofluvial sediments and till units exhibit deformation and thrust structures. Furthermore, strata are characterized by the dipping of layers outward from the ridge crest, which we interpret as a result of compressional flow.

- Other glacial landforms in the area are SSBs, eskers, ice-marginal moraines, and meltwater channels. The superimposition of ribbed moraines on drumlins and the ribbed appearance of some drumlins indicates that the ribbed moraines post-date the formation of the drumlins. Eskers superimposed on ribbed moraines indicate channelized water drainage during the deglaciation and suggest that the ribbed moraines develop within or proximal to areas that were or later became meltwater corridors. The eskers frequently terminate at ice-marginal positions on Jökuldalsheiði, implying an active retreat interrupted by short-lived readvances during the deglaciation.
- We suggest that the ribbed moraines are the result of changes in basal processes and ice dynamics related to shifting lateral and longitudinal ice velocity and changes in meltwater drainage enhancing ice-bed coupling. Based on their distribution and often oblique orientation to former ice flow, it is considered that they formed under the later shear margins of the palaeo-ice stream.
- Based on stratigraphic correlation with the adjacent Bustarfell drumlin field and with reference to the known glacial history in northeast Iceland, we suggest that the lower till formed during the LGM, glaciofluvial sediments formed during the subsequent deglaciation, and the upper subglacial (melt-out) till formed during the Late Glacial readvance. Therefore, the ribbed moraines are considered to have formed during ice-stream shutdown following the YD readvance.
- Further work should focus on mapping ribbed moraines elsewhere in Iceland and their correlation with other glacial landforms, such as eskers, to increase our understanding of the deglaciation history and help improve future modelling of the IIS.

References

Aðalsteinsson, B. (1985). Skessugarður. Náttúrufræðingurinn 55(2), 82.

Aðalsteinsson, B. (1987). Jökulhörfun á Brúaröræfum. Í Jarðfræðafélag Íslands: Ísaldarlok á Íslandi. Geological Society of Iceland spring conference, Reykjavík, 28th of April 1987.

Alley, R.B., Anandakrishnan, S., Dupont, T.K. and Parizek, B.R. (2004). Ice streams – fast, and faster? Comptes Rendus Physique 5, 723-734.

Aradóttir, N., Benediktsson, Í.Ö., Ingólfsson, Ó., Brynjólfsson, S., Farnsworth, W.R., Benjamínsdóttir, M.M., and Ríkharðsdóttir, L.B. (2023a). Ice-stream shutdown during deglaciation: Evidence from crevasse-squeeze ridges of the Iceland Ice Sheet. Earth Surface Processes and Landforms, 48(12), 2412-2430. https://doi.org/10.1002/esp.5636

Aradóttir, N., Benediktsson, Í.Ö., Ingólfsson, Ó., Sturkell, E., Brynjólfsson, S., Farnsworth, W.R. and Phillips, E. (2023b). Drumlin formation within the Bustarfell drumlin field, northeast Iceland: integrating sedimentological and ground-penetrating radar data. Journal of Quaternary Science, 38, 386-402. https://doi.org/10.1002/jqs.3481

Aylsworth, J.M. and Shilts, W.W. (1989). Bedforms of the Keewatin Ice Sheet, Canada. Sedimentary Geology 62, 407–428.

Benediktsson, Í.Ö., Aradóttir, N., Ingólfsson, Ó. and Brynjólfsson, S. (2022b). Cross-cutting palaeo-ice streams in NE-Iceland reveal shifting Iceland Ice Sheet dynamics. Geomorphology, 396, 108009. https://doi.org/10.1016/j.geomorph.2021.108009

Benediktsson, Í.Ö., Brynjólfsson, S. and Ásbjörnsdóttir, L. (2022a). Chapter 55 - Iceland: glacial landforms from the Last Glacial Maximum. In: Palacios, D., Hughes, P., García-Ruiz, J.M., Andrés, N. (Eds), European Glacial Landscapes: Maximum Extent of Glaciations. Chennai: Elsevier, pp. 427-434. https://doi.org/10.1016/B978-0-12-823498-3.00055-8

Benediktsson, Í.Ö., Brynjólfsson, S. and Ásbjörnsdóttir, L. (2023a). Chapter 17 - Iceland: glacial landforms during deglaciation. In: Palacios, D., Hughes, P., García-Ruiz, J.M., Andrés, N. (Eds.), European Glacial Landscapes. Chennai: Elsevier, pp. 149-155. https://doi.org/10.1016/B978-0-323-91899-2.00022-X.

Benediktsson, Í.Ö., Brynjólfsson, S. and Ásbjörnsdóttir, L. (2023b). Chapter 34 - Iceland: glacial landforms from the Bølling-Allerød interstadial. In: Palacios, D., Hughes, P., García-Ruiz, J.M., Andrés, N. (Eds.), European Glacial Landscapes. Chennai: Elsevier, pp. 331-339. https://doi.org/10.1016/B978-0-323-91899-2.00051-6.

Benediktsson, Í.Ö., Brynjólfsson, S. and Ásbjörnsdóttir, L. (2023c). Chapter 52 – Iceland: Glacial landscapes of Iceland from the Younger Dryas Stadial. In: Palacios, D., Hughes, P., García-Ruiz, J.M., Andrés, N. (Eds.), European Glacial Landscapes. Chennai: Elsevier, 2023, pp. 497-507. https://doi.org/10.1016/B978-0-323-91899-2.00054-1.

Benediktsson, Í.Ö., Brynjólfsson, S., Ásbjörnsdóttir, L. & Farnsworth, W. (2024a). Chapter 12 – Holocene glacial history and landforms of Iceland. Editors: Palacios, D., Hughes, P., García-Ruiz, J.M., Andrés, N., European Glacial Landscapes, Elsevier, pp. 193-224.

Benediktsson, Í.Ö. Licciardi, J.M., Brynjólfsson, S., Principato, S., Aradóttir, N., Guðmundsdóttir, E.R. and Farnsworth. Early Holocene deglaciation of eastern Iceland constrained by cosmogenic ^{36}Cl exposure ages and tephrochronology. 36th Nordic Geological Winter Meeting, Gothenburg University, 10-12 January 2024b.

Benn, D. I. and Ballantyne, C. K. (1993). The description and representation of particle shape. Earth Surface Processes and Landforms 18, 665–672.

Bennett, M.R. (2001). The morphology, structural evolution and significance of push moraines. Earth-Science Reviews 53(3-4), 197-236. https://doi.org/10.1016/S0012-8252(00)00039-8.

Bennett, M.R. (2003). Ice stream as the arteries of an ice sheet; their mechanics, stability and significance. Earth-Science Reviews 61, 309-339.

Bingham, R.G., Vaughan, G., King, E.C., Davies, D., Cornford, S. L., Smith, A. M., Arthern, R.J., Brisbourne, A.M., Rydt, J.D., Graham, A.G.C., Spagnolo, M., Marsh, O.J. and Shean, D. E. (2017). Diverse landscapes beneath Pine Island Glacier influence ice flow. Nature Communications, 8(1), 1618. https://doi.org/10.1038/s41467-017-01597-y

Bouchard, M.A. (1989). Subglacial landforms and deposits in central and northern Québec, Canada, with emphasis on Rogen moraines. Sedimentary Geology 62, 293–308.

Boulton, G.S. (1987). A theory of drumlin formation by subglacial deformation. In: Menzies, J., Rose, J. (Eds.), Drumlin Symposium. Balkema, Rotterdam, pp. 25–80.

Bourgeois, O., Dauteuil, O. and Van Vliet-Lanoë, B. (2000). Geothermal control on flow patterns in the last glacial maximum ice sheet of Iceland. Earth Surface Processes and Landforms, 25, 59-76. https://doi.org/10.1002/(SICI)1096-9837(200001)25:1<59::AID-ESP48>3.0.CO;2-T

Chapwanya, M., Clark, C.D. and Fowler, A.C. (2011). Numerical computations of a theoretical model of ribbed moraine formation. Earth Surface Processes and Landforms, 36(8), 1105-1112. https://doi.org/10.1002/esp.2138

Chandler, B.M.P., Evans, D.J.A. and Roberts, D.H. (2016). Characteristics of recessional moraines at a temperate glacier in SE Iceland: Insights into patterns, rates and drivers of glacier

retreat. Quaternary Science Reviews 135, 171–205. https://doi.org/10.1016/j.quascirev.2016.01.025

Cowan, W. (1968). Ribbed moraine: till fabric analysis and origin. Canadian Journal of Earth Sciences 5, 1145–1159.

Delaney, C.A., Adamson, K., Linch, L.D., Davis, S. and McCarron, S. (2023). Reconstructing terrestrial ice sheet retreat dynamics from hummocky topography using multiscale evidence: An example from central Ireland. Quaternary Science Reviews, 308, 108041. https://doi.org/10.1016/j.quascirev.2023.108041

Dunlop, P., and Clark, C.D. (2006). The morphological characteristics of ribbed moraine. Quaternary Science Reviews, 25(13-14), 1668-1691. https://doi.org/10.1016/j.quascirev.2006.01.002

Dunlop, P., Clark, C.D., and Hindmarsh, R.C. (2008). Bed ribbing instability explanation: testing a numerical model of ribbed moraine formation arising from coupled flow of ice and subglacial sediment. Journal of Geophysical Research: Earth Surface, 113(F3). https://doi.org/10.1029/2007JF000954

Dyke, A.S., Morris, T.F., Green, D.E.C. and England, J. (1992). Quaternary geology of Prince of Wales Island, Arctic Canada. Geological Survey of Canada Memoir 433, 142.

Ely, J.C., Stevens, D., Clark, C.D. and Butcher, F.E. (2023). Numerical modelling of subglacial ribs, drumlins, herringbones, and mega-scale glacial lineations reveals their developmental trajectories and transitions. Earth Surface Processes and Landforms. https://doi.org/10.1002/esp.5529

Evans, D.J.A. and Benn, D.I. (Eds.). (2004). A practical guide to the study of glacial sediments. 83-87 & 97-107 pp. Arnold, London.

Evans, D.J.A. and Rea, B.R. (1999). Geomorphology and sedimentology of surging glaciers: a land-systems approach. Annals of Glaciology, 28, 75-82.

Evans, D.J.A. and Rea, B.R. (2003). Surging glacier landsystem. In Glacial landsystems (pp. 259-288). Taylor and Francis.

Evans, D.J.A., Phillips, E.R., Hiemstra, J.F. and Auton, C.A. (2006). Subglacial till: formation, sedimentary characteristics and classification. Earth-Science Reviews, 78(1-2), 115-176. https://doi.org/10.1016/j.earscirev.2006.04.001

Evans, D.J., Storrar, R.D., and Rea, B.R. (2016). Crevasse-squeeze ridge corridors: diagnostic features of late-stage palaeo-ice stream activity. Geomorphology, 258, 40-50. https://doi.org/10.1016/j.geomorph.2016.01.017

Finlayson, A. (2013). Digital surface models are not always representative of former glacier beds: palaeoglaciological and geomorphological implications. Geomorphology, 194, 25-33. https://doi.org/10.1016/j.geomorph.2013.03.026

Finlayson, A.G. and Bradwell, T. (2008). Morphological characteristics, formation and glaciological significance of Rogen moraine in northern Scotland. Geomorphology, 101(4), 607-617. https://doi.org/10.1016/j.geomorph.2008.02.013

Fisher, T.G. and Shaw, J. (1992). A depositional model for Rogen Moraine, with examples from the Avalon Peninsula, Newfoundland. Canadian Journal of Earth Sciences 29, 669–686. https://doi.org/10.1139/e92-058

Fowler, A.C., Chapwanya, M. 2014. An instability theory for the formation of ribbed moraine, drumlins and mega-scale glacial lineations. Proceedings of the Royal Society A: Mathematical, Physical and Engineering Sciences, 470(2171), 20140185. https://doi.org/10.1098/rspa.2014.0185

Frödin, G. (1954). De sista skedena av Central Jämtlands glaciala historia. Geographica 24, 1–251.

Hättestrand, C. (1997). Ribbed moraines in Sweden—distribution pattern and Palaeoglaciological implications. Sedimentary Geology 111, 41–56. https://doi.org/10.1016/S0037-0738(97)00005-5

Hättestrand, C. and Kleman, J. (1999). Ribbed moraine formation. Quaternary Science Reviews 18, 43–61. https://doi.org/10.1016/S0277-3791(97)00094-2

Helgadóttir, E.G. (2020). Ribbed moraines in the Vopnafjörður region, Iceland. Master's thesis, Faculty of Earth Sciences, University of Iceland. 104 p. Available from: http://hdl.handle.net/1946/35879

Hubbard, A., Sugden, J., Dugmore, A., Norðdahl., H. and Pétursson, H.G. (2006). A modelling insight into the Icelandic Late Glacial Maximum ice sheet. Quaternary Science Reviews, 25(17-18), 2283-2296. https://doi.org/10.1016/j.quascirev.2006.04.001

The Icelandic Road and Coastal Administration. https://namur.vegagerdin.is/ (checked 15.10.2023).

Ingólfsson, Ó. and Norðdahl, H. (2001). High relative sea-level during the Bølling interstadial in W Iceland: a reflection of ice-sheet collapse and extremely rapid glacial unloading. Arctic, Antarctic and Alpine Research, 33, 231-243. https://doi.org/10.1080/15230430.2001.12003426

Jóhannesson, H. and Sæmundsson, K. (2009). Geological map of Iceland. 1:500.000. Bedrock (1st edition). Icelandic Institute of Natural History. Reykjavík.

Kamb, B. (2001). Basal zone of the West Antarctic ice streams and its role in lubrication of their rapid motion. The West Antarctic ice sheet: behavior and environment, 77, 157-199. https://doi.org/10.1029/AR077p0157

Krüger, J. and Kjær, K.H. (1999). A data chart for field description and genetic interpretation of glacial diamicts and associated sediments - with examples from Greenland, Iceland, and Denmark. Boreas, 28(3), 386-402. https://doi.org/10.1111/j.1502-3885.1999.tb00228.x

Kurjanski, B., Rea, B.R., Spagnolo, M., Winsborrow, M., Cornwell, D.G., Andreassen, K. and Howell, J. (2019). Morphological evidence for marine ice stream shutdown, central Barents Sea. Marine Geology, 414, 64-76. https://doi.org/10.1016/j.margeo.2019.05.001

Lamsters, K., Vītola, Z., Karušs, J. and Džeriņš, P. (2021). Evidence of ice streaming and ice tongue shutdown in western Latvia: revealed from the mapping of crevasse-squeeze ridges. Baltica, 33(1). DOI: 10.5200/baltica.2021.1.1

Lindén, M., Möller, P. And Adrielsson, L. (2008). Ribbed moraine formed by subglacial folding, thrust stacking and lee-side cavity infill. Boreas, 37(1), 102-131. https://doi.org/10.1111/j.1502-3885.2007.00002.x

Livingstone, S.J., Cofaigh, C.Ó., Stokes, C.R., Hillenbrand, C., Vieli, A. and Jamieson, S.S.R. (2012). Antarctic palaeo-ice streams. Earth-Science Reviews, 111(1-2), 90-128. https://doi.org/10.1016/j.earscirev.2011.10.003

Lundqvist, J. (1969). Problems of the so-called Rogen moraine. Sverige Geologiske Undersökning, Series C, 648, pp. 1-32.

Lundqvist, J., (1989). Rogen (ribbed) moraine: identification and possible origin. Sedimentary Geology 62, 281–292.

Lundqvist, J. (1997). Rogen moraine—an example of two-step formation of glacial landscapes. Sedimentary Geology 111, 27–40. https://doi.org/10.1016/S0037-0738(97)00004-3

Margold, M., Jansson, K.N., Kleman, J. and Stroeven, A.P. (2011). Glacial meltwater landforms of central British Columbia. Journal of Maps, 7(1).

Möller, P. (2006). Rogen moraine—an example of glacial reshaping of preexisting landforms. Quaternary Science Reviews 25, 362–389. https://doi.org/10.1016/j.quascirev.2005.01.011

Möller, P. and Dowling, T.P. (2018). Equifinality in glacial geomorphology: instability theory examined via ribbed moraine and drumlins in Sweden. GFF, 140(2), 106-135. https://doi.org/10.1080/11035897.2018.1441903

Napieralski, J. and Nalepa, N. (2010). The application of control charts to determine the effect of grid cell size on landform morphometry. Computers & Geosciences 36, 222-230.

Norðdahl, H. and Ingólfsson, Ó. (2015). Collapse of the Icelandic ice sheet controlled by sea-level rise? Arktos, 1, 1-18. https://doi.org/10.1007/s41063-015-0020-x

Norðdahl, H. and Pétursson, H.G. (2005). Relative sea-level changes in Iceland. New aspects of the Weichselian deglaciation of Iceland. In: Caseldine C, Russel A, Harðardóttir J, Knudsen Ó (Eds.), Iceland – modern processes and past environments. Elsevier, Amsterdam, pp. 25-78.

Norðdahl, H., Ingólfsson, Ó., Vogler, E.D., Steingrímsson, B.Ó. and Hjartarson, Á. (2019). Glacio-isostatic age modelling and Late Weichselian deglaciation of the Lögurinn basin, East Iceland. Boreas, 48(3), 563-580. https://doi.org/10.1111/bor.12366

Patton, H., Hubbard, A., Bradwell, T. and Schomacker, A. (2017). The configuration, sensitivity and rapid retreat of the Late Weichselian Icelandic ice sheet. Earth-Science Reviews, 166, 223-245. https://doi.org/10.1016/j.earscirev.2017.02.001

Porter, C., Morin, P., Howat, I., et al. 2018, "ArcticDEM", https://doi.org/10.7910/DVN/OHHUKH, Harvard Dataverse, V1.

Powers, M.C. (1953). A new roundness scale for sedimentary particles. Journal of Sedimentary Research, 23(2), 117-119.

Principato, S.M., Moyer, A.N., Hampsch, A.G. and Ipsen, H.A. (2016). Using GIS and streamlined landforms to interpret palaeo-ice flow in northern Iceland. Boreas 45, 470-482. https://doi.org/10.1111/bor.12164

Raunholm, S., Sejrup, H.P. and Larsen, E. (2003). Lateglacial landform associations at Jæren (SW Norway) and their glaci-dynamic implications. Boreas, 32(3), 462-475. https://doi.org/10.1111/j.1502-3885.2003.tb01228.x

Rivers, G.E., Storrar, R.D., Jones, A.H., and Ojala, A.E. (2023). 3D morphometry of De Geer Moraines and Crevasse-Squeeze Ridges: Differentiating between pushing and squeezing mechanisms from remotely sensed data. Quaternary Science Reviews, 321, 108383. https://doi.org/10.1016/j.quascirev.2023.108383

Sarala, P. (2006). Ribbed moraine stratigraphy and formation in southern Finnish Lapland. Journal of Quaternary Science: Published for the Quaternary Research Association, 21(4), 387-398. https://doi.org/10.1002/jqs.995

Shaw, J. (1979). Genesis of the Sveg till and Rogen moraines of central Sweden: a model of basal Melt out. Boreas 8, 409 426.

Sharp, M. (1985) "Crevasse-fill" ridges-a landform type characteristic of surging glaciers? Geografisker Annaler, Series a, Physical Geography, 67(3–4), 213–220. Available from: https://doi.org/10.1080/04353676.1985.11880147

Smith, A.M., Anker., P.G.F., Nicholls., K.W., Makinson, K., Murray, T., Rios-Costas, S., Brisbourne. A.M., Hodgson, D.A., Schlegel., R. and Anandakrishnan, S. (2021). Ice stream subglacial access for ice-sheet history and fast ice flow: the BEAMISH Project on Rutford Ice

Stream, West Antarctica and initial results on basal conditions. Annals of Glaciology 62(85-86), 203–211. https://doi.org/10.1017/aog.2020.82

Spagnolo, M. and Clark C.D. (2009). A geomorphological overview of glacial landforms on the Icelandic continental shelf. Journal of Maps, 2009, 37-52. https://doi.org/10.4113/jom.2009.1049

Stokes, C.R. (2018). Geomorphology under ice streams: Moving from form to process. Earth Surfaces Processes and Landforms, 43, 85-123. https://doi.org/10.1002/esp.4259

Stokes, C.R. and Clark. C.D. (1999). Geomorphological criteria for identifying Pleistocene ice streams. Annals of Glaciology, 28, 67-74. doi:10.3189/172756499781821625

Stokes, C.R. and Clark, C.D. (2001). Palaeo-ice streams. Quaternary Science Reviews 20, 1437-1457. https://doi.org/10.1016/S0277-3791(01)00003-8

Stokes, C. R., Clark, C.D. and Storrar, R. (2009). Major changes in ice stream dynamics during deglaciation of the north-western margin of the Laurentide Ice Sheet. Quaternary Science Reviews, 28(7-8), 721-738. https://doi.org/10.1016/j.quascirev.2008.07.019

Stokes, C.R., Clark, C.D., Lian, O.B. and Tulaczyk, S. (2007). Ice stream sticky spots: a review of their identification and influence beneath contemporary and palaeo-ice streams. Earth-Science Reviews, 81(3-4), 217-249. https://doi.org/10.1016/j.earscirev.2007.01.002

Stokes, C.R., Lian, O.B., Tulaczyk, S. and Clark., C.D. (2008). Superimposition of ribbed moraines on a palaeo-ice-stream bed: implications for ice stream dynamics and shutdown. Earth Surface Processes and Landforms: The Journal of the British Geomorphological Research Group, 33(4), 593-609. https://doi.org/10.1002/esp.1671

Storrar, R. D., Stokes, C. R., & Evans, D. J. (2014a). Increased channelization of subglacial drainage during deglaciation of the Laurentide Ice Sheet. Geology, 42(3), 239-242. https://doi.org/10.1130/G35092.1

Storrar, R.D., Stokes, C.R. and Evans, D.J. (2014b). Morphometry and pattern of a large sample (> 20,000) of Canadian eskers and implications for subglacial drainage beneath ice sheets. Quaternary Science Reviews, 105, 1-25. https://doi.org/10.1016/j.quascirev.2014.09.013

Sæmundsson, K. (1977). Geological Map of Iceland, Sheet 7, NE-Iceland. 1:250.000. Icelandic Institute of Natural History and National Land Survey of Iceland, Reykjavik.

Sæmundsson, Th. 1995. Deglaciation and shoreline displacement in Vopnafjörður, northeastern Iceland. LUNDQUA thesis 33,1-106. Department of Quaternary Geology, Lund University.

Trommelen, M.S., Ross, M., and Ismail, A. (2014). Ribbed moraines in northern Manitoba, Canada: characteristics and preservation as part of a subglacial bed mosaic near the core regions of ice sheets. *Quaternary Science Reviews*, *87*, 135-155. https://doi.org/10.1016/j.quascirev.2014.01.010

Veen C.J. van Der. (1998). Fracture Mechanics Approach to Penetration of Bottom Crevasses on Glaciers. Cold Regions Science and Technology. https://doi.org/10.1016/S0165-232X(98)00006-8

Vérité, J., Livingstone, S. J., Ravier, E., McMartin, I., Campbell, J., Lewington, E.L., Dewald, N., Clark., C.D., Sole, A.J. and Storrar, R.D. (2023). Conceptual model for the formation of bedforms along subglacial meltwater corridors (SMCs) by variable ice-water-bed interactions. Earth Surface Processes and Landforms. DOI: 10.1002/esp.5725

Vérité, J., Ravier, É., Bourgeois, O., Bessin, P., and Pochat, S. (2023). New metrics reveal the evolutionary continuum behind the morphological diversity of subglacial

bedforms. Geomorphology, 427, 108627. https://doi.org/10.1016/j.geomorph.2023.108627

Vérité, J., Ravier, É., Bourgeois, O., Pochat, S., Lelandais, T., Mourgues, R., Clark, C.D., Bessin, P., Peigné, D. and Atkinson, N. (2021). Formation of ribbed bedforms below shear margins and lobes of palaeo-ice streams. The Cryosphere, 15(6), 2889-2916. https://doi.org/10.5194/tc-15-2889-2021